

**$\beta$ -CYCLODEXTRIN FUNCTIONALIZED IONIC LIQUID AS  
HIGH PERFORMANCE LIQUID CHROMATOGRAPHY  
CHIRAL STATIONARY PHASE FOR THE  
ENANTIOSEPARATION OF NATURAL PRODUCTS AND  
PHARMACEUTICALS**

**NURUL YANI BINTI RAHIM**

**FACULTY OF SCIENCE  
UNIVERSITY OF MALAYA  
KUALA LUMPUR**

**2017**

**$\beta$ -CYCLODEXTRIN FUNCTIONALIZED IONIC  
LIQUID AS HIGH PERFORMANCE LIQUID  
CHROMATOGRAPHY CHIRAL STATIONARY PHASE  
FOR THE ENANTIOSEPARATION OF NATURAL  
PRODUCTS AND PHARMACEUTICALS**

**NURUL YANI BINTI RAHIM**

**THESIS SUBMITTED IN FULFILMENT OF THE  
REQUIREMENTS FOR THE DEGREE OF DOCTOR OF  
PHILOSOPHY**

**FACULTY OF SCIENCE  
UNIVERSITY OF MALAYA  
KUALA LUMPUR**

**2017**

**UNIVERSITY OF MALAYA**  
**ORIGINAL LITERARY WORK DECLARATION**

Name of Candidate: Nurul Yani Rahim (I.C/Passport No: )

Registration/Matric No: SHC 120044

Name of Degree: Degree of Doctor of Philosophy

Title of Project Paper/Research Report/Dissertation/Thesis (“this Work”):

$\beta$ -Cyclodextrin functionalized ionic liquid as high performance liquid chromatography chiral stationary phase for the enantioseparation of natural products and pharmaceuticals

Field of Study: Analytical Chemistry

I do solemnly and sincerely declare that:

- (1) I am the sole author/writer of this Work;
- (2) This Work is original;
- (3) Any use of any work in which copyright exists was done by way of fair dealing and for permitted purposes and any excerpt or extract from, or reference to or reproduction of any copyright work has been disclosed expressly and sufficiently and the title of the Work and its authorship have been acknowledged in this Work;
- (4) I do not have any actual knowledge nor do I ought reasonably to know that the making of this work constitutes an infringement of any copyright work;
- (5) I hereby assign all and every rights in the copyright to this Work to the University of Malaya (“UM”), who henceforth shall be owner of the copyright in this Work and that any reproduction or use in any form or by any means whatsoever is prohibited without the written consent of UM having been first had and obtained;
- (6) I am fully aware that if in the course of making this Work I have infringed any copyright whether intentionally or otherwise, I may be subject to legal action or any other action as may be determined by UM.

Candidate’s Signature

Date:

Subscribed and solemnly declared before,

Witness’s Signature

Date:

Name:

Designation:

## ABSTRACT

The demanding for enantiomerically pure (enantiopure) compounds, especially for pharmaceutical field has been attracting great attention during last decades. Direct enantioseparation by chiral stationary phases (CSPs) using high performance liquid chromatography (HPLC) remains as the most important technique for enantioseparation. The development of novel stable and powerful CSPs is therefore important. The first part of this study involved a facile and reliable preparation of CSPs. Thus,  $\beta$ -cyclodextrin was functionalized with ionic liquids (ILs) namely 1-benzylimidazole (1-BzIm) and 1-decyl-2-methylimidazole ( $C_{10}$ MIm) with tosylate as anion produced  $\beta$ -CD-BIMOTs and  $\beta$ -CD-DIMOTs respectively.  $\beta$ -CD-BIMOTs and  $\beta$ -CD-DIMOTs were attached to the modified silica to obtain the CSPs. The performances of the synthesized CSPs were determined by examining the capability of enantioseparation of selected analytes: flavonoids (flavanone, hesperetin, naringenin and eriodictyol),  $\beta$ -blockers (atenolol, metoprolol, pindolol and propranolol) and Non-steroidal anti-inflammatory drug (NSAIDs) (ibuprofen, fenoprofen, ketoprofen and indoprofen). The performance of  $\beta$ -CD-BIMOTs and  $\beta$ -CD-DIMOTs stationary phases was also compared with native  $\beta$ -CD stationary phase. The results indicated that  $\beta$ -CD-BIMOTs stationary phase afforded more favorable enantioseparations than  $\beta$ -CD-DIMOTs and native  $\beta$ -CD based stationary phases. Therefore, the optimization for enantioseparation of selected analytes (flavonoids,  $\beta$ -blockers and NSAIDs) and evaluation of interactions was further investigated on  $\beta$ -CD-BIMOTs stationary phase. The selected flavonoids, flavanone and hesperetin obtained high resolution factor in reverse phase mode. Meanwhile naringenin and eriodictyol attained partial enantioseparation in polar organic mode. In order to understand the mechanism of separation, the interaction of selected flavonoids and  $\beta$ -CD-BIMOTs was studied using spectroscopic methods which are  $^1H$  NMR, NOESY and UV/Vis spectrophotometry. The result for enantioseparation of selected  $\beta$ -blockers, propranolol and metoprolol showed good enantioresolution compared to atenolol and pindolol. The results suggested that the lipophilic property and the structure of propranolol and metoprolol that enable the formation of inclusion complex contribute to better enantioseparation. This observation was proven by  $^1H$  NMR and NOESY of  $\beta$ -CD-BIMOTs/ $\beta$ -blockers. The effect of the types and variation of mobile phase composition on enantioseparation of NSAIDs was also studied on  $\beta$ -CD-BIMOTs CSP. From the result of enantioseparation, ibuprofen and indoprofen achieved the better resolution than ketoprofen and fenoprofen due to their favorable orientation to fit into the  $\beta$ -CD-BIMOTs cavity. This orientation was depending on the structure of NSAIDs.

## ABSTRAK

Permintaan yang tinggi terhadap sebatian enantio yang asli, terutamanya dalam bidang farmaseutikal telah menjadi perhatian sejak berdekad yang lalu. Pemisahan enantio secara langsung oleh fasa pegun kiral (CSP) menggunakan kromatografi cecair prestasi tinggi (HPLC) adalah teknik yang penting untuk pemisahan enantio. Oleh itu, perkembangan penghasilan CSP yang terbaru perlu diambil kira. Bahagian pertama kajian ini adalah melibatkan penyediaan CSP yang sangat mudah. Untuk itu,  $\beta$ -cyclodextrin telah difungsikan dengan cecair ionik (ILs) iaitu 1-benzylimidazole (1 BzIm) dan 1-Decyl-2-methylimidazole ( $C_{10}$ MIm) dengan tosylate sebagai anion masing-masing menghasilkan  $\beta$ -CD-BIMOTs dan  $\beta$ -CD-DIMOTs.  $\beta$ -CD-BIMOTs dan  $\beta$ -CD-DIMOTs dilekatkan pada silika terubahsuai untuk menghasilkan fasa pegun kiral. Prestasi fasa pegun kiral ini diukur dengan keupayaan pemisahan enantio terhadap analit yang terpilih: flavonoid (flavanone, hesperetin, naringenin dan eriodictyol),  $\beta$ -blockers (atenolol, metoprolol, pindolol dan propranolol) dan ubat anti-radang bukan steroid (NSAIDs) (ibuprofen, fenoprofen, ketoprofen dan indoprofen). Prestasi fasa pegun  $\beta$ -CD-BIMOTs dan  $\beta$ -CD-DIMOTs juga telah dibandingkan dengan fasa pegun  $\beta$ -CD asli. Keputusan menunjukkan bahawa fasa pegun  $\beta$ -CD-BIMOTs mencapai pemisahan enantio yang lebih baik daripada fasa pegun  $\beta$ -CD-DIMOTs dan fasa pegun  $\beta$ -CD asli. Oleh itu, pengoptimuman pemisahan enantio terhadap analit yang terpilih (flavonoid,  $\beta$ -blockers dan NSAIDs) dan penilaian interaksi yang terlibat disiasat dengan menggunakan fasa pegun  $\beta$ -CD-BIMOTs. Flavonoid seperti flavanone dan hesperetin memperolehi faktor resolusi yang tinggi dalam mod fasa terbalik. Sementara itu, naringenin dan eriodictyol mencapai separa pemisahan enantio dalam mod organik berkutub. Untuk memahami mekanisma pemisahan, interaksi flavonoid dan  $\beta$ -CD-BIMOTs dikaji menggunakan kaedah spektroskopi iaitu  $^1\text{H}$  NMR, NOESY dan spektrofotometri UV-Vis. Keputusan pemisahan enantio  $\beta$ -blockers menunjukkan resolusi enantio propranolol dan metoprolol adalah lebih baik berbanding atenolol dan pindolol. Ini kerana sifat lipofilik serta struktur propranolol dan metoprolol yang membolehkan pembentukan kompleks kemasukan berlaku dan seterusnya menyumbang kepada pemisahan enantio yang lebih baik. Interaksi ini dibuktikan dengan  $^1\text{H}$  NMR dan NOESY  $\beta$ -CD-BIMOTs/ $\beta$ -blockers. Pemisahan enantio NSAIDs dengan  $\beta$ -CD-BIMOTs turut dikaji berdasarkan jenis dan kepelbagaian komposisi fasa bergerak. Berdasarkan keputusan pemisahan enantio, ibuprofen dan indoprofen mencapai resolusi yang lebih baik berbanding ketoprofen dan fenoprofen kerana orientasi yang sesuai untuk mereka dimuatkan ke dalam rongga  $\beta$ -CD-BIMOTs. Orientasi ini bergantung kepada struktur NSAIDs itu sendiri.

## ACKNOWLEDGEMENTS

It is with great pleasure I convey my sincere appreciation to all who made my doctoral degree a success. First and foremost, I would like to express my gratitude to my research advisor, Dr. Sharifah Mohamad and Dr Tay Kheng Soo, for their support, encouragement, patience and guidance during my graduate studies. I will never forget what I have learned from them and I look forward to our future endeavors. I consider myself extremely fortunate to have the opportunity to work under their supervision.

I greatly appreciate the assistance of all faculty and staff in the Department of Chemistry at the University of Malaya, especially Miss Norzalida Zakaria for assisting me in using NMR, and other lab assistants for helping me to maintain HPLC instruments and training me in the use of other instrumentation. I also thank my lab members (FD-L5-4) and other colleagues (Dr. Muggundha, Dr. Nur Nadhirah, Dr Saliza, Dr. Mazidatul, Siti Farhana, Khalijah, Shabnam, Fairuz Liyana, Naqiyah Farhan, Syed Fariq, Ahmad Razali, Nur Faizah and Nur Atiqah) for their help and friendship.

Last but not least, I would especially like to thank my parents, mother Siti Omar, father Rahim Yussof, sisters Nur Syuhada and Nuratikah for their unconditional love and support during my life.

## TABLE OF CONTENTS

<b>Abstract</b> .....	<b>iii</b>
<b>Abstrak</b> .....	<b>iv</b>
<b>Acknowledgements</b> .....	<b>v</b>
<b>Table of Contents</b> .....	<b>vi</b>
<b>List of Figures</b> .....	<b>ix</b>
<b>List of Tables</b> .....	<b>xii</b>
<b>List of Symbols and Abbreviations</b> .....	<b>xiii</b>
<b>List of Appendices</b> .....	<b>xvi</b>
<b>CHAPTER 1: INTRODUCTION</b> .....	<b>1</b>
1.1 Background of study.....	1
1.2 Objectives of the research .....	7
1.3 Outline of thesis.....	7
<b>CHAPTER 2: LITERATURE REVIEW</b> .....	<b>8</b>
2.1 Chirality .....	8
2.2 Enantiomeric separation technology .....	10
2.2.1 Development of chiral separation technologies .....	10
2.2.2 Development of chiral stationary phase.....	13
2.3 Cyclodextrin and its applications in enantioseparation .....	14
2.4 Ionic liquid in enantioseparation .....	20
2.5 Selected chiral compounds.....	31
2.5.1 Flavonoids .....	31
2.5.2 $\beta$ -blocker drugs.....	35
2.5.3 Non-steroidal anti-inflammatory drugs (NSAIDs).....	36

<b>CHAPTER 3: EXPERIMENTAL.....</b>	<b>39</b>
3.1 Chemicals, materials and reagents .....	39
3.2 Instruments.....	39
3.3 Preparation of $\beta$ -CD based chiral stationary phase .....	40
3.3.1 Synthesis of $\beta$ -CD functionalized ionic liquid .....	40
3.3.2 Immobilization of $\beta$ -CD-BIMOTs and $\beta$ -CD-DIMOTs onto modified silica to obtain the CSP .....	45
3.3.3 Synthesis of native $\beta$ -CD (n- $\beta$ -CD) as chiral stationary phase .....	45
3.4 Column packing approach .....	45
3.5 HPLC analysis instrumentation and conditions .....	46
3.6 Calculations of chromatographic data .....	46
3.7 Preparation of inclusion complex.....	48
3.7.1 Preparation of kneaded complex .....	48
3.7.2 Determination of formation constant.....	49
 <b>CHAPTER 4: RESULTS AND DISCUSSION.....</b>	 <b>50</b>
4.1 Characterization of $\beta$ -CD Based Chiral Stationary Phase .....	50
4.1.1 FT-IR analysis .....	50
4.1.2 Thermalgravimetric analysis .....	55
4.2 Screening performance of CSPs.....	57
4.3 Enantioseparation performance of Flavonoids.....	61
4.4 Enantioseparation performance of $\beta$ -blockers .....	81
4.5 Enantioseparation performance of NSAIDs .....	94
 <b>CHAPTER 5: CONCLUSIONS AND FUTURE RECOMMENDATIONS.....</b>	 <b>107</b>
5.1 Conclusions .....	107
5.2 Future work suggestions .....	109



<b>References .....</b>	<b>110</b>
<b>LIST OF PUBLICATIONS AND PAPERS PRESENTED.....</b>	<b>121</b>
<b>APPENDIX.....</b>	<b>122</b>

## LIST OF FIGURES

Figure 1.1: Chiral molecule.....	1
Figure 1.2 : a) Chemical structure of CD b) Molecular shape of CD.....	4
Figure 1.3: Illustration of the interaction between $\beta$ -CD and enantiomer .....	5
Figure 2.1: Examples of how to design configuration using Cahn-Ingold-Prelog priority rules.....	9
Figure 2.2: Common structures of chiral selectors.....	12
Figure 2.3: Molecular structure of the first commercial chiral column (Pirkle 1-J-column)-Brush type CSP .....	14
Figure 2.4: Illustration of a) $\alpha$ -CD, b) $\beta$ -CD, c) $\gamma$ -CD and d) side view of CD represent the position.....	16
Figure 2.5: The “three point” model.....	17
Figure 2.6: Common derivatives group of CD.....	20
Figure 2.7: Common structures of cation and anion of ILs .....	21
Figure 2.8: Structures of VIMPCCD-POLY and VAMPCCD-POLY CSPs (Wang <i>et al.</i> , 2012c) .....	25
Figure 2.9: Structure of functionalized IL-bonded CSPs (Zhou <i>et al.</i> , 2010).....	26
Figure 2.10: Structure of Thioether-bridged $\beta$ -CD and Triazole-bridged $\beta$ -CD CSPs (Yao <i>et al.</i> , 2014a) .....	27
Figure 2.11: Structure of $\beta$ -CD derivatives functionalized by ILs (Li & Zhou, 2014) ..	28
Figure 2.12: Structure of $\text{Fe}_3\text{O}_4@\text{SiO}_2@\text{HMMDI-EMIMLpro}$ (Liu <i>et al.</i> , 2015b).....	29
Figure 2.13: Structure of tetramethylammonium L-hydroxyproline (Liu <i>et al.</i> , 2015a)	29
Figure 2.14: Novel cationic CSP (Li <i>et al.</i> , 2016).....	30
Figure 2.15: Basic chemical structure of flavonoid.....	31
Figure 2.16: Spatial dispositions of the enantiomers of chiral flavanones .....	32
Figure 2.17: Chemical structures of some flavanones .....	34

Figure 2.18: Structure of studied $\beta$ -blockers.....	36
Figure 2.19: Structure of selected NSAIDs.....	38
Figure 3.1: Synthesis pathways of $\beta$ -CD-BIMOTs CSP .....	42
Figure 3.2: Structure of $\beta$ -CD-BIMOTs .....	43
Figure 3.3: Structure of $\beta$ -CD-DIMOTs.....	44
Figure 3.4: Two enantiomerically related peaks and the measurements required to calculate $k_1'$ , $k_2'$ , $\alpha$ and $R_s$ .....	47
Figure 3.5: Schematic of kneading method .....	48
Figure 4.1: FT-IR spectrum of a) $\beta$ -CD b) $\beta$ -CD-BIMOTs c) $\beta$ -CD-DIMOTs.....	51
Figure 4.2: FT-IR spectrums of a) Si-TDI b) native $\beta$ -CD CSP c) $\beta$ -CD-BIMOTs CSP d) $\beta$ -CD-DIMOTs CSP .....	52
Figure 4.3: Thermogram of a) Si-TDI b) native $\beta$ -CD CSP c) $\beta$ -CD-BIMOTs CSP d) $\beta$ -CD-DIMOTs CSP.....	56
Figure 4.4: Structure of 2'-hydroxyl substituted chalcones.....	62
Figure 4.5: The deduced structure of $\beta$ -CD-BIMOTs .....	65
Figure 4.6: The deduced structure of a) $\beta$ -CD-BIMOTs/flavanone complex, b) $\beta$ -CD-BIMOTs/hesperetin complex, c) $\beta$ -CD-BIMOTs/naringenin complex d) $\beta$ -CD-BIMOTs/eriodictyol complex .....	66
Figure 4.7: NOESY spectra of $\beta$ -CD-BIMOTs/flavanone .....	69
Figure 4.8: NOESY spectra of $\beta$ -CD-BIMOTs/hesperetin.....	71
Figure 4.9: NOESY spectra of $\beta$ -CD-BIMOTs/naringenin .....	73
Figure 4.10: NOESY spectra of $\beta$ -CD-BIMOTs/eriodictyol.....	74
Figure 4.11: HPLC chromatograms of naringenin in polar organic mode. Mobile phase composition, ACN/MeOH/TEA/HOAc (v/v/v/v): a-i) 90/10/1/3, a-ii) 90/10/3/1, b-i) 50/50/1/3, b-ii) 50/50/3/1, c-i) 30/70/1/3 and c-ii) 30/70/3/1.....	76
Figure 4.12: HPLC chromatograms of eriodictyol in polar organic mode. Mobile phase composition, ACN/MeOH/TEA/HOAc (v/v/v/v): a-i) 90/10/1/3, a-ii) 90/10/3/1, b-i) 50/50/1/3, b-ii) 50/50/3/1, c-i) 30/70/1/3 c-ii) 30/70/3/1 .....	77

Figure 4.13: Absorption spectra of a) $\beta$ -CD-BIMOTs/flavanone b) $\beta$ -CD-BIMOTs/hesperetin c) $\beta$ -CD-BIMOTs/naringenin d) $\beta$ -CD-BIMOTs/eriodictyol with $[\beta$ -CD-BIMOTs]: 0.032mM [Flavonoids]: 0.01mM; T = 25 °C.....	79
Figure 4.14: Benesi-Hildebrand plot of $1/A - A_0$ versus $1/[\beta$ -CD-BIMOTs] for a) $\beta$ -CD-BIMOTs/flavanone, b) $\beta$ -CD-BIMOTs/hesperetin, c) $\beta$ -CD-BIMOTs/naringenin d) $\beta$ -CD-BIMOTs/eriodictyol.....	80
Figure 4.15: The deduced structure of $\beta$ -CD-BIMOTs/ $\beta$ -blockers complexes: a) atenolol, b) metoprolol, c) Pindolol, d) Propranolol.....	86
Figure 4.16: 2D NOESY spectra of $\beta$ -CD-BIMOTs/propranolol complex.....	87
Figure 4.17: 2D NOESY spectra of $\beta$ -CD-BIMOTs/metoprolol complex.....	88
Figure 4.18: 2D NOESY spectra of $\beta$ -CD-BIMOTs/pindolol complex.....	90
Figure 4.19: 2D NOESY spectra of $\beta$ -CD-BIMOTs/atenolol complex.....	91
Figure 4.20: The chromatograms of propranolol, metoprolol, pindolol and atenolol responding to different pH of mobile phase.....	93
Figure 4.21: The deduced structure of NSAID/ $\beta$ -CD-BIMOTs complexes: (a) i) ibuprofen ii) $\beta$ -CD-BIMOTs/ibuprofen, (b) i) indoprofen ii) $\beta$ -CD-BIMOTs/indoprofen (c) i) ketoprofen ii) $\beta$ -CD-BIMOTs/ketoprofen, (d) i) fenoprofen ii) $\beta$ -CD-BIMOTs/fenoprofen.....	99
Figure 4.22: NOESY spectra of $\beta$ -CD-BIMOTs/ibuprofen.....	101
Figure 4.23: NOESY spectra of $\beta$ -CD-BIMOTs/indoprofen.....	102
Figure 4.24: NOESY spectra of $\beta$ -CD-BIMOTs/ketoprofen.....	103
Figure 4.25: NOESY spectra of $\beta$ -CD-BIMOTs/fenoprofen.....	104
Figure 4.26: Absorption spectra of a) $\beta$ -CD-BIMOTs/ibuprofen b) $\beta$ -CD-BIMOTs/indoprofen c) $\beta$ -CD-BIMOTs/ketoprofen d) $\beta$ -CD-BIMOTs/fenoprofen with $[\beta$ -CD-BIMOTs]: 0.032mM [NSAIDs]: 0.01mM; T = 25 °C.....	106

## LIST OF TABLES

Table 2.1: Physical and chemical properties of CD molecules (Bender & Komiyama, 2012).....	16
Table 2.2: Chemical structures of the cationic functionalized $\beta$ -CDs (Wang <i>et al.</i> , 2008) .....	24
Table 2.3: Common dietary flavonoids .....	33
Table 4.1: Main IR frequencies for $\beta$ -CD, $\beta$ -CD-BIMOTs and $\beta$ -CD-DIMOTs with assignments .....	53
Table 4.2: Main IR frequencies for Si-TDI, native $\beta$ -CD CSP, $\beta$ -CD-BIMOTs CSP and $\beta$ -CD-DIMOTs CSP with assignments.....	54
Table 4.3: The assignment for temperature of weight loss .....	57
Table 4.4: The chromatogram for the enantioseparation of selected flavonoids, $\beta$ -blockers and NSAIDs on $\beta$ -CD, $\beta$ -CD-BIMOTs and $\beta$ -CD-DIMOTs CSPs.....	59
Table 4.5: Chiral separation data for the flavonoids on $\beta$ -CD-BIMOTs CSP in the reverse mobile phase.....	63
Table 4.6: Chemical shifts ( $\delta$ ) and induced shifts ( $\Delta\delta$ ) of $\beta$ -CD-BIMOTs and $\beta$ -CD-BIMOTs/flavonoids.....	68
Table 4.7: $K$ values for $\beta$ -CD-BIMOTs/flavonoids.....	80
Table 4.8: Chiral separation data for the $\beta$ -blockers on $\beta$ -CD-BIMOTs CSP in neutral pH mobile phase.....	82
Table 4.9: Chemical shifts ( $\delta$ ) corresponding to $\beta$ -CD-BIMOTs in presence of $\beta$ -blockers .....	83
Table 4.10: Induced shifts ( $\Delta\delta$ ) corresponding to $\beta$ -blockers in presence of $\beta$ -CD-BIMOTs .....	84
Table 4.11: Chiral separation data for the NSAIDs on $\beta$ -CD-BIMOTs CSP .....	95
Table 4.12: Chemical shifts ( $\delta$ ) corresponding to $\beta$ -CD-BIMOTs in the presence of NSAIDs.....	97
Table 4.13: Induced shifts ( $\Delta\delta$ ) corresponding to NSAIDs in the presence of $\beta$ -CD-BIMOTs .....	98

## LIST OF SYMBOLS AND ABBREVIATIONS

1-BzIm	:	1-Benzylimidazole
1D	:	1 dimension
2D	:	2 dimension
ACN	:	Acetonitrile
C <sub>10</sub> MIm	:	1-decyl-2-methylimidazole
CD	:	Cyclodextrin
CIP	:	Cahn-Ingold-Prelog priority
CoA	:	Coenzyme A
CSP	:	Chiral stationary phases
DCM	:	Dichloromethane
DMF	:	N, N-Dimethylformamide anhydrous
DMSO-D <sub>6</sub>	:	Dimethyl Sulfoxide
EMIMLpro	:	1-ethyl-3-methyl-imidazolium L-proline
FDA	:	Food and Drug Administration
FT-IR	:	Fourier transforms infrared
HILIC	:	Hydrophilic Interaction Liquid Chromatography
HOAc	:	Acetic acid
HPLC	:	High performance liquid chromatography
HAS	:	Human serum albumin
ILs	:	Ionic liquids
LE-CE	:	Ligand-exchange capillary electrophoresis
LE-MEKC	:	Ligand-exchange micellar electrokinetic capillary chromatography
MD	:	Molecular dynamics

MDPCCD	:	Mono-6-(3-methylimidazolium)-6-deoxyper (3,5-dimethylphenylcarbamoyl)- $\beta$ -cyclodextrin chloride
MeOH	:	Methanol
MPCCD	:	Mono-6-(3-methylimidazolium)-6-deoxy-perphenylcarbamoyl- $\beta$ -cyclodextrin chloride
NaOH	:	Sodium hydroxide
NMR	:	Nuclear Magnetic Resonance
NOESY	:	Nuclear Overhauser Effect Spectroscopy
NSAID	:	Non-steroidal anti-inflammatory drugs
ODPCCD	:	Mono-6-(3-octylimidazolium)-6-deoxyper (3,5-dimethylphenylcarbamoyl)- $\beta$ -cyclodextrin chloride
OH	:	Hydroxyl
OPCCD	:	Mono-6-(3-octylimidazolium)-6-deoxyperphenylcarbamoyl- $\beta$ -cyclodextrin chloride
PG	:	Prostaglandin
T3	:	Triiodothyronin
T4	:	Thyroxin
TDI	:	Toluene 2,4-diisocyanate
TEA	:	Triethylamine
TEAA	:	Triethylamine acetate
TGA	:	Thermo gravimetric analyses
Ts <sub>2</sub> O	:	<i>p</i> -Toluene sulfonic anhydride
VAMPCCD-POLY	:	6 <sup>A</sup> -(N,N-allylmethylammonium)-6-deoxyperphenylcarbamoyl- $\beta$ -cyclodextrin chloride
VIMPCCD-POLY	:	6 <sup>A</sup> -(3-vinylimidazolium)-6-deoxyperphenylcarbamate- $\beta$ -cyclodextrin chloride
$\beta$ -CD	:	$\beta$ -Cyclodextrin
$\beta$ -CD-BIMOTs	:	Mono-6-deoxy-6-(3-benzylimidazolium tosylate)- $\beta$ -CD

$\beta$ -CD-DIMOTs : Mono-6-deoxy-6-(3-decyl-2-methylimidazolium tosylate)- $\beta$ -CD

$\beta$ -CDOTs : 6-O-Monotosyl-6-deoxy- $\beta$ -CD



## LIST OF APPENDICES

Appendix A: NMR spectra for $^1\text{H}$ and $^{13}\text{C}$ of $\text{Ts}_2\text{O}$ .....	122
Appendix B: NMR spectrum for $^1\text{H}$ of $\beta\text{-CDOTs}$ .....	123
Appendix C: NMR spectrum for $^{13}\text{C}$ of $\beta\text{-CDOTs}$ .....	124
Appendix D: NMR spectrum for $^{13}\text{C}$ $\beta\text{-CD-BIMOTs}$ .....	125
Appendix E: NMR spectrum for $^1\text{H}$ $\beta\text{-CD-DIMOTs}$ .....	126
Appendix F: NMR spectrum for $^{13}\text{C}$ $\beta\text{-CD-DIMOTs}$ .....	127

## CHAPTER 1: INTRODUCTION

### 1.1 Background of study

In chemistry, chirality refers to a molecule that containing asymmetric center (chiral atom or chiral center) and thus it can occur in a pair of isomer which is two mirror images of each other. This pair of isomer is called enantiomers or optical isomers (Figure 1.1). Chirality is important because the biological properties of enantiomers may differ significantly. Using ethambutol and thalidomide as examples, one enantiomer of ethambutol is used to treat tuberculosis while the other isomer causes blindness. *R*-thalidomide is a sedative and effective against morning sickness, whereas *S*-thalidomide is causing the birth defect (Sekhon, 2013; Blaschke *et al.*, 1978). A guideline was issued in 1992 by US Food and Drug Administration (FDA) that each drug enantiomer must be studied separately for its pharmacological pathways, and only therapeutically active isomer is allowed to be marketed (Stinson, 2000).

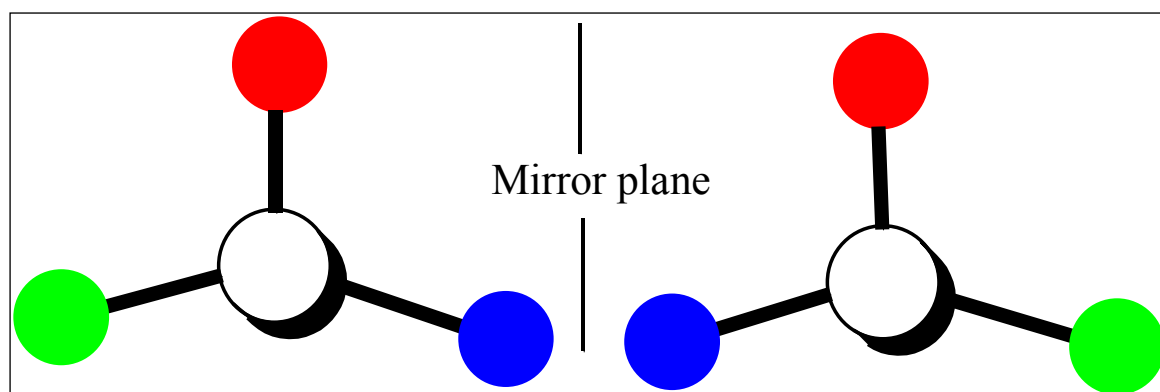


**Figure 1.1:** Chiral molecule

In laboratory, most compounds are produced as racemic mixture that containing equal amount of enantiomers. Ideally, the desired pure enantiomer could be obtained by direct asymmetry synthesis without further treatment (Pazos *et al.*, 2009; Svang-Ariyaskul *et al.*, 2009; Karnik & Kamath, 2008; Kaluzna *et al.*, 2005; Missio & Comasseto, 2003). However, this approach is not always efficient or cost effective. By using chiral catalysts for asymmetric reaction, catalyst efficiency, reaction conditions and kinetics should be considered. Furthermore, there are no general chiral catalysts for all asymmetric reactions. In order to obtain the pure enantiomer, the separation of an enantiomeric mixture or so called enantioseparation is often necessary (Schurig, 2002; Szejtli, 1998). The enantioseparation method includes enzymatic resolution, the diastereomers crystallization or direct chromatographic separation (Lorenz & Seidel-Morgenstern, 2014; Allenmark, 1989).

Recently, high performance liquid chromatography (HPLC) is becoming more widely used instrument for the direct separation of chiral compounds. An advantage of HPLC is that it can be used to separate enantiomers which are non-volatile, polar, or ionic. There are several approaches that have been used to achieve enantioseparation using HPLC. The simplest way to achieve the enantioseparation is to add chiral additives directly into the mobile phase of HPLC (Zhang *et al.*, 2005). This approach affords satisfactory separation with simpler operation. However, the used of chiral additives could not be regenerated after separations. In addition, the preparation of the chiral additives can be laborious and expensive. Consequently, another more practical approach is to use chiral HPLC column that containing chiral stationary phases (CSPs). In this method, the chiral selector is physically adsorbed or covalently bonded to the solid support for the preparation of CSPs. There are several types of CSPs applied in HPLC such as pirkle-type CSPs, polysaccharide-based CSPs, cyclodextrin-based CSPs, macrocyclic antibiotics-based CSPs, chiral crown ether-based CSPs, protein-based

CSPs and molecular imprinting-based CSPs. Herein, this dissertation focuses on cyclodextrin (CD) based CSPs.

CDs are natural cyclic oligosaccharides consisted of six or more glucose units joined through  $\alpha$ -1, 4 linkage (Figure 1.2a). CDs contain hydrophobic center and hydrophilic outer surface (Figure 1.2b). Due to the chair conformation of the glucose units, the CDs are shaped like a truncated cone rather than perfect cylinders as illustrated in Figure 1.2b. CDs are classified by the number of glucose unit.  $\alpha$ -CD,  $\beta$ -CD,  $\gamma$ -CD containing six, seven and eight glucose unit, respectively.  $\beta$ -CD based CSPs are among the most widely used CD in HPLC due its special sizes of its hydrophobic cavity (cavity size:  $\alpha$ -CD <  $\beta$ -CD <  $\gamma$ -CD) (Stalcup *et al.*, 1990; Armstrong *et al.*, 1986; Armstrong *et al.*, 1985; Armstrong & DeMond, 1984).

When  $\beta$ -CD is used as CSP, chiral recognition can be achieved via the interaction between chiral  $\beta$ -CD and enantiomers (Gubitz & Schmid, 2009). The example of interaction is illustrated in Figure 1.3. The  $\beta$ -CD molecule contains 35 chiral centers. Enantiomers can interact via van der Waals dispersion forces with the hydrophobic cavity which is due to methylene hydrogen.  $\beta$ -CD also has a  $C_7$  symmetry axis and 14 hydroxyl groups situated at the exterior of the cavity. Thus, a number of potential interactions might be present between these hydroxyl groups and enantiomers. If the enantiomer has suitable polar substituents group such as hydroxyl, carbonyl, carboxyl, amino and phosphate, one or more favorable hydrogen bonds can be formed with the  $\beta$ -CD CSP. Additionally, repulsive interaction due to steric hindrance around the chiral atoms of CD provides conformational control that can advocate the chiral separation (Hinze *et al.*, 1985; Daffe & Fastrez, 1983). These properties of  $\beta$ -CD has led to its widely used as stationary phase, particularly in HPLC for the separation of chiral compounds (Juvancz & Szejtli, 2002).

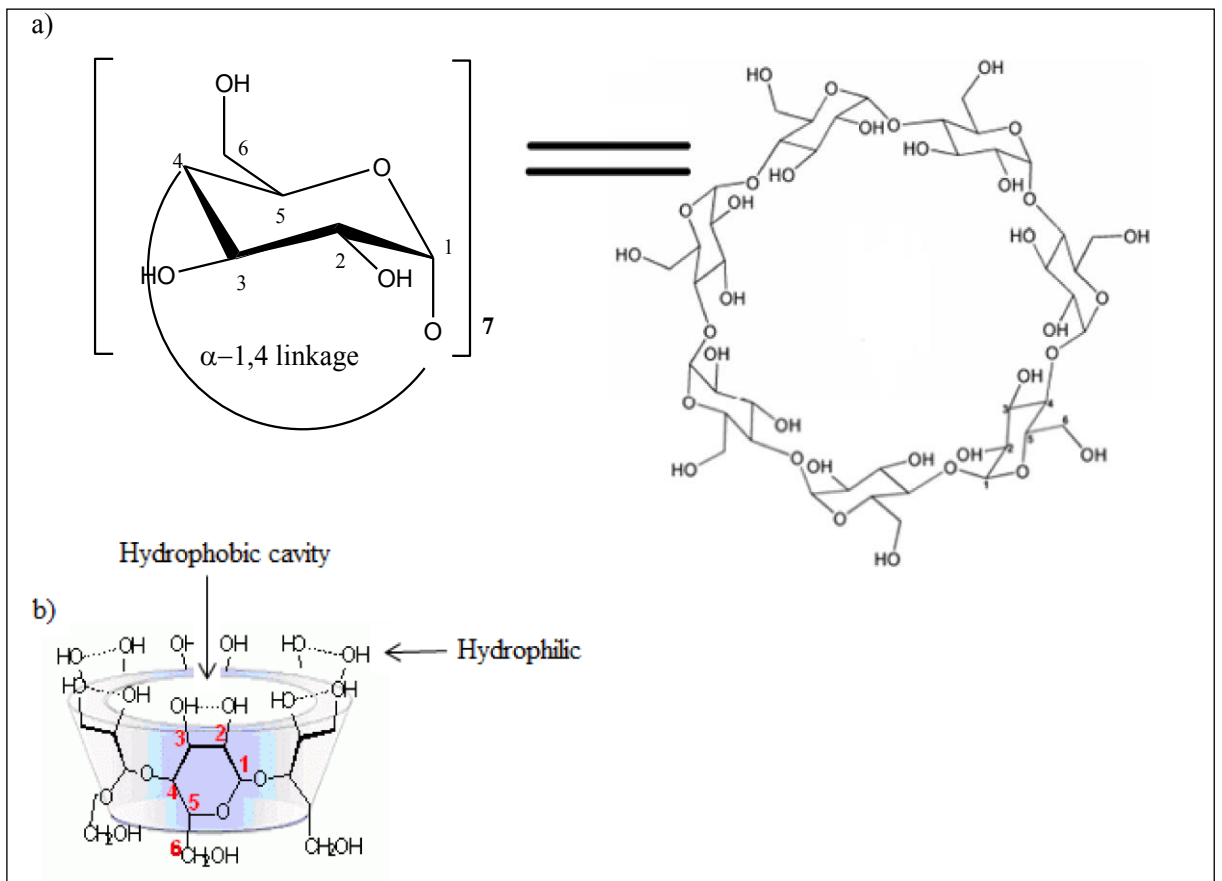


**Figure 1.2 :** a) Chemical structure of CD b) Molecular shape of CD

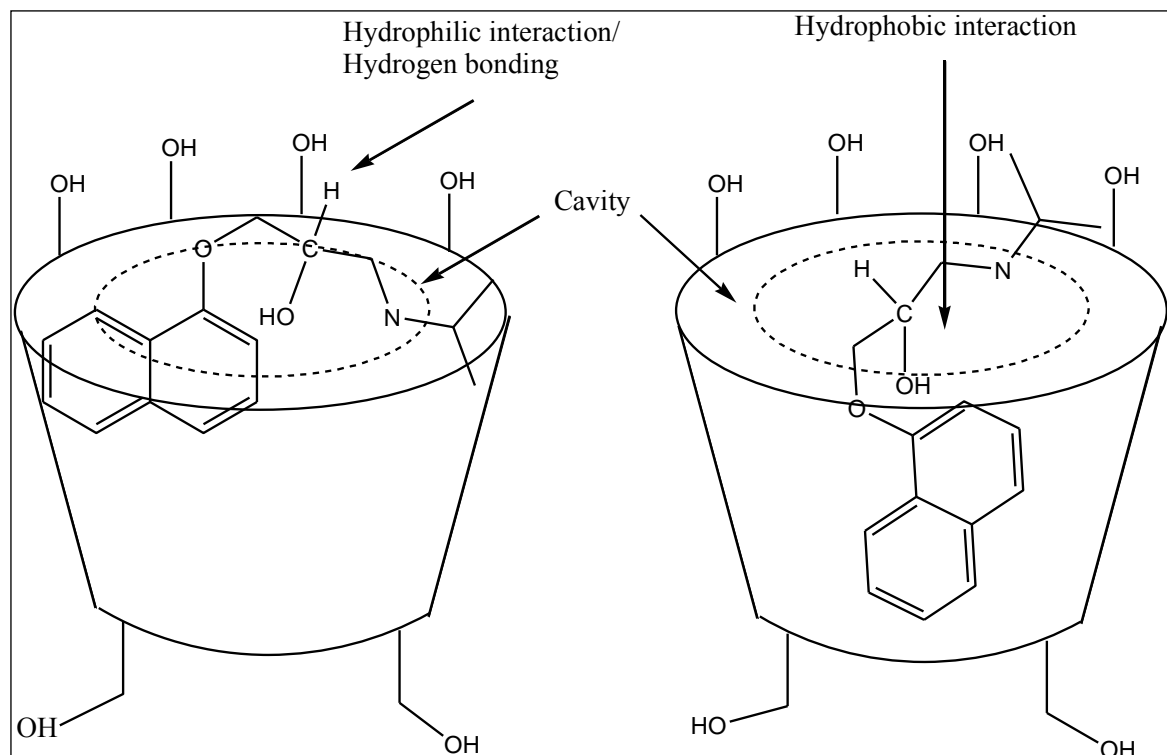


**Figure 1.3:** Illustration of the interaction between  $\beta$ -CD and enantiomer

In most cases, the cylindrical binding cavity of native  $\beta$ -CD is found to be too symmetrical to induce large enantioselectivities (Szejtli, 1994). Due to the native  $\beta$ -CD based CSP is unable to achieve satisfactory separation of enantiomers (Stalcup *et al.*, 1990), additional substituents are often introduced in order to achieve better chiral recognition. Therefore, various efforts have been directed toward developing new  $\beta$ -CD derivative-based CSPs to enhance the chiral separation (Wang *et al.*, 2010; Ciucanu, 1996; Ciucanu & Konig, 1994). Some common substitution groups that have been used to modify  $\beta$ -CD were alkyl, acetyl, benzoyl, hydroxypropyl, phenylcarbamoyl (naphthylethyl carbamoylated or 3,5-dimethylphenyl carbamoylated), *p*-toluoyl, carboxymethyl, pyridylethylene diamine and nitropyridylethylene diamine (Xiao *et al.*, 2009; Han *et al.*, 2005; Tang *et al.*, 2005a; Tang *et al.*, 2005b; Lipka *et al.*, 2003; Armstrong *et al.*, 1998; Chang *et al.*, 1992). Among various substitution groups, the aromatic ring substituted  $\beta$ -CD-based CSPs have been labeled as a multi-modal CSPs due to its ability to interact with enantiomers at various bonding sites. The aromatic

substituted  $\beta$ -CD-based CSPs not only afford hydrogen bonding effects and dipole-dipole interactions, but also hydrophobic and  $\pi$ - $\pi$  interactions during enantioseparation. The different substitution groups on the aromatic ring can further alter the nature of  $\pi$ - $\pi$  interaction to make them more suitable for the separation of various enantiomers. Recently, the 6-hydroxyl group of CD was bonded with ionic liquids (ILs) such as imidazole or pyridine in order to introduce additional  $\pi$ - $\pi$  interaction and ionic interaction (Xiao *et al.*, 2009; Tang *et al.*, 2005a; Tang *et al.*, 2005b).

Ionic liquids (ILs) are a class of salt, in which the ions are poorly coordinated. Consequently, these compounds are in liquid form at the temperature of below 100 °C (Subramaniam *et al.*, 2010; Fontanals *et al.*, 2009). ILs has unique properties, such as non-volatility, non-flammability, low viscosity, and has chemical and electrochemical stability (McEwen *et al.*, 1999), and also can remain in the liquid state over a wide range of temperature. ILs could be hydrophobic and hydrophilic depending on the cationic and anionic characteristic. This dual nature role of ILs indicated their usefulness as stationary phase in chromatography (Anderson & Armstrong, 2003). On the other hand, ILs molecules also consist of high charge region and low charge region (Canongia Lopes & Padua, 2006). This property of ILs contributes to the electrostatic and dispersive interaction which useful for mechanism of enantioseparation (Anderson & Armstrong, 2003).

In this study,  $\beta$ -CD was first functionalized with ILs. The selected ILs were 1-benzylimidazole and 1-decyl-2-methylimidazole with tosylate as anion named  $\beta$ -CD-BIMOTs and  $\beta$ -CD-DIMOTs respectively. Then,  $\beta$ -CD functionalized ILs were then bonded onto modified silica gel to obtain CSPs. The performance of both CSPs for the enantioseparation was evaluated using flavonoids (flavanone, hesperetin, naringenin and eriodictyol),  $\beta$ -blockers (propranolol, metoprolol, pindolol and atenolol) and non-

steroidal anti-inflammatory drugs (NSAIDs) (ibuprofen, fenoprofen, indoprofen and ketoprofen). In addition, the mechanisms of enantioseparation were investigated experimentally through the inclusion complexes formation study. This inclusion complexes study gave an insight into the interaction between CSP and the selected analytes during HPLC separation.

## **1.2 Objectives of the research**

The objectives of this study were:

1. To synthesis  $\beta$ -cyclodextrin functionalized ionic liquid (1-benzylimidazole and 1-decyl-2-methylimidazole) based CSPs.
2. To examine the performance of the synthesized CSPs for the separation of flavonoids,  $\beta$ -blockers and NSAIDs group with optimization of mobile phase.
3. To investigate the mechanism of separation of flavonoids,  $\beta$ -blockers and NSAIDs.

## **1.3 Outline of thesis**

The present thesis is organized into five chapters. Chapter 1 gives a brief introduction on research background, research objectives, and scope of study. A review of related literature is presented in Chapter 2. Chapter 3 presents the experimental procedure for the synthesis of  $\beta$ -CD based-CSP and the preparation of inclusion complex. Chapter 4 discussed the characterization of the synthesized  $\beta$ -CD based-CSP, and the evaluation of synthesized CSPs performance and the mechanism of enantioseparation of flavonoids,  $\beta$ -blockers and NSAIDs. Finally, the overall conclusions, together with recommendations of future works are provided in Chapter 5.



## CHAPTER 2: LITERATURE REVIEW

### 2.1 Chirality

The word “chiral” derives from the greek word “*cheir*” which means hand. In chemistry, chirality was first discovered by Louis Pasteur in 1848. Pasteur conducted an experiment in which he produced crystals salt known as racemic acid. The crystals were of divided into two forms, known as "+" and "-" forms, which is mirror images of one another. Pasteur shone polarized light through each solution of these salts, and found that the two solutions had equal but opposite optical activity. Thus, Pasteur identified, for the first time, the two enantiomers of a chiral substance, and recognized the existence of molecular chirality (Arjomandi-Behzad *et al.*, 2013). Chirality was later defined by Lord Kelvin in 1906 as the non-superimpose ability of a molecule on its mirror image (Evans & Kasprzyk-Hordern, 2014). Chiral molecules are also called optical isomers because the solutions of different enantiomer rotate plane-polarized light in different direction. The optical isomer or enantiomer which rotates plane-polarized light in the clockwise direction is designated as dextrorotatory (*D*) or (+)-enantiomer. In contrast, its antipode (e.g., opposite enantiomer) which rotates plane-polarized light in the counter clockwise direction is designated as levorotatory (*L*) or (–)-enantiomer (Agustian *et al.*, 2016). An equal mixture of each of the enantiomer is known as a racemic mixture (Zhang *et al.*, 2014).

Generally, molecular chirality is mainly due to the stereogenic centers of  $sp^3$  hybridized carbon atoms that bear four different substituents. Apart from carbon, boron, nitrogen, phosphorus and sulphur also have stable chiral centers. The most important nomenclature system for denoting enantiomers is the *R/S* system. Absolute configuration of the isomer are performed by labeling each chiral center *R* or *S* according to a system by which each substituents are assigned a priority, according to

the Cahn-Ingold-Prelog priority rules (CIP), based on atomic number (Zhang *et al.*, 2014).

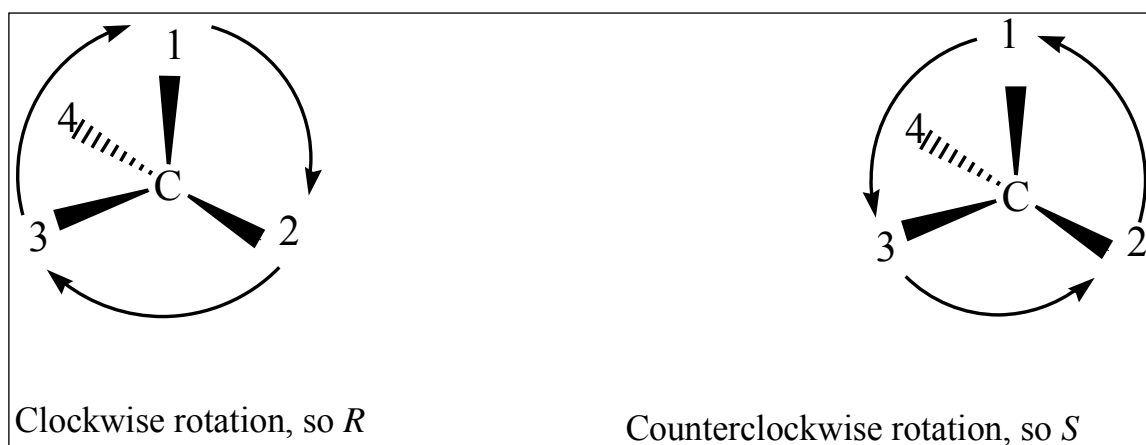


**Figure 2.1:** Examples of how to design configuration using Cahn-Ingold-Prelog priority rules

On a molecular level, chirality represents an intrinsic property of the “building blocks of life”, such as amino acids and sugars, and therefore, of peptides, proteins and polysaccharides (Zhang *et al.*, 2014). For example, amino acids are all presence in *L*-configuration rather than *D*-configuration. Meanwhile, natural sugars are presence in *D*-configuration. Consequently, metabolic and regulatory processes mediated by biological systems are sensitive to stereochemistry and different responses can be often observed when comparing the activities of a pair of enantiomers in biological system. Therefore, stereochemistry is an important consideration when studying xenobiotics, such as drugs, agrochemicals, food additives, flavors or fragrances. Drug action is the result of pharmacological and pharmacokinetic processes, by which it enters, interacts and leaves the body. Thus, straight regulations have been demanded by US Food and Drug Administration (FDA) towards marketing the single-enantiomer of drugs (Zhang *et al.*, 2014). FDA demands full documentation of pharmacological and pharmacokinetic (activity and toxicity) profiles of each individual enantiomer, as well as the racemic

mixture of drugs from the manufacturer. Therefore, it is necessary to have reliable analytical methods for the separation of each individual enantiomer and isolate the pure enantiomers. Chirality is also important in the agrochemical and food industry. In the food industry, a significant number of additives, flavors, fragrances and fumigants, preservatives, growth regulators, pesticides and herbicides are chiral molecules (Sekhon, 2013). Enantiomers in agrochemicals can have diverse effects on plants and insects, and cause negative effects to the environment and human health (Zsila, 2013). For examples, several European governments only allow the application of pesticide mecoprop and dichlorprop in the form of *R*-enantiomers (Author, 2004). All metalaxyl fungicidal activity is resided with the active *R*-enantiomer. The degradation of metalaxyl was shown to be enantioselective with the fungicidally active *R*-enantiomer being degraded faster than the inactive *S*-enantiomer, resulting in residues enriched with *S*-metalaxyl when the racemic compound was applied (Sekhon, 2013). In addition, *R*-enantiomer of fipronil, a phenylpyrazole insecticide, was more toxic to *Ceriodaphnia dubia* (water flea) than the *S*-enantiomer but in other studies the *S*-enantiomer was shown to have significantly more androgen and progesterone activity than the *R*-enantiomer (Negru *et al.*, 2015).

## **2.2 Enantiomeric separation technology**

### **2.2.1 Development of chiral separation technologies**

During the past decades, the requirement of enantiomeric separation emerges rapidly in the area of food safety, environmental analyses, agrochemical and drug industries (Bubalo *et al.*, 2014). In the preparation of single enantiomer, enantioseparation at analytical scale is important for determining enantiomeric purity (Dai *et al.*, 2013). Since enantiomers have identical physical and chemical properties except for the rotation of the plane of polarized light, chiral separation has been

considered as one of the most challenging tasks in chemistry. The enantioseparation can be divided in two classes: non-chromatography and chromatography.

For non-chromatography methods, Louis Pasteur discovered the spontaneous enantiomeric resolution by crystallizing separately each isomers of salt crystal as mentioned previously at section 2.1. After that, a considerable number of optical compounds were resolved mainly by fractional crystallization of the diastereomeric salts (Ismail *et al.*, 2016). Generally, reaction of a racemic acid or base with an optically active base or acid gives a pair of diastereomeric salts. Members of this pair exhibit different physicochemical properties (e.g., solubility, melting point, boiling point, adsorption, phase distribution) and can be separated owing to these differences by crystallization.

For chromatography methods, the earliest report of chiral separation was carried out by Gil-Av and his coworkers in 1966. They found that optically active stationary phase consisting of N-trifluoroacetyl-L-phenylalanine cyclohexyl ester was successfully applied to separate the enantiomers of trifluoroacetyl derivatives of some amino acids (Arjomandi-Behzad *et al.*, 2013). Since then, chromatography approaches are rapidly becoming the most commonly used enantioseparation approach in both analytical and preparative scale.

The publication for HPLC in the area of enantioseparation has been growing rapidly in recent years due to its easy-handling (Lin *et al.*, 2014). Separation of chiral compounds can be carried out using HPLC through direct and indirect methods. Indirect methods are based on the addition of chiral additive to the mobile phase. Direct methods separate the isomers on chiral stationary phases (CSPs). Generally, CSPs is prepared by adsorbing or covalently bonding the chiral selector onto solid support. Chiral selector is the chiral component of the separation system that is able to interact

enantioselectively with the enantiomers to be separated (Saleem *et al.*, 2013). Figure 2.2 illustrates the structures of the various chiral selectors. However, research findings have found that there are no universal CSP or chromatographic conditions which enabling the enantioseparation for all compounds. For most of the CSPs, small changes in the analytes' structures and/or chromatographic conditions would exert a strong impact on the efficiency of enantioseparation. Therefore, many parameters of chromatographic conditions in HPLC need to be optimized to resolve the enantiomers (Ismail *et al.*, 2016).

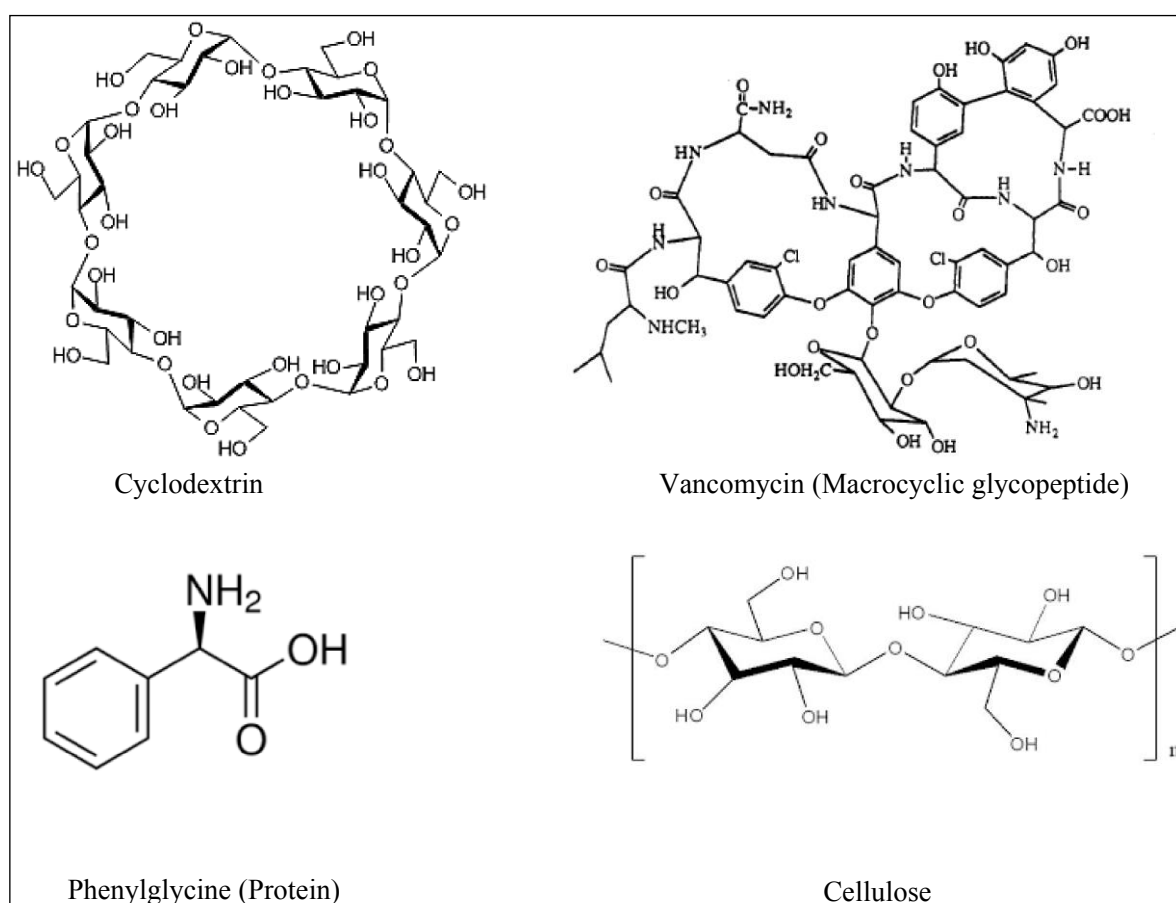


**Figure 2.2:** Common structures of chiral selectors

### 2.2.2 Development of chiral stationary phase

CSPs have been studied extensively since Davankov's review on the application of natural sorbents (proteins, carbohydrates, and optically active quartz) and also artificial dissymmetric sorbents (based on silica gel and activated carbon) as stationary phase for the ion exchange chromatography in the early 1970s (Arjomandi-Behzad *et al.*, 2013). Driven by the growth of asymmetric organic synthesis leading to chiral drugs, food additives, fragrances, agricultural chemicals and many other important chiral intermediates, the development of CSPs has grown rapidly. Various CSPs were developed and applied in various chiral resolution technologies. Firstly, Davankov *et al.* developed metal ion complexes for enantioseparations (Arjomandi-Behzad *et al.*, 2013). After that, by linking small chiral molecules onto stationary phase, brush type chiral stationary phases were prepared (Valente & Soderman, 2014). Pirkle *et al.* developed the first commercial column with brush type chiral stationary phase (Figure 2.3) for HPLC in 1981 (Valente & Soderman, 2014). Most recently, naturally occurred chiral macromolecules such as cyclodextrins, celluloses, macrocyclic glycopeptides and proteins were modified for the application of enantioselective processes (Wang *et al.*, 2011b).

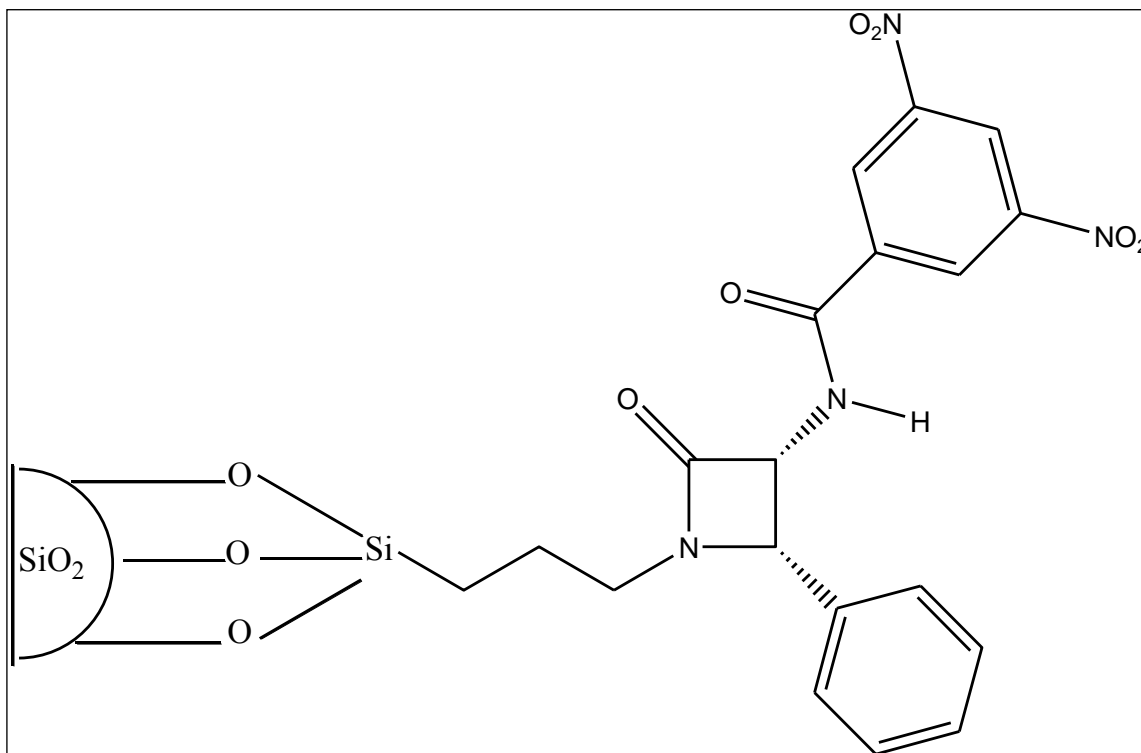


**Figure 2.3:** Molecular structure of the first commercial chiral column (Pirkle 1-J-column)-Brush type CSP

### 2.3 Cyclodextrin and its applications in enantioseparation

Cyclodextrins (CDs) are toroidal structural molecules. The  $\alpha$ -,  $\beta$ -,  $\gamma$ - CD consist of six, seven and eight  $\alpha$ -(1, 4)-linked D-(+)-glucose units, respectively (Figure 2.4). CDs are presence as chiral molecule due to the presence of chiral center of glucose units. The special properties of CDs originate from their unique truncated cone shape structures. The interior cavity of the cone is highly hydrophobic and the exterior is hydrophilic owing to hydroxyl (OH) group (Tang & Tang, 2013). The truncated cone of CDs consists of secondary OH groups at C2 and C3 and primary OH at C6 (Figure 2.4). The hydrogen at C1, C2, and C4 are located at the outside surface of the torus. The OH groups combined with the hydrogen atoms outside surface of CD build up a polar exterior to compatible with polar environments. The cavity interior is lined with the glucose ring oxygen atoms, as well as with the hydrogen atoms at C3 and C5 thus gives

the cavity some Lewis-base character (Zhang *et al.*, 2005). These characteristics endow CDs with a special capacity which can accommodate large variety of organic and inorganic compounds through inclusion complexation (Schurig & Juza, 2014).

As shown in Table 2.1, three types of CDs have different sizes of cavity. A general consideration is that small size hydrophobic organic molecules form the most stable complex with  $\alpha$ -CD but the weakest with  $\gamma$ -CD. Secondly, neutral molecules generally bind more tightly with native CDs than their charged species. Compared with the  $\alpha$ - and  $\gamma$ -CDs,  $\beta$ -CD is more widely investigated in separation science due to their high chemical stability and low cost. In addition,  $\beta$ -CD also has the special size of its hydrophobic cavity (cavity size:  $\alpha$ -CD <  $\beta$ -CD <  $\gamma$ -CD) which affords to form inclusion complexes with numbers of organic and inorganic compounds (Valente & Soderman, 2014).



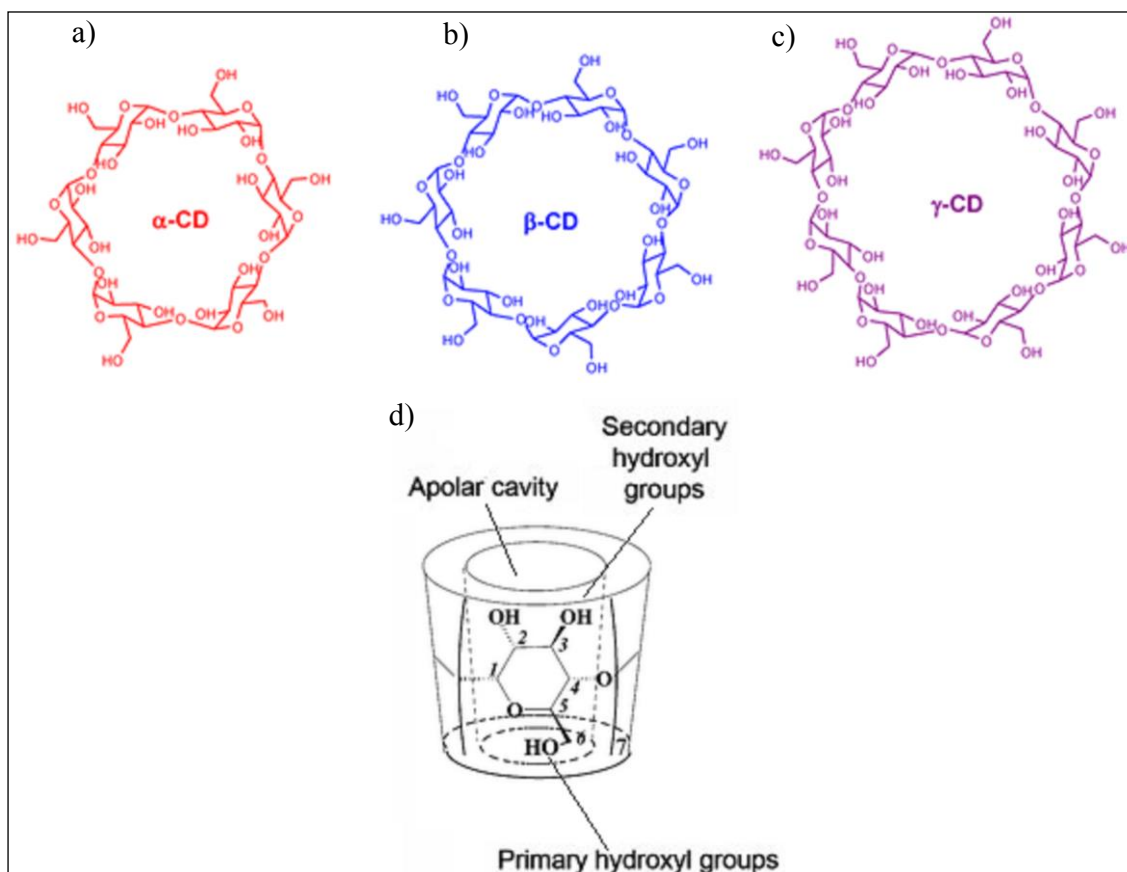


**Figure 2.4:** Illustration of a)  $\alpha$ -CD, b)  $\beta$ -CD, c)  $\gamma$ -CD and d) side view of CD represent the position

**Table 2.1:** Physical and chemical properties of CD molecules (Bender & Komiyama, 2012)

Cyclodextrin	No of glucose units	Molecular mass (g/mol)	Cavity diameter (nm)	No. of stereogenic center	Water solubility (g/100 mL)
$\alpha$	6	972	0.49	30	14.5
$\beta$	7	1135	0.62	35	18.5
$\gamma$	8	1297	0.79	40	23.3

For the mechanism of enantioseparation, according to Armstrong *et al.* (1986), there are a number of requirements for chiral recognition by CD. For example, an inclusion complex must be formed, and there must be relatively tight fit between the complexed moiety and the CD (Wang *et al.*, 2011b). The chiral center and one substituent of the chiral center of an analyte must be near and interacts with the mouth of the CD cavity. The unidirectional OH groups at C2 and C3 located at the mouth of CD cavity are particularly important in chiral recognition in order to satisfy the requirement of the “three-point” model. The “three-point” model was introduced by Pirkle at 1989 to elaborate the enantioseparation on CSPs (Valente & Soderman, 2014). According to Pirkle’s model, chiral recognition requires three interactions with at least one of them has to be stereoselective. Pirkle’s model can be illustrated by a representative enantioseparation in Figure 2.5.

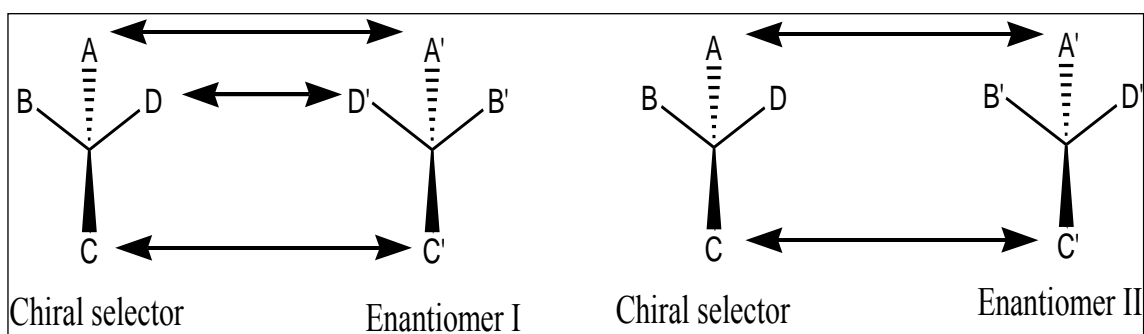


**Figure 2.5:** The “three point” model

As illustrated in Figure 2.5, three interactions of A—A', C—C' and D—D' between the chiral selector and enantiomer (I) whereas, only two interactions A—A' and C—C' are formed between chiral selector and enantiomer (II). The discrimination effect of the two enantiomers falls on the interaction of D—D' and resulting in the different of elution order of the two enantiomers.

The first application of CDs for enantioseparation was reported in 1959 in which CDs were employed as a selective precipitation or crystallization agent for occlusion compounds (Szente & Szemaan, 2013) . From then on, CDs were studied either as mobile phase additives or stationary phases in chromatographic separation (Zhang *et al.*, 2015b). CDs derived stationary phases were originally designed for enantiomeric separation, structural and geometrical isomers separation. Early studies of CDs based stationary phases for enantioseparation focused on the polymerized CDs which were not robust in chiral discrimination and often overloaded with distorted peaks (Bender & Komiyama, 2012). Thereafter, researchers investigated the development of covalently bonded CD based CSPs. In 1984, the first stable CD CSP (Cyclobond I) with high coverage of the CD was developed by Armstrong & DeMond (1984). Subsequently, the CD derived CSPs were also commercialized by their group and hundreds of chiral compounds have been resolved on these CSPs using HPLC (Dai *et al.*, 2013) .

The properties of the CD can be modified by replacing one or more primary or secondary OH groups with different moieties (Ong *et al.*, 2008). For CD, the three OH groups at the glucose units are differ in reactivity due to the different acidities and sterical hindrance. Of the three types of OH groups present in CD rim, the most nucleophilic are primary OH at C6, the least nucleophilic are secondary OH at C2 and the most inaccessible are secondary OH at C3. This forms the basis for a broad spectrum of regioselective alkylations and acylations which have been applied to modify the CDs for CSPs (Schurig & Juza, 2014).

The modified CDs with certain functional moieties can provide potentially additional useful interaction sites and accommodate a variety of spatial requirements to produce highly selective separations for a versatile array of analytes. The substitution groups that have been incorporated onto CDs were alkyl, acetyl, hydroxypropyl,

phenylcarbamoyl groups (naphthylethyl carbamoyl or 3,5-dimethylphenyl carbamoyl) (Figure 2.6) (Dai *et al.*, 2013).

Generally, the OH groups, especially the secondary OH groups allow CD to interact with analytes via hydrogen bonding or dipole-dipole interaction. Although methylation of the OH groups reduced the hydrogen bonding sites but it enlarges the hydrophobic cavity and thus, enhances the steric interactions. These CSPs exhibit good enantioselectivities to some specific solutes such as furan derivatives, tetralins and melatonin ligand. The chiral recognition of these CSPs is implemented through hydrophobic and steric interactions between the analytes and the methoxy groups on the CD rim after inclusion complex formation (Han *et al.*, 2005; Lipka *et al.*, 2003). Since methylation could not introduce diverse effective interaction sites (like hydrogen bonding and  $\pi$ - $\pi$  interaction sites), these CSPs are less effective towards a wide range of chiral compounds.

Hydroxypropylated CD-based CSPs (Figure 2.6 (iii)) have been considered as a very successful CSP. The OH groups of this CD derivative increase the flexibility of hydrogen bonding and provide additional hydrogen bonding sites with analyte. Many chiral compounds that are partially resolved on unmodified CD-based CSP could undergo baseline resolution using similar separation conditions on these hydroxypropylated CSPs. Enhanced enantioseparation of some important drugs like conazoles, methadone, sertraline, Jacobsen's Catalyst and strigol can be achieved using 2-hydroxypropyl- $\beta$ -CD (Liu *et al.*, 2015). However, the preparation process for these CSPs is relatively tedious and costly.

Substituted phenyl or naphthylethyl carbamoylated CD CSPs (Figure 2.6 (iv)) have been labeled as multi-modal CSPs due to their various bonding sites. It is not only afford hydrogen bonding effects and dipole-dipole interactions but also hydrophobic

and  $\pi$ - $\pi$  interactions. In addition, the different substitution groups on the aromatic rings can enhance the nature of  $\pi$ - $\pi$  interaction to make them more suitable for the separation of various racemates. Besides, an ionic interaction site was introduced by incorporating ionic liquid (IL) moiety such as imidazole or pyridine groups into the structure of CD and make them suitable for the enantioseparation of charged and polar analytes (Wang *et al.*, 2012b, 2012a; Wang *et al.*, 2012c; Wang *et al.*, 2008).

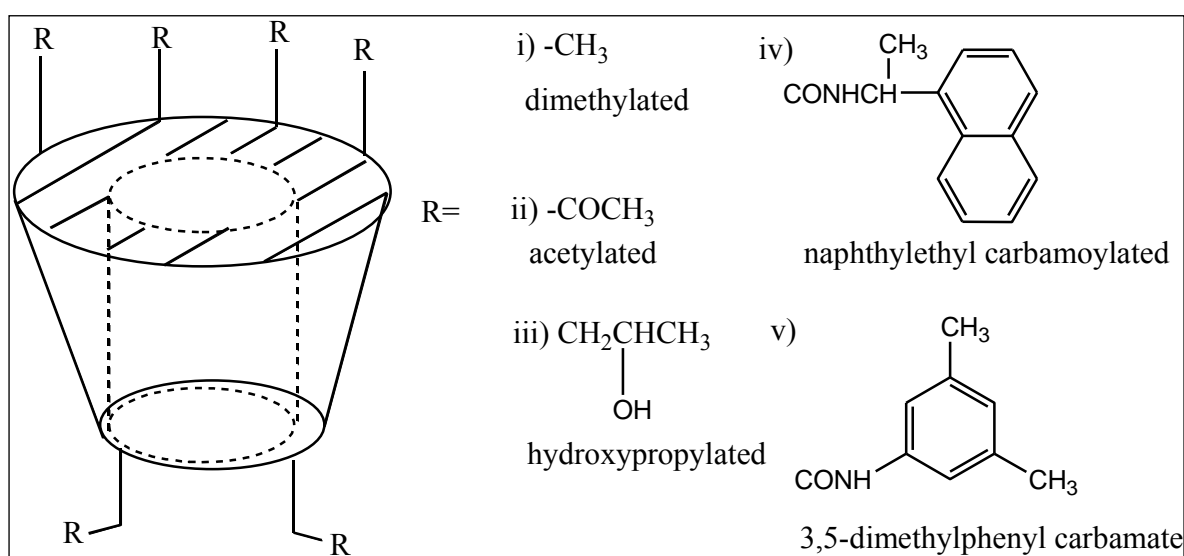


**Figure 2.6:** Common derivatives group of CD

## 2.4 Ionic liquid in enantioseparation

Ionic liquids (ILs) belong to salt-like materials which are liquid below 100 °C and even below room temperature (Yao *et al.*, 2014b). As salts they are by essence made of cation and anion. The term ILs covers inorganic as well as organic molten salts. ILs are usually composed of bulky, nonsymmetrical organic cation such as alkyl-imidazolium, pyridinium or pyrrolidinium, ammonium or phosphonium. Anions could be inorganic, including chloride, tetrafluoroborate, or hexafluorophosphate (Figure 2.7) (Bubalo *et al.*, 2014). The anion is not necessarily to be inorganic; ILs possessing

organic anions such as tosylate and methanesulfonate are also commercially available (Figure 2.7).

Owing to tunable properties which can be selected by choosing appropriate cationic or anionic constituents, they can be applied as mobile phase additive or stationary phase in chromatographic analysis. Compared with ILs used as mobile phase additives in HPLC, the application of ILs as stationary phases is fewer. Armstrong *et al.* (1999) and Anderson and Armstrong (2003) applied the ILs (1-Butyl-3-methylimidazolium hexafluorophosphate [BMIM][PF<sub>6</sub>] and chloride [BMIM][Cl]) as stationary phases for gas chromatography (Zhang *et al.*, 2015a). They claimed that the dual nature of ILs is the main factor that contributed to the effective separation of polar and nonpolar compounds. Afterward, the applications of ILs in chromatography have been increased significantly.

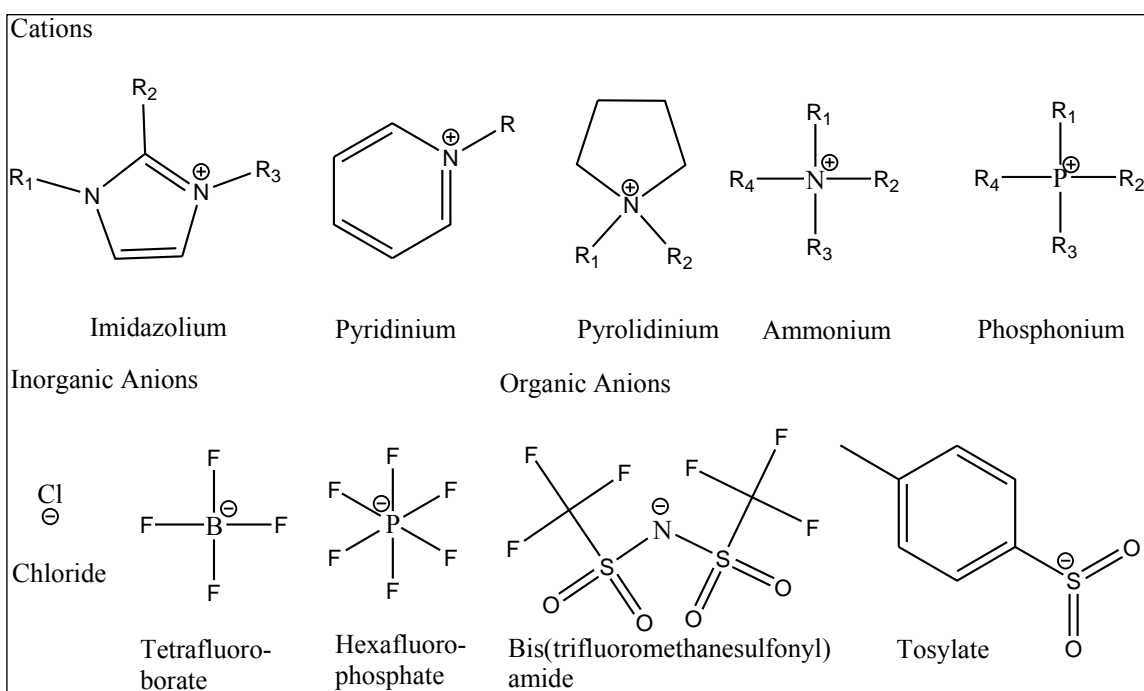


**Figure 2.7:** Common structures of cation and anion of ILs

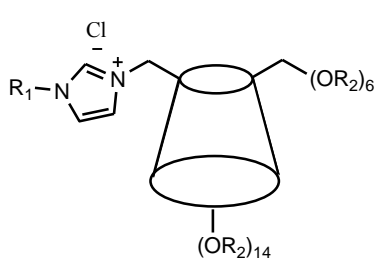
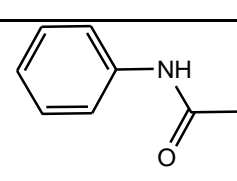
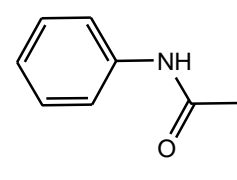
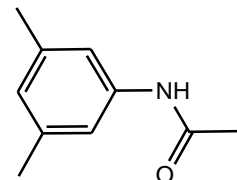
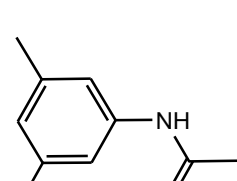
Extending ILs to the realm of chiral separations has been done in two ways: (1) the ILs itself can be chiral or (2) a chiral selector can be dissolved in an achiral ILs. The first approach is not popular since the synthesis of chiral ILs is tedious and required expensive reagents. Thus, the second approach is the most preferred method. Modification of chiral selector with ILs yielded the CSPs with ion exchange properties. Consequently, the chiral separation mechanism involving ILs relies on multi modal interaction such as donor-acceptor interactions (hydrogen bonding,  $\pi$ - $\pi$  interaction) and ionic interactions.

Lately, Wang *et al.* (2008) have physically coated a series of alkyimidazolium modified  $\beta$ -CD onto porous spherical silica gel to develop a series of  $\beta$ -CD-IL based CSPs namely mono-6-(3-methylimidazolium)-6-deoxy-perphenylcarbamoyl- $\beta$ -CD chloride (MPCCD), mono-6-(3-methylimidazolium)-6-deoxyper (3,5-dimethylphenylcarbamoyl)- $\beta$ -CD chloride (MDPCCD), mono-6-(3-octylimidazolium)-6-deoxyperphenylcarbamoyl- $\beta$ -CD chloride (OPCCD) and mono-6-(3-octylimidazolium)-6-deoxyper (3,5-dimethylphenylcarbamoyl)- $\beta$ -CD chloride (ODPCCD) (Table 2.2). These CSPs were used for the chiral separation of 18 aryl alcohols using HPLC and supercritical fluid chromatography (SFC). Among these CSPs, OPCCD, consisting of an *n*-octyl group on the imidazolium moiety and phenylcarbamoyl groups, exhibited the best separation ability for the aryl alcohols. Chromatographic studies revealed that the CSPs consisting of long alkyl group on the imidazolium moiety on the CD ring can provide enhancement of analyte-chiral substrate interactions over CSPs bearing the short alkyl group on the imidazolium moiety on the CD ring.

Later, Wang prepared another two  $\beta$ -CD-ILs CSP by graft polymerization of 6<sup>A</sup>-(3-vinylimidazolium)-6-deoxyperphenylcarbamate- $\beta$ -CD chloride or 6<sup>A</sup>-(N,N-allylmethylammonium)-6-deoxyperphenylcarbamoyl- $\beta$ -CD chloride onto silica to obtain VIMPCCD-POLY and VAMPCCD-POLY CSPs, respectively (Wang *et al.*, 2012b; Wang *et al.*, 2012c). These CSPs were used to separate the enantiomers of 12 pharmaceuticals and six carboxylic acids under reverse phase and normal phase mode. VIMPCCD-POLY exhibited higher enantioselectivities towards most of the selected analytes than VAMPCCD-POLY in normal-phase HPLC (Wang *et al.*, 2012c). The higher enantioselectivity was attributed to the additional  $\pi$ - $\pi$  conjugation and electrostatic interactions formed with the aromatic imidazolium moiety. Meanwhile, the planar imidazolium moiety was found to make the CSP more accessible to the analytes than the tetrahedral ammonium moiety. The chiral separation abilities of VAMPCCD-POLY and VIMPCCDPOLY were also compared in SFC (Wang *et al.*, 2012a). The electrostatic force generated from the cationic imidazolium moiety was found to be important in the retention and chiral separation of 14 racemates, encompassing flavanones, thiazides and amino-acid derivatives.



**Table 2.2:** Chemical structures of the cationic functionalized  $\beta$ -CDs (Wang *et al.*, 2008)

Chemical structure	CSPs	R <sub>1</sub>	R <sub>2</sub>
	MPCCD	-CH <sub>3</sub>	
	OPCCD	-C <sub>8</sub> H <sub>17</sub>	
	MDPCCD	-CH <sub>3</sub>	
	ODPCCD	-C <sub>8</sub> H <sub>17</sub>	

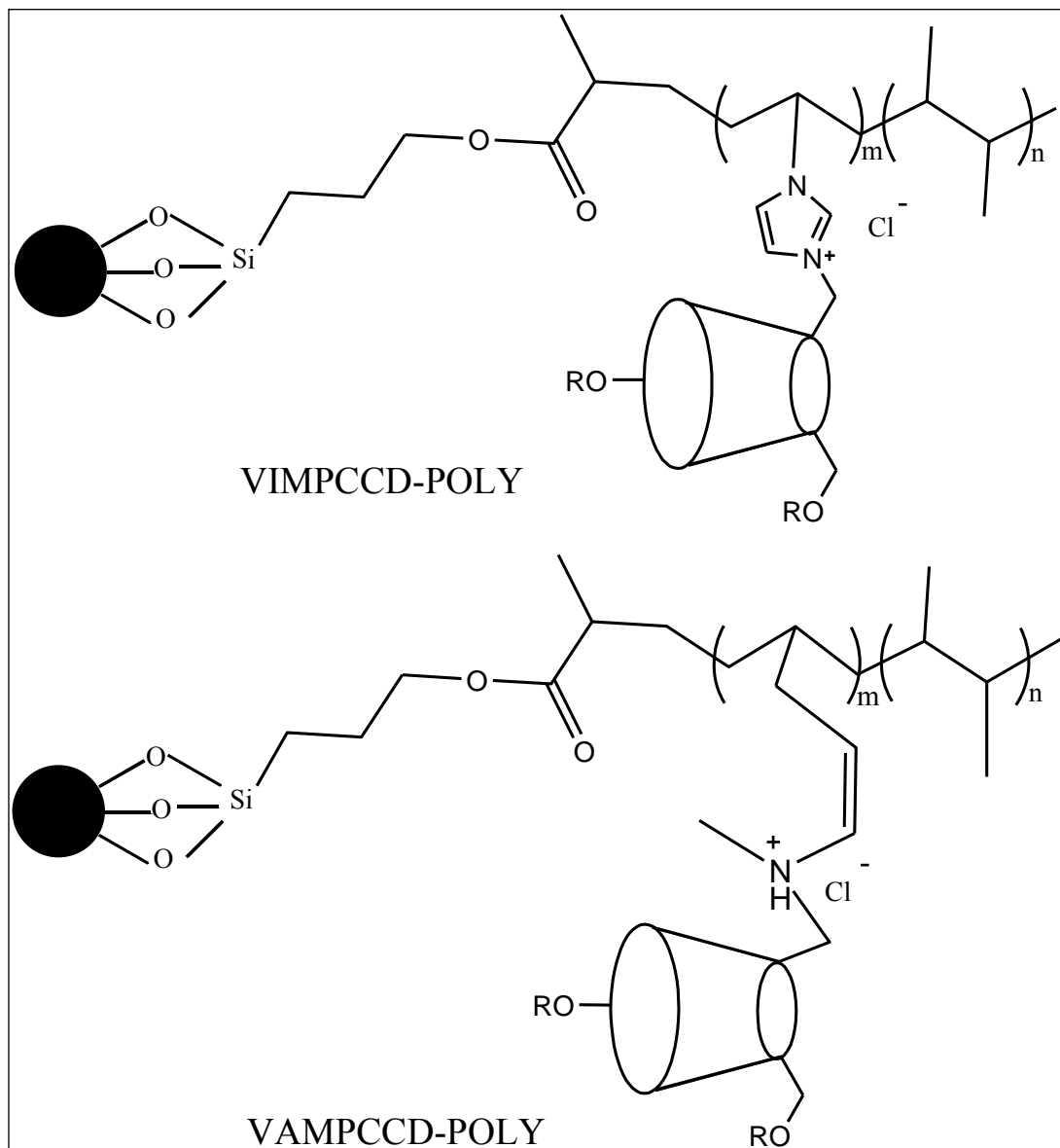


**Figure 2.8:** Structures of VIMPCCD-POLY and VAMPCCD-POLY CSPs (Wang *et al.*, 2012c)

Cooperative effects of  $\beta$ -CD and ILs as CSPs have been studied by Zhou *et al.* (2010) who functionalized  $\beta$ -CDs with ILs. Zhou *et al.* (2010) substituted the 6-tosyl- $\beta$ -CD with 1,2-dimethylimidazole (Figure 2.9 (i)) or 1-amino-1,2,3-triazole (Figure 2.9 (ii)). Then, the functionalized  $\beta$ -CDs-ILs was bonded to silica gel to obtain CSPs. The presence of ILs was found to enhance the enantioselectivity of the synthesized CSPs towards  $\alpha$ -nitro alcohol,  $\alpha$ -hydroxylamine and aromatic alcohol. Zhou *et al.* (2010) stated that the  $\pi$ -conjugation through lone pair electron of  $\text{NH}_2$  in 1-amino-

1,2,3-triazole was electronically stronger than the  $\pi$ -conjugation through the two  $\text{CH}_3$  groups in 1,2-dimethylimidazole. Therefore, 1-amino-1,2,3-triazole cation was much more electronically stabilized. Consequently, 1-amino-1,2,3-triazole cation forming a loose ion pair with its counter ion ( $\text{OTs}^-$  or  $\text{NO}_3^-$ ) and it was more readily participates anionic exchange with analytes. Whereas 1,2-dimethylimidazole cation has a higher affinity to anion and could form a tight ion pair (Zhang & Lv, 2006) with its counter ion ( $\text{OTs}^-$  or  $\text{NO}_3^-$ ). CSPs containing 1-amino-1,2,3-triazole was found to lead to the higher resolution factors for the acidic analytes. Moreover, the CSPs consist of  $\text{NO}_3^-$  anion paired with either 1,2-dimethylimidazole or 1-amino-1,2,3-triazole cation always provided higher resolutions than the CSPs consist of  $\text{OTs}^-$  anion. It was suggested that  $\text{NO}_3^-$  anion has more hydrogen bonding sites and less sterically hindered to easier the interaction with the analytes.

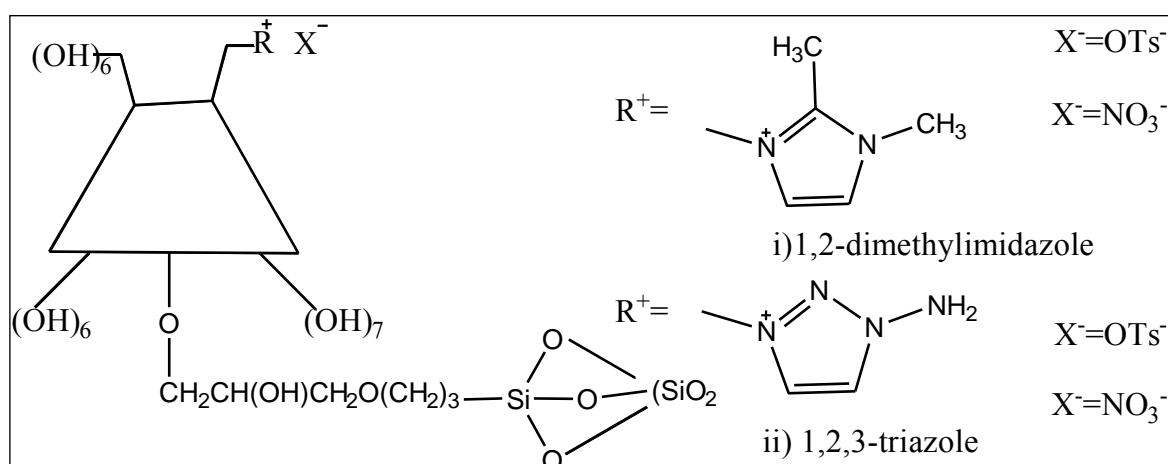


**Figure 2.9:** Structure of functionalized IL-bonded CSPs (Zhou *et al.*, 2010)

Recently, Yao *et al.* (2014b) has applied the simple thiol-ene click chemistry to anchor vinyl imidazolium  $\beta$ -CD onto thiol silica to form a novel  $\beta$ -CD-based CSP with ionic property (Figure 2.10 (i)). This new CSP enhanced chiral separation towards dansyl (Dns) amino acids, carboxylic aryl compounds and flavonoids by HPLC as compared with CSP that prepared through azide/alkynyl click reaction (Yao *et al.*,

2014b) . At the same year, Yao *et al.* (2014a) has synthesized triazole-bridged  $\beta$ -CD CSP. The performance of triazole-bridged  $\beta$ -CD CSP (Figure 2.10 (ii)) was compared with the previous thioether-bridged  $\beta$ -CD CSP (Figure 2.10 (i)) for enantioseparation of 26 isoxazoline derivatives. Most of the selected analytes was well resolved ( $R_s > 1.5$ ) under reversed phase mode for both CSPs.

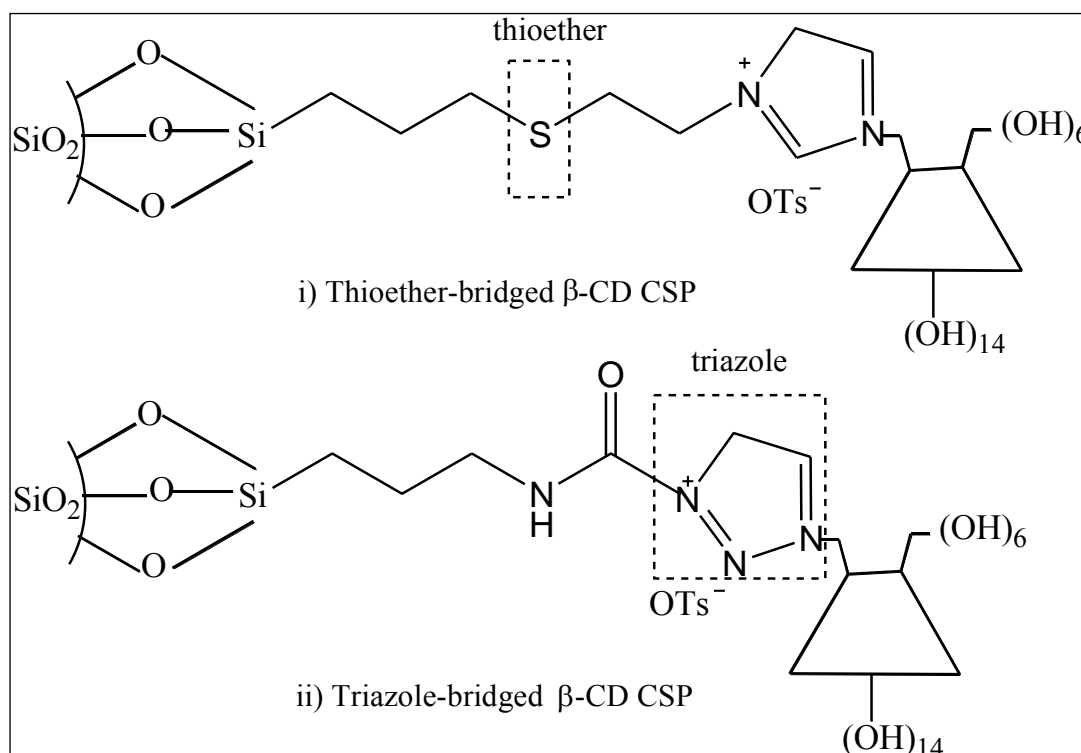


**Figure 2.10:** Structure of Thioether-bridged  $\beta$ -CD and Triazole-bridged  $\beta$ -CD CSPs (Yao *et al.*, 2014a)

Li *et al.* (2014) prepared four  $\beta$ -CD derivatives functionalized by ILs, in which the substituents and  $\beta$ -CD cavity are linked by a  $\text{CH}_2\text{-N}=\text{C}$  bonding and the corresponding CSPs based on silica were namely (a) mono-6-deoxy-6-(p-N,N,N-trimethylaminobenzimide)- $\beta$ -CD nitrate CSP, (b) mono-6-deoxy-6-(p-N,N,N-trimethylamino-benzimide)- $\beta$ -CD tosylate CSP, (c) mono-6-deoxy-6-(p-N-methylimidazolomethyl-benzimide)- $\beta$ -CD nitrate CSP and (d) mono-6-deoxy-6-(p-N-methylimidazolomethylbenzimidide)- $\beta$ -CD tosylate CSP. The excellent enantioseparation

was obtained for most of 1-phenyl-2-nitroethanol derivatives, aromatic alcohol and ferrocene derivatives. The analytes with small volume was found to achieve better enantioseparation on CSP (b) with smaller volume of cation and anion. Thus, they summarized that not only the structure matching between  $\beta$ -CD derivatives and the analytes that contributed to the enantioseparation, but the cooperation of cationic and anionic substituents also play a significant role in the enantioseparation.

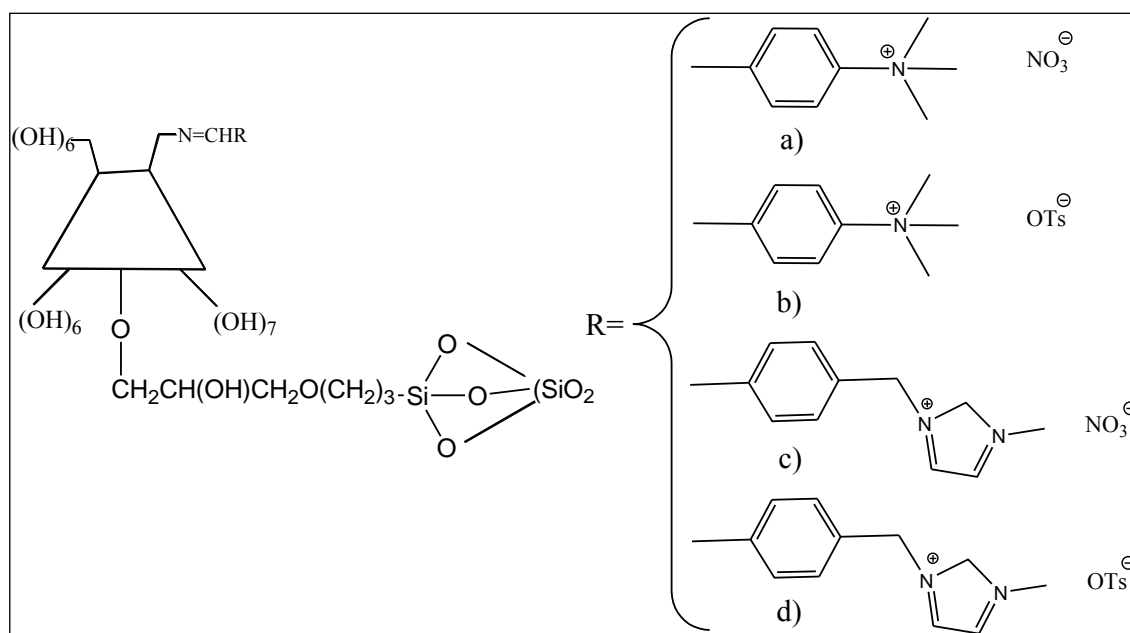


**Figure 2.11:** Structure of  $\beta$ -CD derivatives functionalized by ILs (Li & Zhou, 2014)

Liu *et al.* (2015) successfully fabricated the IL, 1-ethyl-3-methyl-imidazolium L-proline (EMIMLpro) onto the surface of  $\text{Fe}_3\text{O}_4@\text{SiO}_2$  nanospheres. Complete resolution for separation of tryptophan racemate via the  $\text{Fe}_3\text{O}_4@\text{SiO}_2@\text{HMIDI-EMIMLpro}$  nanospheres (Figure 2.12) was eventually achieved by centrifugal chiral chromatography using a spiral tube assembly mounted on a type-J coil planet centrifuge. The newly synthesized nanosphere are promising materials for chiral separation of racemates, because they can provide a huge surface area to accommodate

chiral selectors and are easy to be recycled through an external magnetic field (Liu *et al.*, 2015b) .

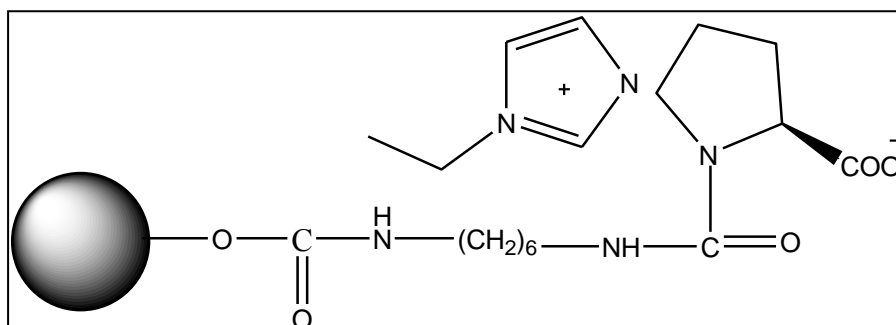


**Figure 2.12:** Structure of  $\text{Fe}_3\text{O}_4@\text{SiO}_2@\text{HMIDI-EMIMLpro}$  (Liu *et al.*, 2015b)

A novel amino acid IL, tetramethylammonium L-hydroxyproline (Figure 2.13), was first applied as a chiral ligand to evaluate its enantioselectivity towards several aromatic amino acids in ligand-exchange capillary electrophoresis (LE-CE) and ligand-exchange micellar electrokinetic capillary chromatography (LE-MEKC) (Liu *et al.*, 2015a). In the LE-CE system, excellent separations were achieved for tryptophan and 3, 4-dihydroxyphenylalanine. Meanwhile, the separations of the enantiomers of tryptophan, phenylalanine, and histidine were all improved in LE-MEKC system.

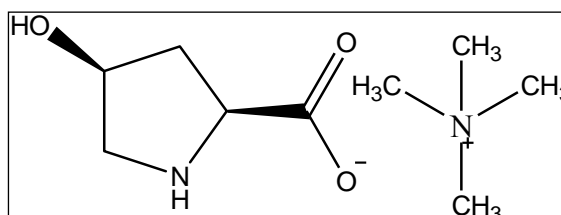


**Figure 2.13:** Structure of tetramethylammonium L-hydroxyproline (Liu *et al.*, 2015a)

The latest research based on CD functionalized IL was reported by Li *et al.* (2016). Li and co-workers were prepared and evaluated four single thioether bridged cationic CD CSPs with different spacer length, selector concentration and rim functionalities (Figure 2.14). The enantioseparation ability of prepared CSPs were evaluated by separating over forty enantiomers including isoxazolines, dansyl amino acids, flavonoids, tröger's base, 4-chromanol, bendroflumethiazide and styrene oxide. Most of the enantiomers were well resolved (Li *et al.*, 2016).

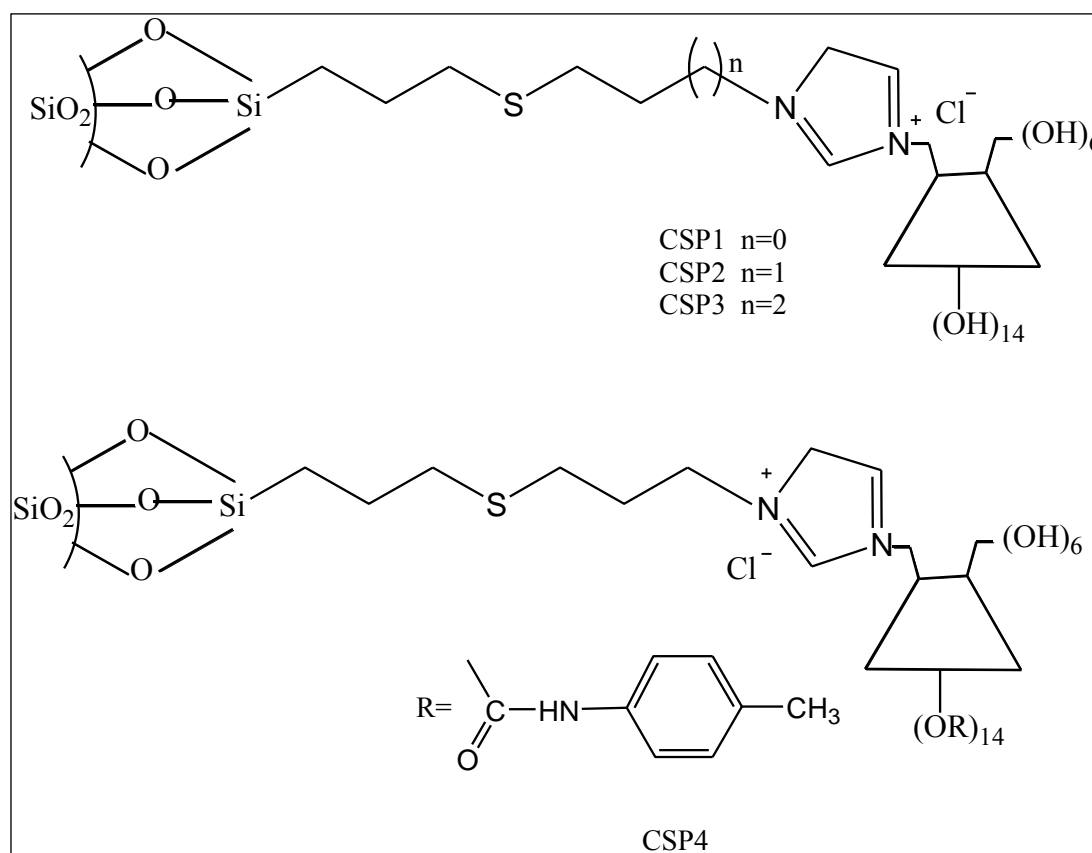


**Figure 2.14:** Novel cationic CSP (Li *et al.*, 2016)

## 2.5 Selected chiral compounds

### 2.5.1 Flavonoids

Flavonoids are a class of secondary metabolites of the plant and fungus. Chemically, they have the general structure of a 15-skeleton (15 carbon atoms), which consists of two phenyl rings (A and B) and a heterocyclic ring (C) (Figure 2.15). Flavonoids are divided into subclasses as showed in Table 2.4.

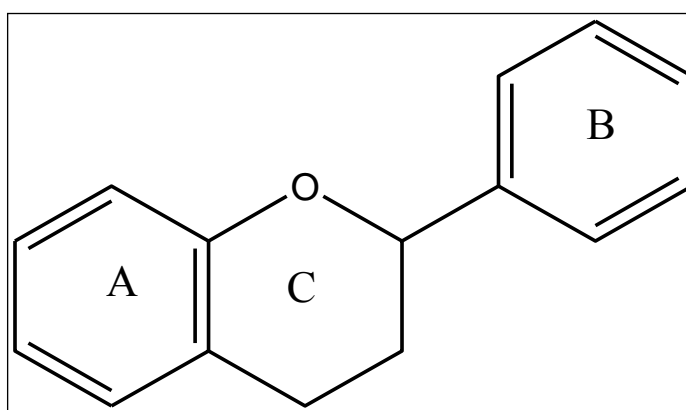


**Figure 2.15:** Basic chemical structure of flavonoid

Within the large family of flavonoids, flavanones possess a unique chiral structural which distinguishes them from all other classes of flavonoids. All the flavanones have a chemical structure based on a  $C_6-C_3-C_6$  (Figure 2.16) configuration consisting of two aromatic rings joined by a three-carbon link (Tiwari *et al.*, 2013). Flavanones present a single stereogenic center at C (2) of chromanone core (Figure 2.16).

Among various flavanones, hesperetin, naringenin and eriodictyol (Figure 2.17) are the most abundant flavonoids that widely distributed in plants. Traditionally, researchers are attracted with the organoleptic properties of flavanones, such as bitterness or taste (Zid *et al.*, 2015). In recent decades, flavanones are increasingly being recognized for their nutritional value since they may reduce the risk of chronic diseases and in general it gives a positive effect to the health (Tucker & Robards, 2008;



Scalbert *et al.*, 2005). Recent studies have shown that naringenin possesses activities such as anti-inflammatory (Park *et al.*, 2012), anticancer (Sabarinathan *et al.*, 2011, 2010), antimetastasis (Qin *et al.*, 2011), normalizing lipids (Cho *et al.*, 2011; Goldwasser *et al.*, 2010), anti-hyperglycemia (Annadurai *et al.*, 2012), and anti-hypercholesterolemia (Chanet *et al.*, 2012). Eriodictyol can provide a cytoprotective effect in ultraviolet (UV)-irradiated keratinocytes (Lee *et al.*, 2011), induce long-term protection in ARPE-19 cells (Johnson *et al.*, 2009), and prevent early retinal and plasma abnormalities in streptozotocin induced diabetic rats (Bucolo *et al.*, 2012).

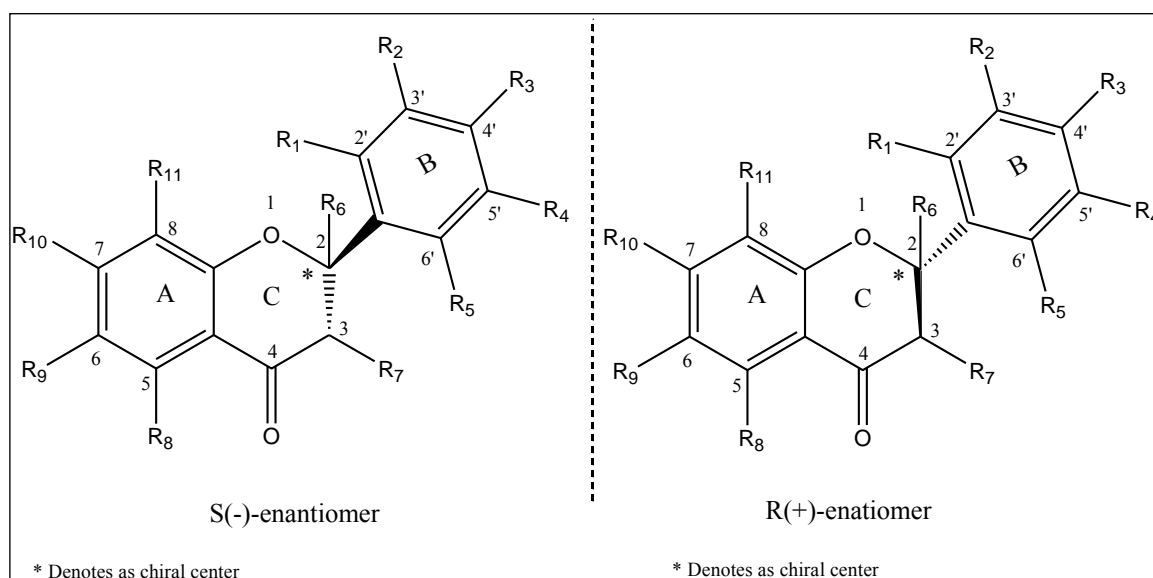


**Figure 2.16:** Spatial dispositions of the enantiomers of chiral flavanones

**Table 2.3:** Common dietary flavonoids

<b>Flavonoids subclass</b>	<b>Dietary flavonoids</b>	<b>Common food source</b>
Antocyanidins	Cyanidin, Delphinidin, Malvidin, Pelargonidin, Peonidin, Petunidin	Red, blue, and purple berries; red and purple grapes; red wine
Flavonols	Monomers (Catechins): Catechin, Epicatechin, Epigallocatechin Epicatechin gallate, Epigallocatechin gallate Dimers and Polymers: Theaflavins, Thearubigins, Proanthocyanidins	Catechins: Teas (particularly green and white), chocolate, grapes, berries, apples Theaflavins, Thearubigins: Teas (particularly black and oolong) Proanthocyanidins: Chocolate, apples, berries, red grapes, red wine
Flavanones	Hesperetin, Naringenin, Eriodictyol	Citrus fruit and juices, e.g., oranges, grapefruit, lemons
Flavonols	Quercetin, Kaempferol, Myricetin, Isorhamnetin	Widely distributed: yellow onions, scallions, kale, broccoli, apples, berries, teas
Flavones	Apigenin, Luteolin	Parsley, thyme, celery, hot peppers
Isoflavones	Daidzein, Genistein, Glycitein	Soybeans, soy foods, legumes

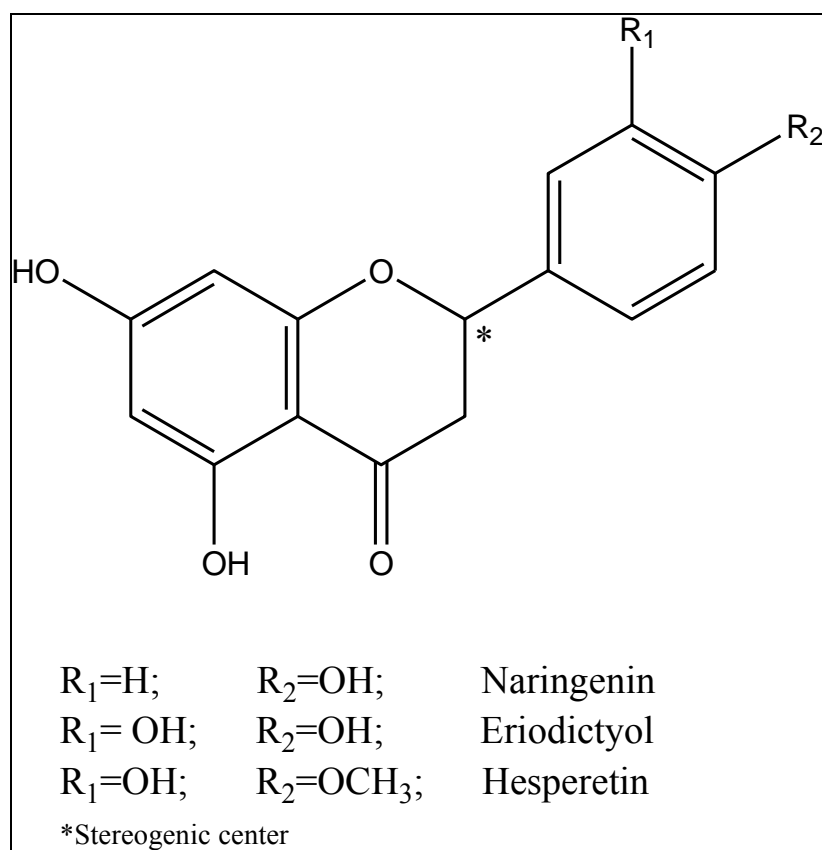


**Figure 2.17:** Chemical structures of some flavanones

The vast majority of flavanones can be purchased from chemical companies, but they are mainly available as racemates. Until now, there are only three stereochemically pure flavanones that are currently marketed internationally. Eriodictyol is marketed as the pure *S*-enantiomer by Fluka (Buchs, Switzerland). Homoeriodictyol is marketed as the pure *S*-enantiomer by Indofine Chemical Company (Hillsborough, NJ), Extrasynthese (Genay, France), and ITI International Inc. (Miami, FL). Finally, taxifolin is marketed as the pure *2R, 3R*-enantiomer by Alexis Biochemicals (San Diego, CA), Fluka (Buchs, Switzerland), and Extrasynthese (Genay, France) (Yanez *et al.*, 2007). As pharmaceutical related compounds, biological activity of flavonoids may result from a single enantiomer. Therefore, there is a need for stereospecific assay methods for the quantitation and effectively isolate the pure flavonoid enantiomers for their pharmacometric study in *in vivo* and *in vitro* models.

### 2.5.2 $\beta$ -blocker drugs

$\beta$ -adrenergic blocking agents ( $\beta$ -blockers) are basic drug that are frequently used for the treatment of angina pectoris and cardiovascular (Saleem *et al.*, 2013).  $\beta$ -blockers competitively binds to  $\beta$ -adrenergic receptor located at the heart and /or nonvascular smooth muscle.  $\beta$ -blockers inhibit the action of adrenergic agents (stimulants) by reducing the force of the heart muscle contraction and tend to reduce the heart rate. These drugs do not seem to produce vasodilation (widening of blood vessels resulting relaxation of the muscular walls of the vessels) as in the case of  $\alpha$ -adrenergic blocking agents (Arjomandi-Behzad *et al.*, 2013). It is well known that  $\beta$ -blockers are chiral and their enantiomers have different potential of pharmacological and therapeutic effects (Evans & Kasprzyk-Hordern, 2014). *L*-isomer of all  $\beta$ -blockers is more potent in blocking  $\beta$ -adrenoceptors than their *D*-isomer. For example, *S*(-)-propranolol is 100 times more active than its *R*(+)-propranolol (Evans & Kasprzyk-Hordern, 2014). It has been demonstrated that *R*-propranolol can inhibit the conversion of thyroxin (T4) to triiodothyronin (T3) (Stoschitzky *et al.*, 1992; Harrower *et al.*, 1977; Wiersinga & Touber, 1977). Therefore, *R*-propranolol might be used as a specific drug without  $\beta$ -blocking effects to reduce plasma concentrations of T3 particularly for patients who suffering from hyperthyroidism. Meanwhile, racemic propranolol cannot be administered because of contraindications for  $\beta$ -blocking drugs (Stoschitzky *et al.*, 1998). Therefore, it is important to isolate and separate the enantiomer of  $\beta$ -blockers for further application in pharmaceutical field since each isomer give the different effect to the body metabolism. Figure 2.18 showed the studied  $\beta$ -blockers.

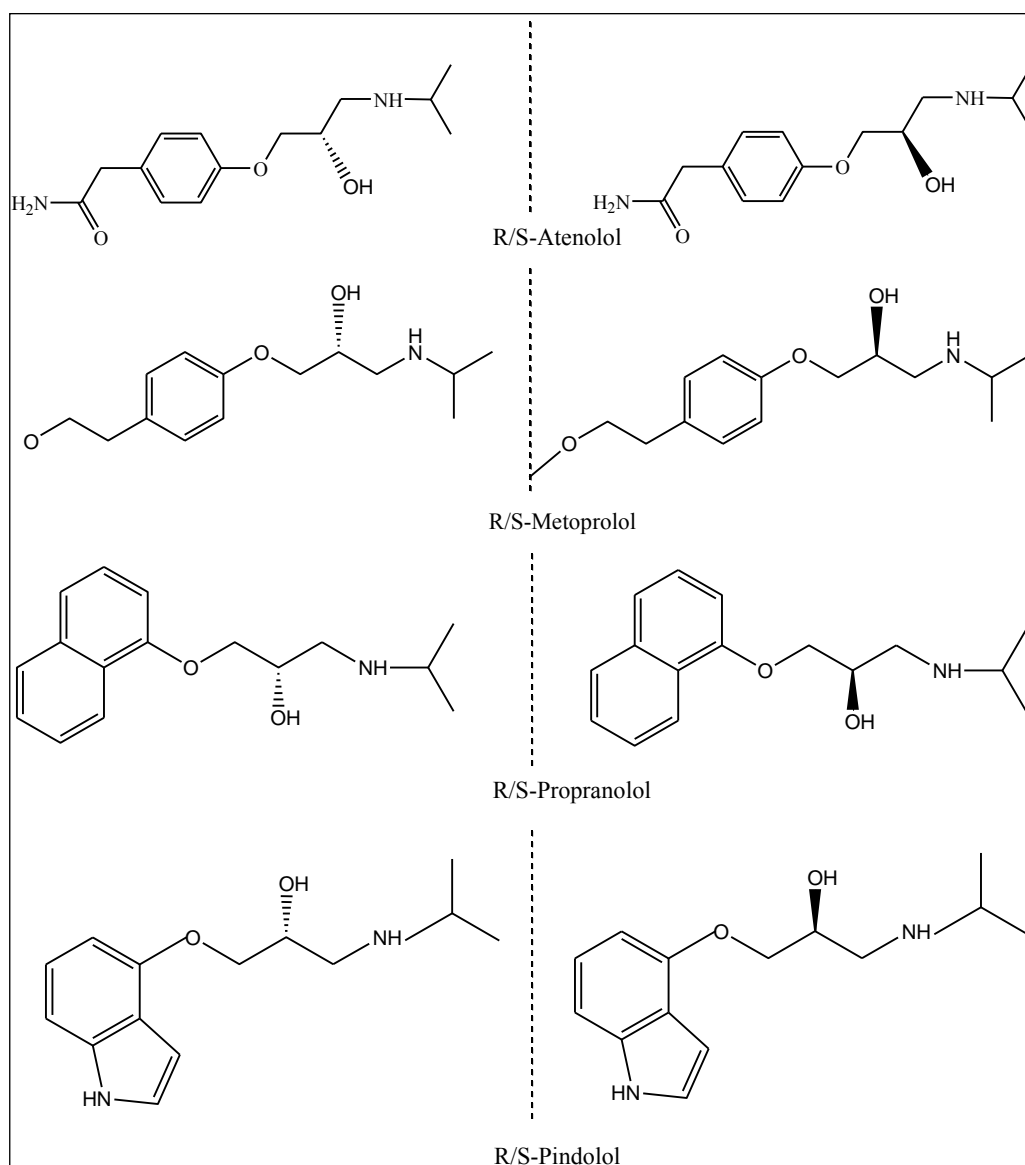


**Figure 2.18:** Structure of studied  $\beta$ -blockers

### 2.5.3 Non-steroidal anti-inflammatory drugs (NSAIDs)

Profen (2-arylpropionic acids) is an important group of non-steroidal anti-inflammatory drugs (NSAIDs), characterized by a chiral carbon atom next to the carboxylic acid group (Figure 2.19). The common anti-inflammatory mechanism of NSAIDs are inhibiting cyclooxygenase or 5-lipoxygenase and reducing the biosynthesis of prostaglandin (PG) to achieve the anti-inflammatory effect. It is well known that the pharmacological activities of the S-enantiomers of many NSAIDs are higher than that

of their *R*-enantiomers (Sekhon, 2013). Some reports have shown that the protein binding to NSAIDs have stereoselectivity (Zsila, 2013).

For ibuprofen, it is mainly the *R*-enantiomer that binds with human serum albumin (HSA) and the two enantiomers can be mutually replaced. In *in vivo* study, the *R*-enantiomer of ibuprofen undergoes unidirectional chiral inversion to *S*-enantiomer. This occurs to the extent about 65%, whereas there is no bio-inversion of *S*- to *R*-ibuprofen (Zhang *et al.*, 2014). Although this would favor the used of racemic ibuprofen, since most of its inactive enantiomer is converted to active form, conversion of racemic ibuprofen to *S*-ibuprofen results in variability of clinical response, including delayed onset of activity, and difficulty in achieving an optimal dose, also the formation of coenzyme A (CoA) thioester during bio-inversion of *R*- to *S*- ibuprofen may resulting toxic effects (e.g. interference of lipid anabolism/catabolism) (Podar *et al.*, 2016). In addition, *R*-ibuprofen bio-activation is susceptible to biological factors and certain drugs.

Most or all cyclooxygenase inhibitory activity of ketoprofen is attributed to the *S*-enantiomer (Podar *et al.*, 2016). The *R*-enantiomer is 30 to 5000 times less potent as an inhibitor of cyclooxygenase-1 and about 100 times less potent as an inhibitor of cyclooxygenase-2 (Negru *et al.*, 2015; Cooper *et al.*, 1998). In addition, *S*-ketoprofen has been found to be significantly less ulcerogenic in the rat gastrointestinal tract as compared to the racemic ketoprofen and that *R*-enantiomer may contribute to the pathogenesis of ulcers (Hardikar, 2008). In order of the different pharmacokinetic effect between each isomer of NSAIDs, they are raising the method to isolate and separate the individual isomers of the NSAIDs via chromatography.

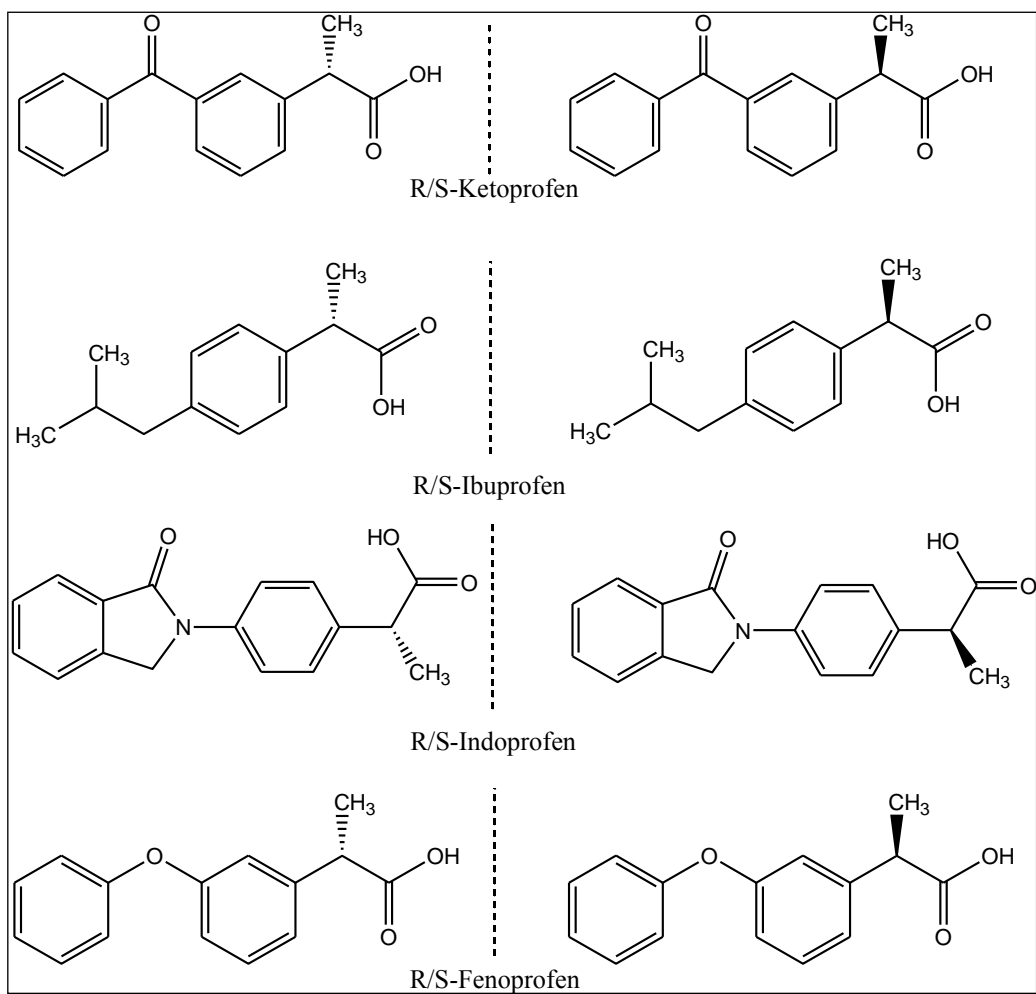


**Figure 2.19:** Structure of selected NSAIDs

## CHAPTER 3: EXPERIMENTAL

### 3.1 Chemicals, materials and reagents

$\beta$ -CD was purchased from Acros (Geel, Belgium) (99%). 1-Benzylimidazole (1-BzIm) (99%), 1-decyl-2-methylimidazole (C<sub>10</sub>MIm) (97%) and toluene 2,4-diisocyanate (TDI) (95%) were supplied by Sigma Aldrich (Buches SG, Switzerland). Anhydrous N,N-Dimethylformamide (DMF), anhydrous hexane, HPLC grade of acetonitrile (ACN) and methanol (MeOH), *p*-toluene sulfonic acid, *p*-toluene sulfonyl chloride and Kromasil spherical silica gel (100Å pore size and 5µm particle size) were purchased from Merck (New York, NY, USA).

Flavonoids group consisting of hesperetin, naringenin and eriodictyol were purchased from Roth Karlsruhe (Germany) while flavanone was purchased from Sigma Aldrich (Buches SG, Switzerland). Propranolol, metoprolol, atenolol and pindolol were supplied from Sigma Aldrich (Buches SG, Switzerland). Ketoprofen, ibuprofen, indoprofen and fenoprofen were also purchased from Sigma Aldrich (Buches SG, Switzerland). The standard stock solutions of flavonoids,  $\beta$ -blockers and NSAIDs (500 mg/L) were prepared separately by dissolving them in MeOH and were stored in a dark amber glass at 4 °C.

### 3.2 Instruments

Fourier transform infrared (FT-IR) spectra were recorded using Perkin–Elmer RX1 FT-IR (Perkin Elmer, Waltham, MA, USA) in the ranged 4000 to 400 (cm<sup>-1</sup>). <sup>1</sup>H NMR, <sup>13</sup>C NMR, and NOESY spectra were recorded on AVN 600 MHz (Bruker, Fällanden, Switzerland), and Dimethyl Sulfoxide (DMSO-D<sub>6</sub>) was used as solvent. Thermogravimetric analyzers were examined using TGA 4000 (Perkin Elmer, USA). A linear heating rate was set at 20 °C per min within the temperature ranged from 50 °C to 900 °C in a stream of nitrogen atmosphere. The chromatographic data was performed



using a HPLC system consisted of a LC-20AT pump, a SPD-M20 detector, a SIL-20AHT auto sampler, a CTO-20AC column oven and CBM-20A communication bus module (Shimadzu, Japan).

### 3.3 Preparation of $\beta$ -CD based chiral stationary phase

The preparation of  $\beta$ -CD based CSP was carried out by synthesizing  $\beta$ -CD functionalized IL and then immobilized onto modified silica.

#### 3.3.1 Synthesis of $\beta$ -CD functionalized ionic liquid

$\beta$ -CD functionalized IL was prepared according to the previous report (Raovv *et al.*, 2013), as shown in Figure 3.1. First, 6-O-monotosyl-6-deoxy- $\beta$ -cyclodextrin ( $\beta$ -CDOTs) was prepared as describe by Zhong (Raovv *et al.*, 2013). Then, the reaction was carried out by reacting  $\beta$ -CDOTs with IL (1-BzIm/C<sub>10</sub>MIm). Since tosylate is a good leaving group, imidazole can easily undergo the nucleophilic substitution.

The reaction was performed as follows: A suspension of  $\beta$ -CD (11.5 g, 10 mmol) and *p*-toluenesulfonic anhydride (Ts<sub>2</sub>O) (4.9 g, 15 mmol) in 250 mL of water was stirred at room temperature for 2 h. Then, solution of NaOH (5.0 g in 50 mL of H<sub>2</sub>O) was added, and after 10 min, the reaction mixture was filtered through the celite on the sintered glass funnel to separate the excess tosylate. The filtrate was brought to pH 8 by the addition of ammonium chloride (13.4 g). The precipitate of  $\beta$ -CDOTs was obtained and cooled at 4 °C overnight. Then, the dried  $\beta$ -CDOTs (1.00 g, 0.78 mmol) and 1-BzIm (10 mole equivalent) were dissolved in anhydrous DMF (40 ml) and the solution was stirred at 90 °C under N<sub>2</sub> atmosphere. After two days, the resultant solution was cooled to room temperature and acetone slowly was added. The mixture was stirred for 30 minutes, and thereafter, filtered and washed the obtained  $\beta$ -CD-

BIMOTs (mono-6-deoxy-6-(3-benzylimidazolium tosylate)- $\beta$ -CD) in excess amount of acetone.

The same procedure was applied for synthesizing  $\beta$ -CD-DIMOTs (mono-6-deoxy-6-(3-decyl-2-methylimidazolium tosylate)- $\beta$ -CD) using  $C_{10}$ MIm replacing 1-BzIm. The characterized results showed that  $\beta$ -CD-BIMOTs and  $\beta$ -CD-DIMOTs had been successfully prepared. From  $^1\text{H}$  NMR result, the chemical shifts of imidazole ring (Hf, He, and Hd) appeared in the downfield region since the protons were deshielded upon functionalization. A new peak was observed in proton (H6\*, 3.9 ppm) and carbon signal (C6\*, 45 ppm), which belonged to the substituted CD. All the protons of  $\beta$ -CD still appeared after the reaction because the functionalization process occurred at only one of the primary hydroxyl groups of  $\beta$ -CD. The obtained product was successfully characterized using several analytical techniques. Both structures of  $\beta$ -CD-BIMOTs and  $\beta$ -CD-DIMOTs are illustrated in Figure 3.2 and Figure 3.3.

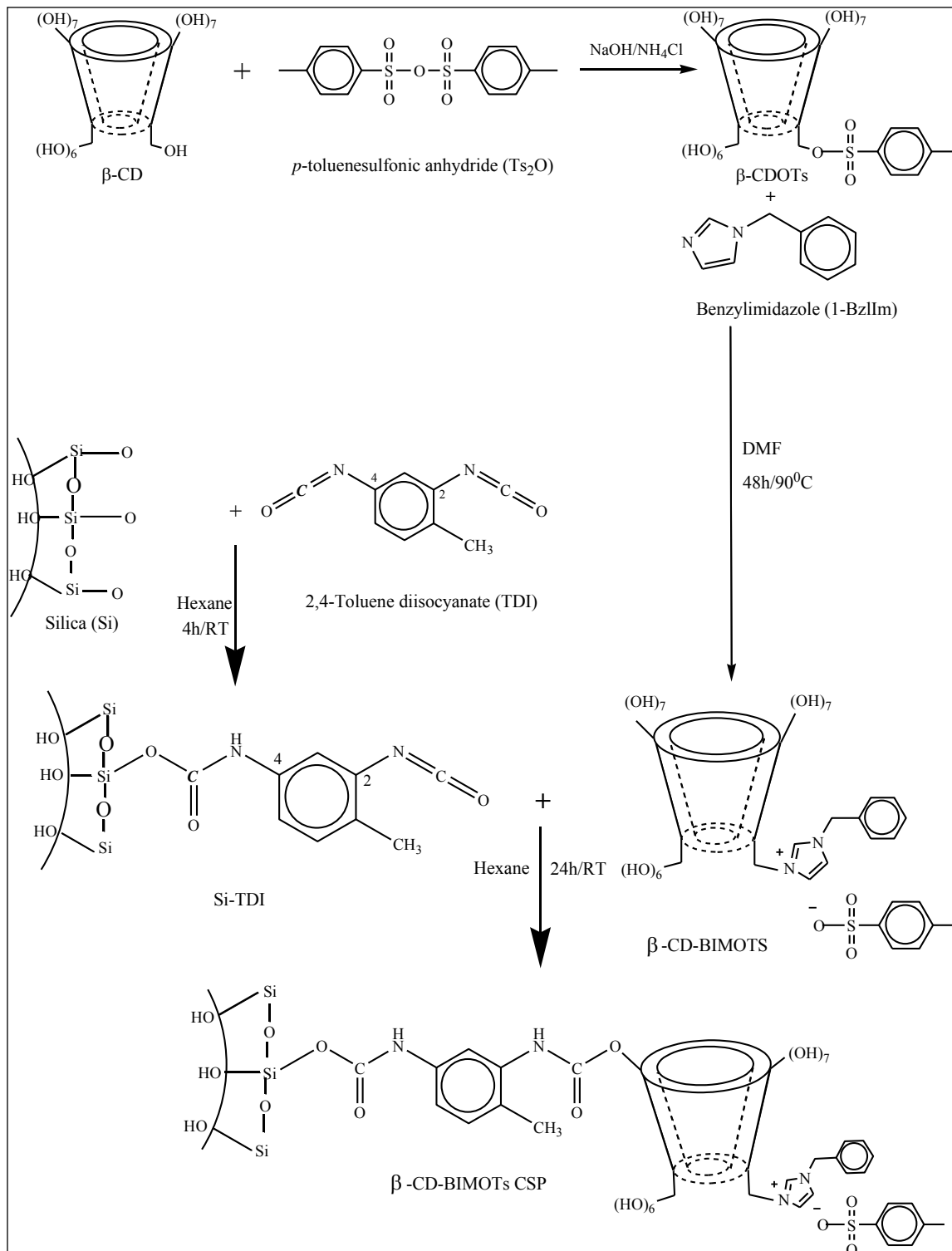


**Figure 3.1:** Synthesis pathways of  $\beta\text{-CD-BIMOTs CSP}$

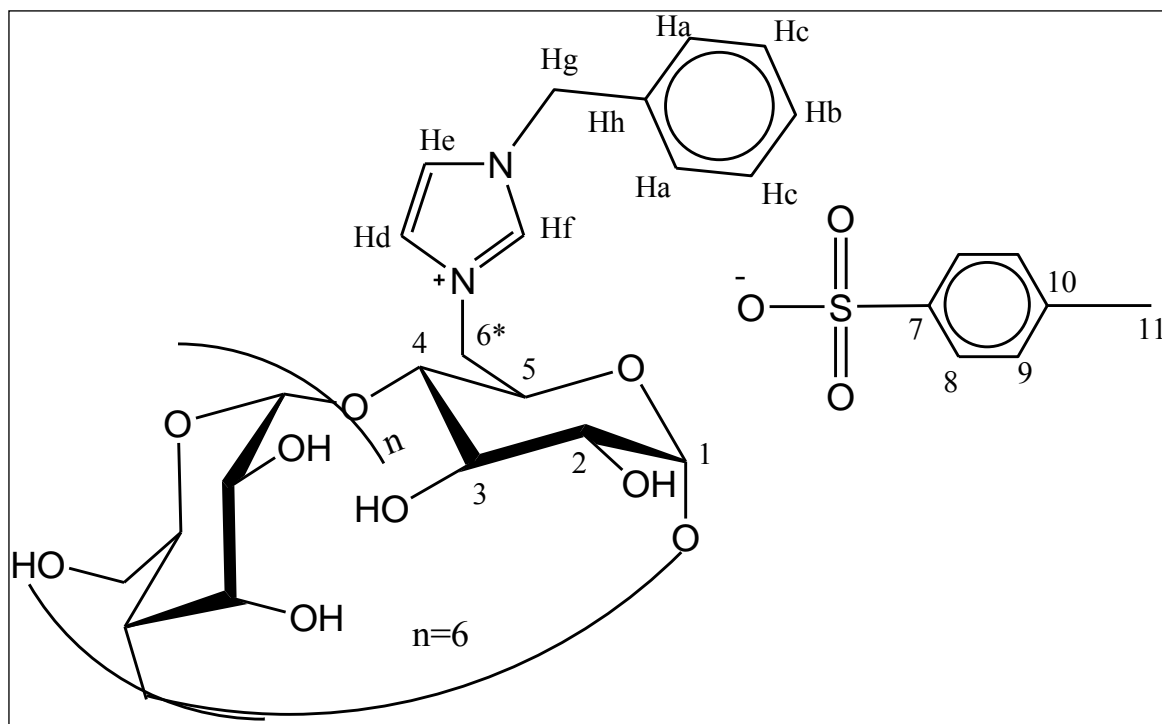


**Figure 3.2:** Structure of  $\beta$ -CD-BIMOTs

FT-IR/KBr,  $\text{cm}^{-1}$ : 3297 (OH), 2922 (C-H), 1652 (C=C), 1152 (C-N).

$^1\text{H}$  NMR, DMSO- $\text{D}_6$ : Hf (9.28, s), He (7.94, s), Hd (8.20, s), Hc (7.75, s), Hb (7.80, t), Ha (7.46, s), Hg (5.18, s), H8 (7.41, d), H9 (7.10, d), OH-2-OH-3 (5.50–5.80, m), H1 (4.83, s), OH-6 (4.47–4.6, m), H6\* (3.91), H3, H5, H6 (3.40–3.63), H2-H4 (3.20–3.40, m), H11 (2.08, s).

$^{13}\text{C}$  NMR, DMSO- $\text{D}_6$ : Ca (127), Cb (123.4), Cc (128.3), Cd (128), Ce (119), Cf (136.9), Cg (52), Ch (137.8), C7 (145.26), C10 (137.3), C9 (128.7), C8 (125.6), C1 (101.8), C4 (81.16), C2 (73.27), C3 (71.6), C5 (69.37), C6 (60.03), C6\* (45.2), C11 (21.97).

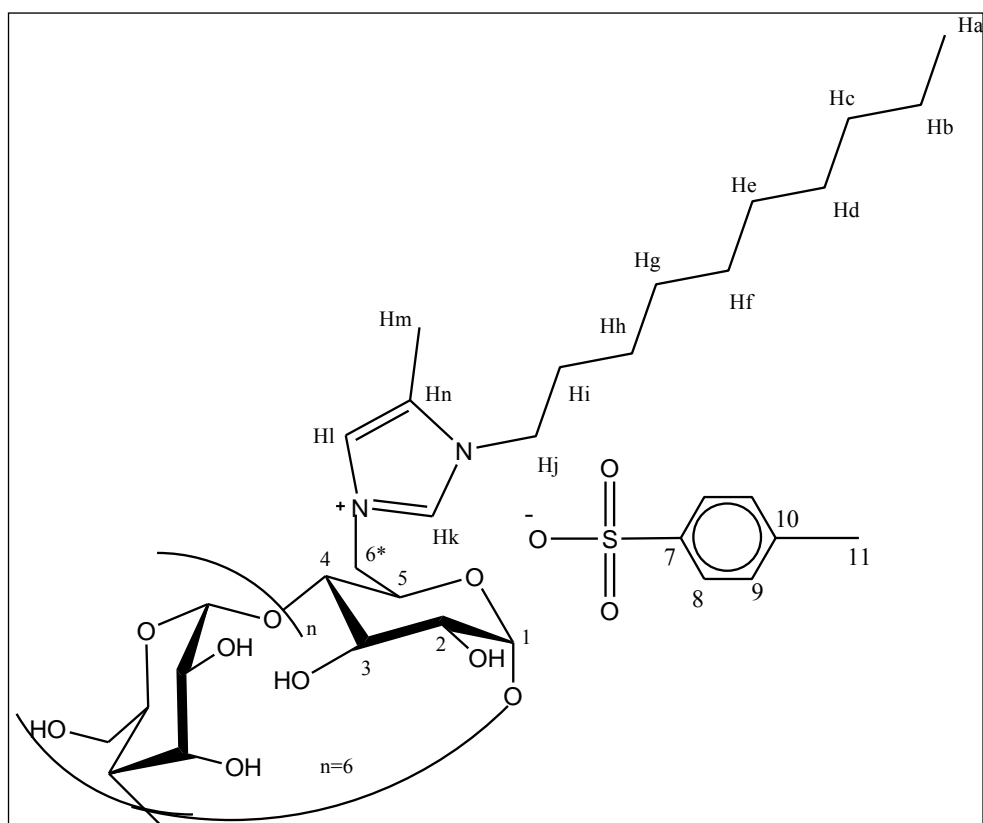


**Figure 3.3:** Structure of  $\beta$ -CD-DIMOTs

FT-IR/KBr,  $\text{cm}^{-1}$ : 3297 (OH), 2922 (C-H), 1652 (C=C), 1152 (C-N).

$^1\text{H}$  NMR, DMSO- $\text{D}_6$ : Hl (7.68, s), Hk (7.61, s), Hb-Hj (1.23-1.28, t), Ha (0.85, t), H8 (7.46, d), H9 (7.11, d), OH-2-OH-3 (5.64-5.79, m), H1 (4.83, s), OH-6 (4.44-4.54, m), H6\* (3.91), H3, H5, H6 (3.54-3.63), H2-H4 (3.20-3.34, m), H11 (2.28, s).

$^{13}\text{C}$  NMR, DMSO- $\text{D}_6$ : Ca (16.13), Cb (19.79), Cc (28.62), Cd (22.48), Cg (22.48), Ch (21.38), Ci (22.48), Cj (31.37), Ck (126.42), Cl (128.75), Cm (14.40), Cn (129.84), C9 (128.17), C8 (126.06), C1 (102.38), C4 (81.95), C2 (73.49), C3 (72.43), C5 (70.74), C6 (60.36), C6\* (45.66).

### **3.3.2 Immobilization of $\beta$ -CD-BIMOTs and $\beta$ -CD-DIMOTs onto modified silica to obtain the CSP**

Silica is the most suitable inert support for stationary phase, because of its high physical strength, chemical inertness and high thermal resistance (Arakaki *et al.*, 2000; Alimarin *et al.*, 1987; Cassim & Yang, 1969). The immobilization was performed by reacting the  $\beta$ -CD functionalized IL with modified silica gel that bearing carbamate group as linker (Zhang *et al.*, 1999).

First, the modified silica gel was prepared as reported (Yatabe & Kageyama, 1994). The modified silica gel was prepared by reacting TDI with silica gel in dry hexane for 4 h at room temperature to obtain Si-TDI. Upon completion of the reaction, the product was filtered, rinsed thoroughly by hexane and dried under reduced pressure. Later, the Si-TDI (5g) was stirred in anhydrous hexane (200 mL) through continuous stream of nitrogen at room temperature. After 30 min, a solution of  $\beta$ -CD functionalized IL ( $\beta$ -CD-BIMOTs or  $\beta$ -CD-DIMOTs) (1.8 g) was added. Stirring was continued for 24 h. The obtained solid was filtered and wash with toluene, acetone and distilled water to afford purified product. The obtained product was characterized using FT-IR and TGA.

### **3.3.3 Synthesis of native $\beta$ -CD (n- $\beta$ -CD) as chiral stationary phase**

Native  $\beta$ -CD as CSP was prepared by immobilizing the native  $\beta$ -CD onto Si-TDI. The procedure was similar as the immobilization of the  $\beta$ -CD-BIMOTs and  $\beta$ -CD-DIMOTs onto Si-TDI.

## **3.4 Column packing approach**

The synthesized CSPs were packed with hexane into empty stainless steel column (250 mm  $\times$  4.6 mm I.D.). First, the CSPs (2.5 g) was suspended in approximately 15 ml of HPLC grade hexane and then poured into the column. The

CSPs were packed into the stainless steel column with a 1525 binary HPLC pump. The flow rate and pressure was first settled at 24.00 ml/min and 4000 Psi respectively. After that, the pressure was increased stepwise until the back pressure reached 8000 Psi. The pressure and flow rate was keep constantly for 1 h.

### 3.5 HPLC analysis instrumentation and conditions

The newly packed column was flushed with 100 % hexane at a flow rate of 0.2 ml/min for 24 hours. The flow rate was increased to 0.5 ml/min for getting the stable baseline. All analyses were performed at ambient temperature at 25 °C. The analytes solutions at concentration of 500 mg/L were prepared by dissolving flavonoids,  $\beta$ -blockers and NSAIDs separately in MeOH. The injection volume was 20  $\mu$ l. The flow rate was fixed at 0.5 ml/min for all analytes. The buffer of triethylamine acetate (TEAA) was prepared by adding triethylamine (TEA) with acetic acid (HOAc) to adjust the pH of mobile phase. The amount of additives in the buffer was recorded as the total weight of both acetic acid and TEA in buffer (w/v).

### 3.6 Calculations of chromatographic data

Figure 3.4 illustrated the example of chromatogram of two well resolved enantiomers and its chromatographic data. Three important terms used in this regard are  $k'$  (capacity factor or retention factor),  $\alpha$  (selectivity factor or separation factor) and  $R_s$  (resolution factor).  $k'$  is a measurement of time of a solute is retained on the column. Retention is a function of affinity of the solute to the stationary phase. The stronger the attraction between the solute and the column material, the longer is the retention.  $\alpha$  is a measurement of selectivity of the column for any pair of solutes.  $R_s$  is a measurement of how well the enantiomers have been separated. The baseline resolution is achieved when  $R_s \geq 1.5$ . The  $k'$ ,  $\alpha$  and  $R_s$  were calculated using the following equations:

$$k' = \frac{(t_R - t_0)}{t_0} \quad 3-2$$

$$\alpha = \frac{k_2'}{k_1'} = \frac{(t_{R2} - t_0)}{(t_{R1} - t_0)} \quad 3-3$$

$$R_s = \frac{2 \times (t_{R2} - t_{R1})}{(W_1 + W_2)} \quad 3-4$$

The dead time ( $t_0$ ) is the time for the mobile phase to pass through the column, which relates to the efficiency of the column. The retention time ( $t_R$ ) is the retention time corresponding to each isomer in the chromatographic separation.  $t_{R2}$  and  $t_{R1}$  represents the retention times of the second and first isomers respectively, and  $W_1$  and  $W_2$  are the corresponding base peak width.

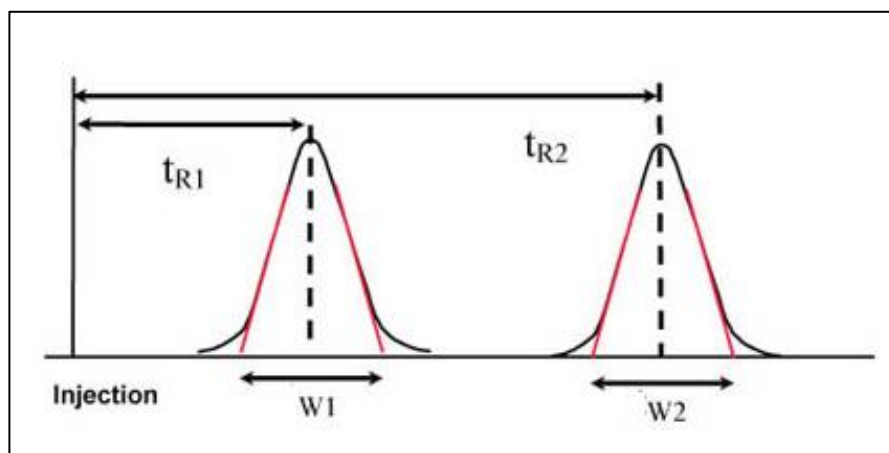


**Figure 3.4:** Two enantiomerically related peaks and the measurements required to calculate  $k_1'$ ,  $k_2'$ ,  $\alpha$  and  $R_s$



### 3.7 Preparation of inclusion complex

#### 3.7.1 Preparation of kneaded complex

The inclusion complex of  $\beta$ -CD-BIMOTs with analytes was prepared using conventional kneading method (Cwiertnia *et al.*, 1999). Equimolar amount of  $\beta$ -CD-BIMOTs and analytes were kneaded with mortar and pestle in minimal ethanol to form homogenous paste (Figure 3.5). The complex was kneaded for 30 min and dried to constant mass. After drying, a white powder was obtained. The final product was characterized in the liquid state by one dimensional (1D)  $^1\text{H}$  NMR and two dimensional (2D)  $^1\text{H}$  NMR NOESY. For  $^1\text{H}$  NMR and NOESY, the spectra were obtained from the samples that prepared using  $\beta$ -CD-BIMOTs and analytes with the ratio of 1:1. The samples were dissolved in  $\text{DMSO-d}_6$ . Seven hundred microliter of solutions were introduced into standard 5 mm NMR tubes and the spectra were recorded at 300.15 K. For NOESY experiments, the spectra were recorded with a mixing time of 700 ms with 256 increments and 40 scans.

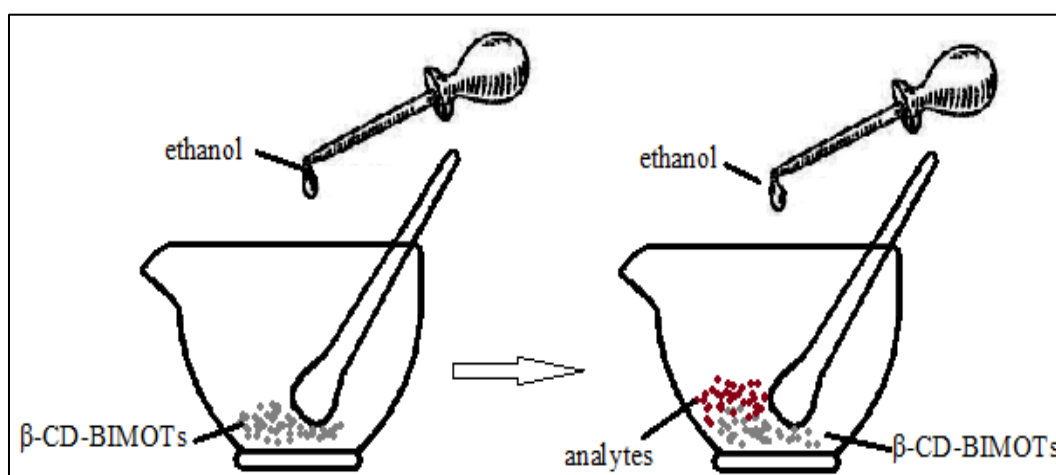


**Figure 3.5:** Schematic of kneading method

### 3.7.2 Determination of formation constant

UV-Visible spectrophotometer with 1 cm quartz cuvette was used for this experiment. The absorption spectrum of  $\beta$ -CD-BIMOTs and analytes complex was recorded against blank reagent. Blank reagent was prepared with the same concentration without the addition of analytes. In addition, absorption spectra of each analyte and  $\beta$ -CD functionalized ionic liquid were also recorded. For the formation constant curve, the concentration of analytes was held constant at 0.01 mM, meanwhile the concentration of  $\beta$ -CD functionalized ionic liquid was varied (0.001, 0.002, 0.003 and 0.005 M). The formation constant and stoichiometry of the  $\beta$ -CD functionalized ionic liquid inclusion complex was obtained from the Benesi-Hildebrand equation (Equation 3-5) (Qian *et al.*, 2008).

$$\frac{1}{(A-A_0)} = \left[ \frac{1}{(A'-A_0)} \right] + \left[ \frac{1}{K(A'-A_0)[\beta\text{-CD-BIMOTs}]} \right] \quad 3-5$$

In the above equations,  $A_0$  is the intensity of absorption of the guest without  $\beta$ -CD functionalized ionic liquid,  $A$  is the absorbance with a particular concentration of  $\beta$ -CD functionalized ionic liquid,  $A'$  is the absorbance at the maximum concentration of  $\beta$ -CD functionalized ionic liquid used and  $K$  is the formation constant. Linearity is obtained in the plot of  $1/(A - A_0)$  versus  $1/K(A' - A_0)[\beta - \text{CD} - \text{BIMOTS}]$  for 1:1 complexes (Equation 3-5). The formation constant ( $K$ ) was calculated from the slope of Benesi-Hildebrand plot using the Equation 3-6.

$$K = \left[ \frac{1}{\text{slope } (A'-A_0)} \right] \quad 3-6$$

## CHAPTER 4: RESULTS AND DISCUSSION

### 4.1 Characterization of $\beta$ -CD Based Chiral Stationary Phase

#### 4.1.1 FT-IR analysis

The spectra of  $\beta$ -CD,  $\beta$ -CD-BIMOTs and  $\beta$ -CD-DIMOTs are shown in Figure 4.1. Meanwhile, the main frequencies of  $\beta$ -CD,  $\beta$ -CD-BIMOTs and  $\beta$ -CD-DIMOTs are shown in Table 4.1. The broad O-H stretching band around 3200-3300  $\text{cm}^{-1}$  (Figure 4.1) for  $\beta$ -CD,  $\beta$ -CD-BIMOTs and  $\beta$ -CD-DIMOTs are corresponded to the multiple -OH functional groups in  $\beta$ -CD molecules. O-H stretching, C-H stretching, and C-N bending (refer Table 4.1 for assignment) were observed as the most obvious band in the IR spectra of both  $\beta$ -CD-BIMOTs and  $\beta$ -CD-DIMOTs. The intense band at 1657  $\text{cm}^{-1}$  referred to C=C aromatic ring of 1-BzIm moieties was observed at  $\beta$ -CD-BIMOTs spectra (Figure 4.1 (b)). The weak bands known as overtones at 1665-2000  $\text{cm}^{-1}$  were correlated to aromatic ring of benzene was also observed at  $\beta$ -CD-BIMOTs spectra. Moreover, the band of C-H of  $\beta$ -CD-BIMOTs and  $\beta$ -CD-DIMOTs spectra (Figure 4.1(b and c)) that occurred at 2925  $\text{cm}^{-1}$  are more intense than the band of C-H of  $\beta$ -CD spectra (Figure 4.1(a)). These prove that  $\beta$ -CD was successful functionalized with 1-BzIm or C<sub>10</sub>MIm and  $\beta$ -CD-BIMOTs and  $\beta$ -CD-DIMOTs were obtained.

The spectra and assignment peak of Si-TDI (modified silica), native  $\beta$ -CD CSP,  $\beta$ -CD-BIMOTs CSP and  $\beta$ -CD-DIMOTs CSP are shown in Figure 4.2 and Table 4.2, respectively. Spectra of Si-TDI (a) shows the presence of the isocyanate (O=C=N-) group at 2280  $\text{cm}^{-1}$ . TDI has two isocyanate groups with different activities towards OH groups that located at the para-position and ortho-position, respectively. The two isocyanate groups in TDI react at different rates with the para-position (approximately four times more reactive than the ortho-position) (Arnold *et al.*, 1957; Simons & Arnold, 1956). Hence, the isocyanate functional groups in TDI (para position) reacted

with OH groups on the surface of silica and formed Si-TDI. The remaining isocyanate group at ortho-position would react with secondary OH group of  $\beta$ -CD or  $\beta$ -CD functionalized ionic liquid. Therefore, the isocyanate peak was disappeared after immobilization of native  $\beta$ -CD,  $\beta$ -CD-BIMOTs and  $\beta$ -CD-DIMOTs onto Si-TDI to obtain CSP as shown in Figure 4.2 (b), (c) and (d).

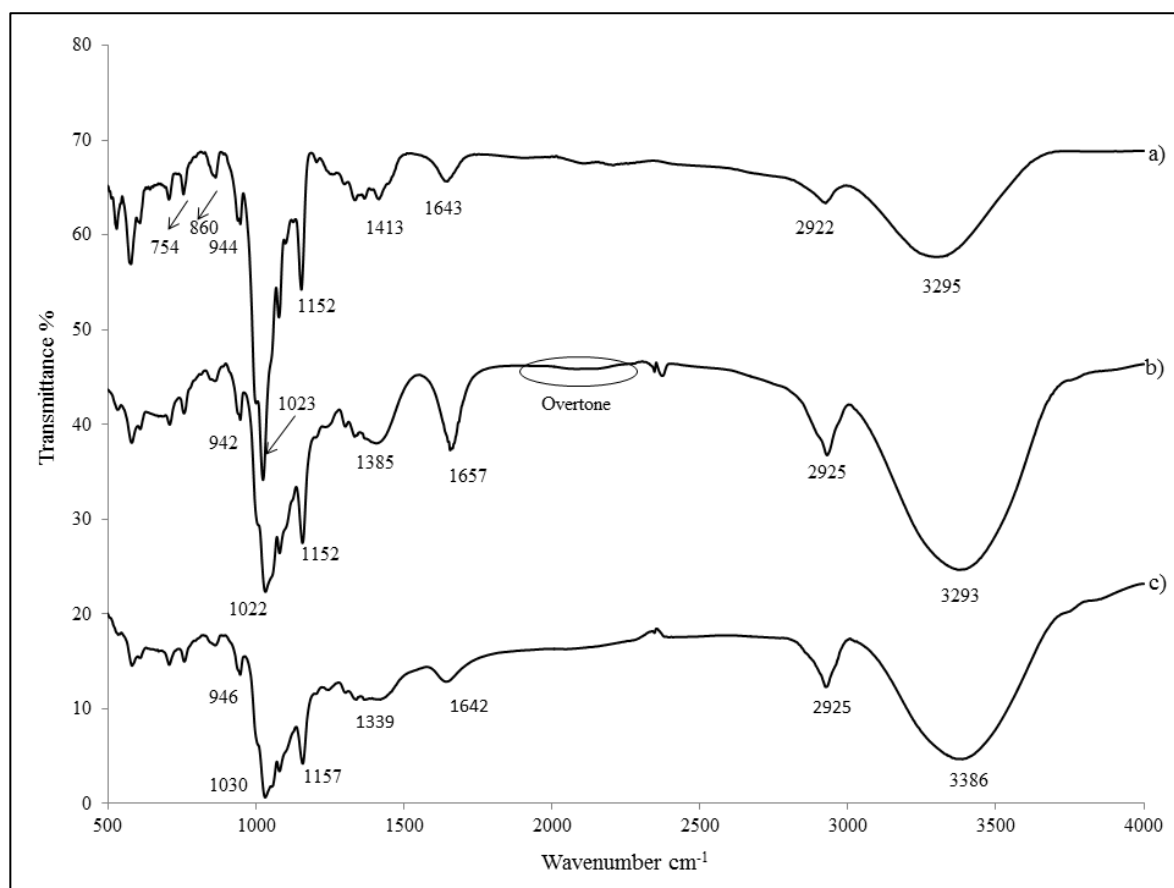


**Figure 4.1:** FT-IR spectrum of a)  $\beta$ -CD b)  $\beta$ -CD-BIMOTs c)  $\beta$ -CD-DIMOTs

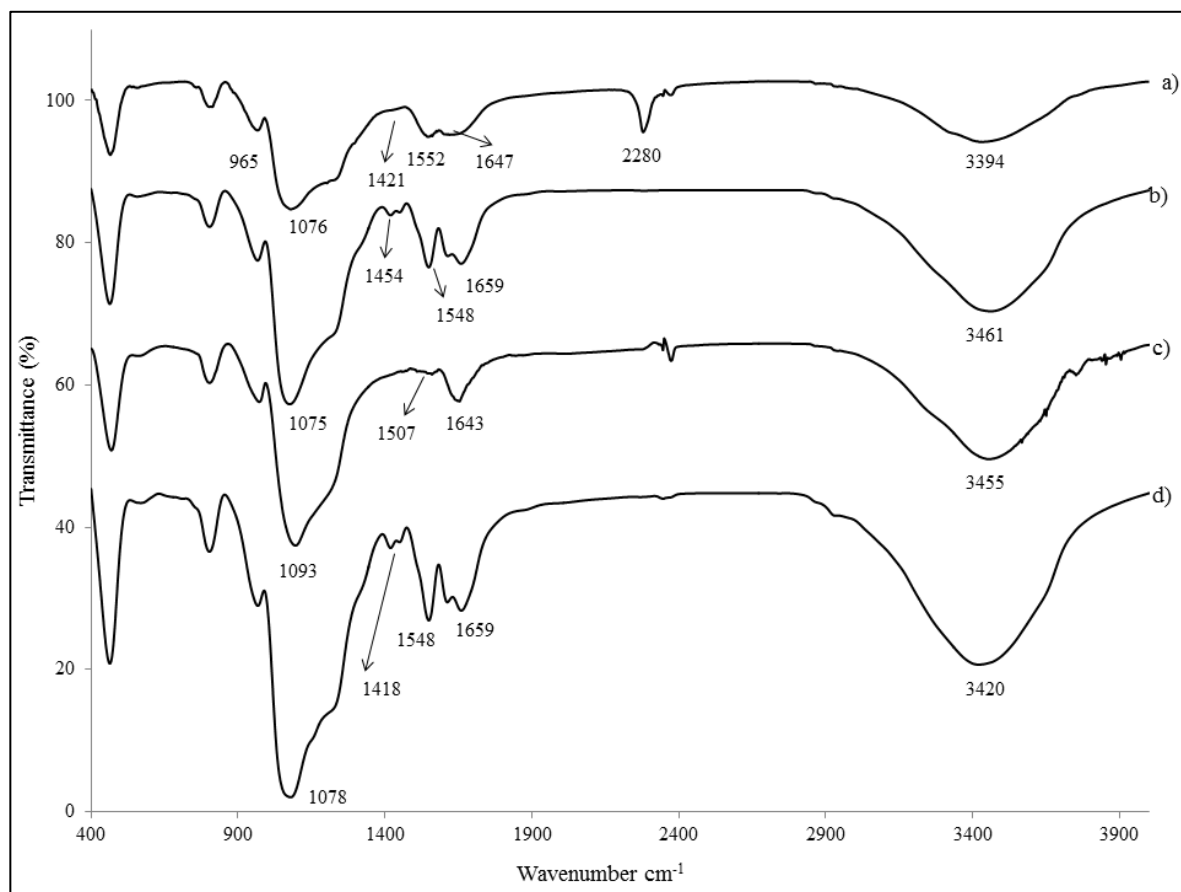


**Figure 4.2:** FT-IR spectrums of a) Si-TDI b) native  $\beta$ -CD CSP c)  $\beta$ -CD-BIMOTs CSP  
d)  $\beta$ -CD-DIMOTs CSP

**Table 4.1:** Main IR frequencies for  $\beta$ -CD,  $\beta$ -CD-BIMOTs and  $\beta$ -CD-DIMOTs with assignments

Wavelength $\text{cm}^{-1}$	Assignments	$\beta$ -CD	$\beta$ -CD-BIMOTs	$\beta$ -CD-DIMOTs
3295	O-H stretch	√		
3293	N-H, O-H stretch		√	
3386	N-H, O-H stretch			√
2922	C-H stretch	√		
2925, 1385	C-H stretch, bend		√	
2925, 1339	C-H stretch, bend			√
1643,1023	C-O stretch	√	√	
1657	C=C aromatic (1-BzIIIm)		√	
1642, 1030	C-O stretch			√
1413	O-H, CH <sub>2</sub>	√		
1152	C-C-C	√		
1157	C-N		√	
1157	C-N			√
944, 860, 754	-CH, =CH <sub>2</sub> , CH	√	√	√

**Table 4.2:** Main IR frequencies for Si-TDI, native  $\beta$ -CD CSP,  $\beta$ -CD-BIMOTs CSP and  $\beta$ -CD-DIMOTs CSP with assignments

Samples	Wavelength $\text{cm}^{-1}$	Assignments
Si-TDI	3297	O-H stretch
	2280	N=C=O stretch
	1647, 1552	NHCO carbamate linkage
	1421	Aromatic group in TDI
Native $\beta$ -CD CSP	3461	O-H stretch
	2280	Absence of N=C=O
	1659, 1548	NHCO carbamate linkage
	1548, 1454	Aromatic group in TDI
$\beta$ -CD-BIMOTs CSP	3455	N-H, O-H stretch and imidazole ring
	2280	Absence of N=C=O
	1653	C=C aromatic (1-BzIIIm)
	1507	C-C stretch in aromatic
	1093	C-O stretch
$\beta$ -CD-DIMOTs CSP	3420	N-H, O-H stretch and imidazole ring
	2280	Absence of N=C=O
	1659, 1078	C-O stretch
	1548, 1418	Aromatic group in TDI

#### 4.1.2 Thermalgravimetric analysis

TGA was performed on the Si-TDI, native  $\beta$ -CD CSP,  $\beta$ -CD-BIMOTs CSP and  $\beta$ -CD-DIMOTs CSP in the temperature range of 50 to 900 °C. Based on the thermograms shown in Figure 4.3, it can be seen that there is an initial loss of weight at temperature below 100 °C for all samples. This was attributed to the removal of physically adsorbed water and/or remaining solvent residues. Physically adsorbed water was removed completely by further heating to around 200 °C. TDI attached to the silica surface decomposed in the region between 125 and 250 °C (Guo *et al.*, 2005). Moreover, Si-TDI revealed a smaller, but noticeable, weight loss in the region from 250-600 °C. This can be attributed to the dehydration of the silica surface, in which silanol groups condense to siloxanes, a process known to occur in this thermal region (Poole, 2003). The thermogram of  $\beta$ -CD-BIMOTs CSP and  $\beta$ -CD-DIMOTs CSP showed two very distinct weight loss that occurred at the range of 210-357 °C and 400-600 °C. The first of these two weight loss was attributed to the decomposition of organic moieties at the surface. The second weight loss was associated with the decomposition of the residual methoxy groups on silica (Antochshuk & Jaroniec, 2000). In addition, the thermogram of native  $\beta$ -CD CSP,  $\beta$ -CD-BIMOTs CSP and  $\beta$ -CD-DIMOTs CSP attributed to the weight loss at 600-900 °C due to decomposition of the  $\beta$ -CD. By comparing Figure (c) and (d), it is clear that  $\beta$ -CD-BIMOTs-CSP shows more pronounced weight loss than  $\beta$ -CD-DIMOTs-CSP at all isothermal temperatures. This may be due to the long alkyl chain of  $\beta$ -CD-DIMOTs-CSP prevent it to be very volatile at high temperatures (Lu *et al.*, 2002). The temperature of weight loss with detail assignment is shown in Table 4.3.



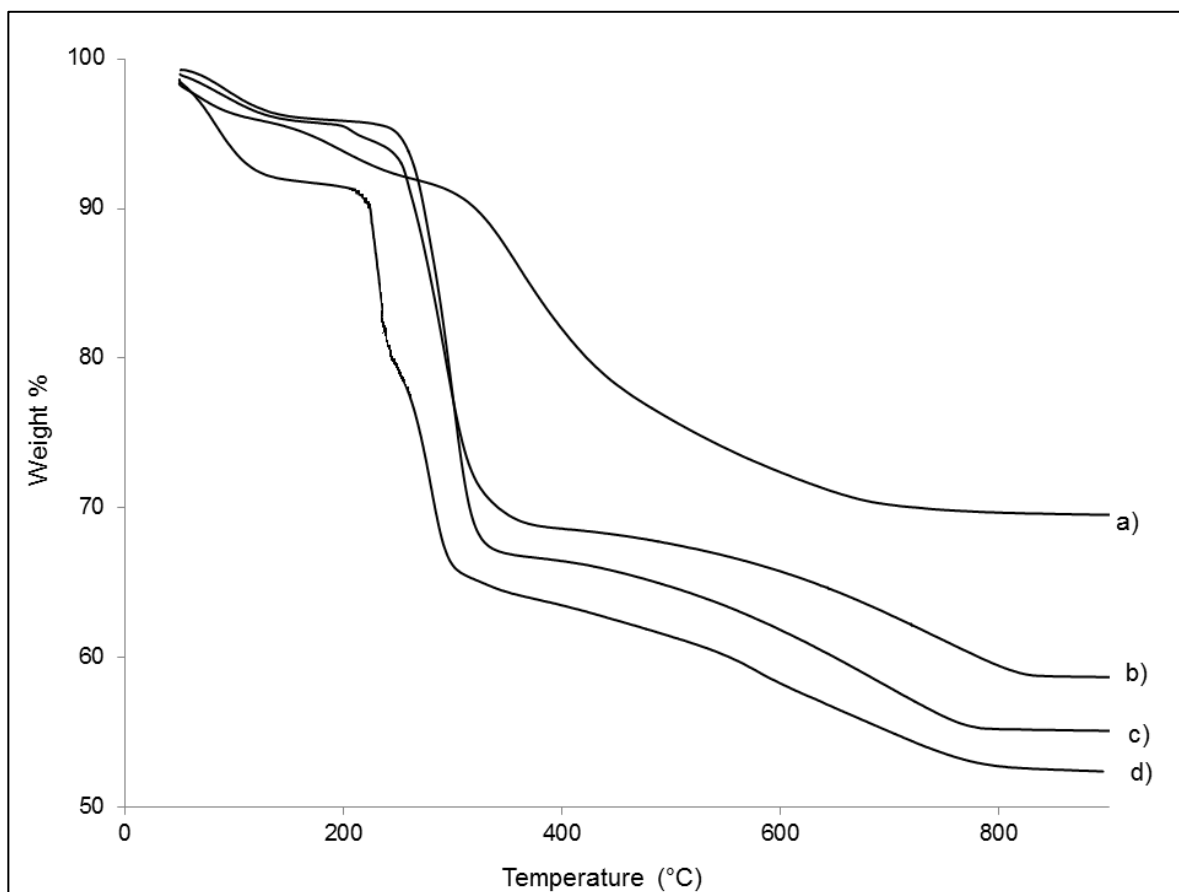


**Figure 4.3:** Thermogram of a) Si-TDI b) native  $\beta$ -CD CSP c)  $\beta$ -CD-BIMOTs CSP d)  $\beta$ -CD-DIMOTs CSP

**Table 4.3:** The assignment for temperature of weight loss

Samples	Region (°C)	Weight loss (%)	Assignment
Si-TDI	50-100	4	Water loss
	125-250	2	TDI
	250-600	28	Silanol condensation
Native $\beta$ -CD CSP	50-100	3	Water loss
	125-250	3	TDI
	250-600	24	Silanol condensation
	600-900	10	$\beta$ -CD
$\beta$ -CD-BIMOTs CSP	50-100	3	Water loss
	125-250	3	TDI
	215-357	26	1-BzIm, OTs
	357-900	11	Silanol condensation, $\beta$ -CD
$\beta$ -CD-DIMOTs CSP	50-100	7	Water loss
	125-250	2	TDI
	211-357	15	C <sub>10</sub> Mim, OTs
	357-900	12	Silanol condensation, $\beta$ -CD

## 4.2 Screening performance of CSPs

Different moieties that functionalized on  $\beta$ -CD possess different effects to the separation of chiral compounds. Herein, the effect of different group at the side chain of imidazolium cation of IL was studied. The performance of  $\beta$ -CD-BIMOTs CSP and  $\beta$ -CD-DIMOTs CSP were compared with native  $\beta$ -CD based CSP for the enantioseparation of flavonoids,  $\beta$ -blockers and NSAIDs. As shown in Table 4.4, the chromatograms showed that most of the flavonoids,  $\beta$ -blockers and NSAIDs were enantioseparated using  $\beta$ -CD-BIMOTs CSP as compared to  $\beta$ -CD-DIMOTs CSP and native  $\beta$ -CD based CSP. This result might due to the  $\beta$ -CD-BIMOTs CSP that displayed additional interaction with analytes which enhanced the enantioseparations.  $\beta$ -CD-BIMOTs CSP is prefer to be approached by planar analytes due to the planar aromatic

of 1-BzIIm (Wang *et al.*, 2012c). This might attributed to the  $\pi$ - $\pi$  interaction between analytes and  $\beta$ -CD-BIMOTs CSP that enhanced the enantioseparation. In addition, the long alkyl chain is preferably covered the partial cavity (Meier-Augenstein *et al.*, 1992) resulting decreased the chiral selectivity of  $\beta$ -CD-DIMOTs CSP. Thus, the optimization of mobile phase for the enantioseparation of flavonoids,  $\beta$ -blockers and NSAIDs on  $\beta$ -CD-BIMOTs CSP was studied. Furthermore, the mechanism of the enantioseparation was also evaluated.

**Table 4.4:** The chromatogram for the enantioseparation of selected flavonoids,  $\beta$ -blockers and NSAIDs on  $\beta$ -CD,  $\beta$ -CD-BIMOTs and  $\beta$ -CD-DIMOTs CSPs

Analytes	CSPs		
	$\beta$ -CD	$\beta$ -CD-BIMOTs	$\beta$ -CD-DIMOTs
Flavonoids			
$\beta$ -blockers			

**Table 4.4, continued**

Analytes	CSPs		
	$\beta$ -CD	$\beta$ -CD-BIMOTs	$\beta$ -CD-DIMOTs
NSAIDs			

Flavonoids: a) flavanone b) hesperetin c) naringenin d) eriodictyol

$\beta$ -blockers: a) propranolol b) metoprolol c) pindolol d) atenolol

NSAIDs : a) fenoprofen b) ibuprofen c) indoprofen d) ketoprofen

Condition: i) 90/10 ACN/water ii) 50/50 ACN/water iii) 30/70 ACN/water

### 4.3 Enantioseparation performance of Flavonoids

The type and composition of organic modifier as mobile phase are important factors that affect the enantioseparations. Adjusting the pH of mobile phase for reverse phase mode would also influence the forms of analytes and thus affect the enantioseparation. As presented in Table 4.5, high  $R_s$  values indicated the good enantioseparation for flavanone ( $R_s=1.63$ ) and hesperetin ( $R_s=1.06$ ) with the mobile phase of MeOH/water:50/50 and ACN/water:50/50, respectively. In addition, flavanone also obtained good enantioseparation ( $R_s=1.86$ ) in ACN/buffer at pH 4. However, a low  $R_s$  value was obtained for flavanone when ACN/buffer pH 9 was selected as mobile phase. Meanwhile, the enantiomers of naringenin and eriodictyol were not resolve at all using all selected mobile phases. Moreover, it can be seen that the  $k_1'$  values of flavonoids decreased with increasing content of organic solvent. This was a common rule in reverse phase mode due to the increasing content of organic solvent that led to the increased of elution strength of mobile phase. Thus, flavonoids easily can be displaced from the stationary phase.

Flavanone obtained good enantioseparation in most of the mobile phase conditions which might due to its hydrophobic properties that facilitated the inclusion complex formation with hydrophobic cavity of  $\beta$ -CD-BIMOTs CSP. Moreover, flavanone with aromatic rings without any substituent may experience less steric hindrance for inclusion complex formation with cavity of  $\beta$ -CD-BIMOTs CSP. In addition, the carbonyl group and aromatic ring of flavanone can form hydrogen bonding and  $\pi$ - $\pi$  interaction, respectively, with  $\beta$ -CD-BIMOTs CSP which can further enhance the enantio-recognition. Flavanone is classified as neutral compound as compared with hesperetin, naringenin and eriodictyol which are weakly acidic in nature (Ng *et al.*, 2002). Thus, at pH 4 and 7, flavanone is remained neutral and preferable to form

inclusion complex with cavity of  $\beta$ -CD (Raovv *et al.*, 2013). Meanwhile, flavanone is known to undergo ring opening under basic condition to the corresponding unstable 2'-hydroxyl substituted chalcones (Figure 4.4) (Wistuba *et al.*, 2006) which might be a reason in the decreasing  $R_s$  value at pH 9.

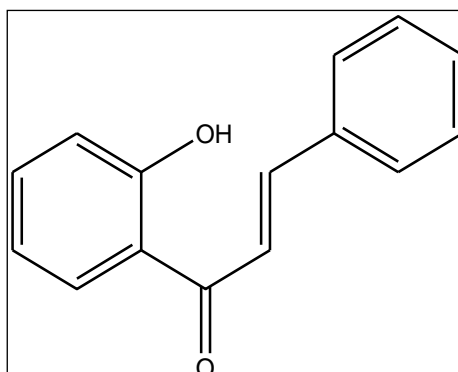


**Figure 4.4:** Structure of 2'-hydroxyl substituted chalcones

**Table 4.5:** Chiral separation data for the flavonoids on  $\beta$ -CD-BIMOTs CSP in the reverse mobile phase

Flavonoids	Conditions	pH 4			pH 7			pH 9		
		$k_1'$	$k_2'$	$R_s$	$k_1'$	$k_2'$	$R_s$	$k_1'$	$k_2'$	$R_s$
Flavanone	a	0.34	0.48	0.64	0.33	0.49	0.45	0.38	0.85	0.79
	b	2.09	5.24	1.86	0.47	0.71	0.81	0.33	0.46	0.46
	c	2.77	2.77	0	2.61	2.61	0	2.51	2.51	0
	d	7.23	7.23	0	1.44	2.05	0.76	1.92	3.34	0.93
	e	2.27	3.58	0.85	2.58	4.31	1.63	6.84	6.84	0
Hesperetin	a	1.18	1.18	0	0.47	0.76	0.45	0.79	0.79	0
	b	1.49	1.49	0	0.37	1.36	1.06	1.61	1.61	0
	c	9.75	9.75	0	4.43	7.14	0.92	4.31	4.31	0
	d	1.35	1.35	0	1.29	1.29	0	1.80	1.80	0
	e	-	-	-	16.19	16.19	0	4.18	4.18	0
Naringenin	a	0.27	0.27	0	0.28	0.28	0	0.28	0.28	0
	b	0.62	0.62	0	0.84	0.84	0	0.97	0.97	0
	c	1.54	1.54	0	4.16	4.16	0	5.29	5.29	0
	d	0.68	0.68	0	0.12	0.12	0	0.83	0.83	0
	e	-	-	-	0.18	0.18	0	3.61	3.61	0
Eriodictyol	a	0.22	0.22	0	0.32	0.32	0	0.34	0.34	0
	b	0.34	0.34	0	0.34	0.34	0	0.34	0.34	0
	c	0.35	0.61	0.26	0.36	0.36	0	0.37	0.37	0
	d	-	-	-	0.19	0.19	0	0.82	0.82	0
	e	-	-	-	0.34	0.34	0	4.09	4.09	0

Conditions pH 7: a) ACN/water-90/10 b) ACN/water-50/50 c) ACN/water-30/70 d) MeOH/water-90/10 e) MeOH/water-50/50

Conditions pH 4 or 9: a) ACN/buffer-90/10 b) ACN/buffer-50/50 c) ACN/buffer-30/70 d) MeOH/buffer-90/10 e) MeOH/buffer-50/50



According Li *et al.* (1992), the formation of inclusion complex is an important interaction to achieve better enantioseparation (Li & Purdy, 1992). In order to study the interaction for the enantioseparation,  $^1\text{H}$  NMR and NOESY of  $\beta$ -CD-BIMOTs/flavonoids complexes were studied. The deduced structures of the  $\beta$ -CD-BIMOTs and  $\beta$ -CD-BIMOTs/flavonoids complexes are shown in Figure 4.5 and Figure 4.6, respectively. Chemical shift ( $\delta$ ) variations can provide evidence for the formation of inclusion complexes in solution. The values of the  $\delta$  for different protons in  $\beta$ -CD-BIMOTs and  $\beta$ -CD-BIMOTs/flavonoids complexes are listed in Table 4.6. The induced shift ( $\Delta\delta$ ) is defined as the difference in chemical shift in the presence or absence of analytes. In this study, the induced shift was calculated using Eq. 4-1:

$$\Delta\delta = \delta(\text{complex}) - \delta(\text{free}) \quad 4-1$$

Normally, the inclusion of an apolar region of an analyte into the hydrophobic cavity would affect the inner protons of the glucose units of  $\beta$ -CD, namely, H3 and H5 (Zhang *et al.*, 1990), whereas the protons on the exterior torus of  $\beta$ -CD (H1, H2 and H4) would also be affected if there are any hydrogen bonding involved. As the result, the chemical shifts of  $\beta$ -CD-BIMOTs protons (H1, H2, H3, H4 and H5) would change as the presence of analytes.

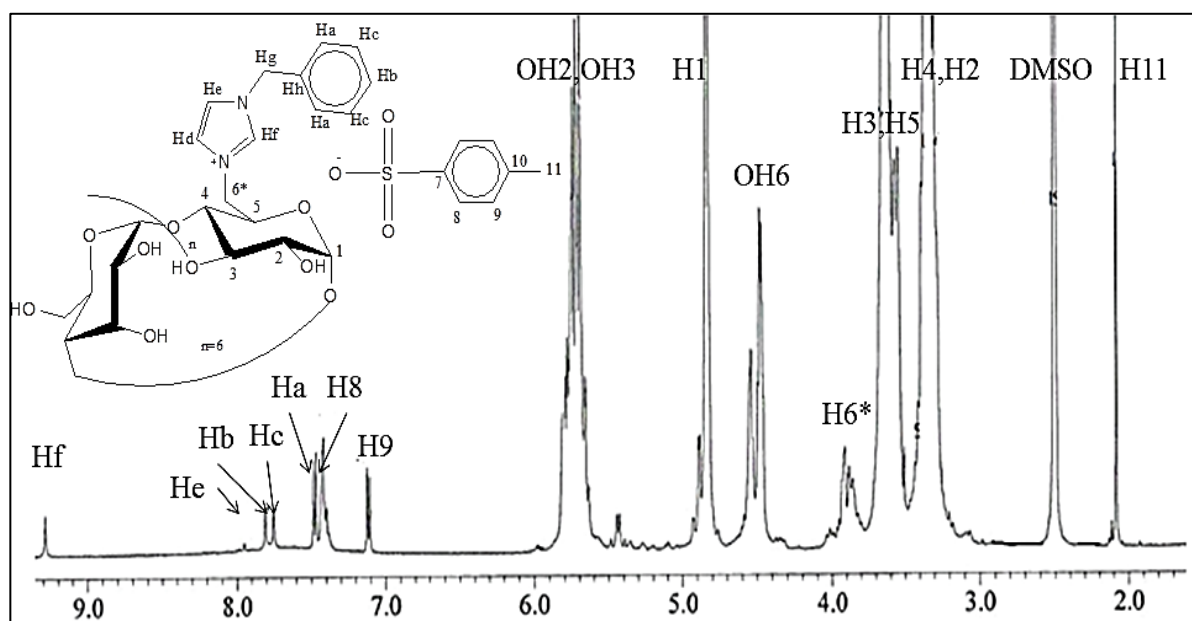


**Figure 4.5:** The deduced structure of  $\beta$ -CD-BIMOTs

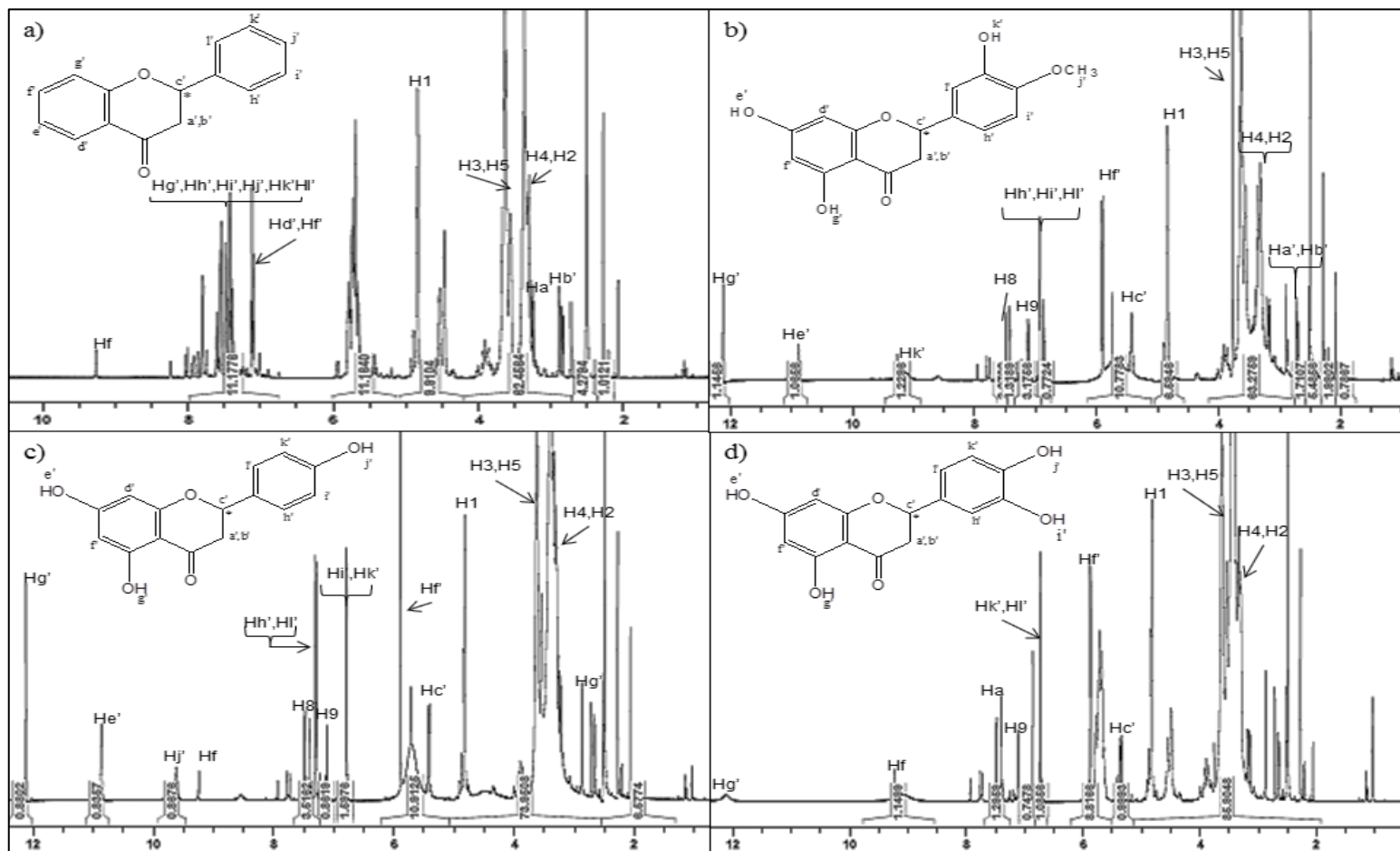


**Figure 4.6:** The deduced structure of a)  $\beta$ -CD-BIMOTs/flavanone complex, b)  $\beta$ -CD-BIMOTs/hesperetin complex, c)  $\beta$ -CD-BIMOTs/naringenin complex d)  $\beta$ -CD-BIMOTs/eriodictyol complex

For  $\beta$ -CD-BIMOTs/flavanone complex (Table 4.6), the significant changes were observed on  $\Delta\delta$  at H5 proton located at the cavity of  $\beta$ -CD-BIMOTs due to inclusion complex formation. In addition, there is large shift at H2 proton located at the exterior torus of  $\beta$ -CD-BIMOTs caused by hydrogen bonding. The NOESY spectra in Figure 4.7 shows the cross-peak between H1, H2 and H5 protons of  $\beta$ -CD-BIMOTs with Hg' and Hj' protons of flavanone proved that the inclusion complex and hydrogen bonding were formed between flavanone and  $\beta$ -CD-BIMOTs.

**Table 4.6:** Chemical shifts ( $\delta$ ) and induced shifts ( $\Delta\delta$ ) of  $\beta$ -CD-BIMOTs and  $\beta$ -CD-BIMOTs/flavonoids

	$\beta$ -CD- BIMOTs	$\beta$ -CD- BIMOTs/Flavanone	$\beta$ -CD- BIMOTs/Hesperetin	$\beta$ -CD- BIMOTs/Naringenin	$\beta$ -CD- BIMOTs/Eriodictyol				
	$\delta$	$\delta$	$\Delta\delta$	$\delta$	$\Delta\delta$	$\delta$	$\Delta\delta$	$\delta$	$\Delta\delta$
H1	4.8405	4.8872	0.0467	4.8381	-0.0024	4.8241	-0.0164	4.8365	-0.004
H2	3.3312	3.2568	<b>-0.0744</b>	3.3214	-0.0138	3.2406	<b>-0.0946</b>	3.34	0.0048
H3	3.6394	3.6392	-0.0002	3.6401	0.0007	3.6253	-0.0141	3.6235	-0.0159
H4	3.3716	3.3797	0.0081	3.3552	<b>-0.0164</b>	3.3989	0.0273	3.4438	<b>0.0722</b>
H5	3.5777	3.5572	<b>-0.0205</b>	3.5586	<b>-0.0191</b>	3.5443	-0.0334	3.5428	-0.0349
H6	3.9225	3.9110	-0.0115	3.9185	-0.004	3.9053	-0.0172	3.8979	-0.0246
H8	7.4215	7.4374	0.0159	7.4276	0.0061	7.4128	-0.0087	7.4105	-0.011
H9	7.1112	7.1142	0.0030	7.1281	0.0169	7.1174	0.0062	7.1199	0.0087
H11	2.0847	2.0821	-0.0026	2.0844	-0.0003	2.0706	-0.0141	2.0698	-0.0149
Ha	7.4314	7.4827	0.0513	7.4995	0.0681	7.4873	0.0559	7.4756	0.0442
Hb	7.7957	7.8025	0.0068	7.8019	0.0062	7.7771	-0.0186	7.765	-0.0307
Hc	7.7542	7.7892	0.035	7.7552	0.001	7.738	-0.0162	7.7274	-0.0268
Hd	-	-	-	-	-	-	-	-	-
He	7.9563	7.9472	-0.0091	7.9456	-0.0107	7.9333	-0.023	7.9312	-0.0251
Hf	9.234	9.2696	0.0302	9.2744	0.035	9.2419	0.0025	9.2252	-0.0142
Hg	5.4371	5.4471	0.0100	5.4191	-0.018	5.4067	-0.0304	5.4000	-0.0371

-: overlap peak

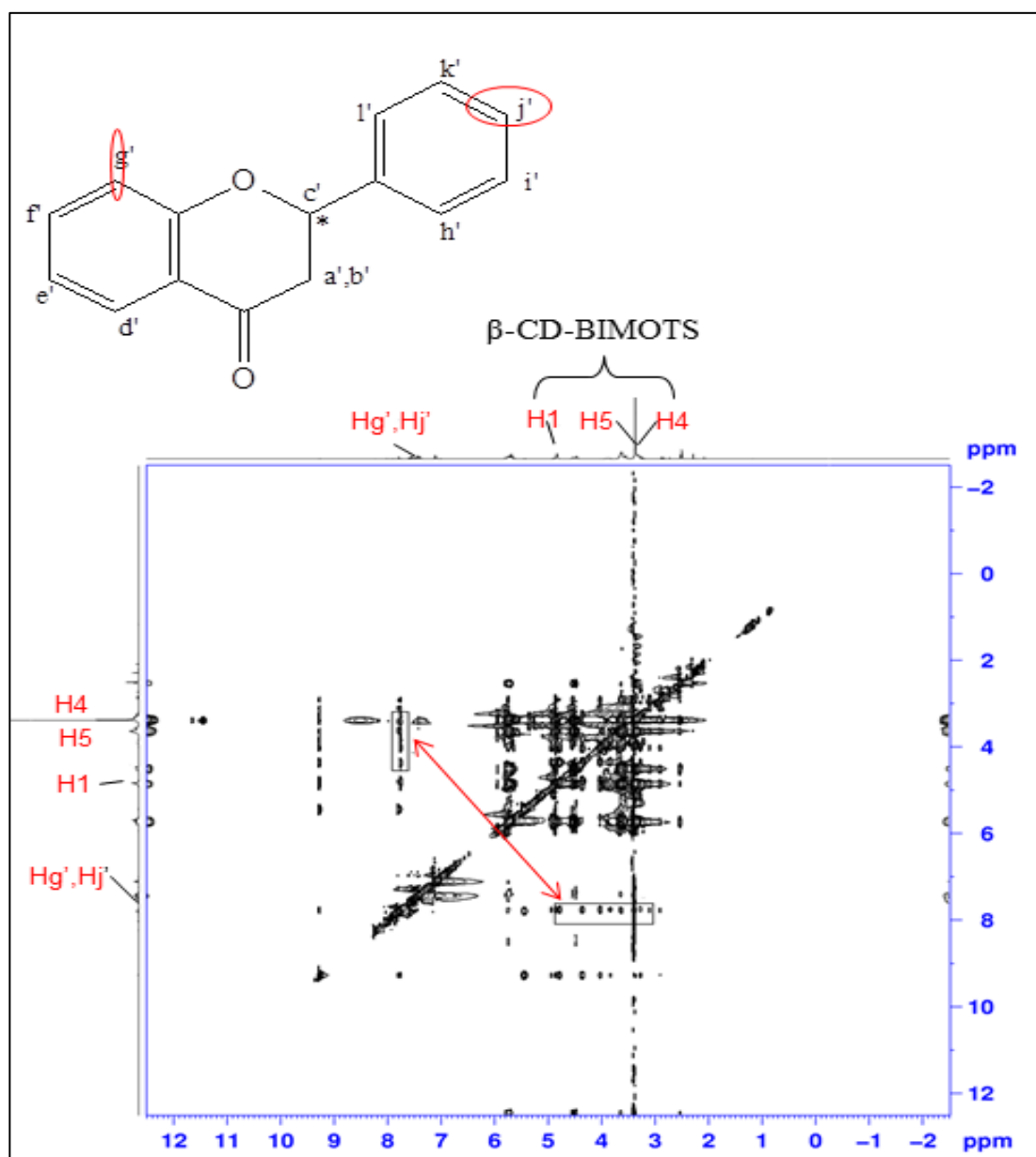


**Figure 4.7:** NOESY spectra of  $\beta$ -CD-BIMOTs/flavanone

Meanwhile, for hesperetin which is weakly acidic ( $pK_a$  7.9) also formed neutral species at pH 7 and able to form inclusion complex with the cavity of  $\beta$ -CD-BIMOTs CSP. Thus, it was effectively enantioseparated using  $\beta$ -CD-BIMOTs based CSP (Table 4.5). Hesperetin bearing methoxy group is more hydrophobic than naringenin and eriodictyol. Therefore, hesperetin has greater affinity towards the cavity of  $\beta$ -CD-BIMOTs CSP as compared to naringenin and eriodictyol. Hesperetin was not enantioseparated at pH 4 and 9. At acidic pH, hesperetin is in neutral form (Ficarra *et al.*, 2002) but the TEAA species in the mobile phase compete with it for the inclusion formation (Kavalirova *et al.*, 2004). Meanwhile, the protonated hesperetin at pH 9 was not favored to form inclusion complex with  $\beta$ -CD (Raovv *et al.*, 2013). This finding further support the role of inclusion complex formation in enantioseparation of  $\beta$ -CD based CSPs. Moreover, OH groups and aromatic rings of hesperetin can form hydrogen bonding and  $\pi$ - $\pi$  interaction with  $\beta$ -CD-BIMOTs CSP and thus enhanced the enantioseparation. These interactions were further proven using  $^1\text{H}$  NMR and NOESY of  $\beta$ -CD-BIMOTs/hesperetin complex. The  $\beta$ -CD-BIMOTs/hesperetin complex shows appreciable shift at H4 proton at exterior torus of  $\beta$ -CD-BIMOTs because of hydrogen bonding. There are also large shift at H5 proton located in cavity of  $\beta$ -CD-BIMOTs (Table 4.6) which related to the formation of inclusion complex. In addition, the NOESY spectra (Figure 4.8) shows the cross-peaks between H3, H4 and H5 protons of  $\beta$ -CD-BIMOTs with He', Hg', and Hk' protons of hesperetin also proved that the inclusion complex and hydrogen bonding were formed with  $\beta$ -CD-BIMOTs which enhanced the enantioseparation.

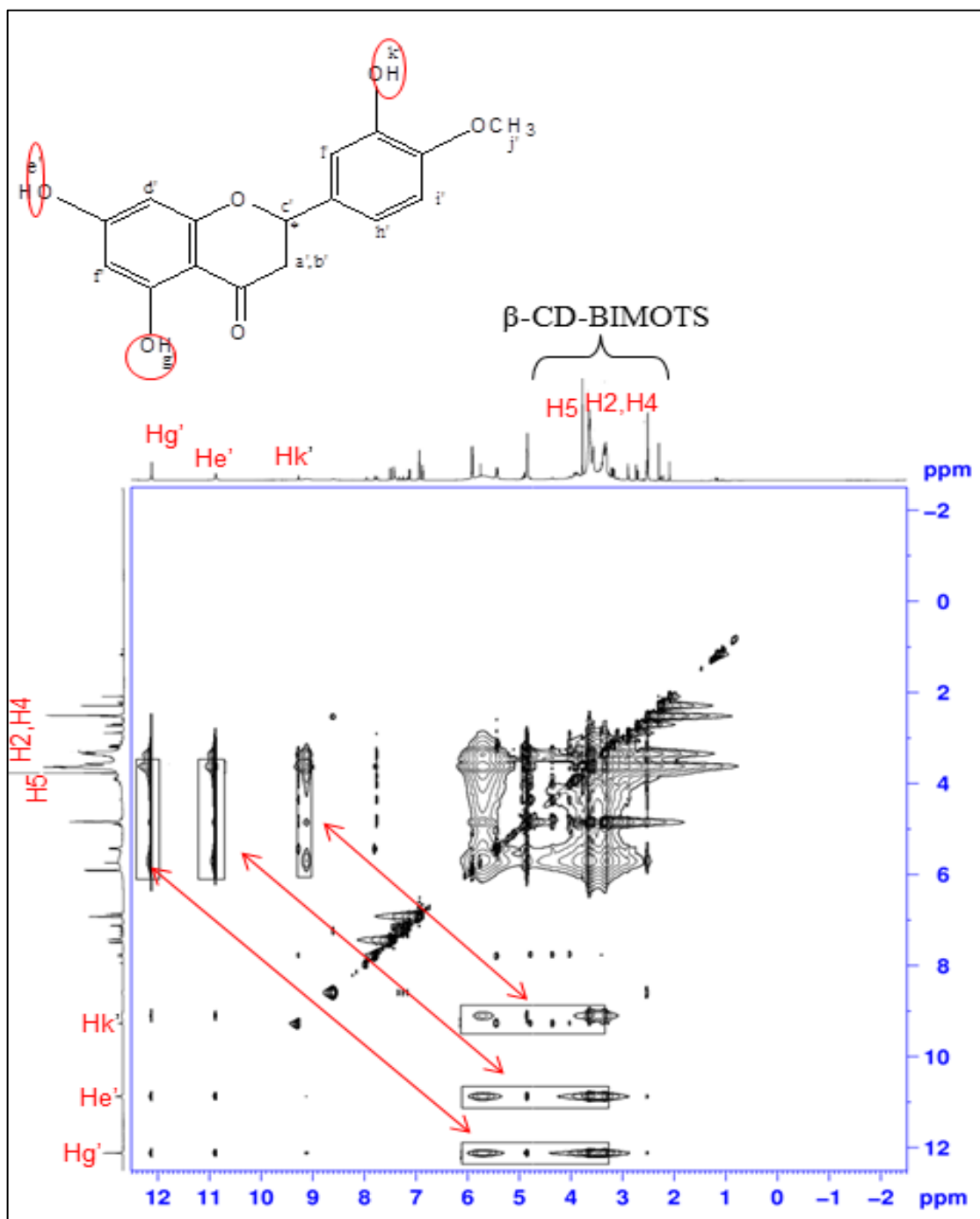
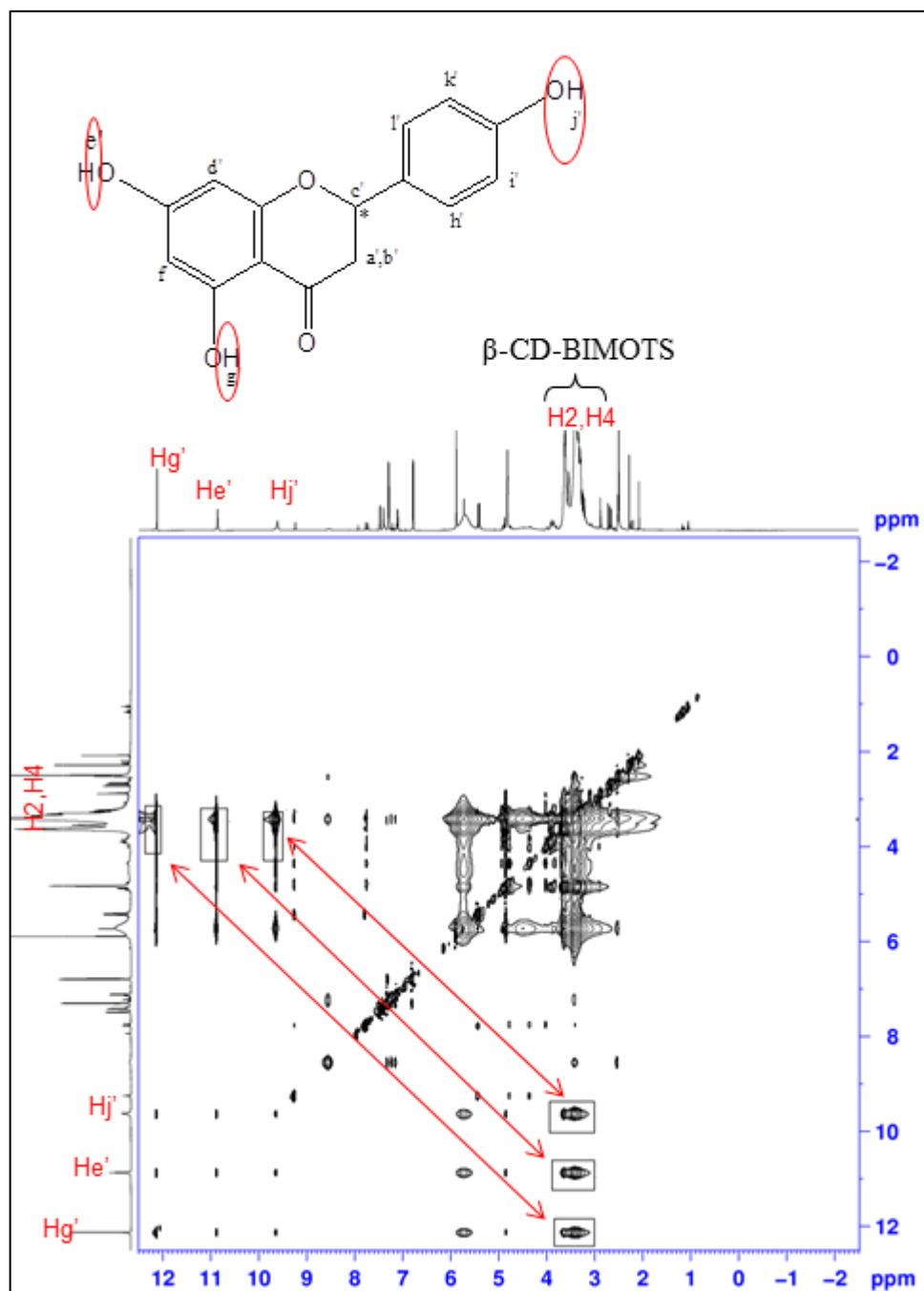


Figure 4.8: NOESY spectra of  $\beta$ -CD-BIMOTs/hesperetin



As shown in Table 4.5, naringenin and eriodictyol are not resolved in the reverse phase mode. Naringenin and eriodictyol contains highly polar moieties (OH) which might weaken the hydrophobic interaction with  $\beta$ -CD-BIMOTs cavity and retard the formation of inclusion complexes. Naringenin and eriodictyol might prefer to form hydrogen bonding at exterior torus instead of interior cavity of  $\beta$ -CD-BIMOTs CSP. Moreover, the presence of OH functionality as electron donating group could increase the electron density of aromatic ring of naringenin and eriodictyol and facilitate the  $\pi$ - $\pi$  repulsion which weaken the  $\pi$ - $\pi$  interaction (Hunter *et al.*, 2001). It can be deduced that hydrogen bonding is not sufficient to produce enantio-recognition.  $^1\text{H}$  NMR of  $\beta$ -CD-BIMOTs/naringenin and  $\beta$ -CD-BIMOTs/eriodictyol complexes were studied to get detail information of the interaction. Large  $\Delta\delta$  of H2 and H4 protons of  $\beta$ -CD-BIMOTs with the presence of naringenin and eriodictyol was observed, respectively (Table 4.6). In addition, NOESY spectra for  $\beta$ -CD-BIMOTs/naringenin complex (Figure 4.9) showed the cross-peak between He', Hg' and Hj' protons of naringenin with H2 proton of  $\beta$ -CD-BIMOTs. In NOESY spectra of  $\beta$ -CD-BIMOTs/eriodictyol complex (Figure 4.10), there are cross-peak between Hc', Hg' and Hf' protons of eriodictyol with H4 proton of  $\beta$ -CD-BIMOTs. These results suggest that there are hydrogen bonding between naringenin and eriodictyol at exterior torus of  $\beta$ -CD-BIMOTs.



**Figure 4.9:** NOESY spectra of  $\beta$ -CD-BIMOTs/naringenin

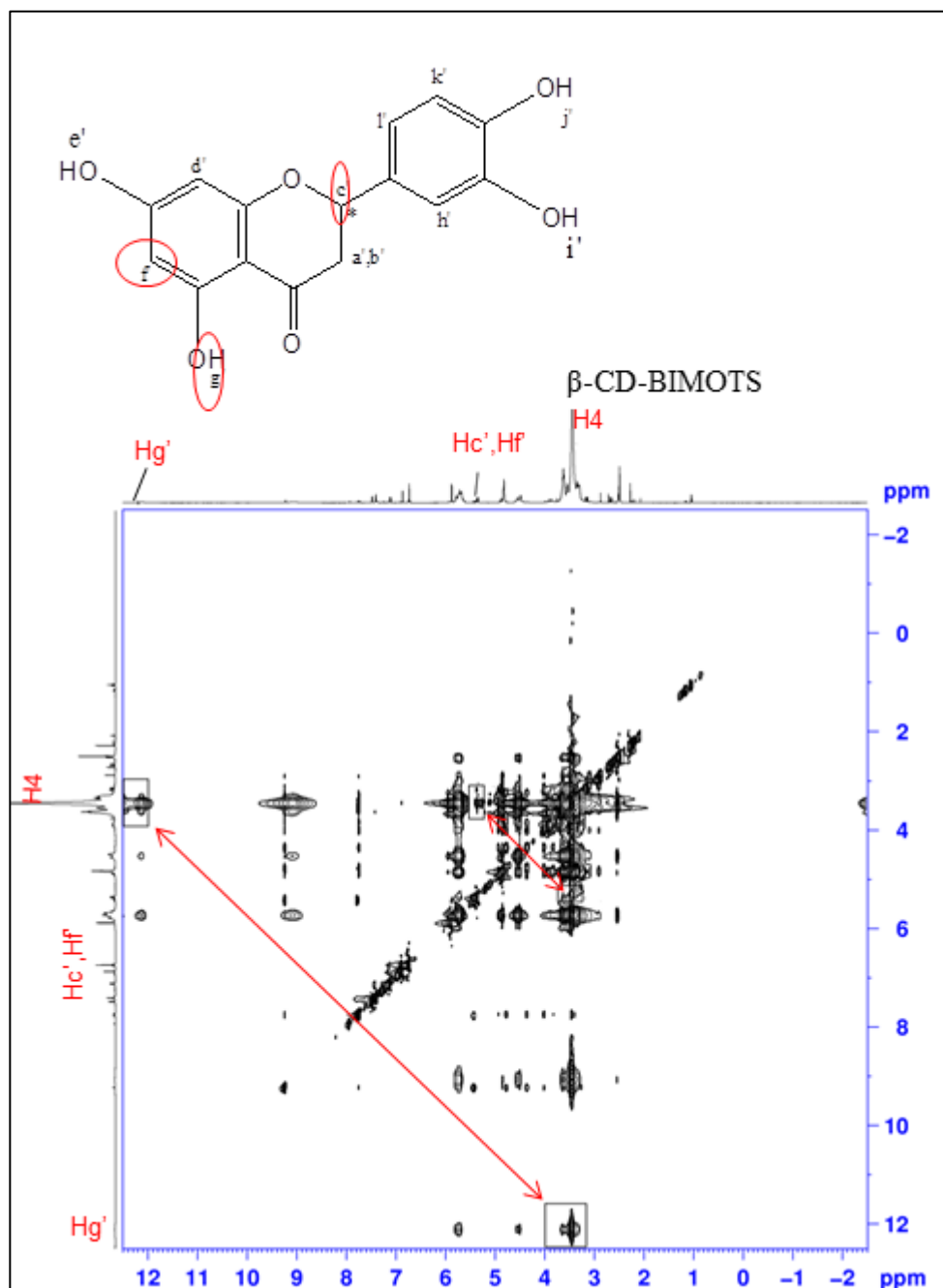


**Figure 4.10:** NOESY spectra of  $\beta$ -CD-BIMOTs/eriodictyol

As a part of the optimization, the polar organic mode with different additives was used to improve the enantioseparation of naringenin and eriodictyol. This system can be used to resolve compounds that cannot be separated in the reverse phase mode. In this study, the mobile phase of polar organic mode was the mixture of ACN and MeOH. The selected additives were TEA and HOAc (Kafkova *et al.*, 2005). In the polar organic mode, the relative high concentration of organic solvents occupies the relatively hydrophobic cavity of  $\beta$ -CD. Armstrong *et al.* (1993) proposed that the analytes may form a “lid” over the “mouth” of the cavity. Moreover, the retention and selectivity are mainly due to the polar OH groups at the rims of  $\beta$ -CD forming hydrogen bonding with analytes (Chang *et al.*, 1993). Thus, the total number of OH moiety at flavonoids would affect the enantioseparation. The HPLC chromatograms shown naringenin achieved better enantioseparation at higher amount of TEA (Figure 4.11) meanwhile eriodictyol was resolved at higher amount of HOAc (Figure 4.12). At higher amount of TEA, naringenin which has less OH groups than eriodictyol tends to carry less number of deprotonated OH. Thus, naringenin prefer to form electrostatic interaction associated with hydrogen bonding which facilitated the enantioseparation. Meanwhile, eriodictyol which has highest number of deprotonated OH led to the stronger electrostatic interaction with  $\beta$ -CD-BIMOTs and thus inhibit the enantioseparation.

At higher ratio of HOAc, both of naringenin and eriodictyol are in neutral form. Under this condition, enantioseparation of eriodictyol was achieved better than naringenin. This might due to the structure of eriodictyol with 4 OH groups that have high capability to form hydrogen bonding at the exterior torus of  $\beta$ -CD-BIMOTs. It can be deduced that the better enantioseparation in the polar organic mode shows the importance of the hydrogen bonding and/or electrostatic interaction for the chiral recognition of naringenin and eriodictyol.

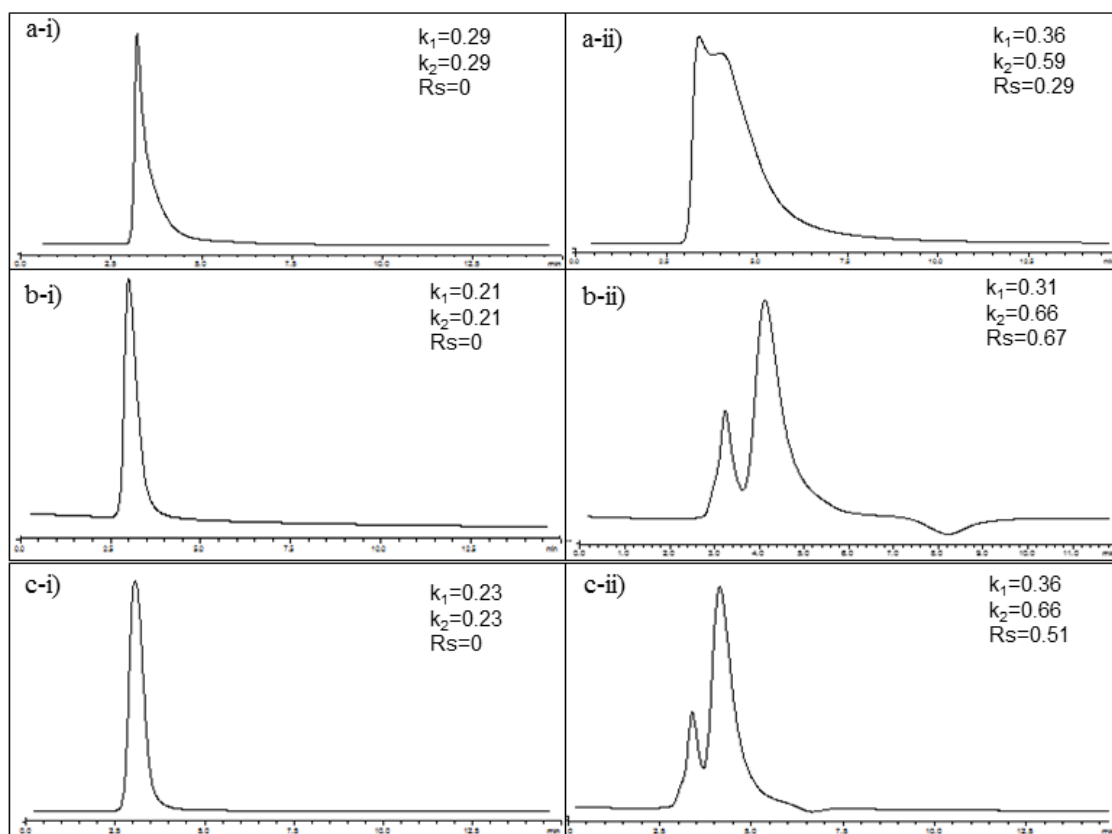


**Figure 4.11:** HPLC chromatograms of naringenin in polar organic mode. Mobile phase composition, ACN/MeOH/TEA/HOAc (v/v/v/v): a-i) 90/10/1/3, a-ii) 90/10/3/1, b-i) 50/50/1/3, b-ii) 50/50/3/1, c-i) 30/70/1/3 and c-ii) 30/70/3/1

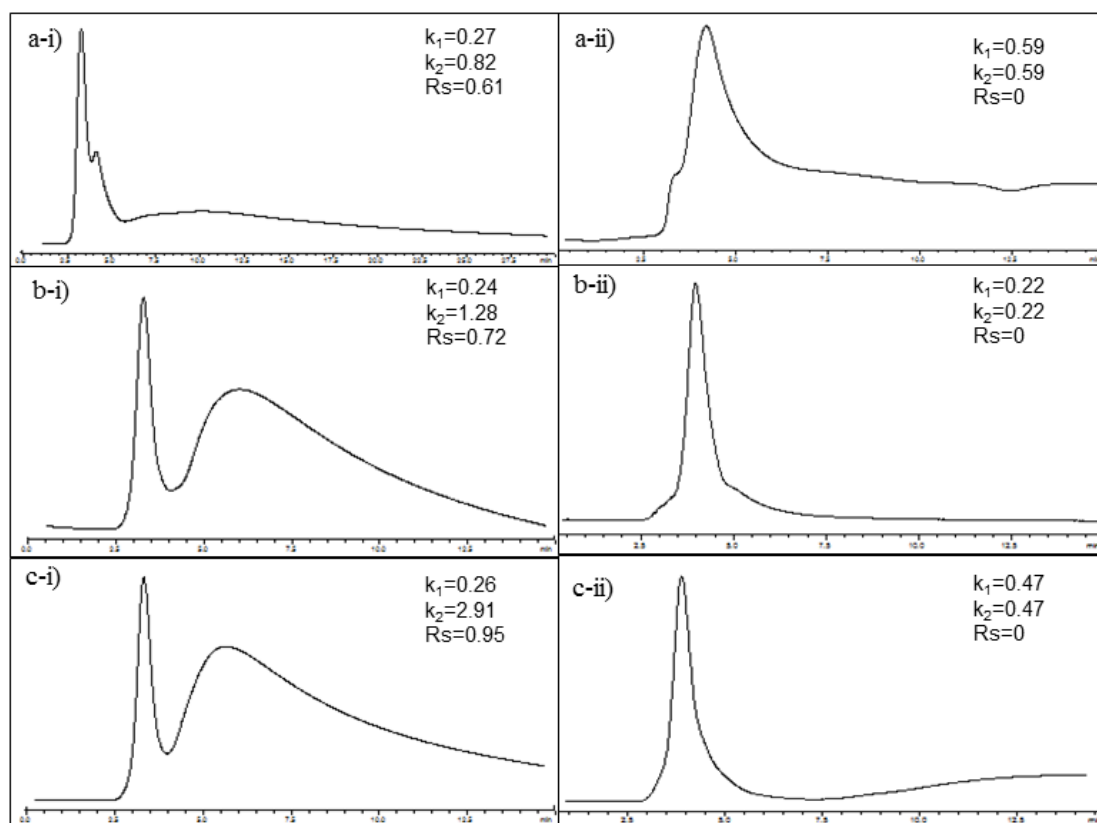


**Figure 4.12:** HPLC chromatograms of eriodictyol in polar organic mode. Mobile phase composition, ACN/MeOH/TEA/HOAc (v/v/v/v): a-i) 90/10/1/3, a-ii) 90/10/3/1, b-i) 50/50/1/3, b-ii) 50/50/3/1, c-i) 30/70/1/3 c-ii) 30/70/3/1

The chromatogram of eriodictyol (Figure 4.12(c-i)) with the broad and tailing peak was caused by the formation of strong hydrogen bonding with  $\beta$ -CD-BIMOTs CSP. Thus, it can be deduced that the higher number of OH groups leads to the stronger interaction with  $\beta$ -CD-BIMOTs CSP and thus, inhibit the enantioseparation. Consequently, the formation constant ( $K$ ) was determined to study the strength of the interaction between flavonoids and  $\beta$ -CD-BIMOTs. In the experiment, the plots of absorption for  $\beta$ -CD-BIMOTs, flavonoids and  $\beta$ -CD-BIMOTs/flavonoids complexes were first measured (Figure 4.13) by monitoring the UV spectra. The results showed that  $\beta$ -CD-BIMOTs had a  $\lambda_{\max}$  in the range of 230-260 nm. The absorption spectra of flavanone displayed two well-defined  $\lambda_{\max}$  at 250 and 320 nm meanwhile naringenin, hesperetin and eriodictyol displayed one  $\lambda_{\max}$  at 320 nm. The  $\lambda_{\max}$  of  $\beta$ -CD-

BIMOTs/flavonoids complex was observed at 230-260 nm referred to  $\beta$ -CD-BIMOTs. Meanwhile, the  $\lambda_{\text{max}}$  at 320 nm of  $\beta$ -CD-BIMOTs/flavonoids complex was referred to flavonoids. It was observed that the absorption spectra of all  $\beta$ -CD-BIMOTs/flavonoids complexes showed both hyperchromic and hypochromic effect. Increase in absorption at  $\lambda_{\text{max}}$  is defined as hyperchromic effect and decrease in the absorption at  $\lambda_{\text{max}}$  is defined as hypochromic effect (Hu *et al.*, 2012; Ventura *et al.*, 2006). Hyperchromic effect that observed in the UV spectra of  $\beta$ -CD-BIMOTs-flavonoids at 320 nm was due to the electron perturbation at the chromophore of flavonoids (Ventura *et al.*, 2006). Meanwhile the hypochromic effect is due to the intercalative mode involving the stacking interaction (Hu *et al.*, 2012) which was mainly referred to  $\pi$ - $\pi$  interaction between aromatic ring of flavonoids and  $\beta$ -CD-BIMOTs. The hypochromic effect for  $\beta$ -CD-BIMOTs-flavanone was not observed due to the overlapping of absorption band at 250 nm (Figure 4.13(a)). Both hyperchromic and hypochromic effects observed in the absorption spectra of  $\beta$ -CD-BIMOTs-flavonoids proved that there were multiple interactions between  $\beta$ -CD-BIMOTs and flavonoids.

The  $K$  values were then calculated (using Equation 3-6) from the slope of  $\frac{1}{(A-A_0)}$  versus  $\frac{1}{[\beta\text{-CD-BIMOTs}]}$  of  $\beta$ -CD-BIMOTs/flavonoids as shown in Figure 4.14. In Table 4.7, the  $K$  values obtained are in the following order:  $\beta$ -CD-BIMOTs/hesperetin <  $\beta$ -CD-BIMOTs/flavanone <  $\beta$ -CD-BIMOTs/naringenin <  $\beta$ -CD-BIMOTs/eriodictyol. This deduced that the strength of interaction is correlated with the substituted OH group at flavonoids. Previous study reported that hydrogen bond is the strongest non-covalent interactions with 2-10 kcal/mol stabilization energy (Frieden, 1975). Naringenin and eriodictyol that possess 3 and 4 OH groups experienced highest  $K$  values indicating the stronger hydrogen bond formation. Indeed, these results clarified that naringenin and eriodictyol interacted at the external torus of  $\beta$ -CD-BIMOT. Meanwhile, the small  $K$

values for flavanone and hesperetin proven that the inclusion complex was formed due to hydrophobic interaction and facilitated the enantioseparation.

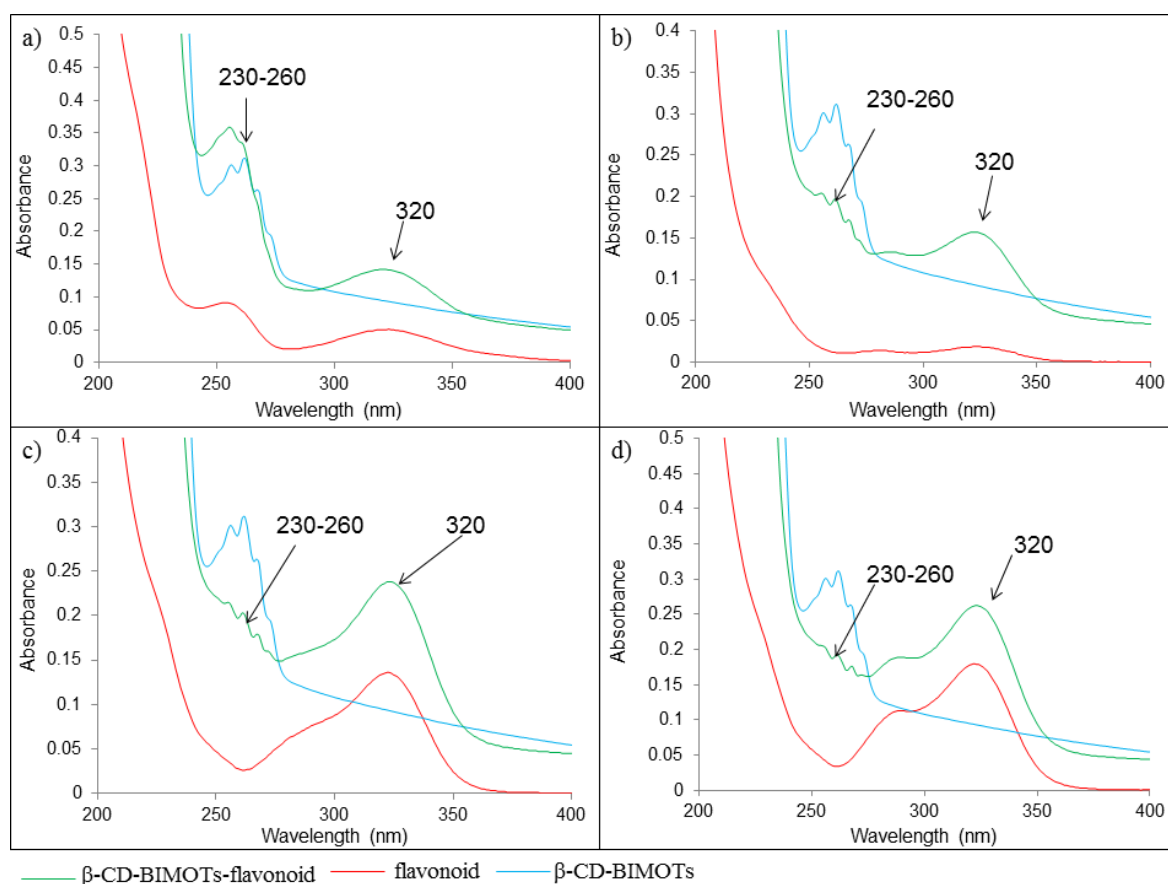


**Figure 4.13:** Absorption spectra of a)  $\beta$ -CD-BIMOTs/flavanone b)  $\beta$ -CD-BIMOTs/hesperetin c)  $\beta$ -CD-BIMOTs/naringenin d)  $\beta$ -CD-BIMOTs/eriodictyol with  $[\beta$ -CD-BIMOTs]: 0.032mM [Flavonoids]: 0.01mM; T = 25 °C



**Table 4.7:**  $K$  values for  $\beta$ -CD-BIMOTs/flavonoids

Flavonoids	$K$
Flavanone	722
Hesperetin	572
Naringenin	1077
Eriodictyol	6032

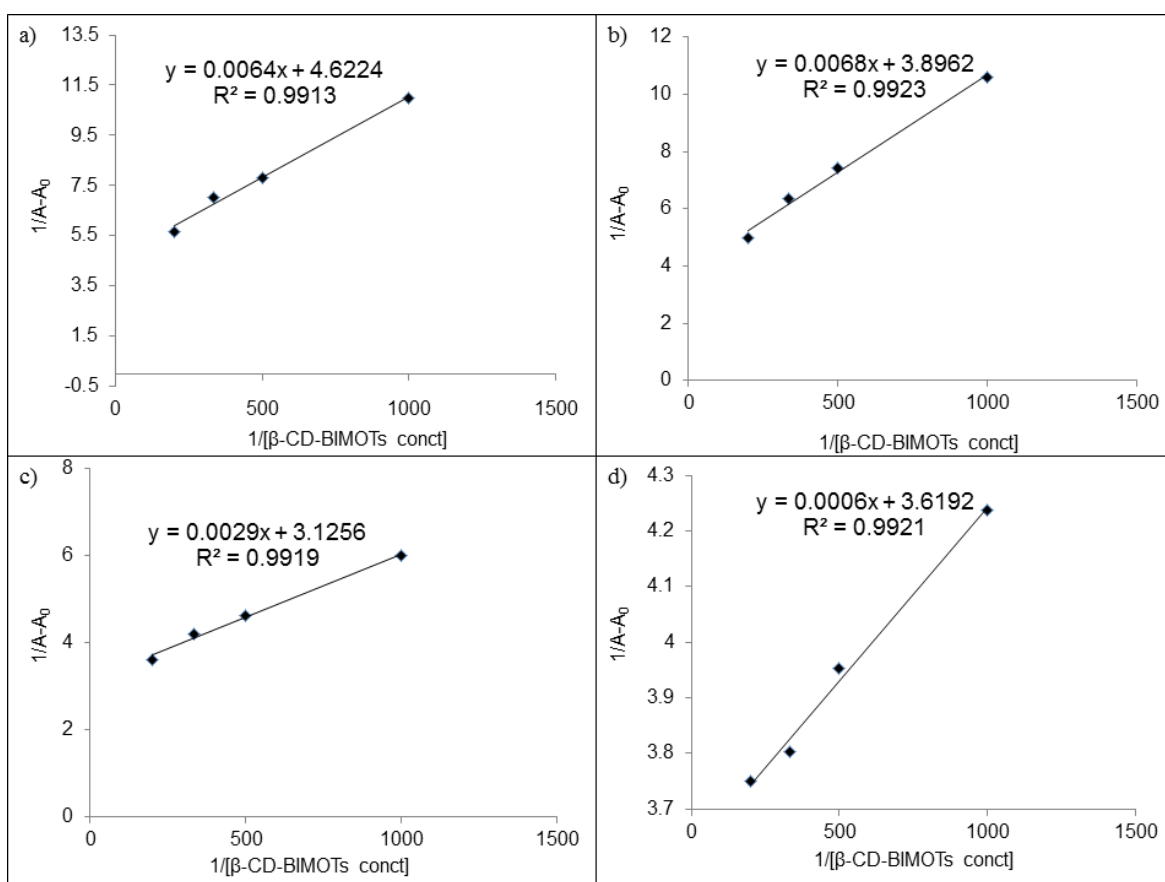


**Figure 4.14:** Benesi-Hildebrand plot of  $1/A-A_0$  versus  $1/[\beta\text{-CD-BIMOTs}]$  for a)  $\beta$ -CD-BIMOTs/flavanone, b)  $\beta$ -CD-BIMOTs/hesperetin, c)  $\beta$ -CD-BIMOTs/naringenin d)  $\beta$ -CD-BIMOTs/eriodictyol

#### 4.4 Enantioseparation performance of $\beta$ -blockers

The enantioselective ability of  $\beta$ -CD-BIMOTs CSP was also examined for chiral compounds with basic properties,  $\beta$ -blockers to study the enantiomeric behavior and the mechanism of enantioseparation. The baseline separation was achieved for the enantiomers of propranolol and metoprolol as shown in Table 4.8. Among the selected  $\beta$ -blockers, propranolol and metoprolol achieved the  $R_s$  values of 3.10 and 2.38, respectively. Complete enantioseparation of propranolol and metoprolol was achieved in 30 min. However, for pindolol and atenolol, no peak was observed even after 120 min due to the high retention of these compounds onto  $\beta$ -CD-BIMOTs CSP.  $\beta$ -Blockers can be divided according to its lipophilic (propranolol and metoprolol) and hydrophilic (pindolol and atenolol) nature (Borchard, 1998). The result indicated hydrophilic atenolol and pindolol with polar amide and indole moiety showed stronger interaction with CSP that contribute to high retention. On the other hand, it is proven that the  $\beta$ -blockers with lipophilicity properties were well enantioseparated than the hydrophilic  $\beta$ -blockers.

The enantioseparation of propranolol and metoprolol were separated excellently using  $\beta$ -CD-BIMOTs CSP and this might due to the formation of inclusion complex between the analytes and  $\beta$ -CD through the stereogenic center of  $\beta$ -CD located at the interior cavity. In order to verified this interaction, the inclusion complexes of  $\beta$ -CD-BIMOTs and selected  $\beta$ -blockers were prepared.  $^1\text{H}$  NMR and NOESY were used to study the interaction between  $\beta$ -CD-BIMOTs and  $\beta$ -blockers in the complexes. The values of the chemical shifts ( $\delta$ ) and induced shifts ( $\Delta\delta$ ) for different protons in  $\beta$ -CD-BIMOTs,  $\beta$ -blockers and  $\beta$ -CD-BIMOTs/ $\beta$ -blockers complexes are listed in Table 4.9 and Table 4.10.

**Table 4.8:** Chiral separation data for the  $\beta$ -blockers on  $\beta$ -CD-BIMOTs CSP in neutral pH mobile phase

$\beta$ -blockers	Conditions	$\beta$ -CD-BIMOTs CSP			
		$k_1'$	$k_2'$	$\alpha$	$R_s$
Atenolol	ACN/water-90/10	n.a	n.a	n.a	n.a
	ACN/water-50/50	n.a	n.a	n.a	n.a
	ACN/water-30/70	n.a	n.a	n.a	n.a
Metoprolol	ACN/water-90/10	2.04	3.64	1.78	2.38
	ACN/water-50/50	0.58	0.58	1.00	0
	ACN/water-30/70	0.65	0.65	1.00	0
Propranolol	ACN/water-90/10	2.83	4.88	1.72	3.10
	ACN/water-50/50	0.79	1.01	1.27	0.46
	ACN/water-30/70	0.84	1.10	1.30	0.43
Pindolol	ACN/water-90/10	n.a	n.a	n.a	n.a
	ACN/water-50/50	n.a	n.a	n.a	n.a
	ACN/water-30/70	n.a	n.a	n.a	n.a

n.a: not available

**Table 4.9:** Chemical shifts ( $\delta$ ) corresponding to  $\beta$ -CD-BIMOTs in presence of  $\beta$ -blockers

	$\beta$ -CD-BIMOTs	$\beta$ -CD-BIMOTs/ atenolol		$\beta$ -CD-BIMOTs/ metoprolol		$\beta$ -CD-BIMOTs/ propranolol		$\beta$ -CD-BIMOTs/ pindolol	
	$\delta$	$\delta$	$\Delta\delta$	$\delta$	$\Delta\delta$	$\delta$	$\Delta\delta$	$\delta$	$\Delta\delta$
H1	4.8405	4.8301	-0.0104	4.8249	-0.0156	4.8285	-0.012	4.8329	-0.0076
H2	3.3312	3.3483	0.0171	3.3425	0.0113	3.3042	-0.027	3.3476	0.0155
H3	3.6394	3.6311	-0.0083	3.6274	-0.0120	3.6309	-0.0085	3.6335	-0.0059
H4	3.3716	3.4304	<b>0.0588</b>	3.4660	<b>0.0944</b>	3.3762	0.0046	3.4391	<b>0.0675</b>
H5	3.5777	3.5488	-0.0289	3.5464	<b>-0.0313</b>	3.5531	<b>-0.0246</b>	3.5580	-0.0197
H6	3.9225	3.9473	0.0248	3.9272	0.0047	3.9041	-0.0184	3.9041	-0.0184
H8	7.4215	7.4212	-0.0003	7.4202	-0.0013	overlap	-	7.4361	0.0146
H9	7.1112	7.1227	0.0115	-	-	7.1192	0.0008	7.1259	0.0147
H11	2.0847	2.0797	-0.0050	-	-	-	-	-	-
Ha	7.4314	7.4798	<b>0.0484</b>	7.4752	<b>0.0438</b>	7.4832	<b>0.0518</b>	7.4896	<b>0.0582</b>
Hb	7.7957	7.7903	-0.0054	7.7892	0.0350	7.8063	0.0106	7.8081	0.0124
Hc	7.7542	7.7402	-0.014	7.7391	-0.0151	7.7490	-0.0052	7.7473	-0.0069
Hd	-	-	-	-	-	-	-	-	-
He	7.9563	7.9440	-0.0123	-	-	-	-	-	-
Hf	9.2394	9.2606	0.0212	9.2807	<b>0.0413</b>	9.3132	<b>0.0738</b>	9.3379	<b>0.0985</b>
Hg	5.4371	5.4400	0.0029	5.4460	0.0089	5.4369	-0.0002	5.4482	0.0111

 $\Delta\delta$ : induced shifts

-: overlap peak

**Table 4.10:** Induced shifts ( $\Delta\delta$ ) corresponding to  $\beta$ -blockers in presence of  $\beta$ -CD-BIMOTs

	$\beta$ -CD- BIMOTs/atenolol	$\beta$ -CD- BIMOTs/metoprolol	$\beta$ -CD- BIMOTs/propranolol	$\beta$ -CD- BIMOTs/pindolol
	$\Delta\delta$	$\Delta\delta$	$\Delta\delta$	$\Delta\delta$
Ha'	<b>0.1059</b>	0.0995	-0.0018	<b>0.1140</b>
Hb'	<b>0.1345</b>	0.0055	-	<b>0.2063</b>
Hc'	<b>0.1060</b>	0.0995	-0.0018	<b>0.1140</b>
Hd'	-	-0.0075	-0.0160	-0.0067
He'	<b>0.1596</b>	-0.0057	-0.0044	<b>0.1766</b>
Hf'	0.0545	-	-0.0063	-
Hg'	-	-0.0075	<b>-0.0246</b>	-0.0067
Hh'	-0.0008	<b>-0.0269</b>	<b>0.0794</b>	0.0248
Hi'	0.0118	0.0048	-0.0012	0.0041
Hj'	0.0096	0.0064	-0.0027	0.0162
Hk'	0.0096	-0.0009	-0.0025	0.0162
Hi'	0.0132	0.0003	<b>-0.0131</b>	<b>0.0836</b>
Hm'	0.0054	-	-0.0037	-0.0006
Hn'	-	-	-0.0011	0.0056
Ho'	-	-	-0.0055	-

-: overlap peak

The deduced structures of  $\beta$ -CD-BIMOTs/ $\beta$ -blockers complexes are shown in Figure 4.15. For  $\beta$ -CD-BIMOTs/ $\beta$ -blockers complexes, the presence of propranolol and metoprolol showed appreciable shift of H5 proton of  $\beta$ -CD-BIMOTs (Table 4.9). The upfield shifts for this proton proved the existence of an interaction between the analytes and the interior proton of  $\beta$ -CD-BIMOTs. Additionally, the larger  $\Delta\delta$  value of H1' proton was observed for propranolol (Table 4.10). This indicated the perturbation at the aromatic ring of propranolol which might due to  $\pi$ - $\pi$  interaction with IL at  $\beta$ -CD-BIMOTs. In contrast, the  $\Delta\delta$  values of aromatic protons (Hi', Hj', Hk', Hl') of metoprolol were relatively small (Table 4.10). This result suggested that propranolol achieved better enantioseparation than metoprolol because of the additional  $\pi$ - $\pi$  interaction that contributed by IL at  $\beta$ -CD-BIMOTs. Moreover, the greater shift of H4 proton of  $\beta$ -CD-BIMOT-metoprolol was observed as compared to other complexes. Higher electronegativity of oxygen atom at the methoxy group of metoprolol caused the lower electron density around the H4 proton. As a result, the proton was deshielded and experienced higher chemical shift. In Figure 4.16, the cross peak between Hm' and Hn' protons of propranolol with H5 proton  $\beta$ -CD-BIMOTs complex was observed in NOESY spectra. Meanwhile, in Figure 4.17, the cross peak between Hi' and Hj' protons of metoprolol with H5 proton of  $\beta$ -CD-BIMOTs complex was also observed. This indicated the interaction of propranolol and metoprolol at the interior protons of  $\beta$ -CD-BIMOTs.

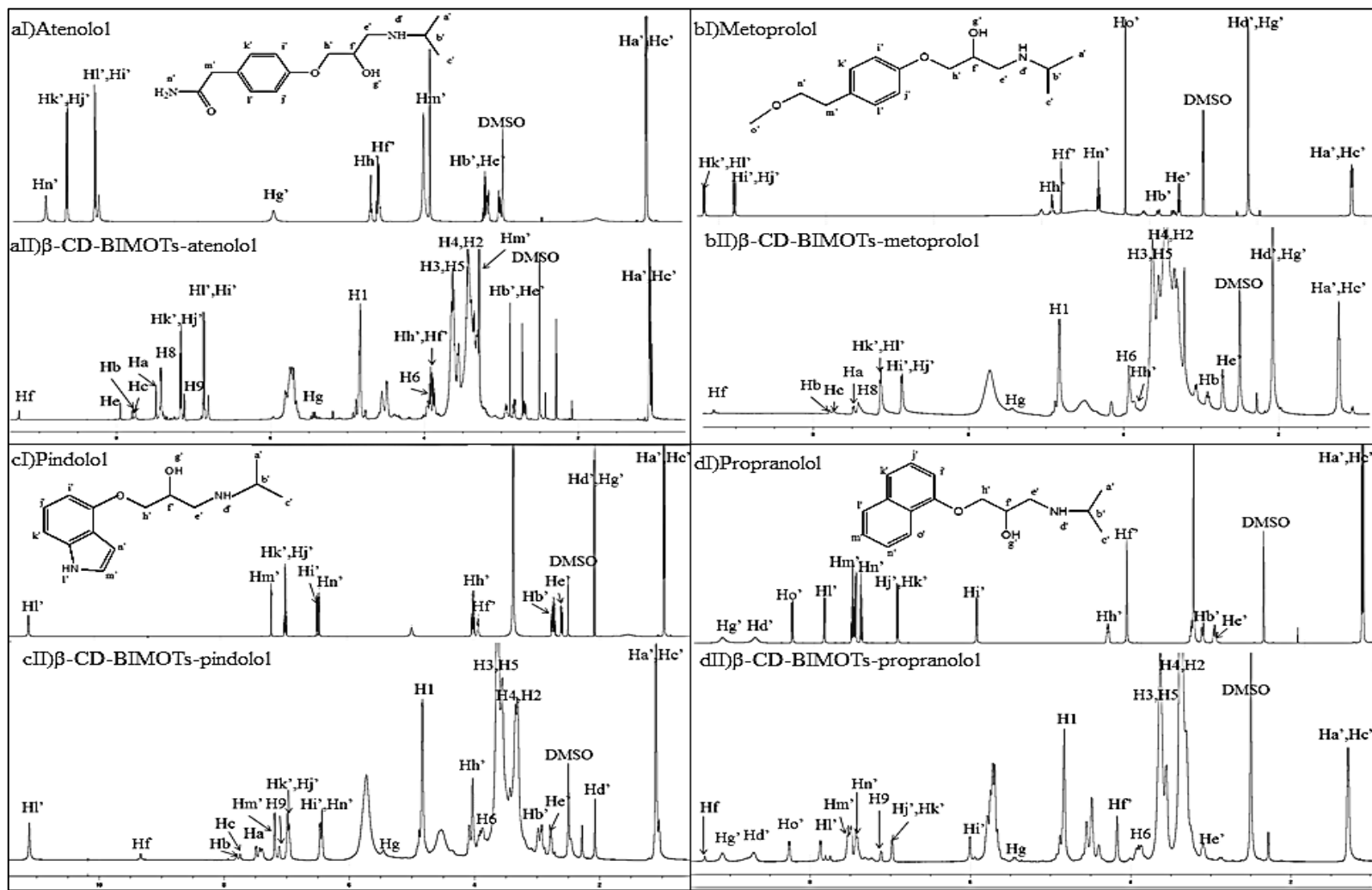


**Figure 4.15:** The deduced structure of  $\beta$ -CD-BIMOTs/ $\beta$ -blockers complexes: a) atenolol, b) metoprolol, c) Pindolol, d) Propranolol

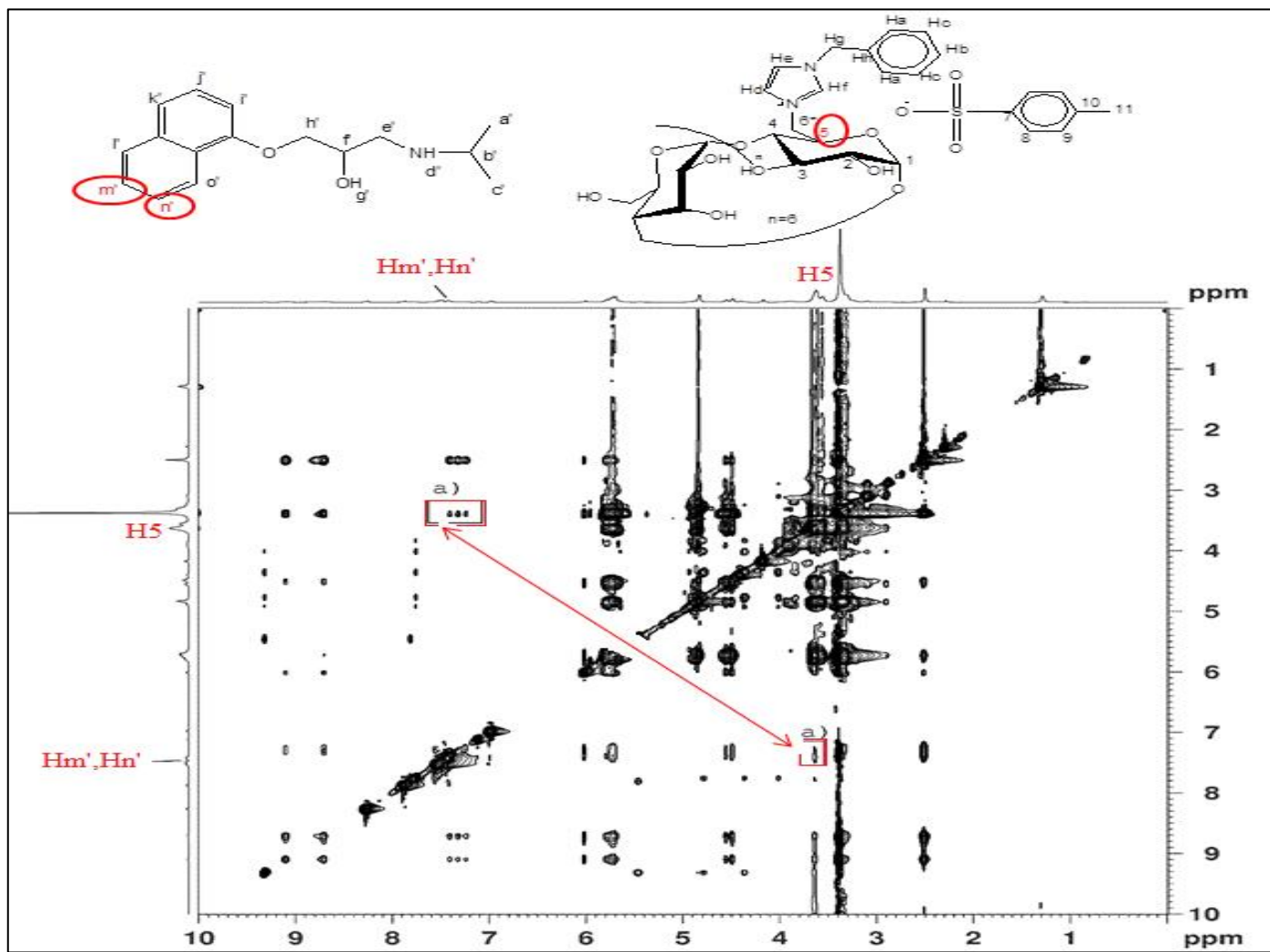


Figure 4.16: 2D NOESY spectra of  $\beta$ -CD-BIMOTs/propranolol complex



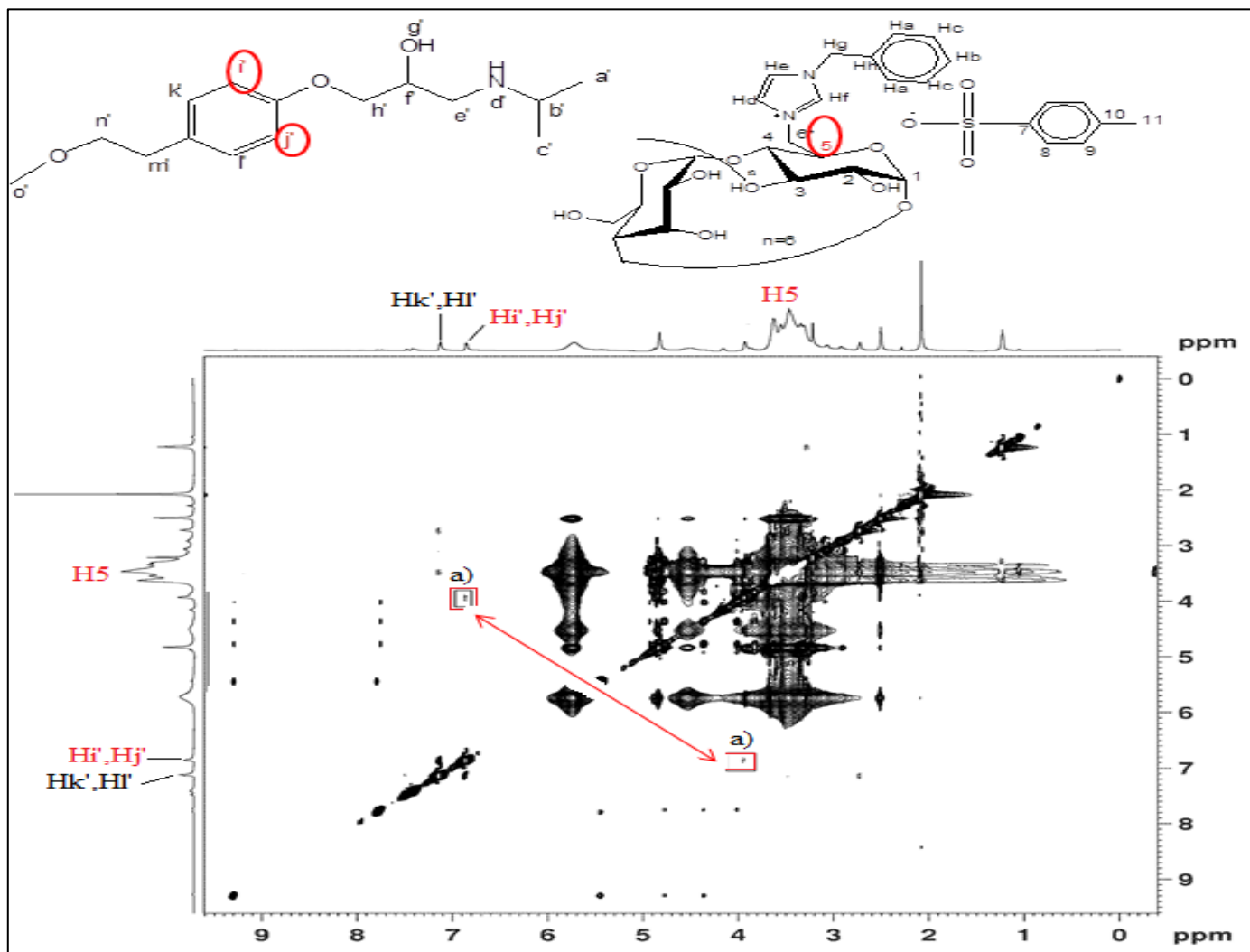
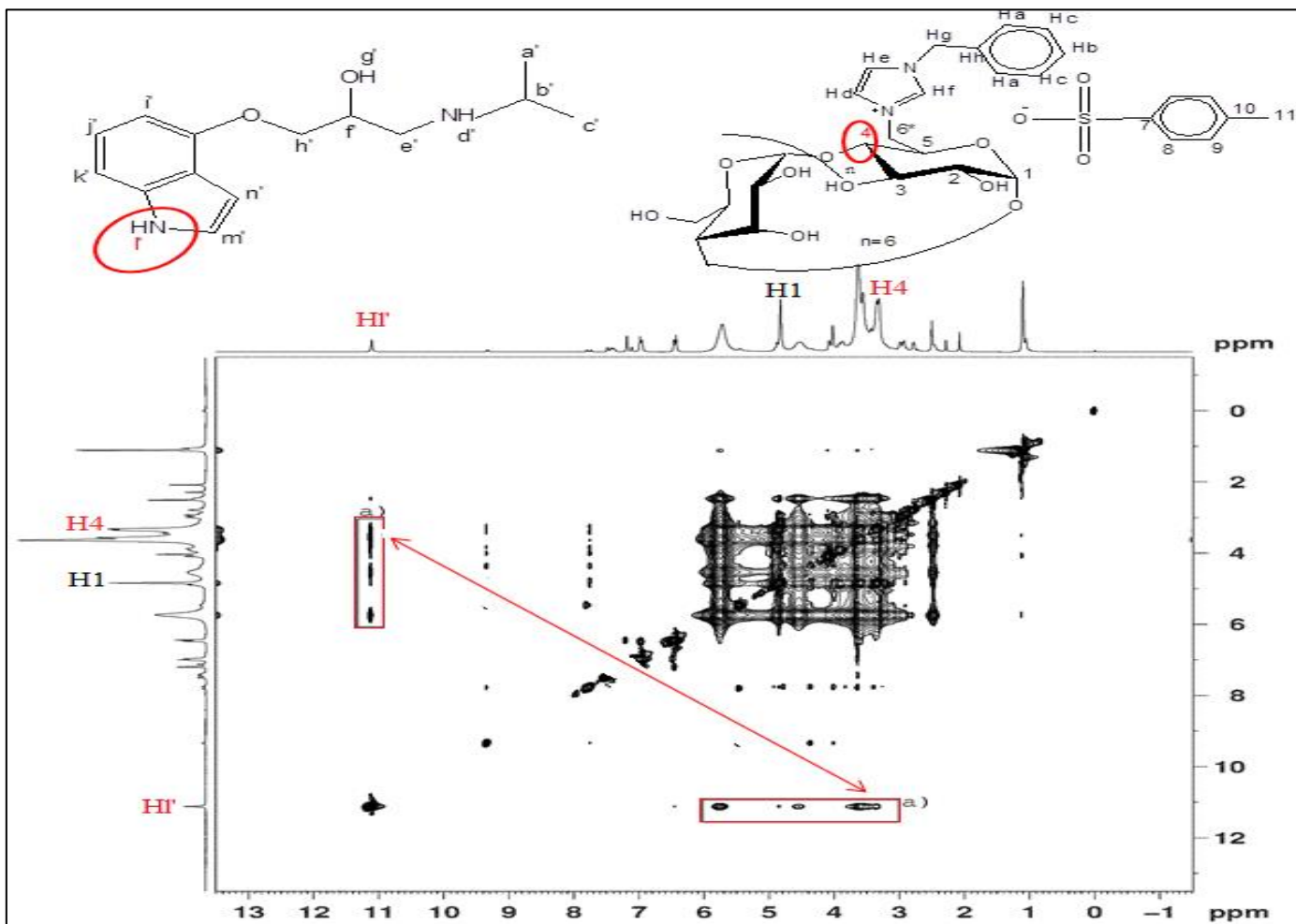


Figure 4.17: 2D NOESY spectra of  $\beta$ -CD-BIMOTs/metoprolol complex

From the  $^1\text{H}$  NMR studied (Table 4.9), H4 (exterior proton) at  $\beta$ -CD-BIMOTs was experienced appreciably shifted downfield after forming complexes with pindolol or atenolol. This result suggested that pindolol and atenolol were not forming inclusion complex but it formed hydrogen bonding with exterior torus of  $\beta$ -CD-BIMOTs. Moreover, the large  $\Delta\delta$  values were observed for Ha', Hb' and Hc' of pindolol and atenolol (Table 4.10). For  $\beta$ -CD-BIMOTs/pindolol complex, the NOESY spectra showed the cross-peak between Hl' proton of pindolol with H1 and H4 protons of  $\beta$ -CD-BIMOTs (Figure 4.18). Meanwhile,  $\beta$ -CD-BIMOTs/atenolol complex showed the cross-peak between Hj' and Hk' protons of atenolol and H4 protons of  $\beta$ -CD-BIMOTs (Figure 4.19). This result indicated the close interaction of pindolol and atenolol at the exterior protons of  $\beta$ -CD-BIMOTs

The composition of the mobile phase also plays an important role in enantioseparation. The effect of ACN contents on enantioseparation of selected  $\beta$ -blockers can be seen from Table 4.8. The high  $k_1'$  and  $k_2'$  of propranolol and metoprolol at high organic content (90 % ACN) showed the normal phase behavior of the  $\beta$ -CD-BIMOTs CSP. On the other hand, when organic content is low (30 % ACN), the high  $k_1'$  and  $k_2'$  of propranolol and metoprolol showed typical reverse phase behavior of  $\beta$ -CD-BIMOTs CSP. Therefore, the retention behavior of  $\beta$ -blockers can be considered as the mixed reverse-normal separation mode (Guo *et al.*, 2009). In this separation mode, the retention mechanism is based on the distribution of the analytes between the ACN-rich mobile phase and water enriched layer adsorbed onto the polar stationary phase (Buszewski & Noga, 2012). Thus, for more hydrophilic analytes (pindolol and atenolol), partitioning equilibrium is shifted towards the immobilized water layer on the stationary phase, causing the analytes retained longer in column.



**Figure 4.18:** 2D NOESY spectra of  $\beta$ -CD-BIMOTs/pindolol complex

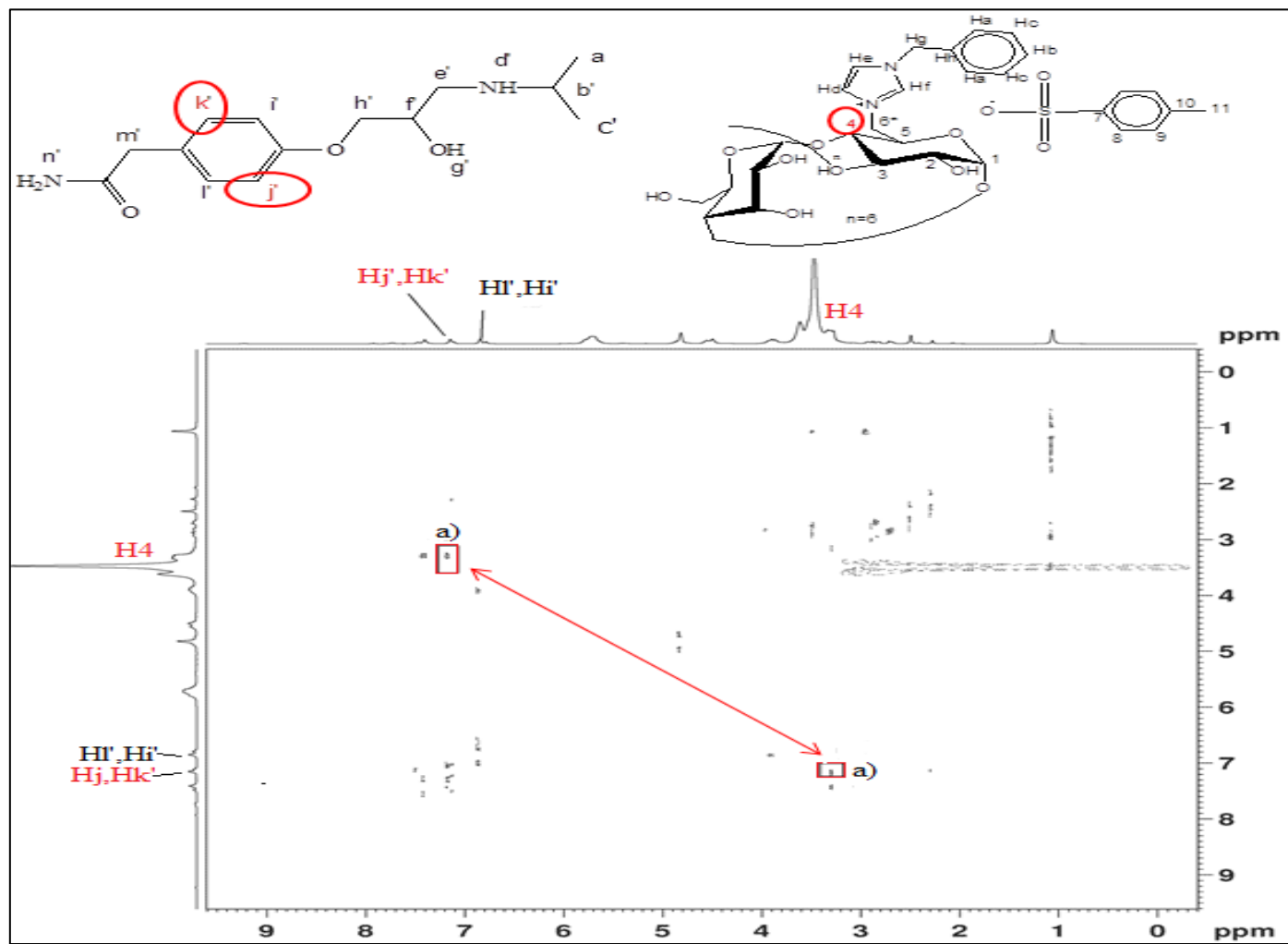
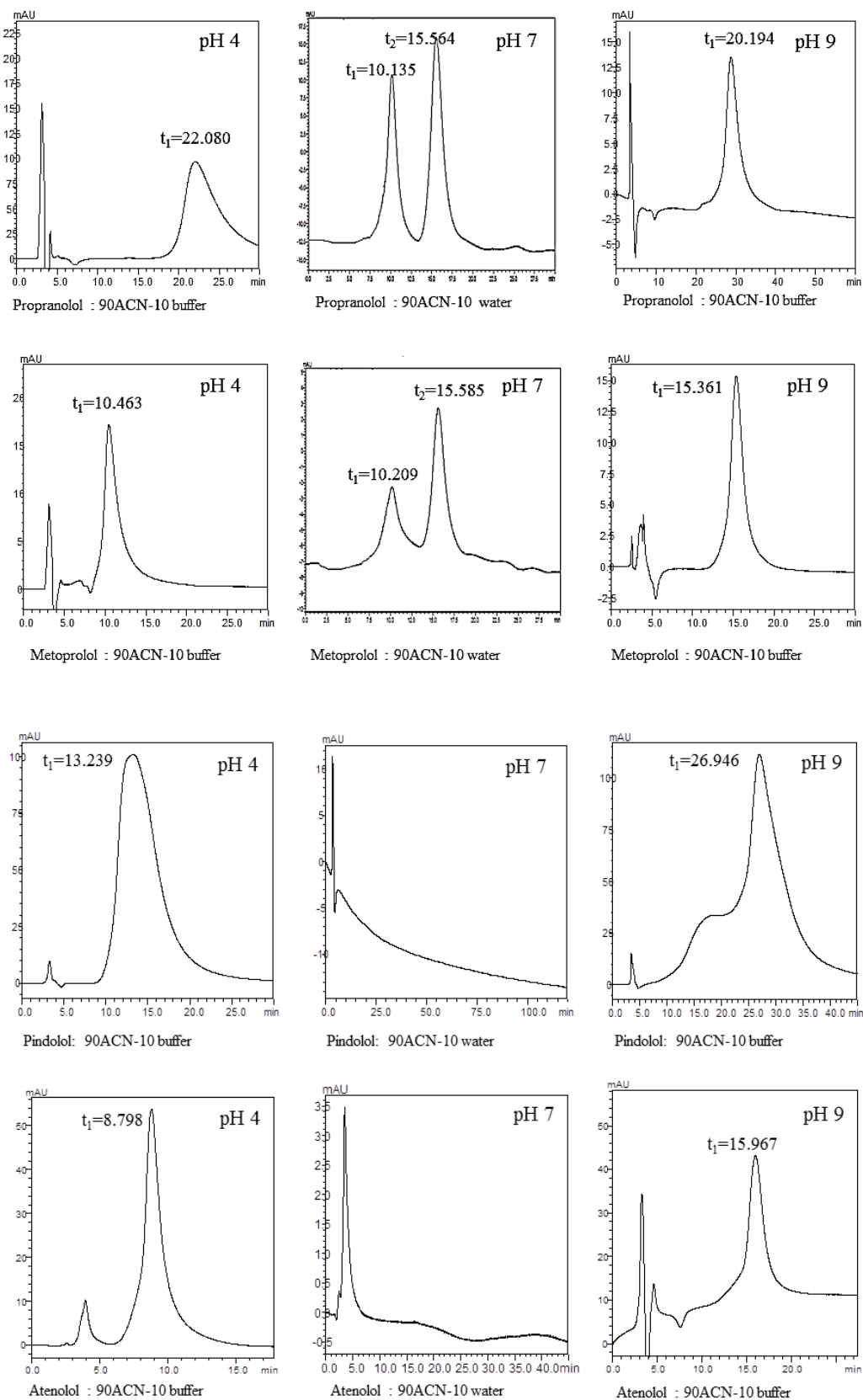


Figure 4.19: 2D NOESY spectra of  $\beta$ -CD-BIMOTs/atenolol complex

TEAA buffer was used to control the pH of mobile phase and ionic strength. Buffer can influence the degree of ionization of analytes and resulting in different retention behavior. The chromatograms in Figure 4.20 show the effect of pH towards the enantioseparation of  $\beta$ -blockers. Propranolol and metoprolol were not enantioseparated at pH 4 and 9. Meanwhile, they are well enantioseparated at pH 7. This is due to the deprotonation and protonation of  $\beta$ -blockers at pH 4 and 9, respectively. Protonated and deprotonated analytes were not favorable for the formation of inclusion complex with  $\beta$ -CD (Raoov *et al.*, 2013). This finding further support the role of inclusion complex formation in enantioseparation of  $\beta$ -CD based CSPs. Meanwhile, the retention time of pindolol and atenolol was reduced at pH 4 and 9 as compared to pH 7. Due to both of analytes and  $\beta$ -CD-BIMOTs CSP acquiring positive charges at pH 4, the electrostatic repulsion occurred and it reduced the retention time of analytes. At basic pH, the abundance of TEAA species reduces the retention time due to the competition between TEAA and protonated analytes.



**Figure 4.20:** The chromatograms of propranolol, metoprolol, pindolol and atenolol responding to different pH of mobile phase

#### 4.5 Enantioseparation performance of NSAIDs

In the final part of this work, the enantioselective ability of  $\beta$ -CD-BIMOTs CSP was examined using chiral compounds with acidic properties, NSAIDs. The influence of mobile phase on the separation of the NSAIDs enantiomers was investigated. The effect of organic solvents (ACN and MeOH) on retention time and resolution was also evaluated (Table 4.11). The  $R_s$  values for all selected NSAIDs were higher in ACN mobile phase. Compared to MeOH, ACN has greater solvent strength, therefore less retention were found at equivalent volume of mobile phase (50 %).

The effect of the amount of ACN on enantioseparation of selected NSAIDs was evaluated by varying the percentage of ACN in mobile phase (Table 4.11). The high  $k_1'$  and  $k_2'$  of NSAIDs at 90 % of ACN showed the normal phase behavior of the  $\beta$ -CD-BIMOTs-CSP. On the other hand, when at 30 % of ACN, the high  $k_1'$  and  $k_2'$  of NSAIDs showed the typical reverse phase behavior of  $\beta$ -CD-BIMOTs CSP. Therefore, the retention behavior of NSAIDs can be considered as the mixed reverse-normal separation mode (Guo *et al.*, 2009) similar with the retention behavior of  $\beta$ -blockers.

As given in Table 4.11, ibuprofen was completely resolved with  $R_s$  value of 2.51. Indoprofen showed partial separation with  $R_s$  value of 1.09. Ketoprofen and fenoprofen also partially enantioseparated with fenoprofen attained the lowest  $R_s$  value of 0.54. The high  $R_s$  values of ibuprofen and indoprofen are probably due to the *para* position of the substituent (containing the chiral center) on the aromatic ring. Previous study revealed that *para*-substituted aromatic rings can fit properly into the CD cavity (Fanali & Aturki, 1995) forming inclusion complex. However, the extent of the penetration mode is also depending on the polarity and feature structure of analytes (Nunez-Aguero *et al.*, 2006). Thus, this result showed that the hydrophobic ibuprofen achieved better enantioseparation than more polar indoprofen (Velkov *et al.*, 2007).

Meanwhile, the relatively low  $R_s$  values of ketoprofen and fenoprofen were because its substituent that located at *meta* position (Fanali & Aturki, 1995) that make their orientation in an unfavorable way to fit into the  $\beta$ -CD-BIMOTs cavity.

**Table 4.11:** Chiral separation data for the NSAIDs on  $\beta$ -CD-BIMOTs CSP

NSAID	Condition	$k_1'$	$k_2'$	$\alpha$	$R_s$
Ibuprofen	ACN/water-90/10	0.29	1.17	4.04	2.51
	ACN/water-50/50	0.43	0.43	1.00	0
	ACN/water-30/70	1.23	1.23	1.00	0
	MeOH/water-90/10	0.16	0.16	1.00	0
	MeOH/water-50/50	0.77	0.77	1.00	0
Indoprofen	ACN/water-90/10	3.35	3.35	1.00	0
	ACN/water-50/50	0.15	0.51	3.39	1.09
	ACN/water-30/70	0.16	0.48	3.02	0.68
	MeOH/water-90/10	0.26	0.26	1.00	0
	MeOH/water-50/50	3.23	3.23	1.00	0
Ketoprofen	ACN/water-90/10	0.76	1.01	1.33	0.43
	ACN/water-50/50	0.46	0.94	2.06	0.72
	ACN/water-30/70	0.52	1.14	2.20	0.88
	MeOH/water-90/10	2.54	2.54	1.00	0
	MeOH/water-50/50	5.12	5.12	1.00	0
Fenoprofen	ACN/water-90/10	1.04	1.04	1.00	0
	ACN/water-50/50	0.07	0.07	1.00	0
	ACN/water-30/70	0.11	0.50	4.55	0.54
	MeOH/water-90/10	0.06	0.06	1.00	0
	MeOH/water-50/50	1.05	1.05	1.00	0



Even though the polarity of fenoprofen and ibuprofen are close to each other ( $\log P_{\text{fenoprofen}}=3.8$ ,  $\log P_{\text{ibuprofen}}=3.7$ ) (Velkov *et al.*, 2007), ibuprofen achieved higher  $R_s$  value at high organic solvent content (90 % ACN) mobile phase. This result suggested that ibuprofen can be fitted into  $\beta$ -CD-BIMOTs cavity whereas fenoprofen with two aromatic rings was less favorable to be fitted into  $\beta$ -CD-BIMOTs cavity due to steric hindrance effect. Previous simulation study (Nunez-Aguero *et al.*, 2006) showed the formation of moderate and weak hydrogen bonding between the carboxyl group of ibuprofen and hydroxyl groups of  $\beta$ -CD during complexation. Therefore, a part of inclusion complex formation, hydrogen bonding also plays a role to enhance the enantioseparation of NSAIDs. Additionally, ketoprofen which composed of almost similar structure (two aromatic rings) as fenoprofen achieved better enantioseparation than fenoprofen. This might due to the presence of carbonyl group in ketoprofen which enhanced the formation of hydrogen bonding with  $\beta$ -CD-BIMOTs rather than ether linkage in fenoprofen (Lommerse *et al.*, 1997).

In order to verify the interactions of enantioseparation,  $^1\text{H}$  NMR and NOESY of  $\beta$ -CD-BIMOTs/NSAIDs complexes were studied. The values of chemical shifts ( $\delta$ ) obtained from  $^1\text{H}$  NMR for different protons in  $\beta$ -CD-BIMOTs, NSAIDs and  $\beta$ -CD-BIMOTs/NSAIDs complexes are listed in Table 4.12 and 4.13. The deduced structures  $\beta$ -CD-BIMOTs/NSAID complexes are shown in Figure 4.21, respectively.

**Table 4.12:** Chemical shifts ( $\delta$ ) corresponding to  $\beta$ -CD-BIMOTs in the presence of NSAIDs

	$\beta$ -CD- BIMOTs	$\beta$ -CD-BIMOTs/ Ibuprofen	$\beta$ -CD-BIMOTs/ Indoprofen	$\beta$ -CD-BIMOTs/ Ketoprofen	$\beta$ -CD-BIMOTs/ Fenoprofen				
	$\delta$	$\delta$	$\Delta\delta$	$\delta$	$\Delta\delta$	$\delta$	$\Delta\delta$	$\delta$	$\Delta\delta$
H1	4.8405	4.8369	-0.0036	4.8316	-0.0089	4.8337	-0.0068	4.8280	-0.0125
H2	3.3312	3.3200	-0.0112	3.3474	0.0162	3.3015	-0.0297	3.3118	-0.0194
H3	3.6394	3.6387	-0.0007	3.6323	-0.0071	3.6284	-0.011	3.6326	-0.0068
H4	3.3716	3.4056	<b>0.0340</b>	3.4292	<b>0.0576</b>	3.3985	0.0269	3.4132	<b>0.0416</b>
H5	3.5777	3.5597	<b>-0.018</b>	3.5536	<b>-0.0241</b>	3.5458	<b>-0.0319</b>	3.5530	<b>-0.0247</b>
H6	3.9225	3.9091	-0.0134	3.9045	-0.018	3.9048	-0.0177	3.8803	-0.0422
H8	7.4215	7.4422	0.0207	7.4318	0.0103	7.4182	-0.0033	7.4209	-0.0006
H9	7.1112	7.1189	-0.0077	7.1268	0.0156	7.1196	-0.0084	-	-
H11	2.0847	-	-	-	-	-	-	-	-
Ha	7.4314	7.4877	<b>0.0563</b>	7.4835	<b>0.0521</b>	7.4737	<b>0.0423</b>	7.4834	<b>0.052</b>
Hb	7.7957	7.8149	0.0192	-	-	-	-	7.7896	-0.0061
Hc	7.7542	7.7516	-0.0026	-	-	-	-	7.7410	-0.0132
Hd	-	-	-	-	-	-	-	-	-
He	7.9563	7.9921	<b>0.0358</b>	-	-	7.9378	-0.0185	7.9399	-0.0164
Hf	9.2394	9.3362	<b>0.0968</b>	9.3202	<b>0.0808</b>	9.2240	-0.0154	9.3217	<b>0.0823</b>
Hg	5.4371	5.4514	0.0143	5.4146	-0.0225	5.4036	-0.0335	5.4459	-0.0088

 $\Delta\delta$ : induced shifts

-: overlap peak

**Table 4.13:** Induced shifts ( $\Delta\delta$ ) corresponding to NSAIDs in the presence of  $\beta$ -CD-BIMOTs

	$\beta$ -CD-BIMOTs/ Ibuprofen	$\beta$ -CD-BIMOTs/ Indoprofen	$\beta$ -CD-BIMOTs/ Ketoprofen	$\beta$ -CD-BIMOTs/ Fenoprofen
	$\Delta\delta$	$\Delta\delta$	$\Delta\delta$	$\Delta\delta$
Ha'	-0.0022	-0.0044	<b>-0.0183</b>	0.0132
Hb'	-0.0041	-0.0022	-0.0048	0.0133
Hc'	<b>0.0072</b>	-0.0044	-0.0083	0.0132
Hd'	-0.0030	<b>-0.0141</b>	-0.0070	<b>0.0677</b>
He'	-0.0033	-0.0051	<b>-0.0119</b>	<b>0.0677</b>
Hf'	-0.0023	-0.0081	-0.0083	0.0237
Hg'	-0.0011	-0.0081	-0.0052	0.0238
Hh'	-0.0020	-0.0086	-0.0046	0.0373
Hi'	-	-0.0086	-0.0042	0.0099
Hj'	-0.0029	-	<b>0.0155</b>	-
Hk'	-	-0.0235	-0.0098	0.0258

-: overlap peak

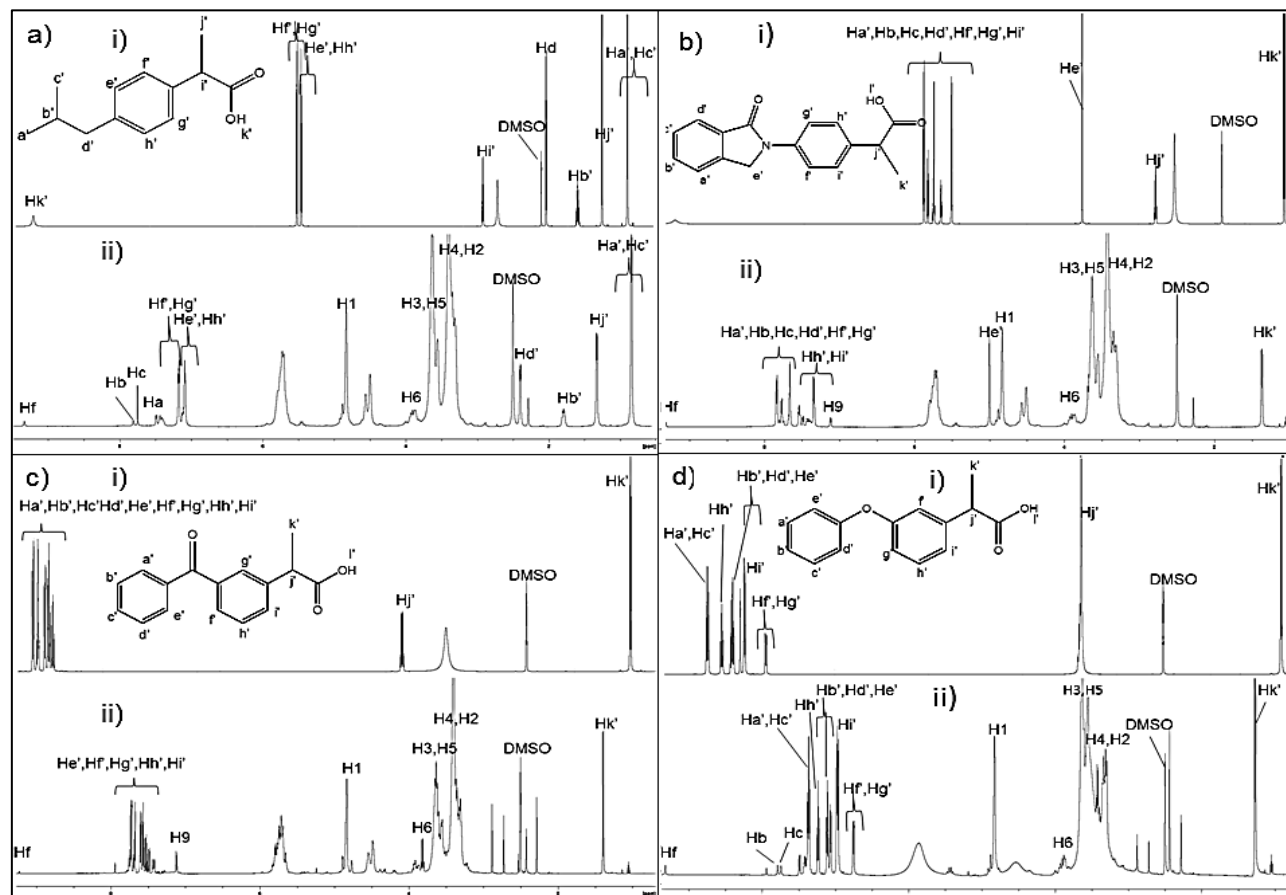


**Figure 4.21:** The deduced structure of NSAID/ $\beta$ -CD-BIMOTs complexes: (a) i) ibuprofen ii)  $\beta$ -CD-BIMOTs/ibuprofen, (b) i) indoprofen ii)  $\beta$ -CD-BIMOTs/indoprofen (c) i) ketoprofen ii)  $\beta$ -CD-BIMOTs/ketoprofen, (d) i) fenoprofen ii)  $\beta$ -CD-BIMOTs/fenoprofen

The presence of ibuprofen, indoprofen, ketoprofen and fenoprofen was found to cause appreciable shift at H4 and H5 protons of  $\beta$ -CD-BIMOTs (Table 4.12) due to the formation of hydrogen bonding and inclusion complex, respectively. Significant change at Hc' proton of ibuprofen (Table 4.13) was observed. This result indicated that isobutyl moiety of ibuprofen was included into the cavity of  $\beta$ -CD-BIMOTs. However, the cross peak between proton of isobutyl ibuprofen with H5 proton of  $\beta$ -CD is absent in the NOESY spectra of  $\beta$ -CD-BIMOTs/ibuprofen (Figure 4.22). Perhaps, the great difference between isobutyl size and the internal  $\beta$ -CD diameter, ( $\approx 4.3$  and  $7.8$  Å, respectively) is responsible for this weak interaction (Nunez-Aguero *et al.*, 2006). But, there were cross peak between Hf', Hg' and Hj' protons of ibuprofen with H5 proton of  $\beta$ -CD-BIMOTs confirmed the penetration aromatic moiety into the  $\beta$ -CD-BIMOTs cavity. The appreciable shift was also observed for the aromatic proton of indoprofen (Hd', Hh', Hi'), ketoprofen (Ha', He') and fenoprofen (Hd', He') (Table 4.13) as evidenced of inclusion complexes. This result was further strengthened with the NOESY spectra of  $\beta$ -CD-BIMOTs/indoprofen,  $\beta$ -CD-BIMOTs/ketoprofen and  $\beta$ -CD-BIMOTs/fenoprofen (Figure 4.23-4.25) showed the cross-peak between Hh', Hi' (proton indoprofen), He' (proton ketoprofen) and Ha', Hc', Hi' (proton fenoprofen) with H5 proton of  $\beta$ -CD-BIMOTs.

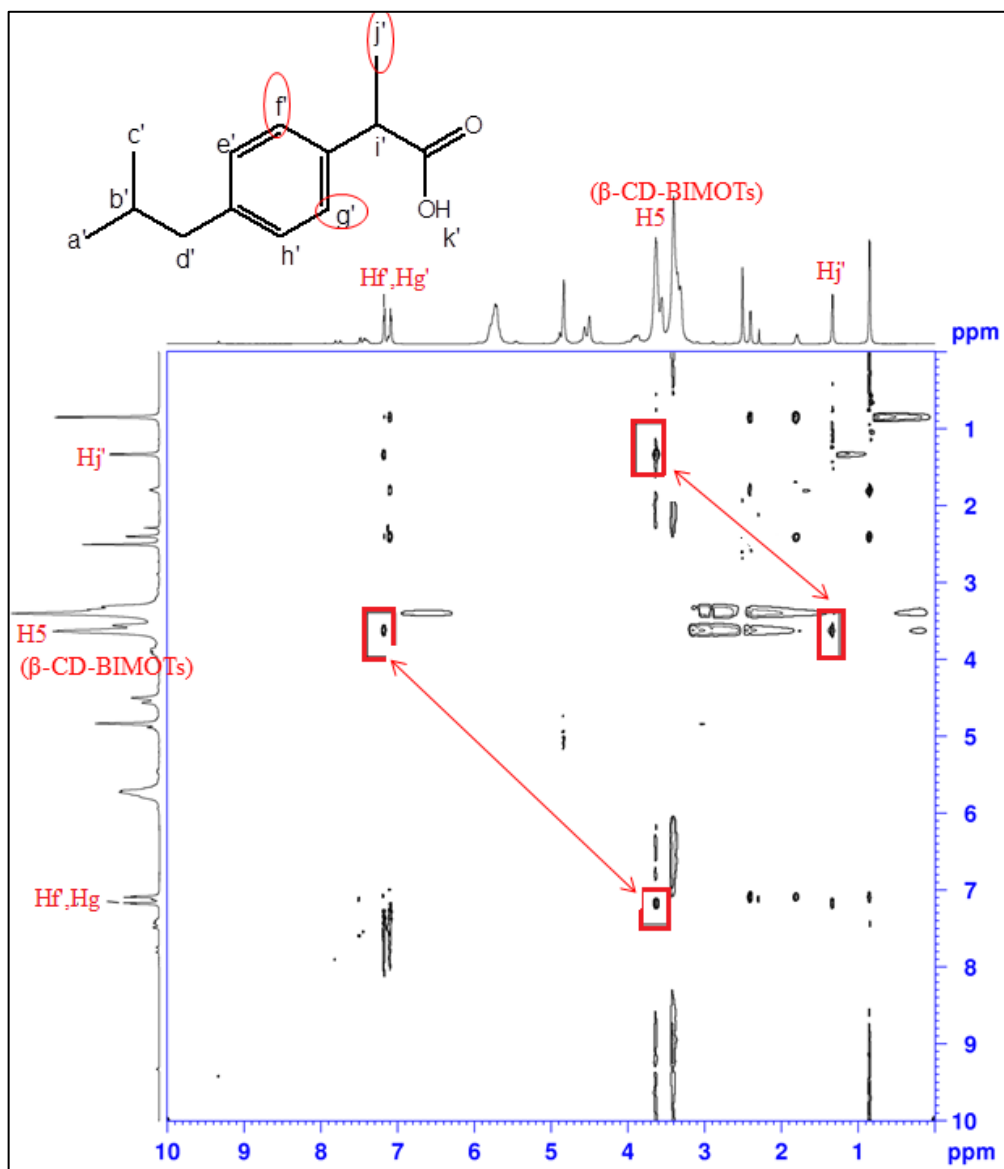


**Figure 4.22:** NOESY spectra of  $\beta$ -CD-BIMOTs/ibuprofen

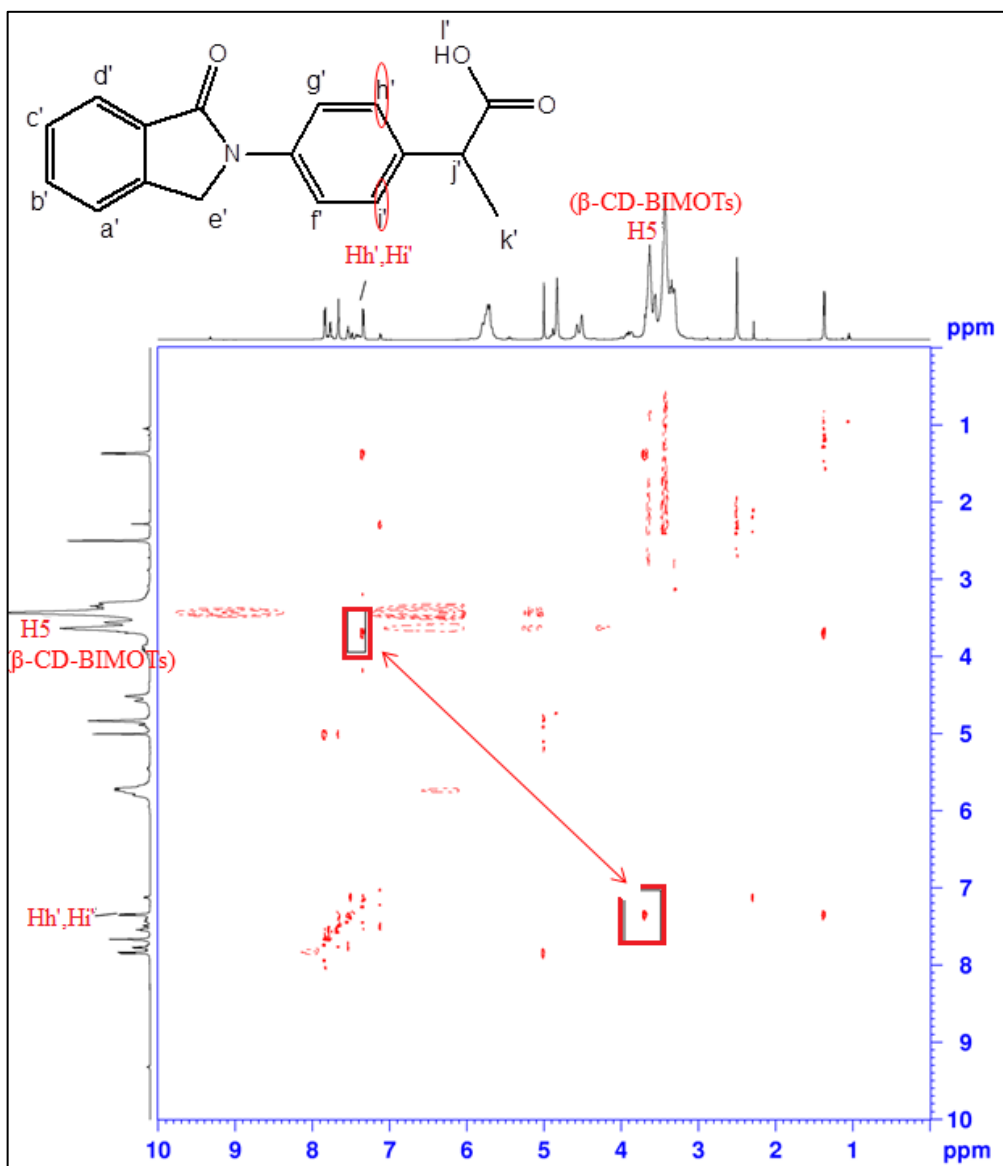


**Figure 4.23:** NOESY spectra of  $\beta$ -CD-BIMOTs/indoprofen

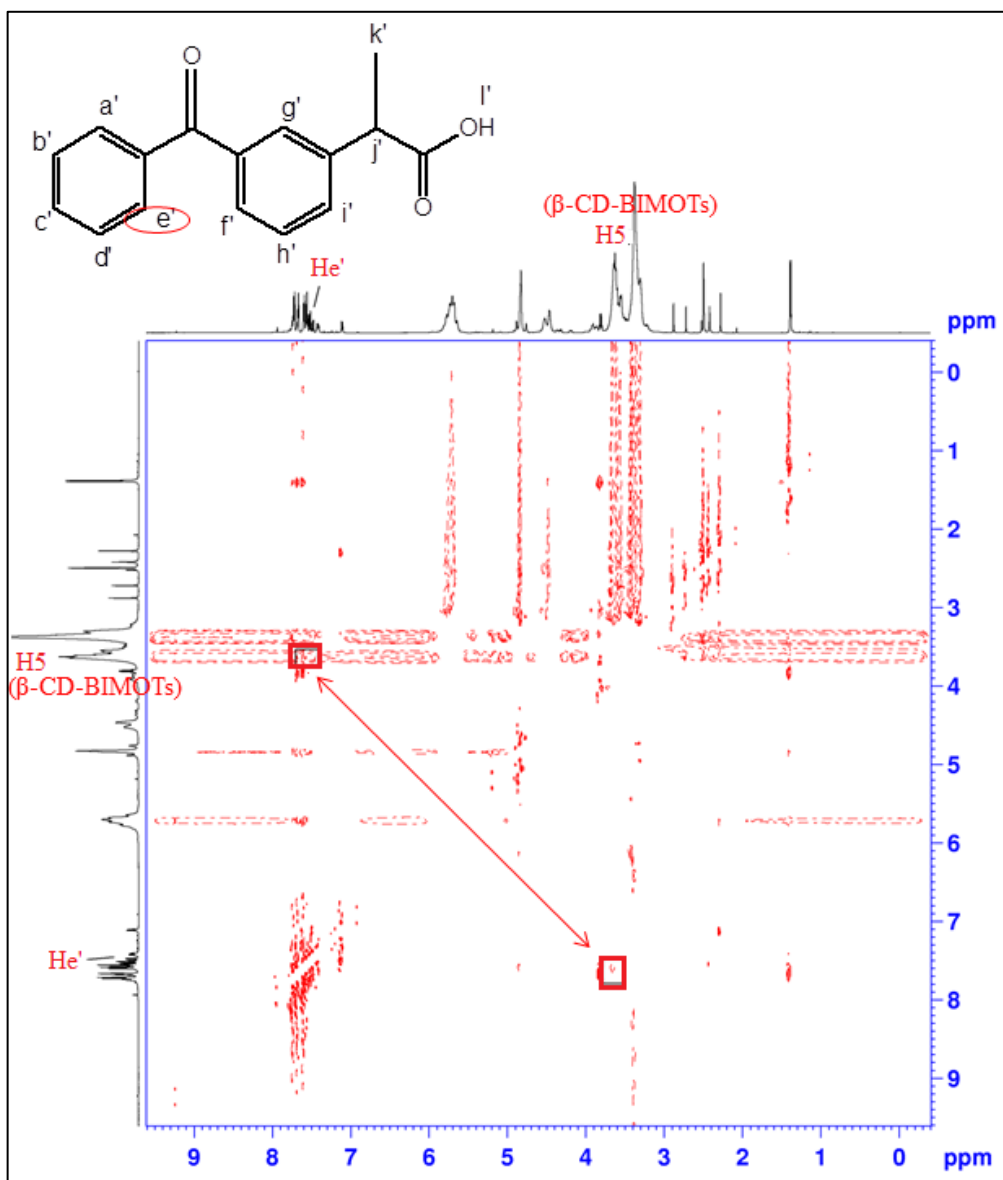


**Figure 4.24:** NOESY spectra of  $\beta$ -CD-BIMOTs/ketoprofen



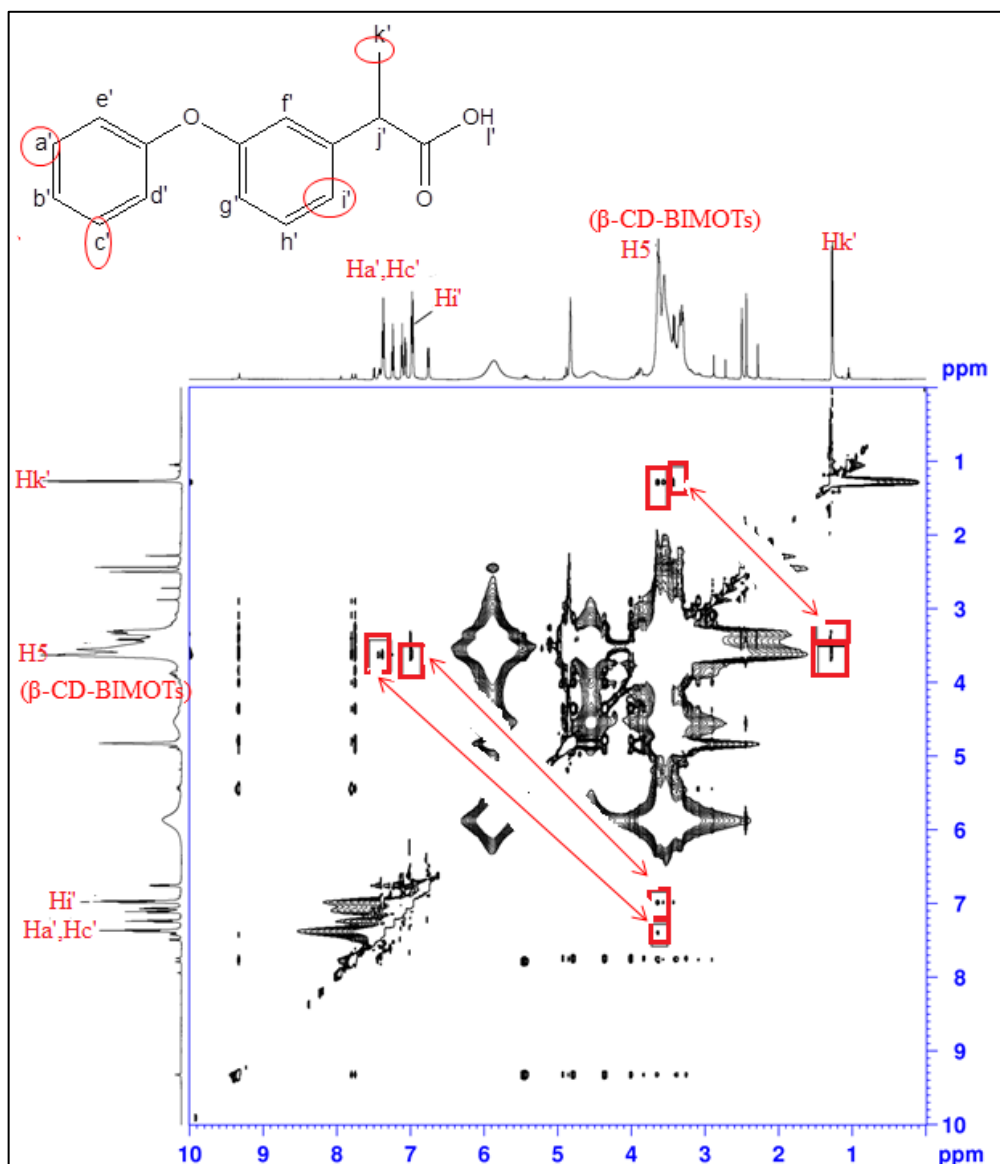


**Figure 4.25:** NOESY spectra of β-CD-BIMOTs/phenopfen

The UV/Vis absorption spectra of  $\beta$ -CD-BIMOTs/NSAIDs complexes were further investigated to acquire more information on the interaction between NSAIDs and  $\beta$ -CD-BIMOTs. The plots of UV/Vis absorption for  $\beta$ -CD-BIMOTs, NSAIDs and  $\beta$ -CD-BIMOTs/NSAIDs complexes are presented in Figure 4.26. The results showed that  $\beta$ -CD-BIMOTs showed a  $\lambda_{\max}$  in the range of 230-260 nm. The  $\lambda_{\max}$  of  $\beta$ -CD-BIMOTs/ibuprofen,  $\beta$ -CD-BIMOTs/indoprofen and  $\beta$ -CD-BIMOTs/fenoprofen complexes appeared at 262, 256 and 256 nm, respectively referring to  $\beta$ -CD-BIMOTs. This absorbance undergoes the hyperchromic effect (increased of absorbance) and shifted bathochromically (change of absorbance to a lower frequency). Meanwhile, the absorbance of  $\beta$ -CD-BIMOTs/ketoprofen experienced the hypochromic effect (decreased of absorbance). The bathochromical shift is because of partial shielding of the chromophore electrons (Wang *et al.*, 2011a) in the  $\beta$ -CD-BIMOTs cavity. Both of hyperchromic and hypochromic effects was due to the  $\pi$ - $\pi^*$  transition of dipole moments of aromatic ring. The transition dipole moment of this chromophore will interact with the induced dipoles of the neighboring chromophores, depending on their relative orientation. If the dipoles are along the same axis and one behind the other, then the intensity of the absorption band will be increased, and hyperchromic effect is observed. Conversely, if the dipoles are parallel and adjacent, a decrease in intensity of the absorption band occurs, and hypochromic effect is observed (Peral & Gallego, 2000). Moreover, hypochromic effect on  $\beta$ -CD-BIMOTs/ketoprofen also attribute by the limitation for  $\pi$ - $\pi^*$  transition because of hydrogen bonding (Peral & Gallego, 2000) at carbonyl group between aromatic rings of ketoprofen. The variations that occur in the UV/Vis spectra are consequence of complexation of NSAIDs with  $\beta$ -CD-BIMOTs accompanied by  $\pi$ - $\pi$  interaction and hydrogen bonding. These results proved the role of IL which provides  $\pi$ - $\pi$  interaction which is the superposition of inclusion complex and hydrogen bond for the enantioseparation of NSAIDs.

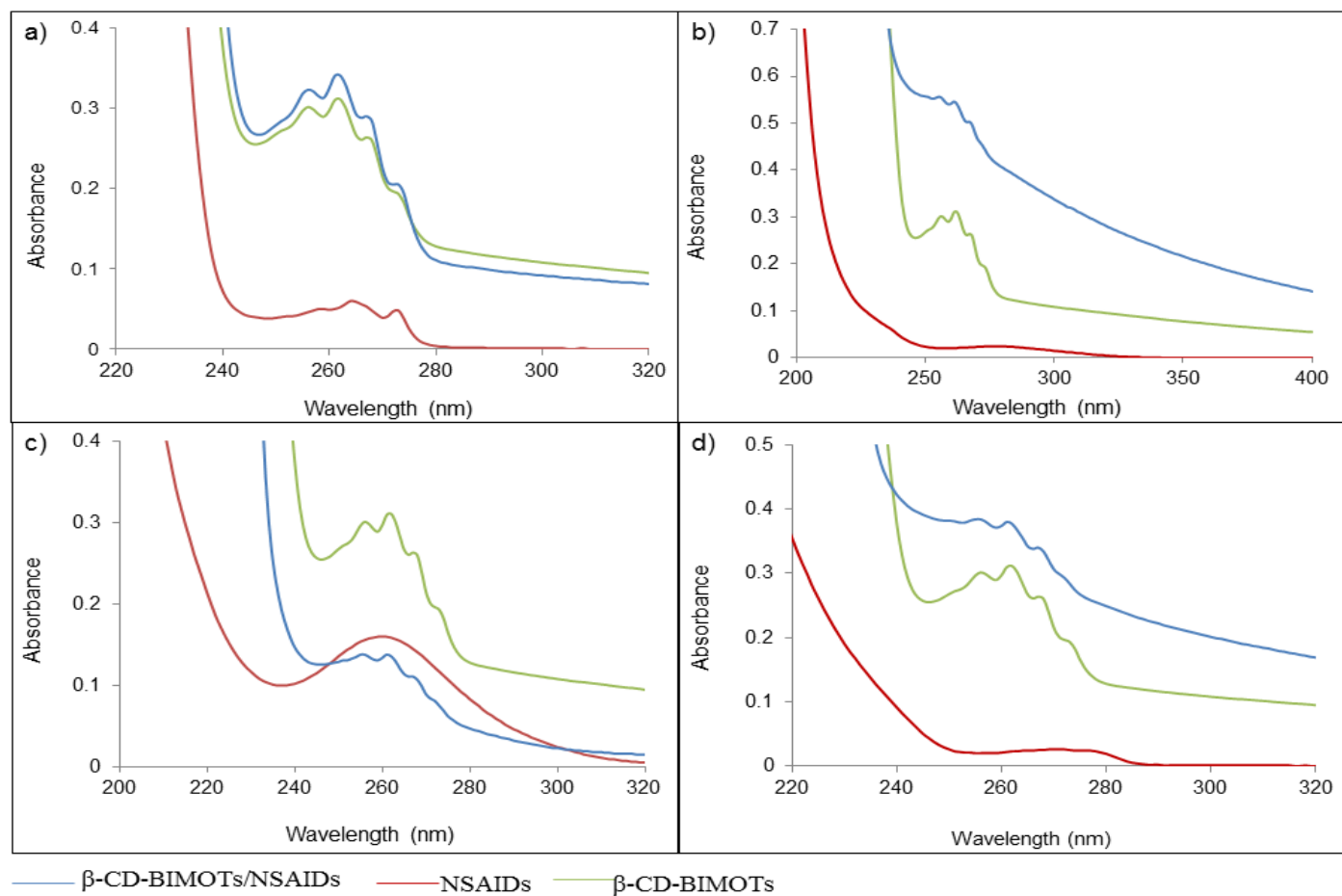


**Figure 4.26:** Absorption spectra of a)  $\beta$ -CD-BIMOTs/ibuprofen b)  $\beta$ -CD-BIMOTs/indoprofen c)  $\beta$ -CD-BIMOTs/ketoprofen d)  $\beta$ -CD-BIMOTs/fenoprofen with  $[\beta\text{-CD-BIMOTs}]$ : 0.032mM  $[\text{NSAIDs}]$ : 0.01mM; T = 25 °C

## CHAPTER 5: CONCLUSIONS AND FUTURE RECOMMENDATIONS

### 5.1 Conclusions

In this study, two new  $\beta$ -CD functionalized IL based CSPs ( $\beta$ -CD-BIMOTs and  $\beta$ -CD-DIMOTs) were successfully synthesized, characterized and compared their performance with native  $\beta$ -CD CSP. The  $\beta$ -CD-BIMOTs and  $\beta$ -CD-DIMOTs CSPs were characterized using various tools and the result obtained was compared with native  $\beta$ -CD CSP.

The performance evaluation of  $\beta$ -CD-BIMOTs,  $\beta$ -CD-DIMOTs and native  $\beta$ -CD as CSPs for the enantioseparation of neutral flavonoids, basic  $\beta$ -blockers and acidic NSAIDs groups was investigated. Although native  $\beta$ -CD has been reported as versatile and efficient for enantioseparation, however it is limited to certain class of analytes. The  $\beta$ -CD-BIMOTs herein have shown even greater chiral resolution capabilities. The result showed that the IL moieties substituted on the  $\beta$ -CD enhanced the enantioseparation. In contrast to the native  $\beta$ -CD CSP, the  $\beta$ -CD functionalized IL based CSP presents the variety interactions with the analytes.  $\beta$ -CD-BIMOTs CSP was more accessible and able to provide more interaction sites compare to  $\beta$ -CD-DIMOTs CSP.

Applying  $\beta$ -CD-BIMOTs as CSP, the influences of organic modifier and analytes's structure was investigated in detail. The following points can be summarized from the series of elaborate investigations of the CSP in reverse phase and polar organic mode HPLC.

- a) The number of OH group substituted at flavonoids strongly affected the choice of mobile phase mode and further affected the enantiomeric separation. In this dissertation,  $\beta$ -CD-BIMOTs CSP was well resolved the enantiomer of flavanone and partially resolved for hesperetin, naringenin and eriodictyol. The broader enantirecognition abilities of  $\beta$ -CD-BIMOTs CSP

towards flavanone and hesperetin were attributable to the hydrophobic interaction, hydrogen bonding and  $\pi$ - $\pi$  interaction. Meanwhile, the chiral recognition for naringenin and eriodictyol were attributed to the exterior interaction with  $\beta$ -CD-BIMOTs CSP such as hydrogen bonding and  $\pi$ - $\pi$  interaction. Different interactions have been proposed to explain these diversities of inclusion complex for different types of flavonoids.

- b) The enantioseparation that attained for the basic  $\beta$ -blockers group is different from the neutral flavonoids group since the mixed mode reverse-normal mobile phase was observed rather than reverse phase. High polarity of atenolol and pindolol retaining them onto the stationary phase and inhibit the chiral recognition. Even though ion pairing reagent such as TEAA was used to accelerate the elution of polar analytes, but the chiral recognition was not improved. Propranolol and metoprolol obtained good enantioresolution as compared to atenolol and pindolol. This result suggested that the lipophilic property and the structure of propranolol and metoprolol enabled the formation of inclusion complex which contributed to better enantioseparation. This observation was proven by  $^1\text{H}$  NMR and NOESY of  $\beta$ -CD-BIMOTs- $\beta$ -blockers inclusion complexes. According to  $^1\text{H}$  NMR and NOESY, propranolol and metoprolol showed the interaction at the interior torus of  $\beta$ -CD-BIMOTs which indicates the formation of inclusion complex. However, atenolol and pindolol showed the strong hydrogen bonding at exterior torus of  $\beta$ -CD-BIMOTs and causing the poor enantioseparation.
- c) The  $\beta$ -CD-BIMOTs CSP depicted good enantioseparation for most of NSAIDs. It was proven through  $^1\text{H}$  NMR, NOESY and UV/Vis studied that all selected NSAIDs were enantioseparated due to the superposition of hydrogen bonding, inclusion complex and  $\pi$ - $\pi$  interactions with  $\beta$ -CD-

BIMOTs CSP. Moreover, the extent of the inclusion mode was affected the enantioseparation. The inclusion mode depends on the polarity and feature structure of analytes. Ibuprofen and indoprofen achieved the good resolution because of the *para* position of the substituent (containing the chiral center) on the aromatic ring can fit properly into the  $\beta$ -CD cavity forming inclusion complex. Meanwhile, the relatively low  $R_s$  values of ketoprofen and fenoprofen was because of its substituent in the *meta* position that make their orientation in an unfavorable way to fit into the  $\beta$ -CD-BIMOTs cavity.

As a whole, the combine effect of hydrophobic inclusion complex, hydrogen bonding and  $\pi$ - $\pi$  interaction resulted in improved the chiral selectivity.  $\beta$ -CD-BIMOTs which provide the additional interaction which is  $\pi$ - $\pi$  interaction showed the important role of IL to enhance the enantioseparation of analytes.

## 5.2 Future work suggestions

In this study,  $\beta$ -CD-BIMOTs and  $\beta$ -CD-DIMOTs CSP have been applied in reverse phase and polar organic mobile phase. Chromatographic conditions have been optimized. The possible chiral recognition mechanisms have been investigated using qualitative tools such as NMR and UV/Visible. However, the influences of  $\pi$ - $\pi$  interaction, hydrogen bonding and hydrophobic inclusion complexation on chiral separation are not quantitatively calculated. Molecular modeling may be useful addition information for theoretical understanding and prediction of the chiral separation mechanism. Only tosylate ion was chosen as the counterion in  $\beta$ -CD-BIMOTs and  $\beta$ -CD-DIMOTs CSPs. Investigations on chiral ionic liquid had revealed that anions may also affect enantioseparation processes. It will be interesting to change the counterions in the CSPs to investigate their influence on chiral resolution as well.

## REFERENCES

- Agustian, J., Kamaruddin, A. H., & Aboul-Enein, H. Y. (2016). Enantio-conversion and-selectivity of racemic atenolol kinetic resolution using free *Pseudomonas fluorescens* lipase (Amano) conducted via transesterification reaction. *RSC Advances*, 6(31), 26077-26085.
- Alimarin, I., Fadeeva, V., Kudryavtsev, G., Loskutova, I., & Tikhomirova, T. (1987). Concentration, separation and determination of scandium, zirconium, hafnium and thorium with a silica-based sulphonic acid cation-exchanger. *Talanta*, 34(1), 103-110.
- Allenmark, S. (1989). *Chromatographic Enantioseparation: Methods & Applications* (pp. 224). New York: Springer.
- Anderson, J. L., & Armstrong, D. W. (2003). High-stability ionic liquids. A new class of stationary phases for gas chromatography. *Analytical Chemistry*, 75(18), 4851-4858.
- Annadurai, T., Muralidharan, A. R., Joseph, T., Hsu, M., Thomas, P., & Geraldine, P. (2012). Antihyperglycemic and antioxidant effects of a flavanone, naringenin, in streptozotocin–nicotinamide-induced experimental diabetic rats. *Journal of Physiology and Biochemistry*, 68(3), 307-318.
- Antochshuk, V., & Jaroniec, M. (2000). Functionalized mesoporous materials obtained via interfacial reactions in self-assembled silica-surfactant systems. *Chemistry of Materials*, 12(8), 2496-2501.
- Arakaki, L. N., Nunes, L. M., Simoni, J. A., & Airoidi, C. (2000). Ethyleneimine anchored on thiol-modified silica gel surface-adsorption of divalent cations and calorimetric data. *Journal of Colloid and Interface Science*, 228(1), 46-51.
- Arjomandi-Behzad, L., Yamini, Y., & Rezazadeh, M. (2013). Pulsed electromembrane method for simultaneous extraction of drugs with different properties. *Analytical Biochemistry*, 438(2), 136-143.
- Armstrong, D. W., & DeMond, W. (1984). Cyclodextrin bonded phases for the liquid chromatographic separation of optical, geometrical, and structural isomers. *Journal of Chromatographic Science*, 22(9), 411-415.
- Armstrong, D. W., Demond, W., & Czech, B. P. (1985). Separation of metallocene enantiomers by liquid chromatography: chiral recognition via cyclodextrin bonded phases. *Analytical Chemistry*, 57(2), 481-484.
- Armstrong, D. W., Lee, J. T., & Chang, L. W. (1998). Enantiomeric impurities in chiral catalysts, auxiliaries and synthons used in enantioselective synthesis. *Tetrahedron: Asymmetry*, 9(12), 2043-2064.
- Armstrong, D. W., Ward, T. J., Armstrong, R. D., & Beesley, T. E. (1986). Separation of drug stereoisomers by the formation of beta-cyclodextrin inclusion complexes. *Science*, 232(4754), 1132-1135.

- Arnold, R., Nelson, J., & Verbanc, J. (1957). Recent advances in isocyanate chemistry. *Chemical Reviews*, 57(1), 47-76.
- Author, A. (2004). On the issue of enantioselectivity of chiral pesticides: a green chemistry opportunity. *Green Chemistry*, 6(12), 77-78.
- Bender, M. L., & Komiyama, M. (2012). Cyclodextrin chemistry (pp. 2-3). New York: Springer.
- Blaschke, G., Kraft, H., Fickentscher, K., & Kohler, F. (1978). Chromatographic separation of racemic thalidomide and teratogenic activity of its enantiomers. *Arzneimittel-forschung*, 29(10), 1640-1642.
- Borchard, U. (1998). Pharmacological properties of beta-adrenoceptor blocking drugs. *Journal of Clinical and Basic Cardiology*, 1(1), 5-9.
- Bubalo, M. C., Radosevic, K., Redovnikovic, I. R., Halambek, J., & Sreck, V. G. (2014). A brief overview of the potential environmental hazards of ionic liquids. *Ecotoxicology and Environmental Safety*, 99, 1-12.
- Bucolo, C., Leggio, G. M., Drago, F., & Salomone, S. (2012). Eriodictyol prevents early retinal and plasma abnormalities in streptozotocin-induced diabetic rats. *Biochemical Pharmacology*, 84(1), 88-92.
- Buszewski, B., & Noga, S. (2012). Hydrophilic interaction liquid chromatography (HILIC)-a powerful separation technique. *Analytical and Bioanalytical Chemistry*, 402(1), 231-247.
- Canongia Lopes, J. N., & Padua, A. A. (2006). Nanostructural organization in ionic liquids. *The Journal of Physical Chemistry B*, 110(7), 3330-3335.
- Cassim, J. Y., & Yang, J. T. (1969). A computerized calibration of the circular dichrometer. *Biochemistry*, 8(5), 1947-1951.
- Chanet, A., Milenkovic, D., Deval, C., Potier, M., Constans, J., & Mazur. (2012). Naringin, the major grapefruit flavonoid, specifically affects atherosclerosis development in diet-induced hypercholesterolemia in mice. *The Journal of Nutritional Biochemistry*, 23(5), 469-477.
- Chang, S., Reid, G., Chen, S., Chang, C., & Armstrong, D. (1993). Evaluation of a new polar-organic high-performance liquid chromatographic mobile phase for cyclodextrin-bonded chiral stationary phases. *Trends in Analytical Chemistry*, 12(4), 144-153.
- Chang, S. C., Wang, L. R., & Armstrong, D. W. (1992). Facile resolution of N-tert-butoxy-carbonyl amino acids: the importance of enantiomeric purity in peptide synthesis. *Journal of Liquid Chromatography & Related Technologies*, 15(9), 1411-1429.



- Cho, K. W., Kim, Y. O., Andrade, J. E., Burgess, J. R., & Kim, Y. C. (2011). Dietary naringenin increases hepatic peroxisome proliferator-activated receptor  $\alpha$  protein expression and decreases plasma triglyceride and adiposity in rats. *European Journal of Nutrition*, 50(2), 81-88.
- Ciucanu, I. (1996). Selective immobilization on silica gel of permethylated  $\beta$ -cyclodextrin for liquid chromatography. *Journal of Chromatography A*, 727(2), 195-201.
- Ciucanu, I., & Konig, W. A. (1994). Immobilization of peralkylated  $\beta$ -cyclodextrin on silica gel for high-performance liquid chromatography. *Journal of Chromatography A*, 685(1), 166-171.
- Cooper, S. A., Reynolds, D. C., Reynolds, B., & Hersh, E. V. (1998). Analgesic efficacy and safety of (R)-ketoprofen in postoperative dental pain. *The Journal of Clinical Pharmacology*, 38(2), 11-18.
- Cwiertnia, B., Hladon, T., & Stobiecki, M. (1999). Stability of diclofenac sodium in the inclusion complex with  $\beta$ -cyclodextrin in the solid state. *Journal of Pharmacy and Pharmacology*, 51(11), 1213-1218.
- Daffe, V., & Fastrez, J. (1983). Cyclodextrin-catalysed hydrolysis of oxazol-5 (4 H)-ones. Enantioselectivity of the acid-base and ring-opening reactions. *Journal of the Chemical Society, Perkin Transactions 2*(6), 789-796.
- Dai, Y., Wang, S., Tang, W., & Ng, S. C. (2013). Cyclodextrin-based chiral stationary phases for high-performance liquid chromatography *Modified Cyclodextrins for Chiral Separation* (pp. 67-101). New York: Springer.
- Evans, S. E., & Kasprzyk-Hordern, B. (2014). Applications of chiral chromatography coupled with mass spectrometry in the analysis of chiral pharmaceuticals in the environment. *Trends in Environmental Analytical Chemistry*, 1, 34-51.
- Fanali, S., & Aturki, Z. (1995). Use of cyclodextrins in capillary electrophoresis for the chiral resolution of some 2-arylpropionic acid non-steroidal anti-inflammatory drugs. *Journal of Chromatography A*, 694(1), 297-305.
- Ficarra, R., Tommasini, S., Raneri, D., Calabro, M., Di Bella, M., Rustichelli, C., Gamberini, M., & Ficarra, P. (2002). Study of flavonoids/ $\beta$ -cyclodextrins inclusion complexes by NMR, FT-IR, DSC, X-ray investigation. *Journal of Pharmaceutical and Biomedical Analysis*, 29(6), 1005-1014.
- Fontanals, N., Ronka, S., Borrull, F., Trochimczuk, A. W., & Marce, R. M. (2009). Supported imidazolium ionic liquid phases: a new material for solid-phase extraction. *Talanta*, 80(1), 250-256.
- Frieden, E. (1975). Non-covalent interactions: key to biological flexibility and specificity. *Journal of Chemical Education*, 52(12), 754-762.

- Goldwasser, J., Cohen, P. Y., Yang, E., Balaguer, P., Yarmush, M. L., & Nahmias, Y. (2010). Transcriptional regulation of human and rat hepatic lipid metabolism by the grapefruit flavonoid naringenin: role of PPARalpha, PPARgamma and LXRalpha. *PloS one*, 5(8), 12399-12408.
- Gubitz, G., & Schmid, M. G. (2009). Cyclodextrin-mediated chiral separations *Chiral separations by capillary electrophoresis* (pp. 47-85). Florida: CRC Press.
- Guo, Z., Jin, Y., Liang, T., Liu, Y., Xu, Q., Liang, X., & Lei, A. (2009). Synthesis, chromatographic evaluation and hydrophilic interaction/reversed-phase mixed-mode behavior of a "Click  $\beta$ -cyclodextrin" stationary phase. *Journal of Chromatography A*, 1216(2), 257-263.
- Guo, Z. X., Liu, W. F., Li, Y., & Yu, J. (2005). Grafting of Poly (ethylene glycol) s onto Nanometer Silica Surface by a One-Step Procedure. *Journal of Macromolecular Science Part A-Pure and Applied Chemistry*, 42(2), 221-230.
- Han, X., Yao, T., Liu, Y., Larock, R. C., & Armstrong, D. W. (2005). Separation of chiral furan derivatives by liquid chromatography using cyclodextrin-based chiral stationary phases. *Journal of Chromatography A*, 1063(1), 111-120.
- Hardikar, M. (2008). Chiral non-steroidal anti-inflammatory drugs-A review. *Journal of the Indian Medical Association*, 106(9), 615-624.
- Harrower, A., Fyffe, J., Horn, D., & Strong, J. (1977). Thyroxine and triiodothyronine levels in hyperthyroid patients during treatment with propranolol. *Clinical Endocrinology*, 7(1), 41-44.
- Hinze, W. L., Riehl, T. E., Armstrong, D. W., DeMond, W., Alak, A., & Ward, T. (1985). Liquid chromatographic separation of enantiomers using a chiral. beta.-cyclodextrin-bonded stationary phase and conventional aqueous-organic mobile phases. *Analytical Chemistry*, 57(1), 237-242.
- Hu, Y. M., Wang, X. M., Pan, H. Z., & Ding, L. S. (2012). Interaction mode between methylene blue-Sm (III) complex and herring sperm DNA. *Bulletin of the Chemical Society of Ethiopia*, 26(3), 395-405.
- Hunter, C. A., Lawson, K. R., Perkins, J., & Urch, C. J. (2001). Aromatic interactions. *Journal of the Chemical Society, Perkin Transactions 2*(5), 651-669.
- Ismail, O. H., Ciogli, A., Villani, C., De Martino, M., Pierini, M., Cavazzini, A., Bell, D. S., & Gasparrini, F. (2016). Ultra-fast high-efficiency enantioseparations by means of a teicoplanin-based chiral stationary phase made on sub-2 $\mu$ m totally porous silica particles of narrow size distribution. *Journal of Chromatography A*, 1427, 55-68.
- Johnson, J., Maher, P., & Hanneken, A. (2009). The flavonoid, eriodictyol, induces long-term protection in ARPE-19 cells through its effects on Nrf2 activation and phase II gene expression. *Investigative Ophthalmology & Visual Science*, 50(5), 2398-2406.

- Juvancz, Z., & Szejtli, J. (2002). The role of cyclodextrins in chiral selective chromatography. *Trends in Analytical Chemistry*, 21(5), 379-388.
- Kafkova, B., Bosakova, Z., Tesarova, E., & Coufal, P. (2005). Chiral separation of beta-adrenergic antagonists, profen non-steroidal anti-inflammatory drugs and chlorophenoxypropionic acid herbicides using teicoplanin as the chiral selector in capillary liquid chromatography. *Journal of Chromatography A*, 1088(1), 82-93.
- Kaluzna, I. A., Rozzell, J. D., & Kambourakis, S. (2005). Ketoreductases: stereoselective catalysts for the facile synthesis of chiral alcohols. *Tetrahedron: Asymmetry*, 16(22), 3682-3689.
- Karnik, A. V., & Kamath, S. S. (2008). Cascade enantioselective synthesis of  $\gamma$ -aryl- $\gamma$ -butyrolactones with a delayed stereoselective step. *Tetrahedron*, 64(13), 2992-2996.
- Kavalirova, A., Pospisilova, M., & Karlicek, R. (2004). Enantiomeric analysis of rivastigmine in pharmaceuticals by cyclodextrin-modified capillary zone electrophoresis. *Analytica Chimica Acta*, 525(1), 43-51.
- Lee, E. R., Kim, J. H., Choi, H. Y., Jeon, K., & Cho, S. G. (2011). Cytoprotective effect of eriodictyol in UV-irradiated keratinocytes via phosphatase-dependent modulation of both the p38 MAPK and Akt signaling pathways. *Cellular Physiology and Biochemistry*, 27(5), 513-524.
- Li, S., & Purdy, W. C. (1992). Direct separation of enantiomers using multiple-interaction chiral stationary phases based on the modified  $\beta$ -cyclodextrin-bonded stationary phase. *Journal of Chromatography A*, 625(2), 109-120.
- Li, X., Jin, X., Yao, X., Ma, X., & Wang, Y. (2016). Thioether bridged cationic cyclodextrin stationary phases: Effect of spacer length, selector concentration and rim functionalities on the enantioseparation. *Journal of Chromatography A*, 1467, 279-287.
- Li, X., & Zhou, Z. (2014). Enantioseparation performance of novel benzimido- $\beta$ -cyclodextrins derivatized by ionic liquids as chiral stationary phases. *Analytica Chimica Acta*, 819, 122-129.
- Lin, C., Fan, J., Liu, W. N., Tan, Y., & Zhang, W. G. (2014). Comparative HPLC enantioseparation on substituted phenylcarbamoyleated cyclodextrin chiral stationary phases and mobile phase effects. *Journal of Pharmaceutical and Biomedical Analysis*, 98, 221-227.
- Lipka, E., Vaccher, M., Fourmaintraux, E., Bonte, J., & Vaccher, C. (2003). Chiral Separation and Determination of the Enantiomeric Purity of Tetrahydronaphthalenic Derivatives, Melatonergic Ligands, by HPLC using  $\beta$ -Cyclodextrins. *Chromatographia*, 58(9-10), 665-670.

- Liu, R., Du, Y., Chen, J., Zhang, Q., Du, S., & Feng, Z. (2015a). Investigation of the enantioselectivity of tetramethylammonium L-hydroxyproline ionic liquid as a novel chiral ligand in ligand-exchange CE and ligand-exchange MEKC. *Chirality*, 27(1), 58-63.
- Liu, Y., Tian, A., Wang, X., Qi, J., Wang, F., Ma, Y., Ito, Y., & Wei, Y. (2015b). Fabrication of chiral amino acid ionic liquid modified magnetic multifunctional nanospheres for centrifugal chiral chromatography separation of racemates. *Journal of Chromatography A*, 1400, 40-46.
- Lommerse, J. P., Price, S. L., & Taylor, R. (1997). Hydrogen bonding of carbonyl, ether, and ester oxygen atoms with alkanol hydroxyl groups. *Journal of Computational Chemistry*, 18(6), 757-774.
- Lorenz, H., & Seidel-Morgenstern, A. (2014). Processes to separate enantiomers. *Angewandte Chemie International Edition*, 53(5), 1218-1250.
- Lu, X., Ng, H. Y., Xu, J., & He, C. (2002). Electrical conductivity of polyaniline-dodecylbenzene sulphonic acid complex: thermal degradation and its mechanism. *Synthetic Metals*, 128(2), 167-178.
- McEwen, A. B., Ngo, H. L., LeCompte, K., & Goldman, J. L. (1999). Electrochemical properties of imidazolium salt electrolytes for electrochemical capacitor applications. *Journal of the Electrochemical Society*, 146(5), 1687-1695.
- Meier-Augenstein, W., Burger, B. V., Spies, H. S., & Burger, W. J. (1992). Conformational analyses of alkylated  $\beta$ -cyclodextrins by NMR spectroscopy. *Zeitschrift für Naturforschung B*, 47(6), 877-886.
- Missio, L. J., & Comasseto, V. (2003). Corrigendum to "Enantioselective synthesis of (-)- $\gamma$ -jasmolactone". *Tetrahedron: Asymmetry*, 14(1), 145.
- Negru, J., Popa, D. S., Vlase, L., Iacob, D., Achim, M., & Dorneanu, V. (2015). High-throughput HPLC method for rapid quantification of ketoprofen in human plasma. *Farmacia*, 63(5), 770-776.
- Ng, S. C., Ong, T. T., Fu, P., & Ching, C. B. (2002). Enantiomer separation of flavour and fragrance compounds by liquid chromatography using novel urea-covalent bonded methylated  $\beta$ -cyclodextrins on silica. *Journal of Chromatography A*, 968(1), 31-40.
- Nunez-Aguero, C. J., Escobar Llanos, C. M., Diaz, D., Jaime, C., & Garduno Juarez, R. (2006). Chiral discrimination of ibuprofen isomers in  $\beta$ -cyclodextrin inclusion complexes: experimental (NMR) and theoretical (MD, MM/GBSA) studies. *Tetrahedron*, 62(17), 4162-4172.
- Ong, T., Wang, R. Q., Muderawan, I. W., & Ng, S. C. (2008). Synthesis and application of mono-6-(3-methylimidazolium)-6-deoxyperphenylcarbamoyl- $\beta$ -cyclodextrin chloride as chiral stationary phases for high-performance liquid chromatography and supercritical fluid chromatography. *Journal of Chromatography A*, 1182(1), 136-140.

- Park, H. Y., Kim, G. Y., & Choi, Y. H. (2012). Naringenin attenuates the release of pro-inflammatory mediators from lipopolysaccharide-stimulated BV2 microglia by inactivating nuclear factor- $\kappa$ B and inhibiting mitogen-activated protein kinases. *International Journal of Molecular Medicine*, 30(1), 204-210.
- Pazos, G., Perez, M., Gandara, Z., Gomez, G., & Fall, Y. (2009). A new enantioselective synthesis of (+)-isolaurepan. *Tetrahedron Letters*, 50(37), 5285-5287.
- Peral, F., & Gallego, E. (2000). Self-association of pyridine-2, 6-dicarboxylic acid in aqueous solution as determined from ultraviolet hypochromic and hyperchromic effects. *Spectrochimica Acta Part A: Molecular and Biomolecular Spectroscopy*, 56(11), 2149-2155.
- Podar, A., Siciu, S., & Oprean, R. (2016). Review-Recent enantiomer separation strategies of nonsteroidal anti-inflammatory drugs (NSAIDs) by capillary electrophoresis. *Farmacia*, 64(2), 159-170.
- Poole, C. F. (2003). The essence of chromatography (pp. 272-278). Netherland: Elsevier.
- Qian, L., Guan, Y., & Xiao, H. (2008). Preparation and characterization of inclusion complexes of a cationic  $\beta$ -cyclodextrin polymer with butylparaben or triclosan. *International Journal of Pharmaceutics*, 357(1), 244-251.
- Qin, L., Jin, L., Lu, L., Lu, X., Zhang, C., Zhang, F., & Liang, W. (2011). Naringenin reduces lung metastasis in a breast cancer resection model. *Protein & cell*, 2(6), 507-516.
- Raoov, M., Mohamad, S., & Abas, M. R. (2013). Removal of 2, 4-dichlorophenol using cyclodextrin-ionic liquid polymer as a macroporous material: Characterization, adsorption isotherm, kinetic study, thermodynamics. *Journal of Hazardous Materials*, 263(2), 501-516.
- Sabarinathan, D., Mahalakshmi, P., & Vanisree, A. J. (2010). Naringenin promote apoptosis in cerebrally implanted C6 glioma cells. *Molecular and Cellular Biochemistry*, 345(1-2), 215-222.
- Sabarinathan, D., Mahalakshmi, P., & Vanisree, A. J. (2011). Naringenin, a flavanone inhibits the proliferation of cerebrally implanted C6 glioma cells in rats. *Chemico-Biological Interactions*, 189(1), 26-36.
- Saleem, K., Ali, I., Kulsum, U., & Aboul-Enein, H. Y. (2013). Recent developments in HPLC analysis of  $\beta$ -blockers in biological samples. *Journal of Chromatographic Science*, 51(8), 807-818.
- Scalbert, A., Manach, C., Morand, C., Remesy, C., & Jimenez, L. (2005). Dietary polyphenols and the prevention of diseases. *Critical Reviews in Food Science and Nutrition*, 45(4), 287-306.
- Schurig, V. (2002). Chiral separations using gas chromatography. *Trends in Analytical Chemistry*, 21(9), 647-661.

- Schurig, V., & Juza, M. (2014). Analytical separation of enantiomers by gas chromatography on chiral stationary phases *Advances in Chromatography* (pp. 117-168). Florida: CRC Press.
- Sekhon, B. S. (2013). Exploiting the power of stereochemistry in drugs: an overview of racemic and enantiopure drugs. *Journal of Modern Medicinal Chemistry, 1*, 10-36.
- Simons, D. M., & Arnold, R. G. (1956). Relative reactivity of the isocyanate groups in toluene-2, 4-diisocyanate. *Journal of the American Chemical Society, 78*(8), 1658-1659.
- Stalcup, A. M., Chang, S. C., Armstrong, D. W., & Pitha, J. (1990). (S)-2-Hydroxypropyl- $\beta$ -cyclodextrin, a new chiral stationary phase for reversed-phase liquid chromatography. *Journal of Chromatography A, 513*, 181-194.
- Stinson, S. C. (2000). Chiral drugs. *Chemical & Engineering News, 78*(43), 55-78.
- Stoschitzky, K., Lindner, W., Egginger, G., Brunner, F., Obermayer-Pietsch, B., Passath, A., & Klein, W. (1992). Racemic (R, S)-propranolol versus half-dosed optically pure (S)-propranolol in humans at steady state: Hemodynamic effects, plasma concentrations, and influence on thyroid hormone levels. *Clinical Pharmacology & Therapeutics, 51*(4), 445-453.
- Subramaniam, P., Mohamad, S., & Alias, Y. (2010). Synthesis and characterization of the inclusion complex of dicationic ionic liquid and  $\beta$ -cyclodextrin. *International Journal of Molecular Sciences, 11*(10), 3675-3685.
- Svang-Ariyaskul, A., Koros, W. J., & Rousseau, R. W. (2009). Chiral separation using a novel combination of cooling crystallization and a membrane barrier: Resolution of DL-glutamic acid. *Chemical Engineering Science, 64*(9), 1980-1984.
- Szejtli, J. (1994). Medicinal applications of cyclodextrins. *Medicinal Research Reviews, 14*(3), 353-386.
- Szejtli, J. (1998). Introduction and general overview of cyclodextrin chemistry. *Chemical Reviews, 98*(5), 1743-1754.
- Szente, L., & Szemaan, J. (2013). Cyclodextrins in analytical chemistry: Host-guest type molecular recognition. *Analytical Chemistry, 85*(17), 8024-8030.
- Tang, J., & Tang, W. (2013). Modification of Cyclodextrin *Modified Cyclodextrins for Chiral Separation* (pp. 1-25). New York: Springer.
- Tang, W., Muderawan, I. W., Ong, T. T., & Ng, S. C. (2005a). Enantioseparation of acidic enantiomers in capillary electrophoresis using a novel single-isomer of positively charged  $\beta$ -cyclodextrin: mono-6A-N-pentylammonium-6A-deoxy- $\beta$ -cyclodextrin chloride. *Journal of Chromatography A, 1091*(1), 152-157.

- Tang, W., Muderawan, I. W., Ong, T. T., & Ng, S. C. (2005b). A family of single• isomer positively charged cyclodextrins as chiral selectors for capillary electrophoresis: Mono-6A-butylammonium-6A-deoxy- $\beta$ -cyclodextrin tosylate. *Electrophoresis*, 26(16), 3125-3133.
- Tiwari, B. K., Brunton, N. P., & Brennan, C. (2013). Polyphenols *Handbook of Plant Food Phytochemicals: Sources, Stability and Extraction* (pp. 1917-1918). New Jersey: John Wiley & Sons.
- Tucker, G., & Robards, K. (2008). Bioactivity and structure of biophenols as mediators of chronic diseases. *Critical Reviews in Food Science and Nutrition*, 48(10), 929-966.
- Valente, A. J., & Soderman, O. (2014). The formation of host-guest complexes between surfactants and cyclodextrins. *Advances in Colloid and Interface Science*, 205, 156-176.
- Velkov, T., Horne, J., Laguerre, A., Jones, E., Scanlon, M. J., & Porter, C. J. (2007). Examination of the role of intestinal fatty acid-binding protein in drug absorption using a parallel artificial membrane permeability assay. *Chemistry & Biology*, 14(4), 453-465.
- Ventura, C. A., Giannone, I., Musumeci, T., Pignatello, R., Ragni, L., Landolfi, C., Milanese, C., Paolino, D., & Puglisi, G. (2006). Physico-chemical characterization of disoxaril–dimethyl- $\beta$ -cyclodextrin inclusion complex and in vitro permeation studies. *European Journal of Medicinal Chemistry*, 41(2), 233-240.
- Wang, J., Cao, Y., Sun, B., & Wang, C. (2011a). Characterisation of inclusion complex of trans-ferulic acid and hydroxypropyl- $\beta$ -cyclodextrin. *Food Chemistry*, 124(3), 1069-1075.
- Wang, R. Q., Ong, T. T., & Ng, S. C. (2008). Synthesis of cationic  $\beta$ -cyclodextrin derivatives and their applications as chiral stationary phases for high-performance liquid chromatography and supercritical fluid chromatography. *Journal of Chromatography A*, 1203(2), 185-192.
- Wang, R. Q., Ong, T. T., & Ng, S. C. (2012a). Chemically bonded cationic  $\beta$ -cyclodextrin derivatives and their applications in supercritical fluid chromatography. *Journal of Chromatography A*, 1224, 97-103.
- Wang, R. Q., Ong, T. T., & Ng, S. C. (2012b). Chemically bonded cationic  $\beta$ -cyclodextrin derivatives as chiral stationary phases for enantioseparation applications. *Tetrahedron Letters*, 53(18), 2312-2315.
- Wang, R. Q., Ong, T. T., Tang, W., & Ng, S. C. (2012c). Cationic cyclodextrins chemically-bonded chiral stationary phases for high-performance liquid chromatography. *Analytica Chimica Acta*, 718, 121-129.
- Wang, Y., Chen, H., Xiao, Y., Ng, C. H., Oh, T. S., Tan, T. T. Y., & Ng, S. C. (2011b). Preparation of cyclodextrin chiral stationary phases by organic soluble catalytic'click'chemistry. *Nature Protocols*, 6(7), 935-942.

- Wang, Y., Young, D. J., Tan, T. T. Y., & Ng, S. C. (2010). "Click" immobilized perphenylcarbomated and permethylated cyclodextrin stationary phases for chiral high-performance liquid chromatography application. *Journal of Chromatography A*, 1217(31), 5103-5108.
- Wiersinga, W., & Touber, J. (1977). The influence of  $\beta$ -adrenoceptor blocking agents on plasma thyroxine and triiodothyronine. *The Journal of Clinical Endocrinology & Metabolism*, 45(2), 293-298.
- Wistuba, D., Trapp, O., Gel-Moreto, N., Galensa, R., & Schurig, V. (2006). Stereoisomeric separation of flavanones and flavanone-7-O-glycosides by capillary electrophoresis and determination of interconversion barriers. *Analytical Chemistry*, 78(10), 3424-3433.
- Xiao, Y., Ong, T. T., Tan, T. T. Y., & Ng, S. C. (2009). Synthesis and application of a novel single-isomer mono-6-deoxy-6-(3R, 4R-dihydroxypyrrolidine)- $\beta$ -cyclodextrin chloride as a chiral selector in capillary electrophoresis. *Journal of Chromatography A*, 1216(6), 994-999.
- Yanez, J. A., Andrews, P. K., & Davies, N. M. (2007). Methods of analysis and separation of chiral flavonoids. *Journal of Chromatography B*, 848(2), 159-181.
- Yao, X., Gong, Y., Mamuti, R., Xing, W., Zheng, H., Tang, X., & Wang, Y. (2014a). Chiral differentiation of novel isoxazoline derivatives on "clicked" thioether and triazole bridged cyclodextrin chiral stationary phases. *RSC Advances*, 4(58), 30492-30499.
- Yao, X., Tan, T. T. Y., & Wang, Y. (2014b). Thiol-ene click chemistry derived cationic cyclodextrin chiral stationary phase and its enhanced separation performance in liquid chromatography. *Journal of Chromatography A*, 1326, 80-88.
- Yatabe, J., & Kageyama, T. (1994). Preparation of Hydrophobic Silica with Isocyanates. *Journal of the Ceramic Society of Japan*, 102(6), 594-597.
- Zhang, C., Ingram, I. C., Hantao, L. W., & Anderson, J. L. (2015a). Identifying important structural features of ionic liquid stationary phases for the selective separation of nonpolar analytes by comprehensive two-dimensional gas chromatography. *Journal of Chromatography A*, 1386, 89-97.
- Zhang, D., Zhao, P., Huang, N., Wu, Y., & Zhai, Y. (1990, 28-30 March). *Study of H-NMR spectra of  $\alpha$ -cyclodextrin or dimethylcyclodextrin/toluene complexes in  $CF_3COOD/D_2O$* . Paper presented at the Minutes of the 5th Int. Symp. on Cyclodextrins, Paris.
- Zhang, L., Yu, W., Rong, Y., Guo, X., Ye, J., Shen, Z., & Zeng, S. (2014). Enantiomeric separation of 2-arylpropionic acid nonsteroidal anti-inflammatory drugs and  $\beta$ -blockers by RP-HPLC using an amylose chiral stationary phase for the enantioselective skin permeation study. *Analytical Methods*, 6(15), 6058-6065.

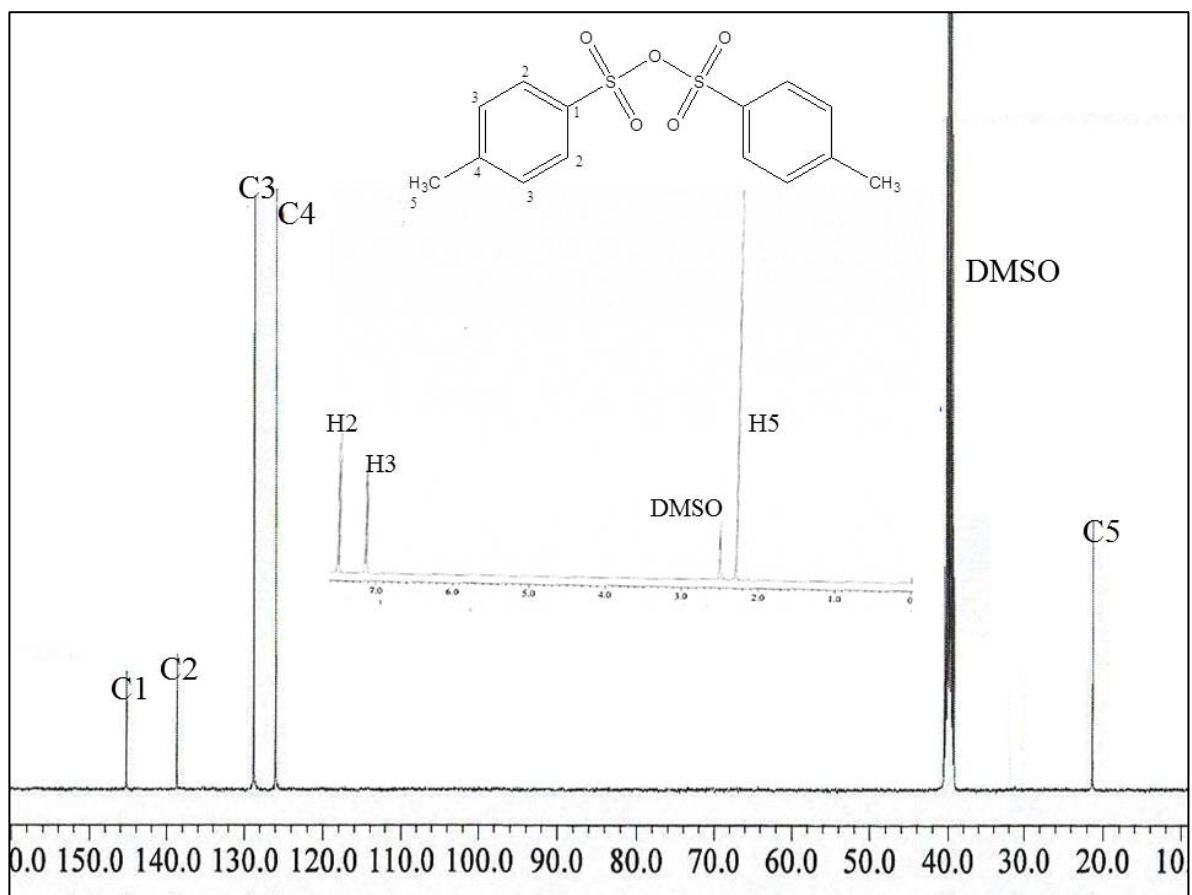


- Zhang, L. F., Wong, Y. C., Chen, L., Ching, C. B., & Ng, S. C. (1999). A facile immobilization approach for perfunctionalised cyclodextrin onto silica via the Staudinger reaction. *Tetrahedron letters*, 40(9), 1815-1818.
- Zhang, M., Mallik, A. K., Takafuji, M., Ihara, H., & Qiu, H. (2015b). Versatile ligands for high-performance liquid chromatography: an overview of ionic liquid-functionalized stationary phases. *Analytica Chimica Acta*, 887, 1-16.
- Zhang, S., & Lv, X. (2006). Ionic liquids: from fundamentals to applications (pp. 33). China: Science Press.
- Zhang, Y., Wu, D. R., Wang Iverson, D. B., & Tymiak, A. A. (2005). Enantioselective chromatography in drug discovery. *Drug Discovery Today*, 10(8), 571-577.
- Zhou, Z., Li, X., Chen, X., & Hao, X. (2010). Synthesis of ionic liquids functionalized  $\beta$ -cyclodextrin-bonded chiral stationary phases and their applications in high-performance liquid chromatography. *Analytica Chimica Acta*, 678(2), 208-214.
- Zid, M. B., Dhuique-Mayer, C., Bellagha, S., Sanier, C., Collignan, A., Servent, A., & Dornier, M. (2015). Effects of blanching on flavanones and microstructure of *Citrus aurantium* peels. *Food and Bioprocess Technology*, 8(11), 2246-2255.
- Zsila, F. (2013). Subdomain IB is the third major drug binding region of human serum albumin: toward the three-sites model. *Molecular Pharmaceutics*, 10(5), 1668-1682.

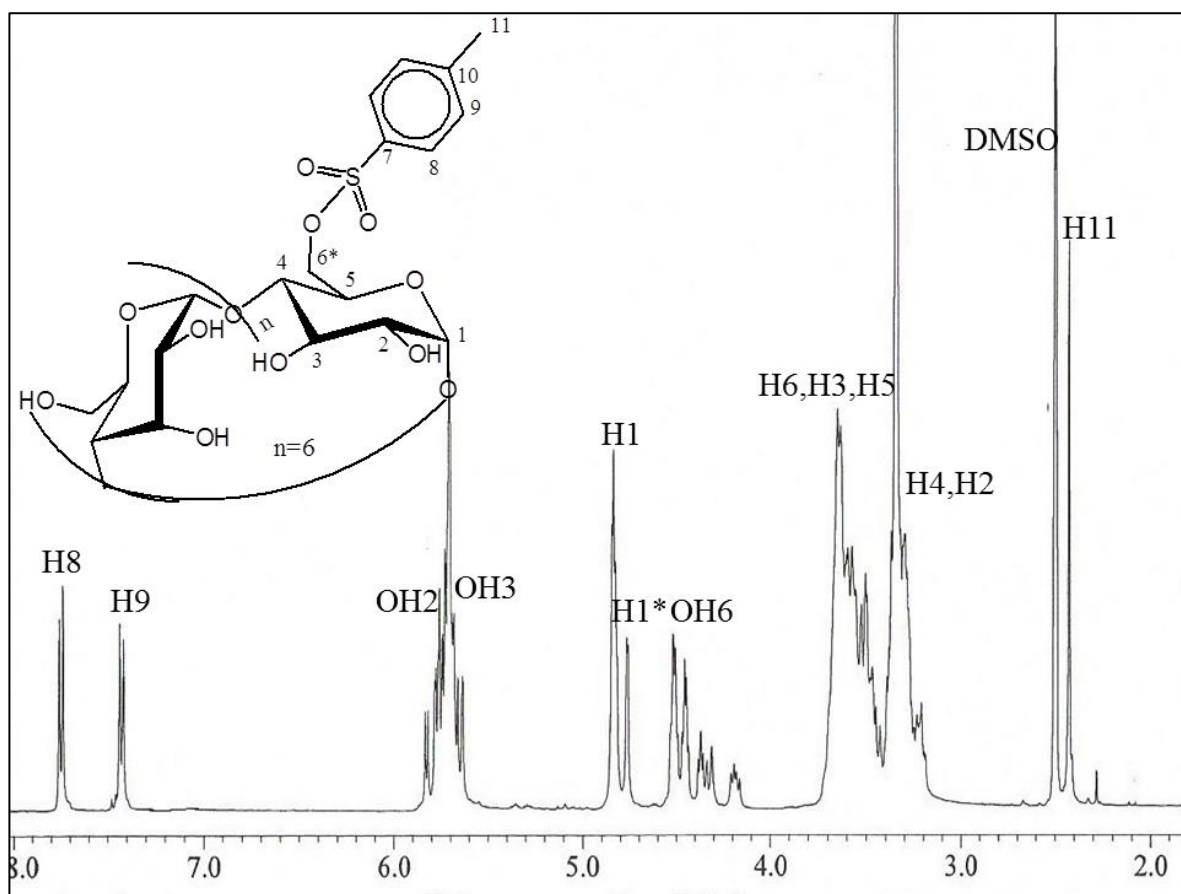
## LIST OF PUBLICATIONS AND PAPERS PRESENTED

1. Rahim, Nurul Yani, Tay, Kheng Soo, Mohamad, Sharifah. “ $\beta$ -cyclodextrin functionalized Ionic liquid as chiral stationary phase for  $\beta$ -blockers enantioseparation.” *Journal of Inclusion Phenomena and Macrocyclic Chemistry*, (2016) 85, 303-315.
2. Rahim, Nurul Yani, Tay Kheng Soo, Sharifah Mohamad. “Chromatographic and spectroscopic studies on the chiral recognition of ionic liquids functionalized  $\beta$ -cyclodextrin as chiral stationary phase: Enantioseparation of flavonoids.” *Chromatographia*. 79(21-22), 1445-1455.
3. Rahim, Nurul Yani, Tay Kheng Soo, Sharifah Mohamad.” Chromatographic and spectroscopic studies on the  $\beta$ -cyclodextrin functionalized ionic liquid as chiral stationary phase: Enantioseparation of NSAIDs”. *Adsorption and Separation Technology*, DOI: 10.1177/0263617416686798.
4. Nurul Yani Rahim, Sharifah Mohamad, Tay Kheng Soo. 2013. Ionic cyclodextrins chemically-bonded chiral stationary phases for high-performance liquid chromatography. International Conference on Ionic Liquids 2013 (ICIL 13). 11-13 December 2013, Langkawi Island, Kedah.
5. Nurul Yani Rahim, Sharifah Mohamad, Tay Kheng Soo. 2014. Preparation of ionic liquid  $\beta$ -cyclodextrin immobilization on functionalized silica gel as chiral stationary phase for High Performance Liquid Chromatography. 6<sup>th</sup> International Conference on Postgraduate Education (ICPE-6). 17-18 December 2014, University Teknikal Malaysia Melaka.
6. Nurul Yani Rahim, Sharifah Mohamad, Tay Kheng Soo. 2015. 28<sup>th</sup> Regional Symposium of Malaysian Analytical Sciences. 17-20 August 2015, Weil Hotel, Ipoh, Perak.

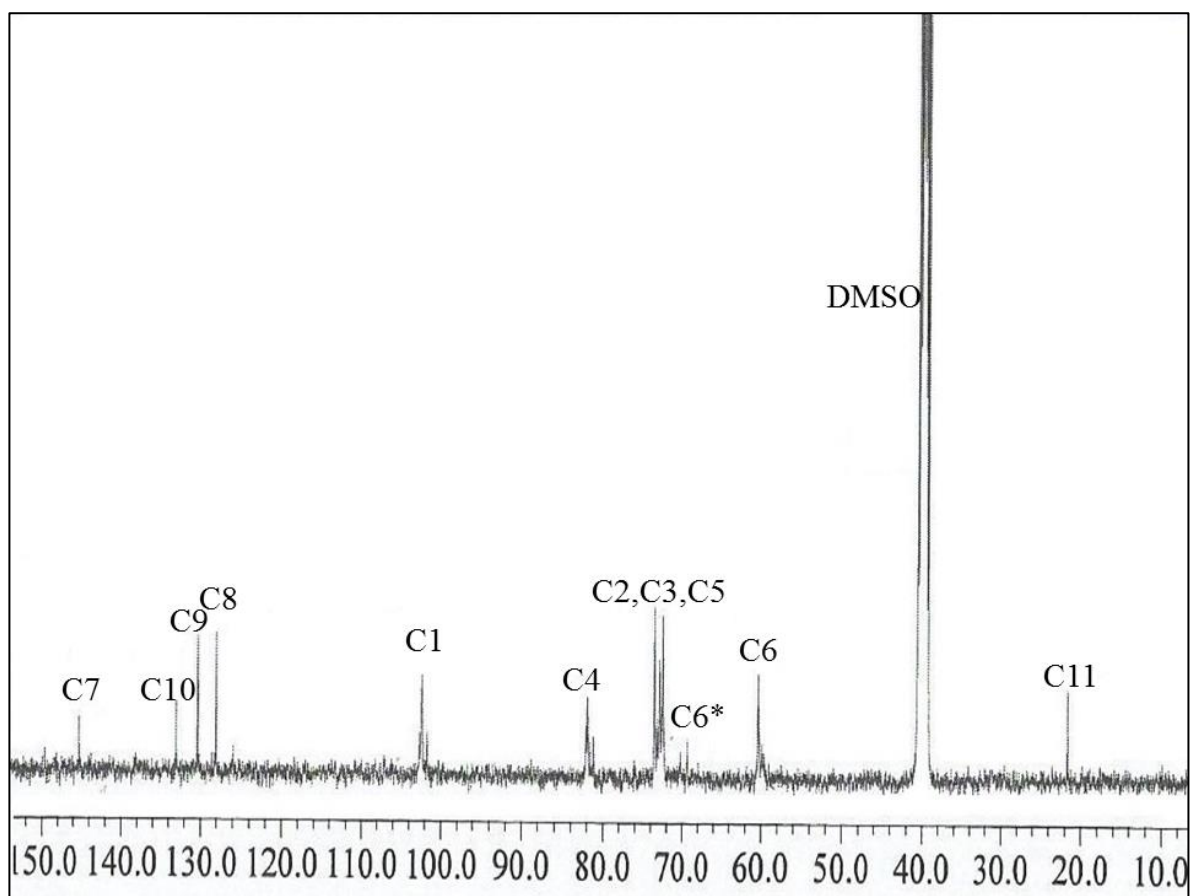
## APPENDIX



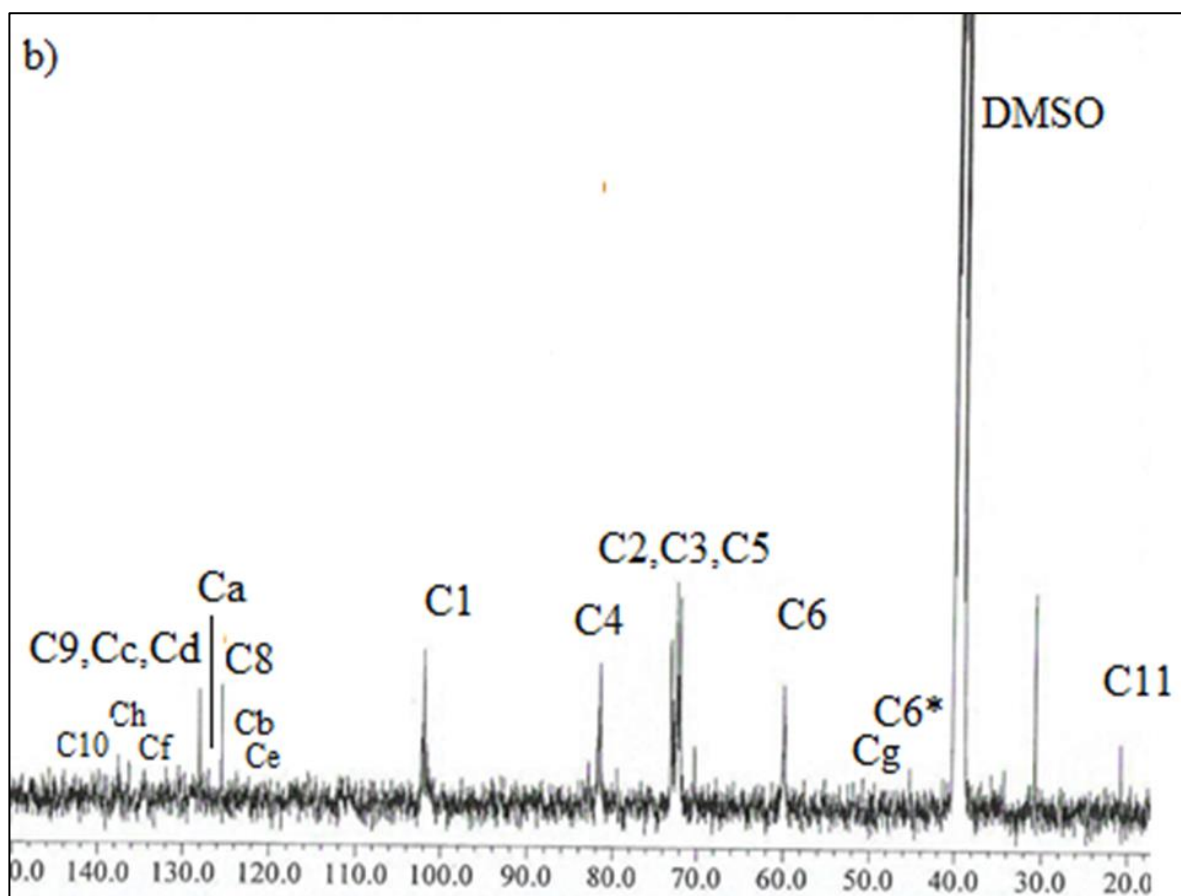
**Appendix A:** NMR spectra for <sup>1</sup>H and <sup>13</sup>C of Ts<sub>2</sub>O



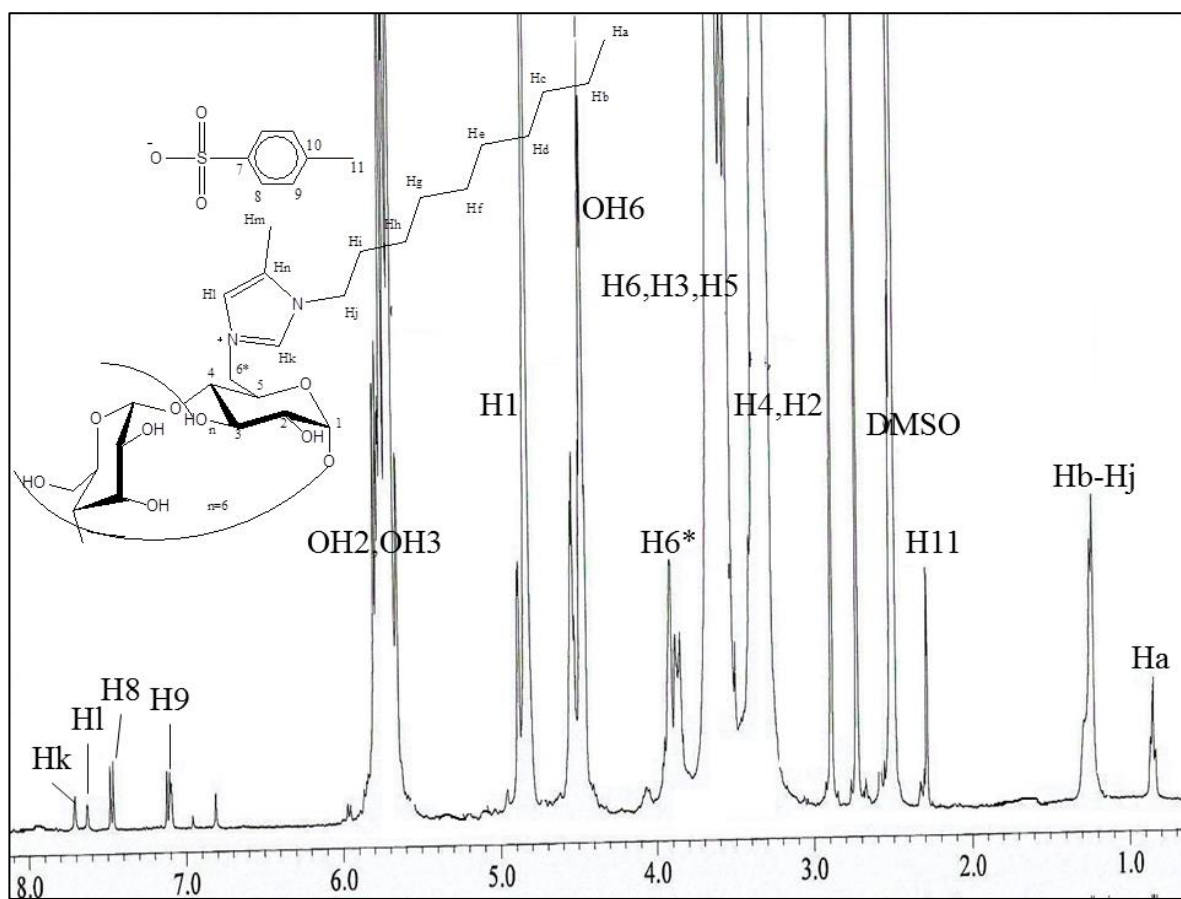
**Appendix B:** NMR spectrum for <sup>1</sup>H of β-CDOTs



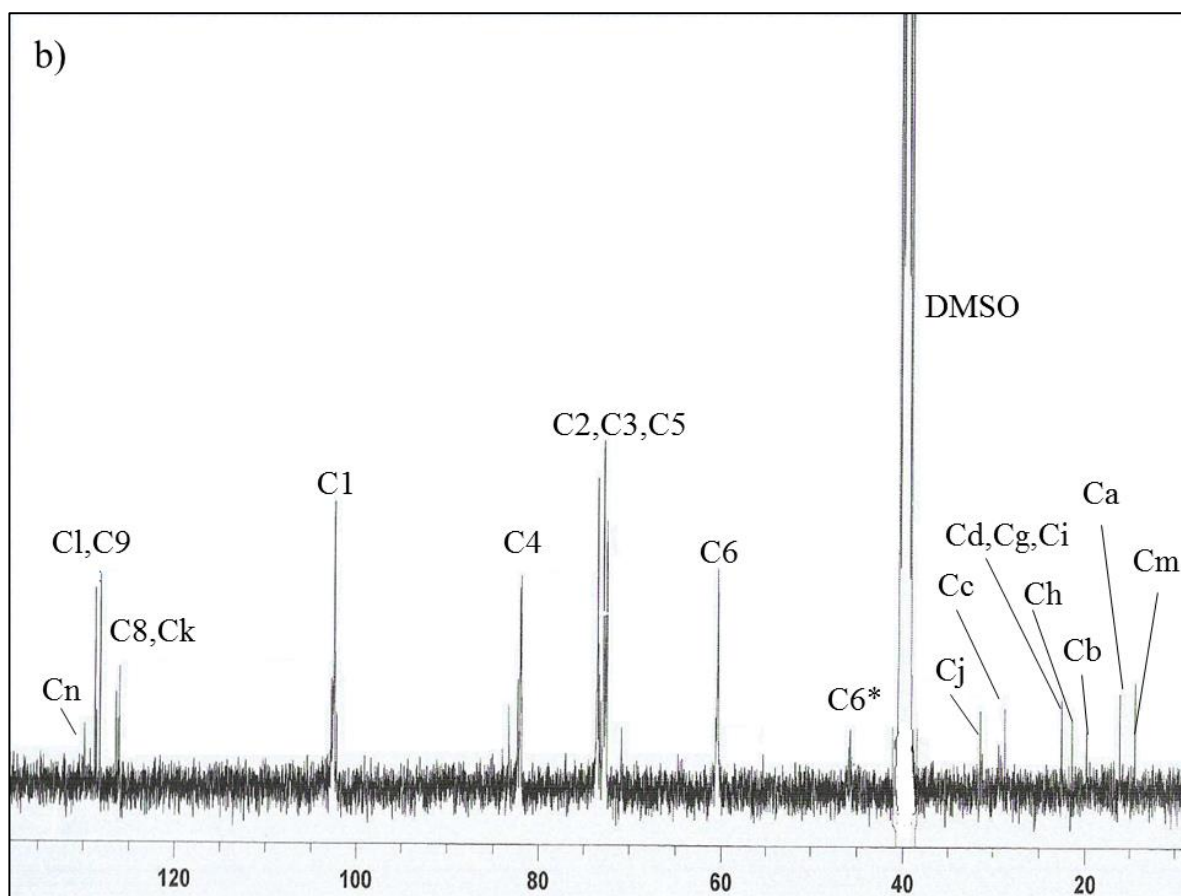
**Appendix C: NMR spectrum for  $^{13}\text{C}$  of  $\beta$ -CDOTs**



**Appendix D:** NMR spectrum for  $^{13}\text{C}$   $\beta$ -CD-BIMOTs



**Appendix E:** NMR spectrum for  $^1\text{H}$   $\beta$ -CD-DIMOTs



**Appendix F:** NMR spectrum for  $^{13}\text{C}$   $\beta$ -CD-DIMOTs



*$\beta$ -Cyclodextrin functionalized ionic liquid as chiral stationary phase of high performance liquid chromatography for enantioseparation of  $\beta$ -blockers*

**Nurul Yani Rahim, Kheng Soo Tay & Sharifah Mohamad**

**Journal of Inclusion Phenomena and  
Macrocyclic Chemistry**  
and Macrocyclic Chemistry

ISSN 1388-3127

J Incl Phenom Macrocycl Chem  
DOI 10.1007/s10847-016-0629-9



**Your article is protected by copyright and all rights are held exclusively by Springer Science +Business Media Dordrecht. This e-offprint is for personal use only and shall not be self-archived in electronic repositories. If you wish to self-archive your article, please use the accepted manuscript version for posting on your own website. You may further deposit the accepted manuscript version in any repository, provided it is only made publicly available 12 months after official publication or later and provided acknowledgement is given to the original source of publication and a link is inserted to the published article on Springer's website. The link must be accompanied by the following text: "The final publication is available at [link.springer.com](http://link.springer.com)".**

# $\beta$ -Cyclodextrin functionalized ionic liquid as chiral stationary phase of high performance liquid chromatography for enantioseparation of $\beta$ -blockers

Nurul Yani Rahim<sup>1</sup> · Kheng Soo Tay<sup>1</sup> · Sharifah Mohamad<sup>1,2</sup>Received: 3 January 2016 / Accepted: 1 June 2016  
© Springer Science+Business Media Dordrecht 2016

**Abstract** Two covalently bonded  $\beta$ -Cyclodextrin ( $\beta$ -CD) based CSPs were prepared by immobilizing the native  $\beta$ -CD and mono-6-deoxy-6-(3-benzylimidazolium tosylate)- $\beta$ -CD ( $\beta$ -CD-BIMOTs) onto modified silica gel.  $\beta$ -CD-BIMOTs is a  $\beta$ -CD based CSP with ionic liquid (3-benzylimidazolium tosylate) substituent. The enantioseparation capability of the synthesized CSPs was examined using 4 racemic mixtures of  $\beta$ -blockers (propranolol, metoprolol, pindolol and atenolol). The results indicated that  $\beta$ -CD-BIMOTs based CSP afforded more favorable enantioseparations than native  $\beta$ -CD based CSP. In order to study the mechanism of enantioseparation, inclusion complexes  $\beta$ -CD-BIMOTs and  $\beta$ -blockers were prepared and these inclusion complexes were characterized by using <sup>1</sup>H NMR and NOESY. In addition, the separation conditions such as pH and composition of mobile phase were varied to study the role of  $\beta$ -CD and ionic liquid in enantioseparation. In general, it can be concluded that the complete enantioseparation of propranolol and metoprolol is achieved through the formation of inclusion complex with  $\beta$ -CD-BIMOTs and the formation  $\pi$ - $\pi$  interaction with the ionic liquid moiety of  $\beta$ -CD-BIMOTs. The result also showed the poor enantioseparation of pindolol and atenolol

on the  $\beta$ -CD-BIMOTs based CSP due to the strong interaction at the exterior torus of  $\beta$ -CD-BIMOTs.

**Keywords** Cyclodextrin · Ionic Liquid · Enantio recognition · Chiral · Inclusion complex

## Introduction

$\beta$ -Blockers are a class of pharmaceuticals used to treat cardiovascular diseases [1, 2]. Propranolol, metoprolol, pindolol and atenolol are the most frequently used  $\beta$ -blockers in the markets [3].  $\beta$ -blockers are chiral compounds with different enantiomers showing different potential on pharmacological and therapeutic effects [4]. Most biological receptors act stereoselectively by interacting with only one enantiomer of a chiral substance, while the other enantiomer can be inactivated at the specific receptors. Mehvar and Brocks [1] reported that  $\beta$ -blockers inherent high degree of enantioselectivity in binding to the  $\beta$ -adrenergic receptors. For example, some of the enantiomers possess higher affinity for binding to the  $\beta$ -adrenergic receptors than antipode. Other enantiomers of  $\beta$ -blockers may possess other effects, such as antagonism at  $\alpha$ -adrenergic receptors. Therefore, the development of an efficient enantiomeric separation has attracted considerable attention due to the awareness that compounds of biological active such as pharmaceuticals can be chiral and their enantiomers are often exhibited different bioactivities and bio-toxicities [5]. For example, *S*-propranolol is 100 times more active than its *R*-propranolol [6]. So far, the enantioseparation of  $\beta$ -blockers are achieved using various chiral stationary phases (CSPs) and chiral mobile phase additives at analytical scale [7, 8].

Among various chiral stationary phases,  $\beta$ -cyclodextrins ( $\beta$ -CD) and their derivatives are among the most widely

**Electronic supplementary material** The online version of this article (doi:10.1007/s10847-016-0629-9) contains supplementary material, which is available to authorized users.

✉ Sharifah Mohamad  
sharifahm@um.edu.my

<sup>1</sup> Chemistry Department, Faculty Science, University Malaya, 50603 Kuala Lumpur, Malaysia

<sup>2</sup> University of Malaya Centre for Ionic Liquids (UMCiL), University of Malaya, 50603 Kuala Lumpur, Malaysia

used stationary phases in high-performance liquid chromatography (HPLC) [8–12].  $\beta$ -CD is a natural cyclic oligosaccharides comprised of seven glucose units joined through  $\alpha$ -1,4 linkage. When  $\beta$ -CD is used as CSP, chiral recognition can be achieved via the inclusion complex formation between chiral  $\beta$ -CD and enantiomers [13]. A  $\beta$ -CD molecule contains 35 chiral centers, and enantiomers can interact via van der Waals dispersion forces with its hydrophobic cavity.  $\beta$ -CD also has a C7 symmetry axis and 14 hydroxyl groups situated at the mouth of the cavity. Thus, a number of potential interactions might be present between these hydroxyl groups and enantiomers during the formation of inclusion complex. For instance, if the enantiomer has suitable polar substituents, one or more favorable hydrogen bonds can be formed with the  $\beta$ -CD CSP. Additionally, repulsive steric interactions could also occur

between any groups of the analytes and hydroxyl groups of CD [14, 15]. These properties of  $\beta$ -CD have led to its widely use as CSP particularly in HPLC for chiral separation [16].

On the other hand, native  $\beta$ -CD based CSP are unable to achieve satisfactory separation of enantiomers [11] because of the cylindrical binding cavity of  $\beta$ -CD which is too symmetry to induce large enantioselectivities [17]. Therefore, additional substituents are often introduced in order to achieve better chiral recognition. Various efforts have been directed toward developing new modified  $\beta$ -CD based CSP to enhance the chiral separation [18–20]. For example,  $\beta$ -CD containing ionic-liquid (IL) substituent have been extensively explored for the application of CSPs [21–25].

IL is defined as salt that melt at or below 100 °C to afford liquid. IL is usually composed of organic cation and inorganic or organic anion [26]. It was been used in environmentally benign chemical processing and chemical analysis [27]. IL molecules consist of high charge region and low charge region [28]. In IL based CSP, this dual properties of IL contribute to the enantioseparation through electrostatic and dispersive interaction [29]. In addition to the hydrophobic interaction, hydrogen bonding and dipole-dipole interaction of  $\beta$ -CD based CSP, the presence of IL can provide additional electrostatic interaction and  $\pi$ - $\pi$  interaction which can enhance the enantioseparation.

This study investigated the applicability of the new  $\beta$ -CD functionalized IL, mono-6-deoxy-6-(3-benzylimidazolium tosylate)- $\beta$ -CD ( $\beta$ -CD-BIMOTs) (Fig. 1) as CSP for enantioseparation of  $\beta$ -blockers (Fig. 2). The chromatographic performance of  $\beta$ -CD-BIMOTs against native  $\beta$ -CD based CSP was also evaluated. Based on literature reviews, most of the researches on the mechanism of enantioseparation

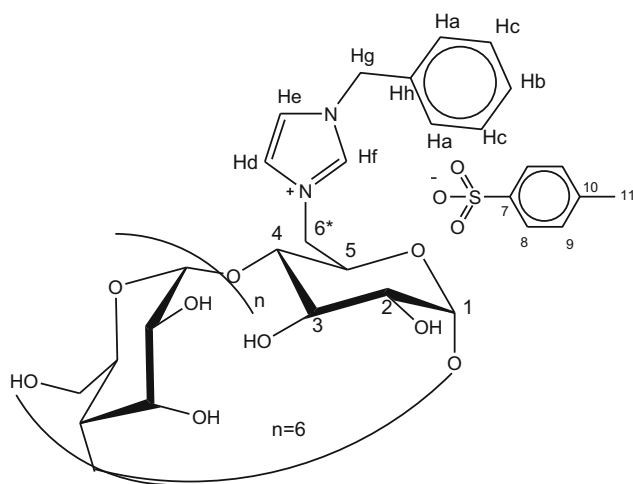


**Fig. 1** Structure of  $\beta$ -CD-BIMOTs

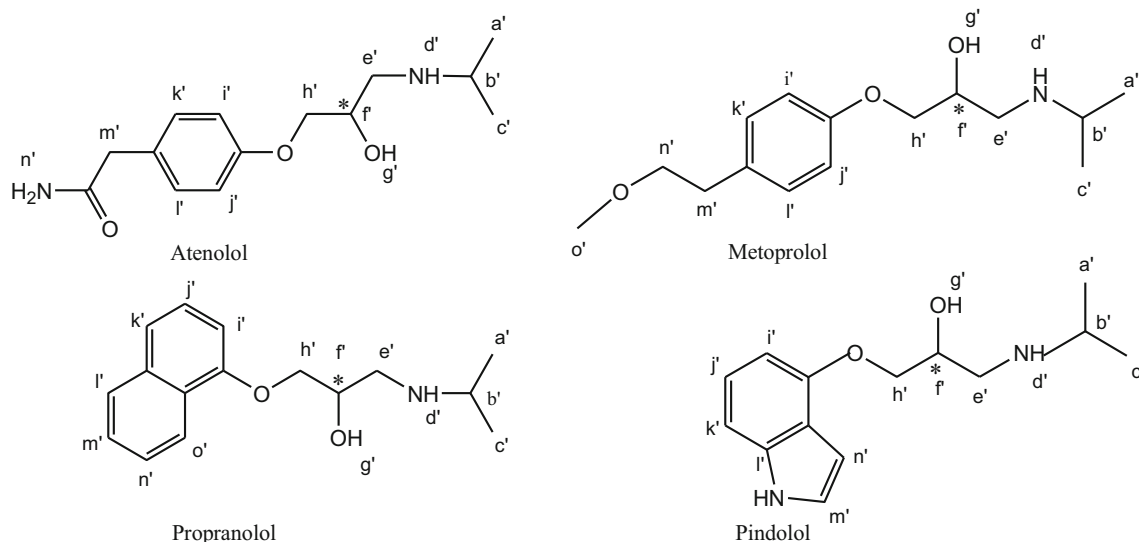


**Fig. 2** Structure and assignments of the hydrogen atoms of the studied  $\beta$ -blockers

were elaborated through hypothesis or computational study [30, 31]. This study investigated the mechanism of enantioseparation using the spectroscopic technique. This mechanism of enantioseparation provides an insight into the interaction between  $\beta$ -CD-BIMOTs CSP and  $\beta$ -blockers.

## Experimental

### Chemicals

All chemicals obtained were used without further purification. HPLC grade solvents were purchased from Merck (Germany).  $\beta$ -CD was purchased from Acros (Belgium) (99 %). 1-benzylimidazole (1-BzIIm), 2,4-toluene diisocyanate (TDI), propranolol, metoprolol, atenolol and pindolol (Fig. 2), Celite (60 Å and 60–200  $\mu$ m particle size) were supplied from Aldrich (USA). The Kromasil spherical silica gel (100 Å pore size and 5  $\mu$ m particle size) was purchased from Merck.

### Instruments

A Perkin–Elmer RX1 FT-IR (Perkin Elmer, Waltham, MA, USA) spectrophotometer was used to obtain infrared (IR) spectra. IR data were recorded in the range of 400–4000  $\text{cm}^{-1}$ . Thermogravimetric analyses (TGA) curves were obtained using a TA Instruments Q500 (Perkin Elmer, Waltham, MA, USA). In a stream of nitrogen atmosphere, a linear heating rate was set at 20  $^{\circ}\text{C}$  per min and the temperature range was 50 to 900  $^{\circ}\text{C}$ . All NMR spectra were recorded using an Avance 600 MHz (Bruker, Fällanden, Switzerland). Proton shifts are reported in parts per million (ppm) using the residual signal of dimethyl sulfoxide (DMSO- $d_6$ ). Evaluation of the CSPs performance was performed using a HPLC system consisting of a LC-20AT pump, a SPD-M20 detector, a SIL-20AHT auto sampler, a CTO-20AC column oven and CBM-20A communication bus module (Shimadzu, Japan).

### Synthesis of chiral stationary phase (CSP)

The synthesis pathway of CSP is illustrated in Fig. 3. There are 3 steps to synthesis the CSP: (a) preparation of 6-O-Monosyl-6-deoxy- $\beta$ -cyclodextrin ( $\beta$ -CDOTs), (b) preparation of Mono-6-deoxy-6-(3-benzylimidazolium tosylate)- $\beta$ -CD ( $\beta$ -CD-BIMOTs), (c) immobilization of  $\beta$ -CD-BIMOTs onto modified silica to obtain  $\beta$ -CD-BIMOTs CSP.

#### (a) Preparation of 6-O-Monosyl-6-deoxy- $\beta$ -cyclodextrin ( $\beta$ -CDOTs) (1)

$\beta$ -CDOTs was prepared as previously reported method [32]. Briefly, a suspension of  $\beta$ -CD (11.5 g, 10 mmol) and

*p*-toluene sulfonic anhydride ( $\text{Ts}_2\text{O}$ ) (4.9 g, 15 mmol) in 250 mL of water was stirred at room temperature for 2 h. Thereafter, a solution of NaOH (5.0 g in 50 mL of  $\text{H}_2\text{O}$ ) was then added. After 10 min, the reaction mixture was filtered through the Celite to separate the excess  $\text{Ts}_2\text{O}$ . The filtrate was adjusted to pH 8 by the addition of ammonium chloride (13.4 g).  $\beta$ -CDOTs as a precipitate was collected after cooling at 4  $^{\circ}\text{C}$  overnight.

(IR/KBR,  $\text{cm}^{-1}$ ) 3285 (O–H), 2925 (C–H), 1637 (C=C), 1598 (C–C), 1359 ( $\text{SO}_2$ , Assy.), 1154 ( $\text{SO}_2$ , Sym), 1024 (C–O).

( $^1\text{H}$  NMR/ppm, DMSO- $d_6$ ) 7.53(d, HAr, 2H), 7.21 (d, HAr, 2H), 4.55 (s, OH-6), 5.40–5.80 (m, H-6, 2H), 4.0 (m, H-6), 3.20–3.55 (m, H-3, H-5, H-6), 5.40–5.80 (br, OH-2, OH-3), 2.90–3.20 (m, H-2, H-4) 4.63 (d, H-1, 7H), 2.21, (s, -CH<sub>3</sub>, 3H).

#### (b) Preparation of Mono-6-deoxy-6-(3-benzylimidazolium tosylate)- $\beta$ -CD ( $\beta$ -CD-BIMOTs) (2)

The preparation of the mono-functionalized  $\beta$ -CD with IL was carried out according to a reported procedure [33]. Briefly, dried  $\beta$ -CDOTs (1.00 g, 0.78 mmol) and an appropriate amount of 1-BzIIm (10 mol equivalent) were dissolved in anhydrous DMF (40 mL) and the solution was stirred at 90  $^{\circ}\text{C}$  under nitrogen atmosphere. After 2 days, the resultant solution was cooled to room temperature and acetone was added slowly. Then, the mixture was stirred for 30 min and the resulting product was filtered and washed with excess amount of acetone. The final product obtained was re-crystallized thrice from hot water and a white yellow solid was obtained.

(IR/KBR,  $\text{cm}^{-1}$ ) 3291 (OH), 2925 (C–H), 1655 (C=C), 1152 (C–N).

( $^1\text{H}$  NMR/ppm, DMSO- $d_6$ ) Hf (9.2, s), He (7.93, s), Hc (7.47, s) Hb (7.74, t), Ha (7.45, s), Hg (5.18, s), H8 (7.38, d), H9 (7.09, d), OH2–OH3 (5.6–5.7, m), H1 (4.81, s), OH6(4.4–4.5, m), H6\* (3.89), H3, H5, H6 (3.4–3.6, m), H2–H4 (3.2–3.4, m), H11 (2.07, s).

#### (c) Immobilization of $\beta$ -CD-BIMOTs onto modified silica ( $\beta$ -CD-BIMOTs CSP) (3)

The immobilization of  $\beta$ -CD-BIMOTs with modified silica to obtain CSP is presented in Fig. 3. Silica was reacted with TDI with hexane as solvent for 4 h at room temperature. The Si-TDI was filtered and rinsed thoroughly using hexane and dried under vacuum [34]. The immobilization of  $\beta$ -CD-BIMOTs onto Si-TDI was then carried out by stirring Si-TDI (5 g) in anhydrous hexane (200 mL) under nitrogen atmosphere. After 30 min, a solution of  $\beta$ -CD-BIMOTs (1.8 g) in anhydrous hexane was added. Stirring was continued for 24 h. The obtained  $\beta$ -CD-BIMOTs CSP



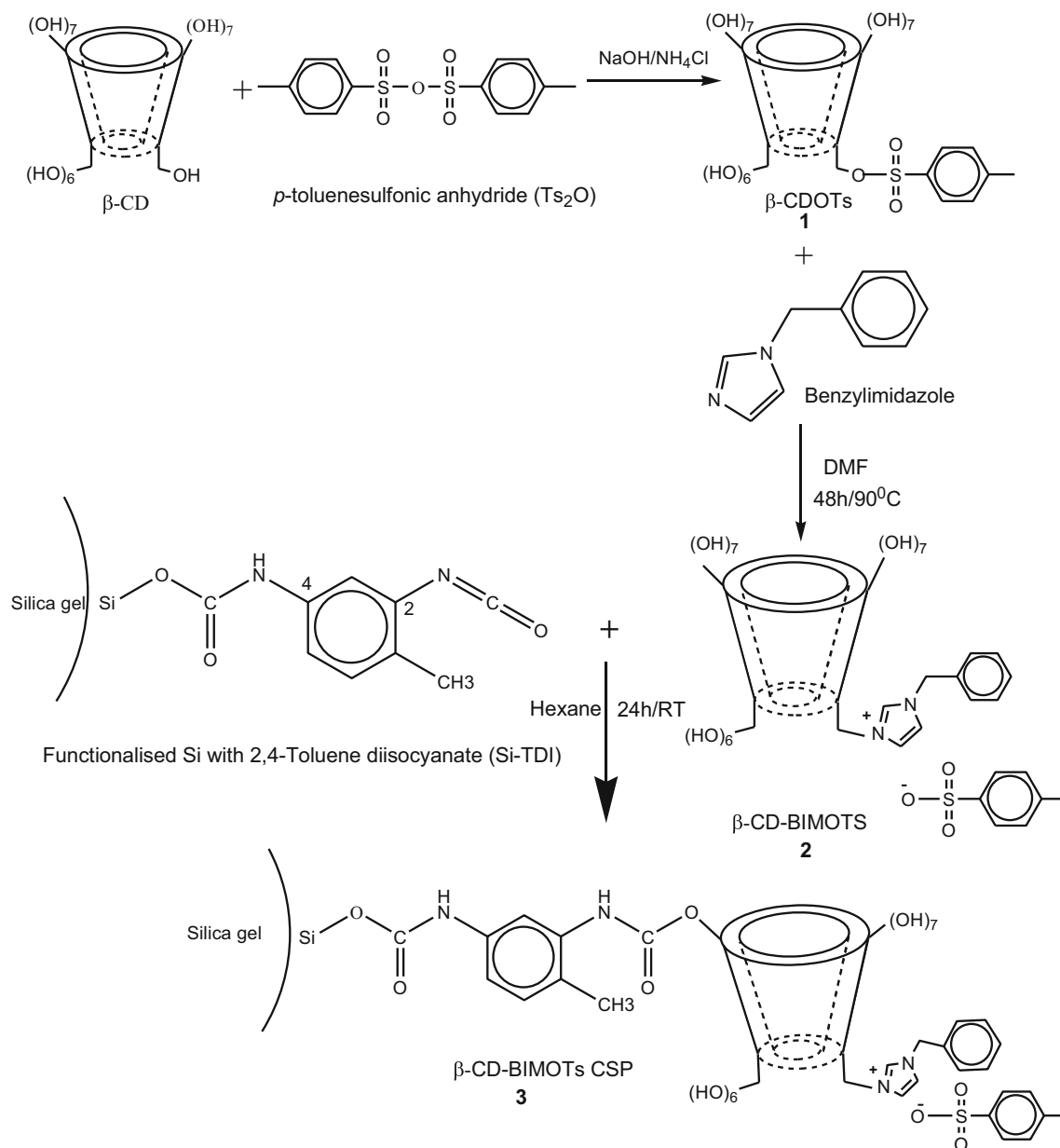


**Fig. 3** Synthesis pathways of  $\beta$ -CD-BIMOTs CSP

was filtered and washed with toluene, acetone and distilled water. The same procedure was applied to immobilize the native  $\beta$ -CD onto the Si-TDI by replacing  $\beta$ -CD-BIMOTs with unmodified  $\beta$ -CD. The obtained product was characterized using FT IR and TGA.

### Chromatographic method and column evaluation

Prepared CSPs (2.5 g) was suspended in approximately 15 ml of HPLC grade hexane to form slurry. The slurry was packed into an empty stainless steel HPLC column (250 mm  $\times$  4.6 mm I.D.) with hexane as packing solvent.

The CSPs were packed under 35 MPa with hexane for about 24 h.

The enantioseparation of  $\beta$ -blockers was performed by using acetonitrile (ACN) as organic eluent and ultrapure water or 1 % (v/v) triethylammonium acetate buffer (denoted as TEAA, adjusted with acetic acid to the desired pH) as aqueous eluent. Selected  $\beta$ -blockers were dissolved in methanol and filtered through a 0.22  $\mu\text{m}$  membrane filter. The injection volume was set at 20  $\mu\text{L}$ . The dead time was determined by injecting the methanol with water/acetonitrile (1/1, v/v) as mobile phase. The column temperature was controlled at  $30^\circ\text{C}$  and the flow rate was  $0.5\text{ mL min}^{-1}$ .

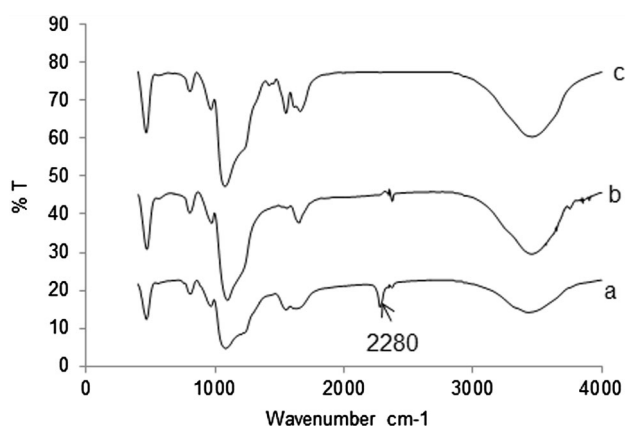


**Fig. 4** FTIR spectra of a) Si-TDI b)  $\beta$ -CD-BIMOTs CSP c) native  $\beta$ -CD CSP

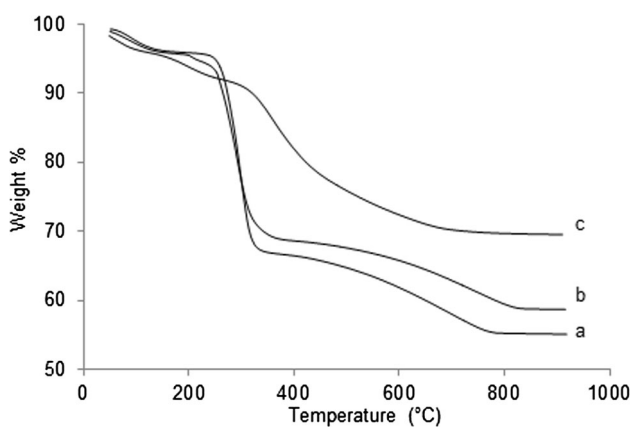


**Fig. 5** Thermogravimetric profiles of a)  $\beta$ -CD-BIMOTs CSP b) native  $\beta$ -CD CSP c) Si-TDI

### Calculations of chromatographic data

The retention factor ( $k'$ ), selectivity factor ( $\alpha$ ) and enantioresolution ( $R_s$ ) were used to describe the chromatographic separation of the selected enantiomers. They were calculated using the below equations:

$$k' = (t_R - t_0)/t_0 \quad (1)$$

$$\alpha = k'_2/k'_1 = (t_{R2} - t_0)/(t_{R1} - t_0) \quad (2)$$

$$R_s = 2 \times (t_{R2} - t_{R1})/(W_1 + W_2) \quad (3)$$

The dead time ( $t_0$ ) is the time for the mobile phase to pass through the column, which relates to the efficiency of the column. The retention time ( $t_R$ ) is the retention time corresponding to each enantiomer in the chromatographic separation  $t_{R1}$  and  $t_{R2}$  represents the retention times of the second and first enantiomers respectively, and  $W_1$  and  $W_2$  are the corresponding base peak width.

### Synthesis and characterization of inclusion complexes

The inclusion complex of  $\beta$ -CD-BIMOTs with  $\beta$ -blockers was prepared using the conventional kneading method [35, 36]. Equimolar amounts of  $\beta$ -CD-BIMOTs and  $\beta$ -blockers were kneaded with mortar and pestle in minimal amount of ethanol to form homogenous paste. The complex was kneaded for 30 min and dried to constant mass. After drying, a white powder ( $\beta$ -CD-BIMOTs- $\beta$ -blockers) was obtained. The final product was characterized in the liquid state by 1D  $^1\text{H}$  NMR and NOESY. For  $^1\text{H}$  NMR and NOESY, the spectra were obtained from the samples that

**Table 1** Chiral separation data for the  $\beta$ -blockers on  $\beta$ -CD-BIMOTs CSP and  $\beta$ -CD CSP in neutral pH mobile phase

$\beta$ -blockers	Conditions	$\beta$ -CD-BIMOTs CSP				$\beta$ -CD CSP			
		$k'_1$	$k'_2$	$\alpha$	$R_s$	$k'_1$	$k'_2$	$\alpha$	$R_s$
Atenolol	ACN/water-90/10	Na	Na	Na	Na	Na	Na	Na	Na
	ACN/water-50/50	Na	Na	Na	Na	Na	Na	Na	Na
	ACN/water-30/70	Na	Na	Na	Na	Na	Na	Na	Na
Metoprolol	ACN/water-90/10	2.04	3.64	1.78	2.38	0.05	0.05	1.00	0
	ACN/water-50/50	0.58	0.58	1.00	0	2.52	2.52	1.00	0
	ACN/water-30/70	0.65	0.65	1.00	0	–	–	–	–
Propranolol	ACN/water-90/10	2.83	4.88	1.72	3.10	Na	Na	Na	Na
	ACN/water-50/50	0.79	1.01	1.27	0.46	Na	Na	Na	Na
	ACN/water-30/70	0.84	1.10	1.30	0.43	Na	Na	Na	Na
Pindolol	ACN/water-90/10	Na	Na	Na	Na	0.41	0	1.00	0
	ACN/water-50/50	Na	Na	Na	Na	0.46	0	1.00	0
	ACN/water-30/70	Na	Na	Na	Na	0.49	0	1.00	0

Na not available

**Table 2** Chemical shifts corresponding to  $\beta$ -CD-BIMOTs in presence of  $\beta$ -blockers

	$\beta$ -CD-BIMOTs		$\beta$ -CD-BIMOTs-atenolol		$\beta$ -CD-BIMOTs-metoprolol		$\beta$ -CD-BIMOTs-propranolol		$\beta$ -CD-BIMOTs-pindolol	
	$\delta$	$\Delta$	$\Delta \delta$	$\Delta$	$\Delta \delta$	$\delta$	$\Delta \delta$	$\delta$	$\Delta \delta$	
H1	4.8405	4.8301	-0.0104	4.8249	-0.0156	4.8285	-0.012	4.8329	-0.0076	
H2	3.3312	3.3483	0.0171	3.3425	0.0113	3.3042	-0.027	3.3476	0.0155	
H3	3.6394	3.6311	-0.0083	3.6274	-0.0120	3.6309	-0.0085	3.6335	-0.0059	
H4	3.3716	3.4304	0.0588	3.4660	0.0944	3.3762	0.0046	3.4391	0.0675	
H5	3.5777	3.5488	-0.0289	3.5464	-0.0313	3.5531	-0.0246	3.5580	-0.0197	
H6	3.9225	3.9473	0.0248	3.9272	0.0047	3.9041	-0.0184	3.9041	-0.0184	
H8	7.4215	7.4212	-0.0003	7.4202	-0.0013	overlap	-	7.4361	0.0146	
H9	7.1112	7.1227	0.0115	Overlap	-	7.1192	0.0008	7.1259	0.0147	
H11	2.0847	2.0797	-0.0050	Overlap	-	-	-	-	-	
Ha	7.4314	7.4798	0.0484	7.4752	0.0438	7.4832	0.0518	7.4896	0.0582	
Hb	7.7957	7.7903	-0.0054	7.7892	0.0350	7.8063	0.0106	7.8081	0.0124	
Hc	7.7542	7.7402	-0.014	7.7391	-0.0151	7.7490	-0.0052	7.7473	-0.0069	
Hd	-	-	-	-	-	-	-	-	-	
He	7.9563	7.9440	-0.0123	-	-	-	-	-	-	
Hf	9.2394	9.2606	0.0212	9.2807	0.0413	9.3132	0.0738	9.3379	0.0985	
Hg	5.4371	5.4400	0.0029	5.4460	0.0089	5.4369	-0.0002	5.4482	0.0111	

**Table 3** Induced shifts corresponding to  $\beta$ -blockers in presence of  $\beta$ -CD-BIMOTs

	$\beta$ -CD-BIMOTs-atenolol $\Delta \delta$	$\beta$ -CD-BIMOTs-metoprolol $\Delta \delta$	$\beta$ -CD-BIMOTs-propranolol $\Delta \delta$	$\beta$ -CD-BIMOTs-pindolol $\Delta \delta$
Ha'	0.1059	0.0995	-0.0018	0.1140
Hb'	0.1345	0.0055	-	0.2063
Hc'	0.1060	0.0995	-0.0018	0.1140
Hd'	-	-0.0075	-0.0160	-0.0067
He'	0.1596	-0.0057	-0.0044	0.1766
Hf'	0.0545	-	-0.0063	-
Hg'	-	-0.0075	-0.0246	-0.0067
Hh'	-0.0008	-0.0269	0.0794	0.0248
Hi'	0.0118	0.0048	-0.0012	0.0041
Hj'	0.0096	0.0064	-0.0027	0.0162
Hk'	0.0096	-0.0009	-0.0025	0.0162
Hi'	0.0132	0.0003	-0.0131	0.0836
Hm'	0.0054	-	-0.0037	-0.0006
Hn'	-	-	-0.0011	0.0056
Ho'	-	-	-0.0055	-

- overlap peak

prepared using  $\beta$ -CD-BIMOTs and  $\beta$ -blockers with the ratio of 1:1. The samples were dissolved in DMSO- $d_6$ . Seven hundred microliter of solutions were introduced into standard 5 mm NMR tubes and the spectra were recorded at 300.15 K. For NOESY experiments, the spectra were recorded with a mixing time of 700 ms with 256 increments and 40 scans.

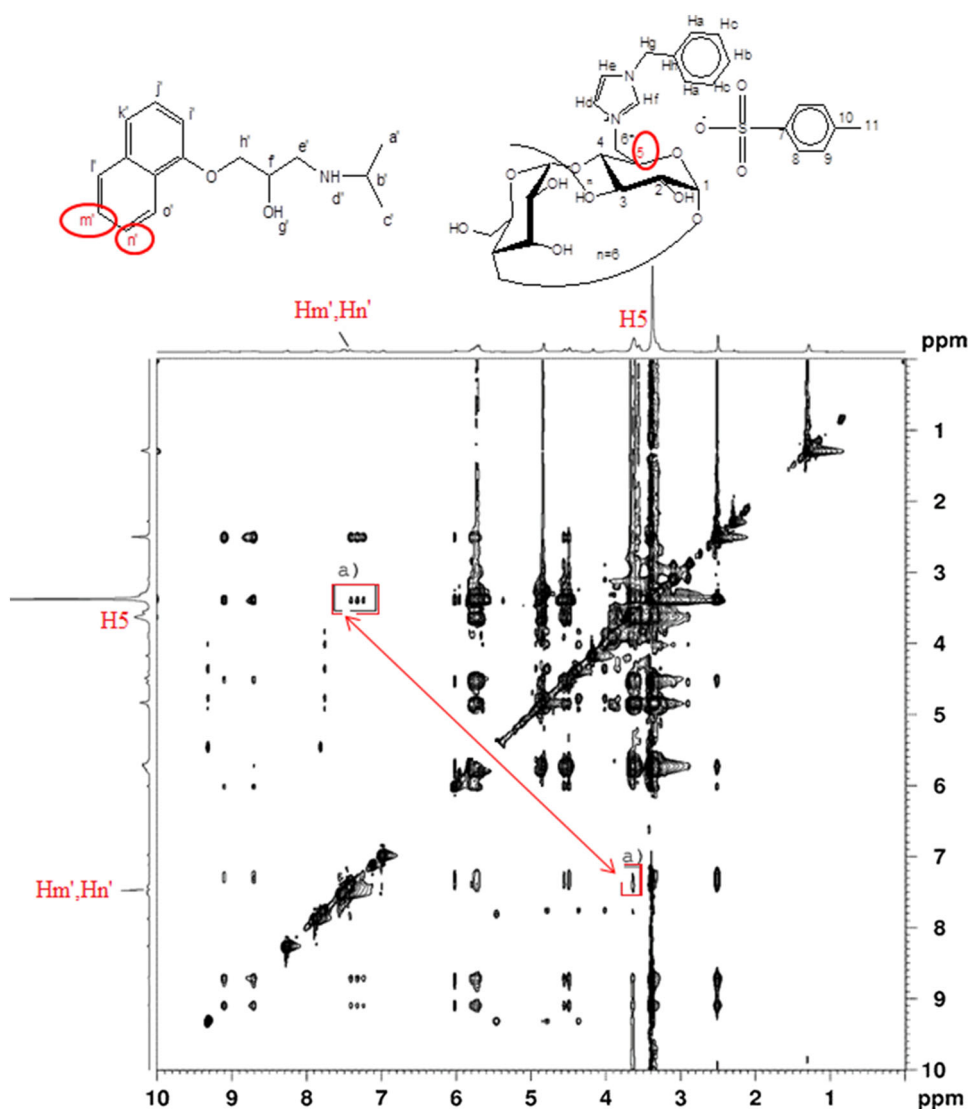
## Result and discussion

### FTIR Characterization of Si-TDI, native $\beta$ -CD CSP and $\beta$ -CD-BIMOTs CSP

The silica was modified using TDI as the linker. TDI has two isocyanate groups with different activities towards



**Fig. 6** 2D NOESY spectra of  $\beta$ -CD-BIMOTs-propranolol complex



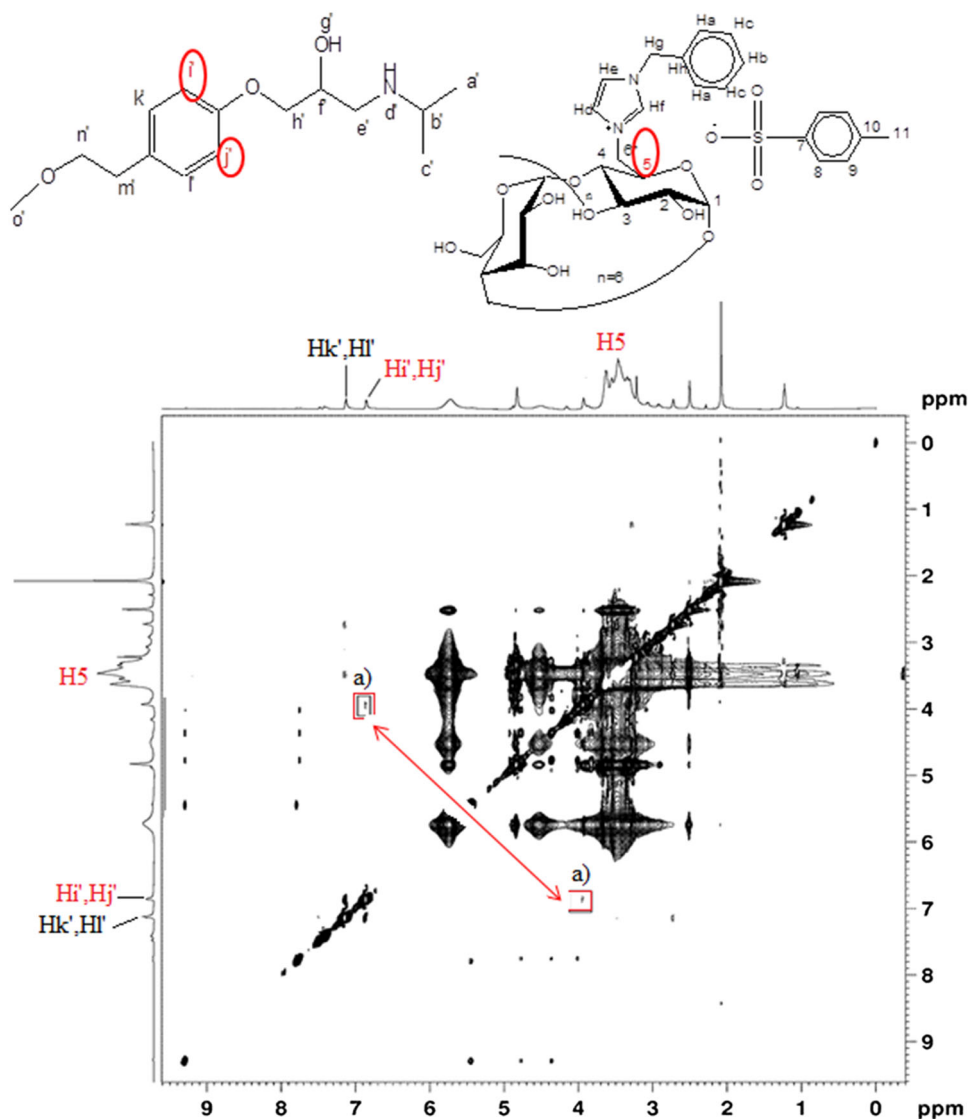
hydroxyl groups located at the para-position and ortho-position, respectively. The isocyanate functional groups in TDI (para position) reacted with hydroxyl groups at the surface of silica and formed Si-TDI. The two isocyanate groups in TDI reacted at different rates with the para-position (approximately four times more reactive than the ortho-position) [37, 38]. Figure 4 shows the disappearance of the absorption peak of isocyanate group at  $2280\text{ cm}^{-1}$  indicated that the reserved isocyanate groups had reacted with  $\beta$ -CD or  $\beta$ -CD-BIMOTs.

#### TGA Characterization of Si-TDI, native $\beta$ -CD CSP and $\beta$ -CD-BIMOTs CSP

Thermogravimetry was employed to further determine the presence of  $\beta$ -CD and  $\beta$ -CD-BIMOTs on the synthesized

CSPs. In this experiment, weight loss that attributed to the loss of the organic group of the synthesized CSPs was observed between 200 to 600 °C [39]. Figure 5 shows the thermogravimetric curves of Si-TDI, native  $\beta$ -CD CSP and  $\beta$ -CD-BIMOTs CSP. The curve of all CSPs and Si-TDI exhibited the first weight loss below 250 °C which was due to the loss of the physisorbed water as well as the condensation of the silanol groups. In native  $\beta$ -CD CSP and  $\beta$ -CD-BIMOTs CSP, the larger weight loss was observed above 280 °C. This weight loss can be attributed to the thermal decomposition of  $\beta$ -CD and  $\beta$ -CD-BIMOTs moieties on the synthesized CSPs. As compared with  $\beta$ -CD CSP, higher weight loss was observed for  $\beta$ -CD-BIMOTs CSP indicating the presence of higher organic content. This result provides further evidence for the presence of  $\beta$ -CD and  $\beta$ -CD-BIMOTs on the synthesized CSPs.

**Fig. 7** 2D NOESY spectra of  $\beta$ -CD-BIMOTs-metoprolol complex



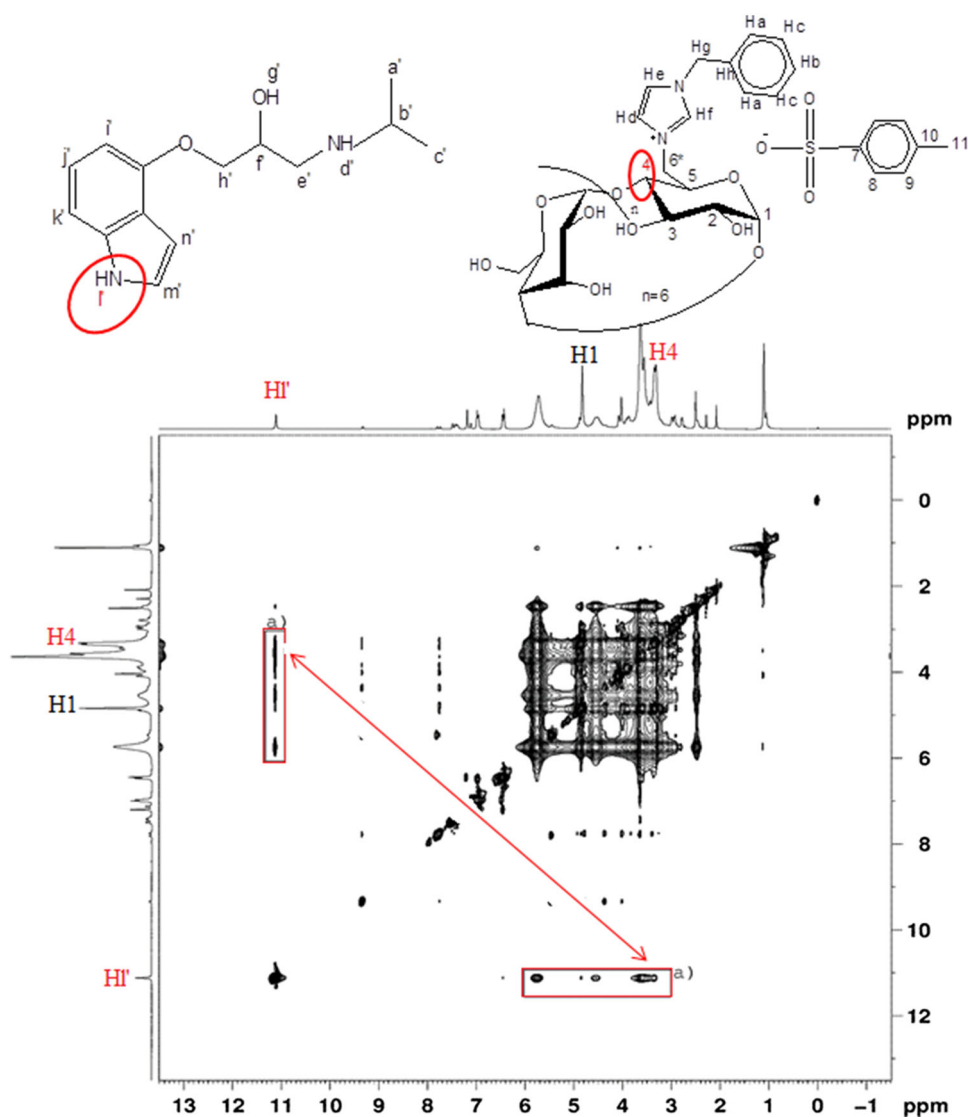
### Chromatographic performance and inclusion complex evaluation

The enantioselectivity of  $\beta$ -CD-BIMOTs CSP was first compared with native  $\beta$ -CD CSP for enantioseparation of  $\beta$ -blockers as shown in Table 1. The results indicated that baseline separation was achieved for the enantiomers of propranolol and metoprolol on  $\beta$ -CD-BIMOTs CSP. Meanwhile, all the  $\beta$ -blockers were not enantioseparated by using native- $\beta$ -CD CSP. This proved that the presence of IL moieties at  $\beta$ -CD-BIMOTs CSP play an important role to improve the enantioseparation for some of  $\beta$ -blockers. This result indicated that the contribution of multi-modal retention properties of IL which involved hydrogen bonding, hydrophobic,  $\pi$ - $\pi$  and electrostatic interactions could enhance the chiral recognition [40]. Table 1 also shows the higher  $R_s$  values were obtained for

propranolol ( $R_s = 3.10$ ) and metoprolol ( $R_s = 2.38$ ) on  $\beta$ -CD-BIMOTs CSP. Complete enantioseparation of propranolol and metoprolol was achieved in 30 min. For pindolol and atenolol, no peak was observed even after 120 min due to the high retention of these compounds onto  $\beta$ -CD-BIMOTs CSP.  $\beta$ -Blockers can be divided into lipophilic (propranolol and metoprolol) and hydrophilic (pindolol and atenolol) nature [3]. Atenolol and pindolol with polar amide and indole moiety respectively tends to interact stronger with CSP through hydrogen bonding which contribute to high retention. Thus, it is proven that the  $\beta$ -blockers with lipophilicity properties are well enantioseparated than the hydrophilic  $\beta$ -blockers.

The enantioseparation of propranolol and metoprolol were separated excellently using  $\beta$ -CD-BIMOTs CSP might due to the formation of inclusion complex between the analytes and  $\beta$ -CD through the stereogenic center of

**Fig. 8** 2D NOESY spectra of  $\beta$ -CD-BIMOTs-pindolol complex



CD which is located at the interior of the cavity of  $\beta$ -CD. According Li et al. [41], the formation of inclusion complex is an important interaction to achieve better enantioselectivity. In order to verify this interaction, the formation of inclusion complexes of  $\beta$ -CD-BIMOTs and selected  $\beta$ -blockers were prepared.  $^1\text{H}$  NMR and NOESY were used to study the interaction between  $\beta$ -CD-BIMOTs and  $\beta$ -blockers. The values of the chemical shifts ( $\delta$ ) for different protons in  $\beta$ -CD-BIMOTs,  $\beta$ -blockers and  $\beta$ -blockers- $\beta$ -CD-BIMOTs complexes are listed in Table 2 and 3. The deduced structures of the  $\beta$ -CD-BIMOTs and  $\beta$ -CD-BIMOTs- $\beta$ -blockers complexes are shown in supplementary data, Figs. S1 and S2, respectively. Normally, the inclusion of an apolar region of an analyte into the hydrophobic cavity would affect the inner protons of the glucose units of  $\beta$ -CD, namely, H3 and H5, whereas the protons on the exterior torus of  $\beta$ -CD (H1, H2 and H4)

would remain unaffected [42]. For  $\beta$ -CD-BIMOTs- $\beta$ -blockers complexes, the presence of propranolol and metoprolol show appreciable  $\Delta\delta$  of H5 proton of  $\beta$ -CD-BIMOTs (Table 2). The upfield shifts for this proton proved the existence of an interaction between the analytes and the interior proton of  $\beta$ -CD-BIMOTs. Additionally, the larger  $\Delta\delta$  of H1' proton of propranolol as shown in Table 3 indicated that a perturbation occurs at the aromatic ring of propranolol which might be due to  $\pi$ - $\pi$  interaction with IL at  $\beta$ -CD-BIMOTs. In contrast, the  $\Delta\delta$  values of aromatic protons (H1', Hj', Hk', Hl') of metoprolol were relatively weak (Table 3). This suggested that propranolol achieved better enantioselectivity than metoprolol because of the additional  $\pi$ - $\pi$  interaction contributed by IL at  $\beta$ -CD-BIMOTs. Moreover, the greater  $\Delta\delta$  of H4 proton of  $\beta$ -CD-BIMOT-metoprolol was observed as compared to other complexes. Higher electronegativity of oxygen atom at the

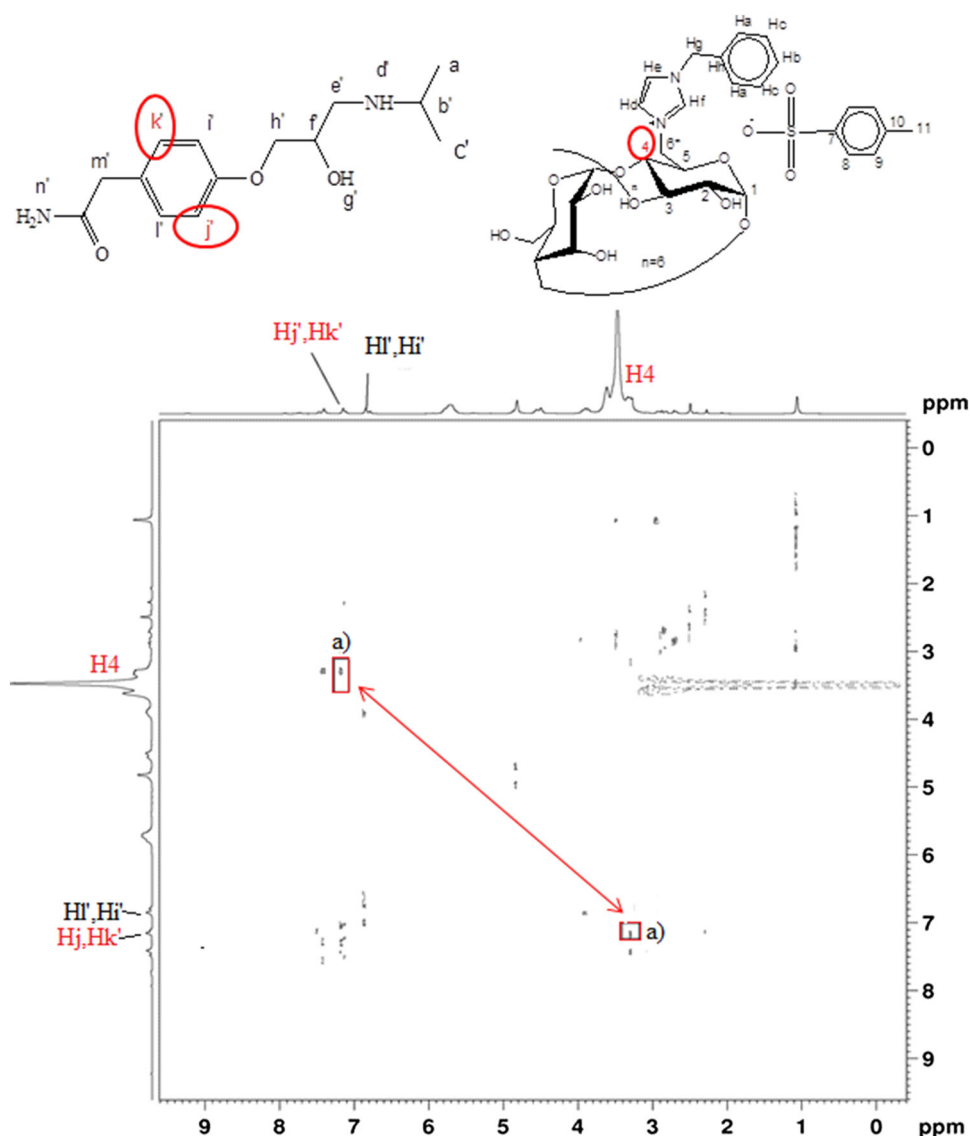
methoxy group of metoprolol caused the lower electron density around the H4 proton. As a result, the proton was deshielded and experienced higher chemical shift. In Fig. 6, the cross peak between Hm' and Hn' protons of propranolol with H5 proton  $\beta$ -CD-BIMOTs complex was observed in NOESY spectra. Meanwhile, in Fig. 7, the cross peak between Hi' and Hj' protons of metoprolol with H5 proton of  $\beta$ -CD-BIMOTs complex was also observed. This indicated that propranolol and metoprolol interact with interior protons of  $\beta$ -CD-BIMOTs.

From the  $^1\text{H}$  NMR studied, the  $\Delta\delta$  of H4 (exterior proton) at  $\beta$ -CD-BIMOTs was appreciably shifted downfield after forming complexes with pindolol or atenolol. This suggests that pindolol and atenolol are not forming inclusion complex but it formed hydrogen bonding with exterior torus of  $\beta$ -CD-BIMOTs. Moreover, the large  $\Delta\delta$  were observed for Ha', Hb' and Hc' of pindolol and

atenolol (Table 3). For  $\beta$ -CD-BIMOTs-pindolol complex, the NOESY spectra show the cross-peak between Hi' proton of pindolol with H1 and H4 protons of  $\beta$ -CD-BIMOTs (Fig. 8). Meanwhile,  $\beta$ -CD-BIMOTs-atenolol complex shows the cross-peak between Hj' and Hk' protons of atenolol and H4 protons of  $\beta$ -CD-BIMOTs (Fig. 9). This result indicated the close interaction of pindolol and atenolol at the exterior protons of  $\beta$ -CD-BIMOTs.

The composition of the mobile phase also plays an important role in enantioseparation. The effect of ACN contents on enantioseparation of selected  $\beta$ -blockers can be seen from Table 1. The high  $k'_1$  and  $k'_2$  of propranolol and metoprolol at high organic content (90 % ACN) showed the normal phase behavior of the  $\beta$ -CD-BIMOTs CSP. On the other hand, when organic content is low (30 % ACN), the high  $k'_1$  and  $k'_1$  of propranolol and metoprolol showed typical reverse phase behavior of  $\beta$ -CD-BIMOTs CSP. Therefore,

**Fig. 9** 2D NOESY spectra of  $\beta$ -CD-BIMOTs-atenolol complex



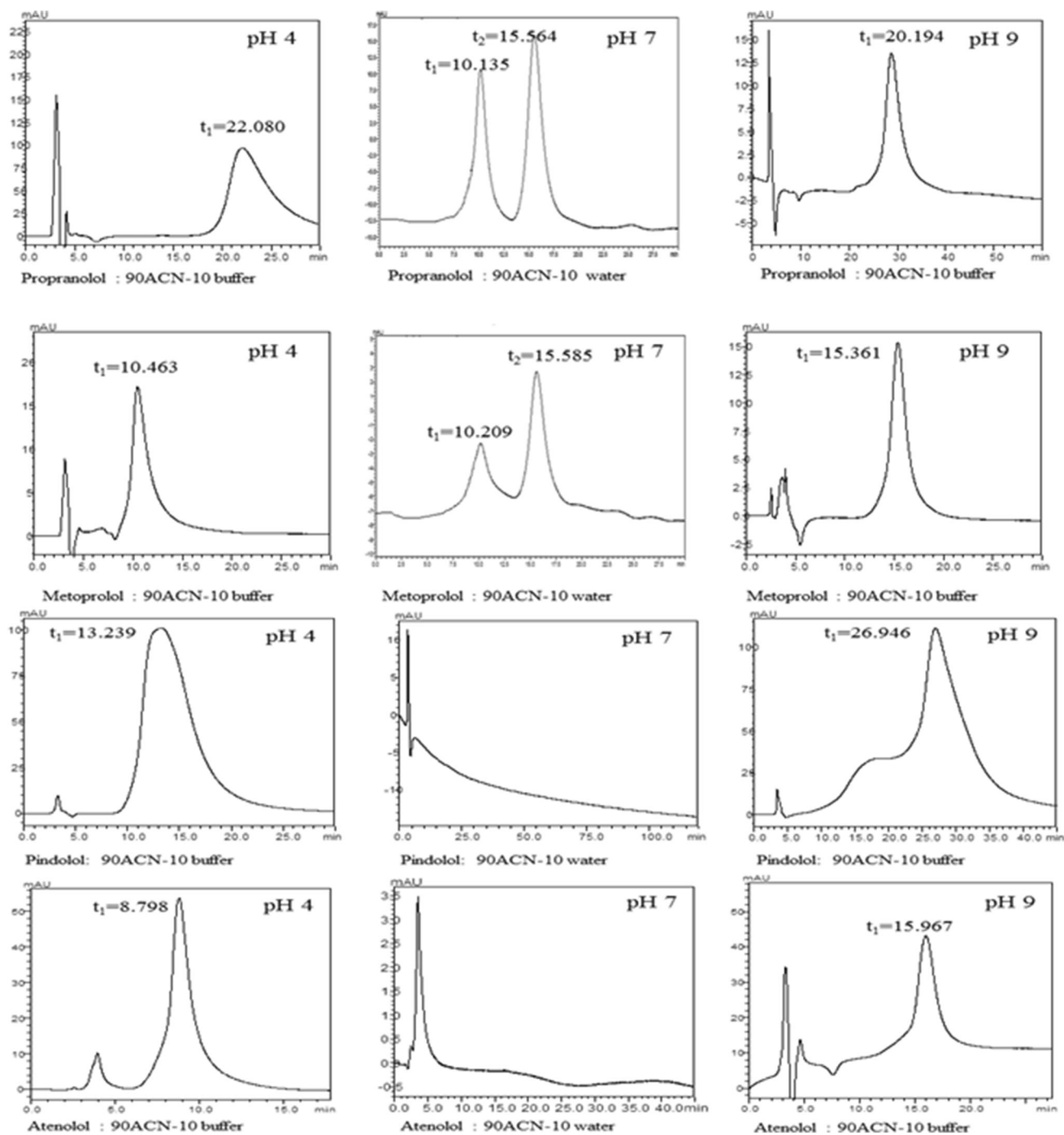


**Fig. 10** The chromatograms of propranolol, metoprolol, pindolol and atenolol responding to different pH of mobile phase

the retention behavior of  $\beta$ -blockers can be considered as the mixed aqueous-normal separation mode [43]. In this separation mode, the retention mechanism is based on the distribution of the analytes between the ACN-rich mobile phase and water enriched layer adsorbed onto the polar stationary phase [44]. Thus, for more hydrophilic analytes (pindolol and atenolol), partitioning equilibrium is shifted towards the immobilized water layer on the stationary phase, causing the analytes retained longer in column.

TEAA buffer was used to control the mobile phase pH and ion strength. Buffer can influence the degree of ionization of analytes and resulting in different retention behavior. The chromatograms in Fig. 10 show the effect of pH towards the enantioseparation of  $\beta$ -blockers. Propranolol and metoprolol were not enantioseparated at pH 4 and 9. Meanwhile, they are well enantioseparated at pH 7. This is due to the deprotonation and protonation of  $\beta$ -blockers at pH 4 and 9, respectively. Protonated and



deprotonated analytes were not favorable for the formation of inclusion complex with  $\beta$ -CD [45]. This finding further support the role of inclusion complex formation in enantioseparation of  $\beta$ -CD based CSPs. Meanwhile, the retention time of pindolol and atenolol was reduced at pH 4 and 9 as compared to pH 7. Due to both of analytes and  $\beta$ -CD-BIMOTs CSP acquiring positive charges at pH 4, the electrostatic repulsion occurred and reduced the retention time. At basic pH, the abundance of TEAA species reduces the retention time due to the competition between TEAA and protonated analytes.

## Conclusion

In this study, the  $\beta$ -CD-BIMOTs and native  $\beta$ -CD was successfully synthesized and immobilized onto the modified silica to obtain CSPs. The enantioseparation of  $\beta$ -blockers using  $\beta$ -CD-BIMOTs CSP with ionic liquid moiety was found to be better than native  $\beta$ -CD CSP. This proved the critical role of ionic liquid in enhancing the enantioseparation for some of  $\beta$ -blockers. Propranolol and metoprolol obtained good enantioresolution compared to atenolol and pindolol. The results suggested that the lipophilic property and the structure of propranolol and metoprolol that enable the formation of inclusion complex contribute to better enantioseparation. This observation was proven by  $^1\text{H}$  NMR and NOESY of  $\beta$ -CD-BIMOTs- $\beta$ -blockers inclusion complexes. According to  $^1\text{H}$  NMR and NOESY, propranolol and metoprolol showed the interaction at the interior torus of  $\beta$ -CD-BIMOTs which indicates the formation of inclusion complex. However, atenolol and pindolol showed the strong interaction at exterior torus of  $\beta$ -CD-BIMOTs and resulting in the poor enantioseparation.

**Acknowledgments** Authors would like to seize this opportunity to express their gratitude to the University Malaya for the IPPP grant PG027/2013A and UMRG grant (RP006A-13SUS and RP011B-14SUS). The authors also acknowledge Ministry of Higher Education (MOHE) for providing fellowship to one of the authors-cum-researchers, Ms. NurulYani Rahim.

## Compliance with ethical standards

**Conflict of interest** The authors declare that they have no conflict of interest.

## References

- Mehvar, R., Brocks, D.R.: Stereospecific pharmacokinetics and pharmacodynamics of beta-adrenergic blockers in humans. *J. Pharm. Pharm. Sci.* **4**, 185–200 (2001)
- Wilson, A.G., Brooke, O.G., Lloyd, H.J., Robinson, B.F.: Mechanism of action of  $\beta$ -adrenergic receptor blocking agents in angina pectoris: comparison of action of propranolol with dexpropranolol and practolol. *Br. Med. J.* **4**, 399–401 (1969)
- Borchard, U.: Pharmacological properties of beta-adrenoceptor blocking drugs. *J. Clin. Bas. Cardiol.* **1**, 5–9 (1998)
- Hoffman, B.B.: Catecholamines, sympathomimetic drugs, and adrenergic receptor antagonists, *The pharmacological basis of therapeutics* (1996)
- Armstrong, D.W.: Direct enantiomeric separations in liquid chromatography and gas chromatography. In: Issaq, H.J. (ed.) *A Century of Separation Science*, pp. 555–578. Marcel Dekker, New York (2002)
- Stoschitzky, K., Lindner, W., Zernig, G.: Racemic beta-blockers-fixed combinations of different drugs. *J. Clin. Bas. Cardiol.* **1**, 15–19 (1998)
- Hedeland, M., Isaksson, R., Pettersson, C.: Cellobiohydrolase I as a chiral additive in capillary electrophoresis and liquid chromatography. *J. Chromatogr. A* **807**, 297–305 (1998)
- Aboul-Enein, H.Y., Abou-Basha, L.I.: HPLC separation of nadolol and enantiomers on chiralcel OD column. *J. Liq. Chrom. Rel. Techno.* **19**, 383–392 (1996)
- Armstrong, D.W., DeMond, W.: Cyclodextrin bonded phases for the liquid chromatographic separation of optical, geometrical, and structural isomers. *J. Chromatogr. Sci.* **22**, 411–415 (1984)
- Armstrong, D.W., Ward, T.J., Armstrong, R.D., Beesley, T.E.: Separation of drug stereoisomers by the formation of beta-cyclodextrin inclusion complexes. *Science* **232**, 1132–1135 (1986)
- Stalcup, A.M., Chang, S.C., Armstrong, D.W., Pitha, J.: (S)-2-Hydroxypropyl- $\beta$ -cyclodextrin, a new chiral stationary phase for reversed-phase liquid chromatography. *J. Chromatogr. A* **513**, 181–194 (1990)
- Armstrong, D.W., Stalcup, A.M., Hilton, M.L., Duncan, J.D., Faulkner Jr., J.R., Chang, S.C.: Separation of metallocene enantiomers by liquid chromatography: chiral recognition via cyclodextrin bonded phases. *Anal. Chem.* **57**, 481–484 (1985)
- Scriba, G.K., Altria, K.: Using cyclodextrins to achieve chiral and non-chiral separations in capillary electrophoresis. *LC GC EUROPE.* **22**, 420 (2009)
- Hinze, W.L., Riehl, T.E., Armstrong, D.W., Demond, W., Alak, A., Ward, T.: Liquid chromatography separation of enantiomers using a chiral  $\beta$ -cyclodextrin bonded stationary phase and conventional aqueous-organic mobile phase. *Anal. Chem.* **57**, 237–242 (1985)
- Daffé, V., Fastrez, J.: Cyclodextrin-catalysed hydrolysis of oxazol-5(4H)-ones. Enantioselectivity of the acid-base and ring-opening reactions. *J. Chem. Soc. Perkin Trans.* **2**, 789–796 (1983)
- Juvancz, Z., Szejtli, J.: The role of cyclodextrins in chiral selective chromatography. *Trends Anal. Chem.* **21**, 379–388 (2002)
- Szejtli, J.: Medicinal applications of cyclodextrins. *Med. Res. Rev.* **14**, 353–386 (1994)
- Wang, Y., Young, D.J., Tan, T.T.Y., Ng, S.C.: “Click” immobilized perphenylcarbamated and permethylated cyclodextrin stationary phases for chiral high-performance liquid chromatography application. *J. Chromatogr. A* **1217**, 5103–5108 (2010)
- Poon, Y.F., Muderawan, I.W., Ng, S.C.: Synthesis and application of mono-2 A-azido-2 A-deoxyperphenylcarbamoylated  $\beta$ -cyclodextrin and mono-2 A-azido-2 A-deoxyperacetylated  $\beta$ -cyclodextrin as chiral stationary phases for high-performance liquid chromatography. *J. Chromatogr. A* **1101**, 185–197 (2006)
- Ahuja, S.: *Chiral Separations by Chromatography*. American Chemical Society, Oxford University Press, Oxford (2000)
- Zhou, Z., Li, X., Chen, X.: Synthesis of ionic liquids functionalized  $\beta$ -cyclodextrin-bonded chiral stationary phases and their

- applications in high-performance liquid chromatography. *Anal. Chim. Acta* **678**, 208–214 (2010)
22. Wang, R.Q., Ong, T.T., Ng, S.C.: Chemically bonded cationic  $\beta$ -cyclodextrin derivatives as chiral stationary phases for enantioseparation applications. *Tetrahedron Lett.* **53**, 2312–2315 (2012)
  23. Wang, R.Q., Ong, T.T., Tang, W., Ng, S.C.: Cationic cyclodextrins chemically-bonded chiral stationary phases for high-performance liquid chromatography. *Anal. Chim. Acta* **718**, 121–129 (2012)
  24. Zhang, J., Shen, X., Chen, Q.: Separation processes in the presence of cyclodextrins using molecular imprinting technology and ionic liquid cooperating approach. *Curr. Org. Chem.* **15**, 74–85 (2011)
  25. Zhou, Z., Li, X., Chen, X., Hao, X.: Synthesis of ionic liquids functionalized  $\beta$ -cyclodextrin-bonded chiral stationary phases and their applications in high-performance liquid chromatography. *Anal. Chim. Acta* **678**, 208–214 (2010)
  26. Wasserscheid, P., Keim, W.: Ionic liquids—new “solutions” for transition metal catalysis. *Angew. Chem.* **39**, 3772–3789 (2000)
  27. Pandey, S.: Analytical applications of room-temperature ionic liquids: a review of recent efforts. *Anal. Chim. Acta* **556**, 38–45 (2006)
  28. Canongia Lopes, J.N., Pádua, A.A.: Nanostructural organization in ionic liquids. *J. Phys. Chem. B* **110**, 3330–3335 (2006)
  29. Anderson, J.L., Armstrong, D.W.: High-stability ionic liquids. A new class of stationary phases for gas chromatography. *Anal. Chem.* **75**, 4851–4858 (2003)
  30. Li, X., Zhou, Z.: Enantioseparation performance of novel benzimidazole- $\beta$ -cyclodextrins derivatized by ionic liquids as chiral stationary phases. *Anal. Chim. Acta* **819**, 122–129 (2014)
  31. Li, X., Zhou, Z., Dai, W.L., Li, Z.: Preparation of a novel cyclodextrin derivative of benzimidazole- $\beta$ -cyclodextrin and its enantioseparation performance in HPLC. *Analyst* **136**, 5017–5024 (2011)
  32. Zhong, N., Byun, H.S., Bittman, R.: An improved synthesis of 6-O-monotosyl-6-deoxy- $\beta$ -cyclodextrin. *Tetrahedron Lett.* **39**, 2919–2920 (1998)
  33. Ong, T.T., Tang, W., Muderawan, W., Ng, S.C., Chan, H.S.O.: Synthesis and application of single-isomer 6-mono (alkylimidazolium)- $\beta$ -cyclodextrins as chiral selectors in chiral capillary electrophoresis. *Electrophoresis* **26**, 3839–3848 (2005)
  34. Yatabe, J., Kageyama, T.: Preparation of hydrophobic silica with isocyanate. *J. Ceram. Soc. Jpn.* **102**, 595–598 (1994)
  35. Cwiertnia, B., Hladon, T., Stobiecki, M.: Stability of diclofenac sodium in the inclusion complex with  $\beta$ -cyclodextrin in the solid state. *J. Pharm. Pharmacol.* **51**, 1213–1218 (1999)
  36. Daruházi, Á.E., Szente, L., Balogh, B., Mátyus, P., Béni, S., Takács, M., Lemberkovics, E.: Utility of cyclodextrins in the formulation of genistein: Part I. Preparation and physicochemical properties of genistein complexes with native cyclodextrins. *J. Pharm. Biomed. Anal.* **48**, 636–640 (2008)
  37. Arnold, R.G., Nelson, J.A., Verbanc, J.J.: Recent advances in isocyanate chemistry. *Chem. Rev.* **57**, 47–76 (1957)
  38. Simons, D.M., Arnold, R.G.: Relative reactivity of the isocyanate groups in toluene 2,4-diisocyanate. *J. Am. Chem. Soc.* **78**, 1658–1659 (1956)
  39. Lumley, B., Khong, T.M., Perrett, D.: The characterization of chemically bonded chromatographic stationary phases by thermogravimetry. *Chromatographia* **60**, 59–62 (2004)
  40. Pino, V., Afonso, A.M.: Surface-bonded ionic liquid stationary phases in high-performance liquid chromatography—a review. *Anal. Chim. Acta* **714**, 20–37 (2012)
  41. Li, S., Purdy, W.C.: Direct separation of enantiomers using multiple-interaction chiral stationary phases based on the modified  $\beta$ -cyclodextrin-bonded stationary phase. *J. Chromatogr. A* **625**, 109–120 (1992)
  42. Zhang, D.D., Zhao, P.Y., Huang, N.J., Wu, Y.L., Zhai, Y.M.: Study of  $\alpha$ -cyclodextrin or dimethylcyclodextrin/toluene in CF COOD/DO. In: *The 5th International Symposium on Cyclodextrins*. Editions de Santé, pp. 146–149 (1990)
  43. Guo, Z., Jin, Y., Liang, T., Liu, Y., Xu, Q., Liang, X., Lei, A.: Synthesis, chromatographic evaluation and hydrophilic interaction/reversed-phase mixed-mode behavior of a “Click  $\beta$ -cyclodextrin” stationary phase. *J. Chromatogr. A* **1216**, 257–263 (2009)
  44. Buszewski, B., Noga, S.: Hydrophilic interaction liquid chromatography (HILIC)—a powerful separation technique. *Anal. Bioanal. Chem.* **402**, 231–247 (2012)
  45. Raoov, M., Mohamad, S., Abas, M.R.: Removal of 2, 4-dichlorophenol using cyclodextrin-ionic liquid polymer as a macroporous material: characterization, adsorption isotherm, kinetic study, thermodynamics. *J. Hazard. Mater.* **263**, 501–516 (2013)

# *Chromatographic and Spectroscopic Studies on $\beta$ -Cyclodextrin Functionalized Ionic Liquid as Chiral Stationary Phase: Enantioseparation of Flavonoids*

**Nurul Yani Rahim, Kheng Soo Tay & Sharifah Mohamad**

## **Chromatographia**

An International Journal for Rapid Communication in Chromatography, Electrophoresis and Associated Techniques

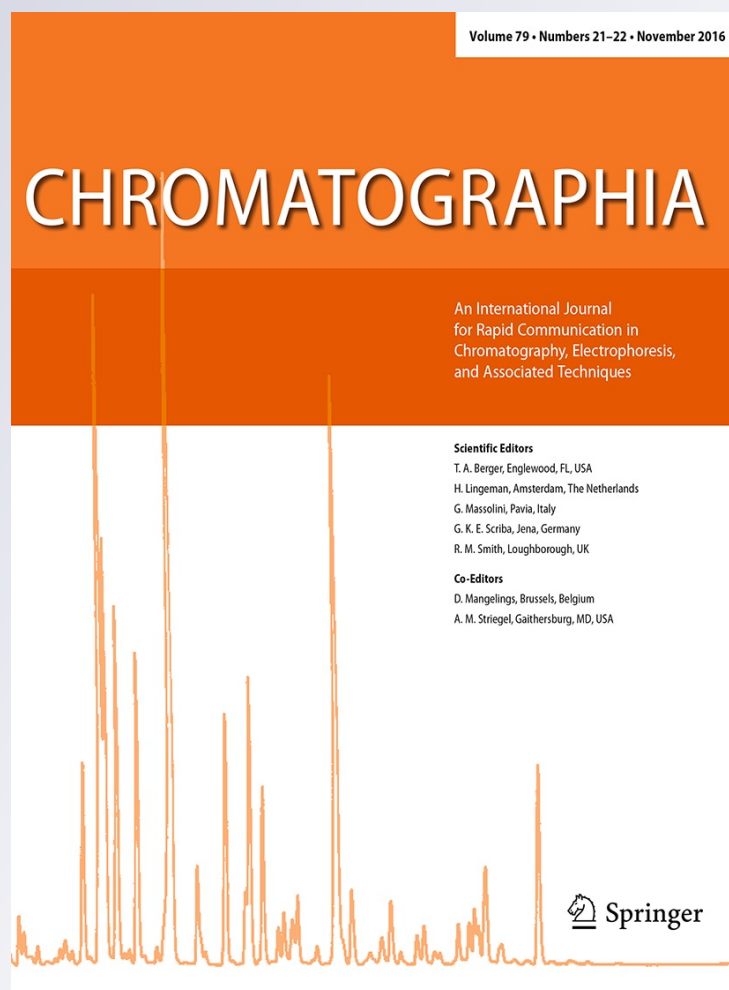
ISSN 0009-5893

Volume 79

Combined 21-22

Chromatographia (2016) 79:1445-1455

DOI 10.1007/s10337-016-3169-y





**Your article is protected by copyright and all rights are held exclusively by Springer-Verlag Berlin Heidelberg. This e-offprint is for personal use only and shall not be self-archived in electronic repositories. If you wish to self-archive your article, please use the accepted manuscript version for posting on your own website. You may further deposit the accepted manuscript version in any repository, provided it is only made publicly available 12 months after official publication or later and provided acknowledgement is given to the original source of publication and a link is inserted to the published article on Springer's website. The link must be accompanied by the following text: "The final publication is available at [link.springer.com](http://link.springer.com)".**

# Chromatographic and Spectroscopic Studies on $\beta$ -Cyclodextrin Functionalized Ionic Liquid as Chiral Stationary Phase: Enantioseparation of Flavonoids

Nurul Yani Rahim<sup>1</sup> · Kheng Soo Tay<sup>1</sup> · Sharifah Mohamad<sup>1,2</sup>

Received: 13 May 2016 / Revised: 31 August 2016 / Accepted: 6 September 2016 / Published online: 15 September 2016  
© Springer-Verlag Berlin Heidelberg 2016

**Abstract** In this study,  $\beta$ -cyclodextrin functionalized ionic liquid was prepared by adding 1-benzylimidazole onto 6-monotosyl-6-deoxy- $\beta$ -cyclodextrin ( $\beta$ -CDOTs) to obtain  $\beta$ -CD-BIMOTs.  $\beta$ -CD-BIMOTs were then bonded onto the modified silica to produce chiral stationary phases ( $\beta$ -CD-BIMOTs-CSP). The performance of  $\beta$ -CD-BIMOTs-CSP was evaluated by observing the enantioseparation of flavonoids. The performance of  $\beta$ -CD-BIMOTs stationary phase was also compared with native  $\beta$ -CD stationary phase. For the selected flavonoids, flavanone and hesperetin obtained a high resolution factor in reverse phase mode. Meanwhile, naringenin and eriodictyol attained partial enantioseparation in polar organic mode. In order to understand the mechanism of separation, the interaction of selected flavonoids and  $\beta$ -CD-BIMOTs was studied using spectroscopic methods (<sup>1</sup>H NMR, NOESY and UV–Vis spectrophotometry). The enantioseparated flavanone and hesperetin were found to form an inclusion complex with  $\beta$ -CD-BIMOTs. However, naringenin and eriodictyol were not enantioseparated due to the formation of hydrogen bonding at exterior torus of  $\beta$ -CD-BIMOTs.

**Keywords** Column liquid chromatography ·  $\beta$ -Cyclodextrin · Ionic liquid · Flavonoids · Enantioseparation

## Introduction

Flavonoids are biological active organic molecules that occur in various vascular plants [1]. Flavanone, hesperetin, naringenin and eriodictyol are the most abundant flavonoids in nature. These flavonoids can be easily extracted from grape fruits and citrus fruits [2]. The protective effect of these flavonoids against lipid peroxidation of membranes and their role in physiological and pathological disorders (such as aging, inflammation, atherosclerosis and ischemia) have been extensively reported [3, 4]. Recently, chirality of the flavonoids has been taken into consideration since enantiomers of the chiral compound can have different biological and toxicological effects on living organisms [5]. In most studies, preparation of pure enantiomer is mainly through (1) asymmetric (enantioselective) synthesis and (2) chiral separation of racemic mixtures [6]. Enantioselective synthesis is of great importance to pure enantiomer preparation, but it can be difficult to achieve. Thus, chiral separation of racemic mixtures is an alternative method used to obtain the desired enantiomer [7].

In this study, the enantioseparation of selected flavonoids was carried out using the  $\beta$ -cyclodextrin ( $\beta$ -CD) based chiral stationary phase (CSP).  $\beta$ -CD is a natural cyclic oligosaccharides comprised of seven glucose units joined through  $\alpha$ -1,4 linkage. A  $\beta$ -CD molecule contains 35 chiral centers which led to its widely used as stationary phase in HPLC for the chiral separation [8]. In  $\beta$ -CD based CSP, chiral separation is achieved through hydrogen bonding or dipole–dipole interaction of analytes with the OH groups of

**Electronic supplementary material** The online version of this article (doi:10.1007/s10337-016-3169-y) contains supplementary material, which is available to authorized users.

✉ Sharifah Mohamad  
sharifahm@um.edu.my

<sup>1</sup> Department of Chemistry, Faculty of Science, University of Malaya, 50603 Kuala Lumpur, Malaysia

<sup>2</sup> University of Malaya Centre for Ionic Liquids (UMCiL), University of Malaya, 50603 Kuala Lumpur, Malaysia

$\beta$ -CD. In addition, formation of inclusion complex between analytes with hydrophobic cavity of  $\beta$ -CD was found to enhance the chiral separation [9]. On the other hand, native  $\beta$ -CD based CSP is not always provide satisfactory separation of enantiomers [10]. As a result, various efforts have been directed towards developing new  $\beta$ -CD derivatives to enhance the chiral separation [11]. Ionic liquid (IL) is an example of new substituent group that have been used to modify  $\beta$ -CD [12, 13]. IL is composed of organic cation and inorganic or organic anion [14]. IL is widely used in environmentally benign chemical processing and chemical analysis [15]. IL molecule consists of high charge region and low charge region [16]. In IL based CSP, the dual properties of IL contribute to the enantioseparation through additional electrostatic and dispersive interaction [17]. Therefore, in addition to the hydrophobic interaction, hydrogen bonding and dipole–dipole interaction of  $\beta$ -CD based CSP with enantiomers, the presence of IL can provide additional electrostatic interaction and  $\pi$ - $\pi$  interaction which can further enhance the enantioseparation [12].

In this study, mono-6-deoxy-6-(3-benzylimidazolium tosylate)- $\beta$ -CD ( $\beta$ -CD-BIMOTs) was bonded to modified silica gel to obtain a modified- $\beta$ -CD based CSP ( $\beta$ -CD-BIMOTs-CSP). The performance of  $\beta$ -CD-BIMOTs-CSP was then compared with native  $\beta$ -CD based CSP for enantioseparation of flavonoids. Based on literature reviews, most of the researches on the mechanism of enantioseparation on  $\beta$ -CD functionalized IL based CSP were elaborated through hypothesis or computational study [12, 13]. This study investigated the mechanism of enantioseparation using the spectroscopic and spectrophotometric techniques

( $^1\text{H}$  NMR, NOESY and UV–Vis). The result from the spectroscopic and spectrophotometric techniques provides the information on the intermolecular interactions between analytes and CSP that involved in the chiral discrimination of flavonoids by  $\beta$ -CD-BIMOTs-CSP.

## Experimental

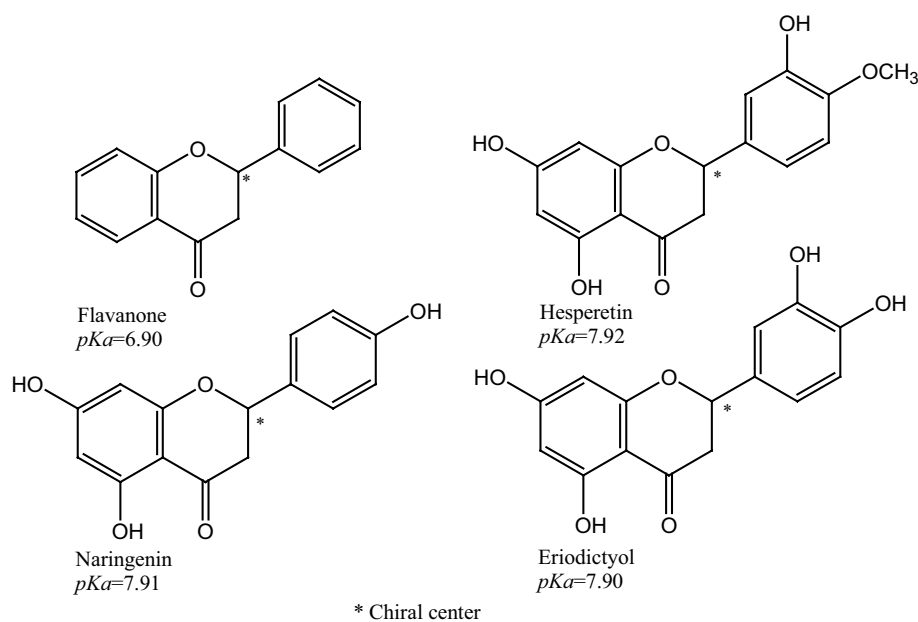
### Materials

$\beta$ -CD was purchased from Acros (Geel, Belgium) (99 %). 1-benzylimidazole (1-BzIm), 2,4-toluene diisocyanate (TDI) and racemic flavanone (Fig. 1) were purchased from Aldrich (St. Louis, MO, USA). The HPLC grade solvents (acetonitrile (ACN), methanol (MeOH) and hexane) and Kromasil spherical silica gel (100 Å pore size and 5  $\mu\text{m}$  particle size) were purchased from Merck (Darmstadt, Germany). The racemic hesperetin, naringenin and eriodictyol (Fig. 1) were purchased from Carl Roth (Karlsruhe, Germany). All chemicals obtained were used without further purification.

### Instruments

A Perkin-Elmer RX1 FT-IR (Waltham, USA) spectrophotometer was used to record all infrared (IR) spectra. IR data were recorded from 400 to 4000  $\text{cm}^{-1}$ . Absorption spectra measurements were carried out with a Shimadzu UV 1800 (Kyoto, Japan) spectrophotometer in the range of 190–800 nm. All NMR spectra were recorded using

**Fig. 1** The structure of studied flavonoids



Bruker Avance 600 MHz (Fällanden, Switzerland). Proton shifts are reported in parts per million (ppm) using the residual signal of dimethyl sulfoxide ( $\text{DMSO-}d_6$ ). The enantioseparation was monitored using a Shimadzu HPLC system consisted of a LC-20AT pump, a SPD-M20 detector, a SIL-20AHT auto sampler, a CTO-20AC column oven and CBM-20A communication bus module (Kyoto, Japan).

### Synthesis of Chiral Stationary Phase (CSP)

#### Synthesis of $\beta$ -CD-BIMOTs

$\beta$ -CD-BIMOTs (Fig. 2) was prepared according to the previously reported method [18, 19]. The substitution of IL onto  $\beta$ -CD was confirmed by IR and the simple proton NMR [18]. New peak was observed in proton NMR ( $\text{H6}^*$ , 3.9 ppm) which belonged to substituted  $\beta$ -CD [19]. The yield was 90 %.

#### Immobilization of $\beta$ -CD-BIMOTs onto Si-TDI

The synthesis of TDI modified silica gel (Si-TDI) and the immobilization of  $\beta$ -CD-BIMOTs onto the Si-TDI were presented in Electronic Supplementary Material (Fig. S1). Si-TDI was first prepared as reported by Yatabe [20]. Then, the obtained Si-TDI was reacted with  $\beta$ -CD-BIMOTs in anhydrous hexane for 24 h to obtain  $\beta$ -CD-BIMOTs-CSP.  $\beta$ -CD-BIMOTs-CSP was then filtered and washed with hexane, acetone and distilled water. The same procedure was applied to immobilize the native  $\beta$ -CD onto the Si-TDI by replacing  $\beta$ -CD-BIMOTs with  $\beta$ -CD. The products was then characterized using FT-IR.

### Chromatographic Conditions

$\beta$ -CD-BIMOTs-CSP (2.5 g) were packing into a stainless steel column (250 mm  $\times$  4.6 mm I.D.). The CSPs were packed under 35 MPa with hexane for about 24 h. The enantioseparation of the selected flavonoids on  $\beta$ -CD-BIMOTs-CSP was evaluated in both reverse phase and polar organic mobile phases. The reverse phase mode was prepared by mixing different amounts of ACN or MeOH with ultra-pure water or triethylammonium acetate (TEAA) buffer pH 4 and 9 (0.1 M, ionic strength 0.21) [21]. TEAA was prepared with addition of acetic acid (HOAc) into solution of triethylamine (TEA). Whereas, polar organic mobile phase consisted of varies volume fraction mixture of ACN/MeOH/TEA/HOAc started at 90/10/1/3 (0.09 ionic strength) or 90/10/3/1 (0.06 ionic strength).

Flavonoids were dissolved in MeOH and filtered through a 0.22  $\mu\text{m}$  membrane filter. The injection volume was set at 20  $\mu\text{L}$ . The dead time was determined by injecting MeOH with ACN/water (1/1, v/v) as mobile phase. The column temperature was controlled at 30  $^\circ\text{C}$  and the flow rate was fixed at 0.5 mL/min.

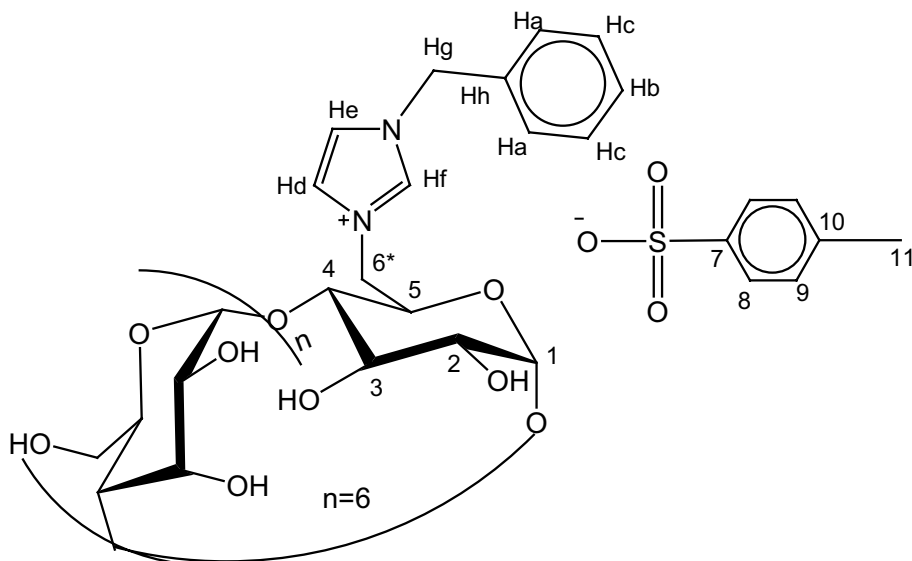
### Data Processing

The relative retentions ( $k$ ) was calculated using the following equations:

$$k_1 = \frac{(t_{R1} - t_0)}{t_0}, \quad (1)$$

$$k_2 = \frac{(t_{R2} - t_0)}{t_0}, \quad (2)$$

**Fig. 2** Structure of  $\beta$ -CD-BIMOTs



where the dead time ( $t_0$ ) is the time for the mobile phase to pass through the column,  $t_{R1}$  and  $t_{R2}$  represent the retention time of the first and second enantiomers, respectively. The resolution factor ( $R_s$ ) was calculated using Eq. (3):

$$R_s = 2 \times \frac{(t_{R2} - t_{R1})}{(W_1 + W_2)}, \quad (3)$$

where  $W_1$  and  $W_2$  are the corresponding base peak width.

### Preparation of $\beta$ -CD-BIMOTs-Flavonoids Complexes

The  $\beta$ -CD-BIMOTs-flavonoid complexes were prepared using the conventional kneading method [22].  $\beta$ -CD-BIMOTs and flavonoids with the molar ratio of 1:1 were pulverised in a ceramic mortar with the presence of minimum amount of ethanol to form homogenous paste. The complex was kneaded for 30 min and dried to constant mass. The final product was characterized using  $^1\text{H}$  NMR and NOESY.  $^1\text{H}$  NMR and NOESY spectra of  $\beta$ -CD-BIMOTs-flavonoid complexes were recorded at 27 °C using a Bruker Avance 600 MHz NMR spectrometer in  $\text{DMSO-}d_6$ . For NOESY experiments, the spectra were recorded with a mixing time of 700 ms with 256 increments and 40 scans.

### Determination the Formation Constant of $\beta$ -CD-BIMOTs-Flavonoids Complexes

The solution of  $\beta$ -CD-BIMOTs-flavonoids complexes were prepared by adding a 2.0 mL of 0.01 mM flavonoids aliquot and 3.2 mL of 0.0032 M  $\beta$ -CD-BIMOTs solution into a 10.0 mL standard volumetric flask and diluted to the mark with ultra-pure water. The absorption spectra of  $\beta$ -CD-BIMOTs-flavonoids complexes were recorded against blank reagent which was prepared with the same reagent concentration but without the addition of flavonoids. The absorption spectra of flavonoids and  $\beta$ -CD-BIMOTs alone were also recorded.

The formation constant ( $K$ ) of the  $\beta$ -CD-BIMOTs-flavonoids complexes were obtained from the slope of Benesi–Hildebrand plot that generated using Eqs. (4) and (5). For the formation constant curve, the concentration of flavonoids was held constant at 0.01 mM, meanwhile the concentration of  $\beta$ -CD-BIMOTs was varied (0.001, 0.002, 0.003 and 0.005 M). In this experiment, water was used as blank in all measurements.

$$\frac{1}{(A - A_0)} = \left[ \frac{1}{(A' - A_0)} \right] + \left[ \frac{1}{K(A' - A_0)[\beta\text{-CD-BIMOTs}]} \right], \quad (4)$$

$$K = \left[ \frac{1}{\text{Slope}(A' - A_0)} \right], \quad (5)$$

where  $A_0$  and  $A$  are the absorbances of the free guest and the  $\beta$ -CD-BIMOTs, respectively.  $A'$  is the absorbance at the maximum concentration of  $\beta$ -CD-BIMOTs.

## Results and Discussion

### FTIR Characterization of CSPs

The FT-IR spectra of silica gel, Si-TDI, native  $\beta$ -CD based CSP and  $\beta$ -CD-BIMOTs-CSP are shown in Fig. 3. In the Fig. 3a, the sharp peaks at 1059 and 3332  $\text{cm}^{-1}$  were attributed to Si–O bond and O–H stretching, respectively. Compared to silica gel, Si-TDI (Fig. 3b) showed a characteristic peak of isocyanate (O=C=N–) group at 2280  $\text{cm}^{-1}$ . This indicated that the reaction of TDI with Si took place through the formation of urethane bond [23]. In the spectra of native  $\beta$ -CD based CSP and  $\beta$ -CD-BIMOTs-CSP (Fig. 3c, d), the broad O–H stretching band was observed at 3461 and 3455  $\text{cm}^{-1}$  attributed to  $\beta$ -CD. The absence of the peak at 2280  $\text{cm}^{-1}$  (corresponding to isocyanate group) at Fig. 3c, d was clearly observed. This result indicated that the completion of reaction for immobilization of both native  $\beta$ -CD and  $\beta$ -CD-BIMOTs onto modified silica [18, 19]. In addition, the band at 1643  $\text{cm}^{-1}$  that attributed to C=C bond of aromatic ring of 1-BzlIm further proven the anchoring  $\beta$ -CD-BIMOTs on to the Si-TDI (Fig. 3d).

### Screening Performance of $\beta$ -CD-BIMOTs-CSP

This study was started by comparing the performance of  $\beta$ -CD-BIMOTs-CSP with native  $\beta$ -CD based CSP in order to investigate the effect of IL substituent on the enantio-separation of flavonoids. The results (Fig. 4a) of this study

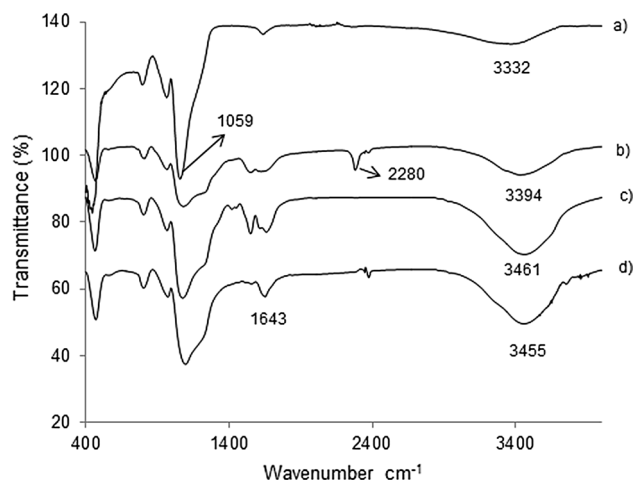


**Fig. 3** FT-IR spectrum of **a** silica, **b** Si-TDI, **c** native  $\beta$ -CD-CSP, **d**  $\beta$ -CD-BIMOTs-CSP



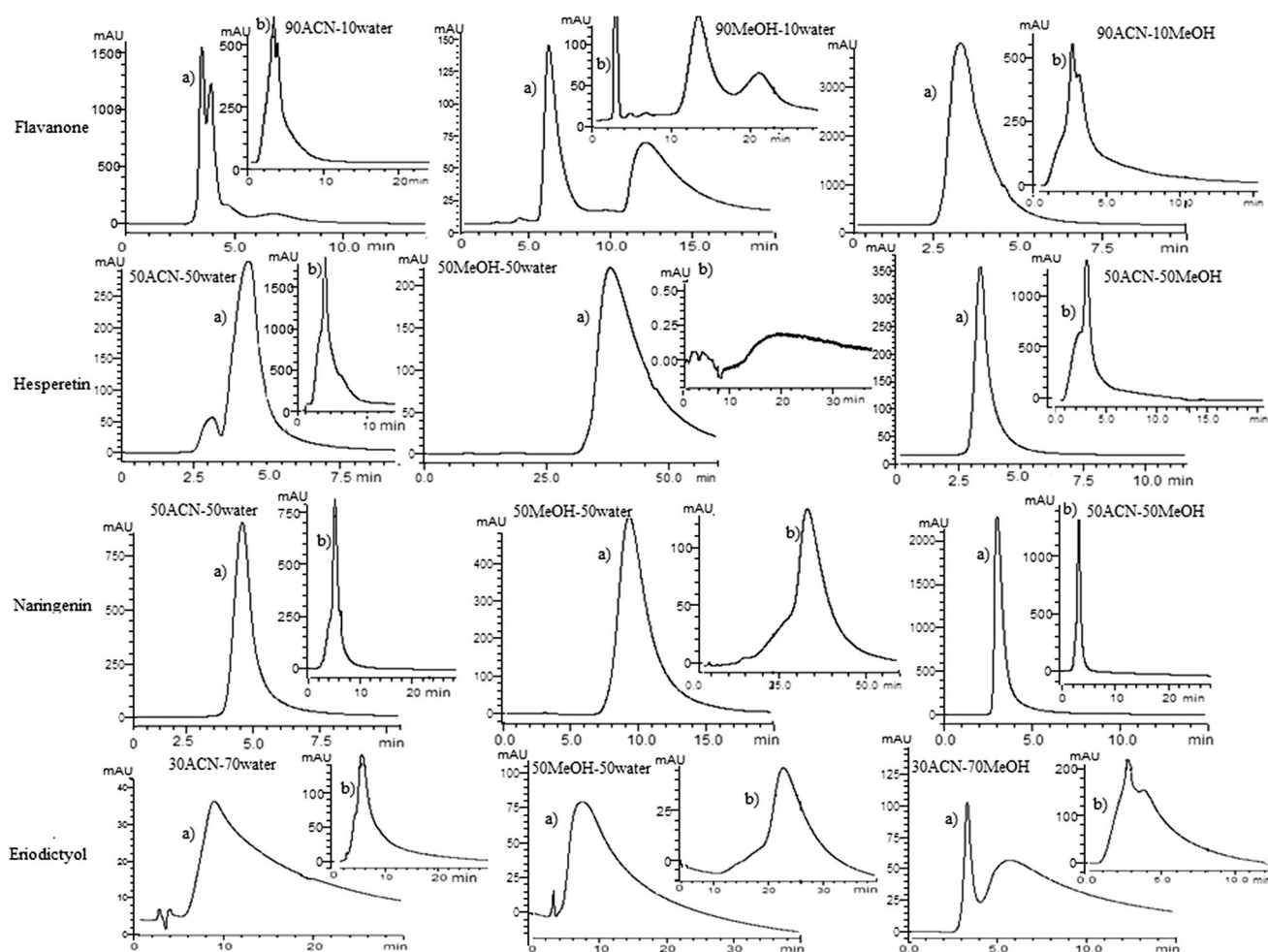


**Fig. 4** Separation of flavonoids on **a**  $\beta$ -CD-BIMOTs-CSP, **b** native  $\beta$ -CD-CSP

showed that better enantioseparation of flavanone, hesperetin and eriodictyol was obtained using  $\beta$ -CD-BIMOTs-CSP as compared to native  $\beta$ -CD based CSP (Fig. 4b). This results showed that the presence of IL substituent on  $\beta$ -CD might provide additional interaction which enhanced the enantioseparation of the selected flavonoids. The effects of mobile phase on the enantioseparation of flavonoids on  $\beta$ -CD-BIMOTs-CSP were further investigated.

### Chromatographic Data and Evaluation on the Mechanism of Enantioseparation

The type and composition of organic modifier as mobile phase are important factors that affect the enantioseparations. Adjusting the pH of mobile phase for reverse phase mode would also influence the forms of analytes and thus affect the enantioseparation. As presented in Table 1, high  $R_s$  values indicated the good enantioseparation for flavanone ( $R_s = 1.63$ ) and hesperetin ( $R_s = 1.06$ ) with the mobile phase of MeOH/water:50/50 and ACN/water:50/50,

respectively. In addition, good enantioseparation ( $R_s = 1.86$ ) was obtained for flavanone when ACN/buffer at pH 4 was used as mobile phase. However, low  $R_s$  values ( $R_s = 0.46$ ) was obtained for flavanone when ACN/buffer pH 9 was selected as mobile phase. Meanwhile, the enantiomers of naringenin and eriodictyol were not resolved using all selected mobile phases. Moreover, it can be seen that the  $k_1$  values of flavonoids decreased with increasing content of organic solvent. This was a common rule in reverse phase mode due to the increasing content of organic solvent which leads to the increase of elution strength of mobile phase. Thus, flavonoids were easily displaced from the stationary phase.

Flavanone obtained good enantioseparation in most of the mobile phase conditions and it might due to its hydrophobic properties that facilitated the inclusion complex formation with hydrophobic cavity of  $\beta$ -CD-BIMOTs-CSP. Moreover, flavanone with aromatic rings that without any substituent may experience less steric hindrance for inclusion complex formation with cavity of  $\beta$ -CD-BIMOTs-CSP.

**Table 1** Chiral separation data for the flavonoids on  $\beta$ -CD-BIMOTs-CSP in the reverse mobile phase

Flavonoids	Conditions	pH 4			pH 7			pH 9		
		$k_1$	$k_2$	$R_s$	$k_1$	$k_2$	$R_s$	$k_1$	$k_2$	$R_s$
Flavanone	a	0.34	0.48	0.64	0.33	0.49	0.45	0.38	0.85	0.79
	b	2.09	5.24	1.86	0.47	0.71	0.81	0.33	0.46	0.46
	c	2.77	2.77	0	2.61	2.61	0	2.51	2.51	0
	d	7.23	7.23	0	1.44	2.05	0.76	1.92	3.34	0.93
	e	2.27	3.58	0.85	2.58	4.31	1.63	6.84	6.84	0
Hesperetin	a	1.18	1.18	0	0.47	0.76	0.45	0.79	0.79	0
	b	1.49	1.49	0	0.37	1.36	1.06	1.61	1.61	0
	c	9.75	9.75	0	4.43	7.14	0.92	4.31	4.31	0
	d	1.35	1.35	0	1.29	1.29	0	1.80	1.80	0
	e	–	–	–	16.19	16.19	0	4.18	4.18	0
Naringenin	a	0.27	0.27	0	0.28	0.28	0	0.28	0.28	0
	b	0.62	0.62	0	0.84	0.84	0	0.97	0.97	0
	c	1.54	1.54	0	4.16	4.16	0	5.29	5.29	0
	d	0.68	0.68	0	0.12	0.12	0	0.83	0.83	0
	e	–	–	–	0.18	0.18	0	3.61	3.61	0
Eriodictyol	a	0.22	0.22	0	0.32	0.32	0	0.34	0.34	0
	b	0.34	0.34	0	0.34	0.34	0	0.34	0.34	0
	c	0.35	0.61	0.26	0.36	0.36	0	0.37	0.37	0
	d	–	–	–	0.19	0.19	0	0.82	0.82	0
	e	–	–	–	0.34	0.34	0	4.09	4.09	0

Conditions pH 7: a: ACN/water:90/10, b: ACN/water:50/50, c: ACN/water:30/70, d: MeOH/water:90/10, e: MeOH/water:50/50

Conditions pH 4 or 9: a: ACN/buffer:90/10, b: ACN/buffer:50/50, c: ACN/buffer:30/70, d: MeOH/buffer:90/10, e: MeOH/buffer:50/50

In addition, the carbonyl group and aromatic ring of flavanone also can form hydrogen bonding and  $\pi$ - $\pi$  interaction, respectively, with  $\beta$ -CD-BIMOTs-CSP which might further enhance the enantio-recognition. Flavanone is a neutral compound as compared with hesperetin, naringenin and eriodictyol which are weakly acidic in nature [24]. Thus, at pH 4, 7 and 9, flavanone is remained neutral and preferable to form inclusion complex with cavity of  $\beta$ -CD [19]. As compared to other flavonoids, flavanone was enantioseparated at pH 4, 7 and 9 but the extent of  $R_s$  was depend on type and composition of mobile phase.

In order to study the interaction that involved in enantioseparation,  $^1\text{H}$  NMR and NOESY spectra of  $\beta$ -CD-BIMOTs-flavonoids complexes were studied. The deduced structures of the  $\beta$ -CD-BIMOTs and  $\beta$ -CD-BIMOTs-flavonoids complexes are presented in Electronic Supplementary Material Fig. S2 and Fig. S3, respectively. Chemical shift ( $\delta$ ) variations provide evidence for the formation of inclusion complexes in solution. The values of the  $\delta$  for different protons in  $\beta$ -CD-BIMOTs and  $\beta$ -CD-BIMOTs-flavonoids complexes are listed in Table 2. The induced shift ( $\Delta\delta$ ) is defined as the difference in chemical shift in the presence or absence of analytes. In this study, the induced shift was calculated using Eq. (6):

$$\Delta\delta = \delta(\text{complex}) - \delta(\text{free}) \quad (6)$$

For  $\beta$ -CD-BIMOTs-flavanone complex (Table 2), the significant changes were observed on  $\Delta\delta$  at H5 proton which located in the cavity of  $\beta$ -CD-BIMOTs due to inclusion complex formation. In addition, large shift at H2 proton located at the exterior torus of  $\beta$ -CD-BIMOTs was due to the hydrogen bonding. The NOESY spectra of  $\beta$ -CD-BIMOTs-flavonoids complexes are presented in Electronic Supplementary Material Fig. S5. The NOESY spectra [see Electronic Supplementary Material Fig. S4(a)] show the cross-peak between H1, H2 and H5 protons of  $\beta$ -CD-BIMOTs with Hg' and Hj' protons of flavanone proved that the inclusion complex and hydrogen bonding were formed between flavanone and  $\beta$ -CD-BIMOTs.

For hesperetin which is a weakly acidic flavonoid with pKa 7.9 also formed neutral species at pH 7 and able to form inclusion complex with cavity of  $\beta$ -CD-BIMOTs-CSP and thus effectively enantioseparated using  $\beta$ -CD-BIMOTs-CSP (Table 1). Hesperetin bearing methoxy group is more hydrophobic than naringenin and eriodictyol. Therefore, hesperetin has greater affinity towards the cavity of  $\beta$ -CD-BIMOTs-CSP as compared to naringenin and eriodictyol. The OH groups and aromatic rings of hesperetin

**Table 2** Chemical shifts ( $\delta$ ) of  $\beta$ -CD-BIMOTs, and  $\beta$ -CD-BIMOTs-flavonoids

	$\beta$ -CD-BIMOTs	$\beta$ -CD-BIMOTs-flavanone		$\beta$ -CD-BIMOTs-hesperetin		$\beta$ -CD-BIMOTs-naringenin		$\beta$ -CD-BIMOTs-eriodictyol	
	$\delta$	$\delta$	$\Delta\delta$	$\delta$	$\Delta\delta$	$\delta$	$\Delta\delta$	$\delta$	$\Delta\delta$
H1	4.8405	4.8872	0.0467	4.8381	-0.0024	4.8241	-0.0164	4.8365	-0.0040
H2	3.3312	3.2568	<b>-0.0744</b>	3.3214	-0.0138	3.2406	<b>-0.0946</b>	3.3400	0.0048
H3	3.6394	3.6392	-0.0002	3.6401	0.0007	3.6253	-0.0141	3.6235	-0.0159
H4	3.3716	3.3797	0.0081	3.3552	<b>-0.0164</b>	3.3989	0.0273	3.4438	<b>0.0722</b>
H5	3.5777	3.5572	<b>-0.0205</b>	3.5586	<b>-0.0191</b>	3.5443	-0.0334	3.5428	-0.0349
H6	3.9225	3.9110	-0.0115	3.9185	-0.0040	3.9053	-0.0172	3.8979	-0.0246
H8	7.4215	7.4374	0.0159	7.4276	0.0061	7.4128	-0.0087	7.4105	-0.0110
H9	7.1112	7.1142	0.0030	7.1281	0.0169	7.1174	0.0062	7.1199	0.0087
H11	2.0847	2.0821	-0.0026	2.0844	-0.0003	2.0706	-0.0141	2.0698	-0.0149
Ha	7.4314	7.4827	0.0513	7.4995	0.0681	7.4873	0.0559	7.4756	0.0442
Hb	7.7957	7.8025	0.0068	7.8019	0.0062	7.7771	-0.0186	7.7650	-0.0307
Hc	7.7542	7.7892	0.0350	7.7552	0.0010	7.7380	-0.0162	7.7274	-0.0268
Hd	-	-	-	-	-	-	-	-	-
He	7.9563	7.9472	-0.0091	7.9456	-0.0107	7.9333	-0.0230	7.9312	-0.0251
Hf	9.2340	9.2696	0.0302	9.2744	0.0350	9.2419	0.0025	9.2252	-0.0142
Hg	5.4371	5.4471	0.0100	5.4191	-0.0180	5.4067	-0.0304	5.4000	-0.0371

Values in bold refer to the highest induced shift of that particular proton

can form hydrogen bonding and  $\pi$ - $\pi$  interaction with  $\beta$ -CD-BIMOTs-CSP and thus enhanced the enantioseparation at pH 7. However, the result from the enantioseparation revealed that hesperetin was not enantioseparated at pH 4 and 9. At acidic pH, there are interaction of buffer salt with analyte molecule which would significantly affect the inclusion interactions between analyte and cavity of  $\beta$ -CD-BIMOTs [25]. Meanwhile, the deprotonated hesperetin at pH 9 is not favorable for the formation of inclusion complex with  $\beta$ -CD-BIMOTs [19]. This finding further support the role of inclusion complex formation in enantioseparation of  $\beta$ -CD based CSPs. These interactions were further proven using the data from  $^1\text{H}$  NMR and NOESY. The  $\beta$ -CD-BIMOTs-hesperetin complex shows appreciable shift at H4 proton at exterior torus of  $\beta$ -CD-BIMOTs because of hydrogen bonding. A large shift at H5 proton located in cavity of  $\beta$ -CD-BIMOTs (Table 2) was attributed to the formation of inclusion complex. In addition, the cross-peaks between H3, H4 and H5 protons of  $\beta$ -CD-BIMOTs with He', Hg', and Hk' protons of hesperetin showed in NOESY spectra [see Electronic Supplementary Material Fig. S4(b)] further proved the formation of inclusion complex and hydrogen bonding which enhanced the enantioseparation.

As shown in Table 1, naringenin and eriodictyol were not resolved using the reverse phase mode. Naringenin and eriodictyol contains highly polar moieties (OH) which might weaken the hydrophobic interaction with  $\beta$ -CD-BIMOTs cavity and retard the formation of inclusion complexes. Naringenin and eriodictyol might prefer to form hydrogen bonding at exterior torus instead of

interior cavity of  $\beta$ -CD-BIMOTs-CSP. Moreover, the presence of OH functionality as electron donating group could increase the electron density of aromatic ring of naringenin and eriodictyol and facilitate the  $\pi$ - $\pi$  repulsion which led to weak  $\pi$ - $\pi$  interaction [26]. It can be deduced that hydrogen bonding is not sufficient to obtain the enantio-recognition.  $^1\text{H}$  NMR spectra of complexes was recorded to obtain the information of intermolecular interaction. With the presence of naringenin and eriodictyol, large  $\Delta\delta$  of H2 and H4 protons of  $\beta$ -CD-BIMOTs was observed. In addition, NOESY spectra for  $\beta$ -CD-BIMOTs-naringenin complex [see Electronic Supplementary Material Fig. S4(c)] showed the cross-peak between He', Hg' and Hj' protons of naringenin with H2 proton of  $\beta$ -CD-BIMOTs. In NOESY spectra of  $\beta$ -CD-BIMOTs-eriodictyol complex [see Electronic Supplementary Material Fig. S4(d)], there are cross-peak between Hc', Hg' and Hf' protons of eriodictyol with H4 proton of  $\beta$ -CD-BIMOTs. These results suggested that hydrogen bonding between naringenin and eriodictyol was formed at the exterior torus of  $\beta$ -CD-BIMOTs.

As a part of the optimization, the polar organic mode with different additives was used to improve the enantioseparation of naringenin and eriodictyol. This system can be used to resolved compounds that cannot be separated in the reverse phase mode. In this study, the mobile phase of polar organic mode was composed of ACN and MeOH. The selected additives were TEA and HAOc [27]. In the polar organic mode, the relative high concentration of organic solvents occupies the relatively hydrophobic cavity of  $\beta$ -CD. Armstrong et al. [28] proposed that the



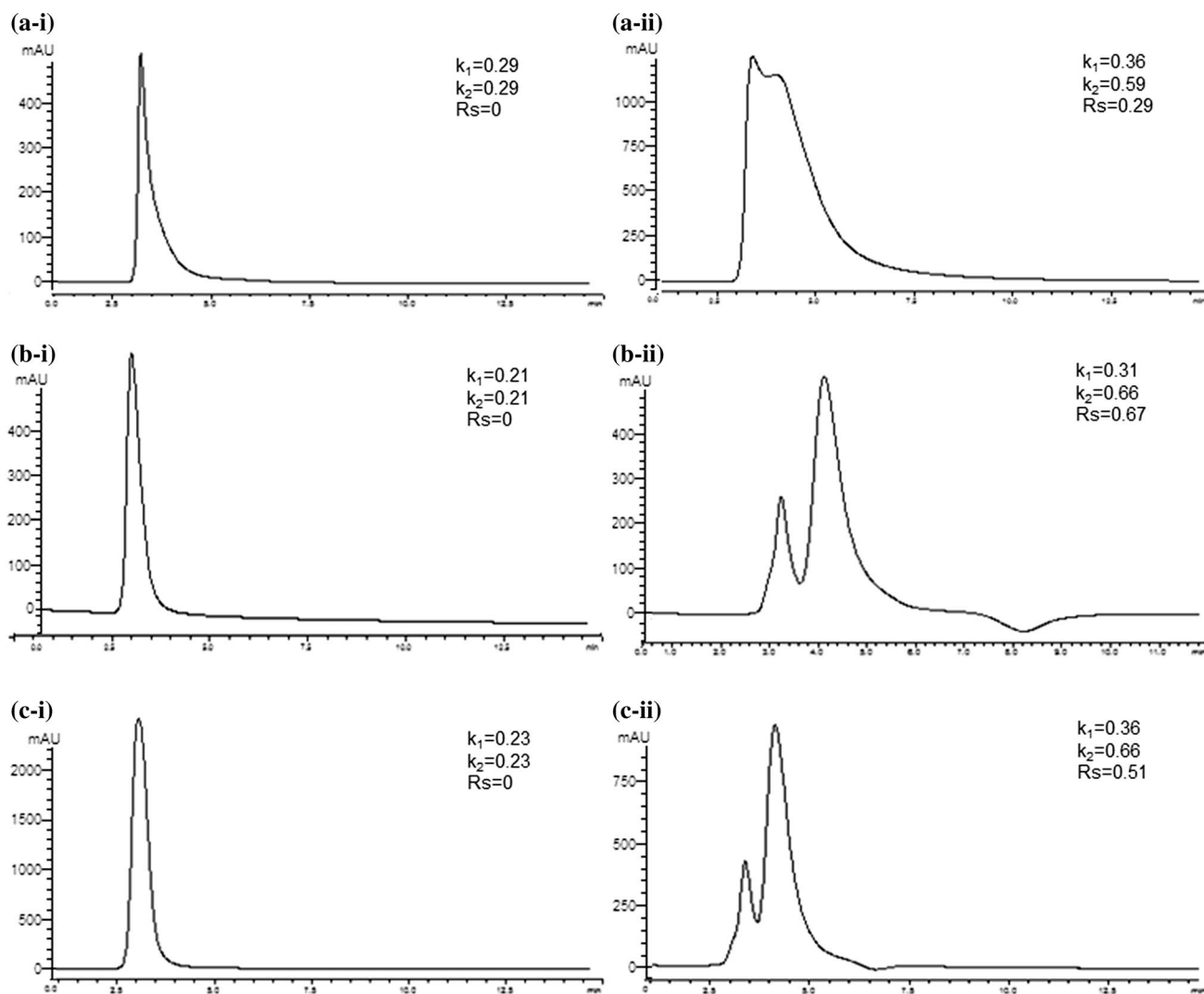


**Fig. 5** HPLC chromatograms of naringenin in polar organic mode. Mobile phase composition, ACN/MeOH/TEA/HAc (v/v/v/v): **a-i** 90/10/1/3, **a-ii** 90/10/3/1, **b-i** 50/50/1/3, **b-ii** 50/50/3/1, **c-i** 30/70/1/3 and **c-ii** 30/70/3/1

analytes may form a “lid” over the “mouth” of the cavity. Moreover, the retention and selectivity are mainly due to the polar OH groups at the rims of  $\beta$ -CD forming hydrogen bond with analytes. Thus, the total number of OH moiety at flavonoids would affect the enantioseparation. The HPLC chromatograms shown naringenin achieved better enantioseparation at higher amount of TEA (Fig. 5a–c-ii) meanwhile eriodictyol was resolved at higher amount of HAc (Fig. 6a–c-ii). Higher amount of TEA increased the pH value of mobile phase, thus favors the dissociation of naringenin and eriodictyol into ionic species. It has been showed that the dissociation constant of eriodictyol is higher than naringenin depending on the number of OH substitutions [29]. This might lead to the strong electrostatic interaction between eriodictyol and IL of CSP which inhibit the enantioseparation.

At higher ratio of HAc, both of naringenin and eriodictyol are in neutral form. However, enantioseparation of eriodictyol was better as compared with naringenin. This might due to the structure of eriodictyol with 4 OH groups that has high capability to form hydrogen bonding at the exterior torus of  $\beta$ -CD-BIMOTs. It can be deduced that the better enantioseparation in the polar organic mode shows the importance of the hydrogen bonding and/or electrostatic interaction for the chiral recognition mechanism of naringenin and eriodictyol.

The optimized chromatogram of eriodictyol (Fig. 6c-i) showed the broad and tailing peak. This might due to the formation of strong hydrogen bonding between eriodictyol and  $\beta$ -CD-BIMOTs-CSP. Thus, it can be deduced that the more OH group substituents at naringenin and eriodictyol leads to the stronger interaction with  $\beta$ -CD-BIMOTs-CSP

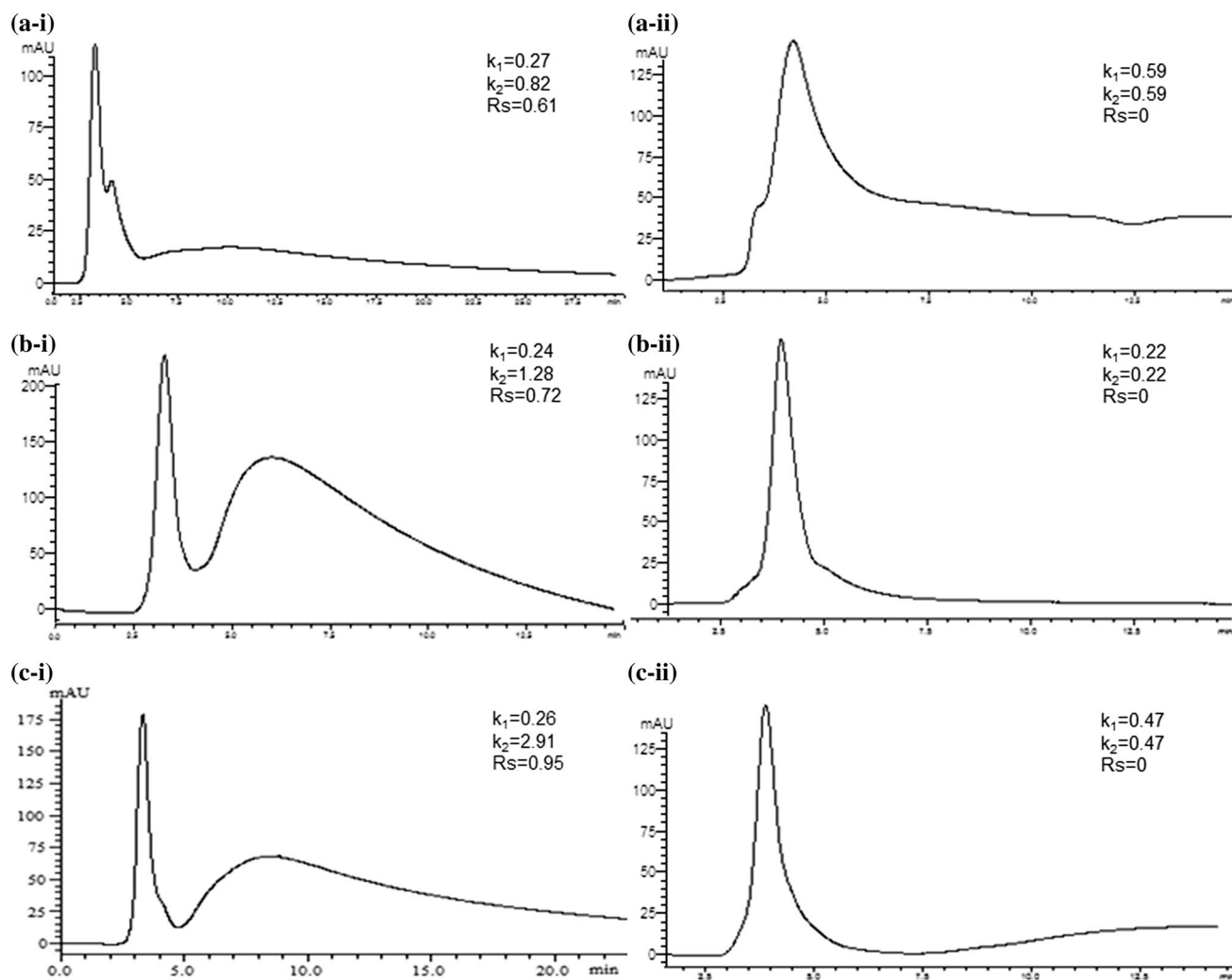


**Fig. 6** HPLC chromatograms of eriodictyol in polar organic mode. Mobile phase composition, ACN/MeOH/TEA/HAc (v/v/v/v): **a-i** 90/10/1/3, **a-ii** 90/10/3/1, **b-i** 50/50/1/3, **b-ii** 50/50/3/1, **c-i** 30/70/1/3 and **c-ii** 30/70/3/1

and thus inhibit the enantioseparation. Therefore, the formation constant ( $K$ ) was determined to indicate the strength of the interaction between flavonoids and  $\beta$ -CD-BIMOTs. The plots of absorption for  $\beta$ -CD-BIMOTs, flavonoids and  $\beta$ -CD-BIMOTs-flavonoids complexes were first measured (Fig. 7) by monitoring the change in the UV spectra. Results showed that  $\beta$ -CD-BIMOTs had a  $\lambda_{\max}$  in the range of 230–260 nm. The absorption spectra of flavanone displayed two well-defined  $\lambda_{\max}$  at 250 and 320 nm meanwhile naringenin, hesperetin and eriodictyol displayed one  $\lambda_{\max}$  at 320 nm. The  $\lambda_{\max}$  of  $\beta$ -CD-BIMOTs-flavonoids complex was observed at 230–260 and 320 nm refer to the wavelength of  $\beta$ -CD-BIMOTs and flavonoids, respectively. It was observed that the absorption spectra of all  $\beta$ -CD-BIMOTs-flavonoids complexes showed both hyperchromic and hypochromic effect. Increase in absorption is defined as hyperchromic effect

and decrease in the absorption is defined as hypochromic effect [30, 31].

Hyperchromic effect observed on  $\beta$ -CD-BIMOTs-flavonoids at 320 nm is due to the electron perturbation at chromophore of flavonoids [30]. Meanwhile, the hypochromic effect is due to the intercalative mode involving the stacking interaction [31] which is mainly referred to  $\pi$ - $\pi$  interaction between aromatic flavonoids and  $\beta$ -CD-BIMOTs. The hypochromic effect for  $\beta$ -CD-BIMOTs-flavanone was not observed due to the overlapping of absorbance at 250 nm (Fig. 7a). Both of hyperchromic and hypochromic effects that observed in the absorption spectra of  $\beta$ -CD-BIMOTs-flavonoids proved that there were multiple interactions for the formation of complex between  $\beta$ -CD-BIMOTs and flavanoids.

The  $K$  values were then calculated from the slope of  $\frac{1}{(A-A_0)}$  versus  $\frac{1}{[\beta\text{-CD-BIMOTs}]}$  of  $\beta$ -CD-BIMOTs-flavonoids as

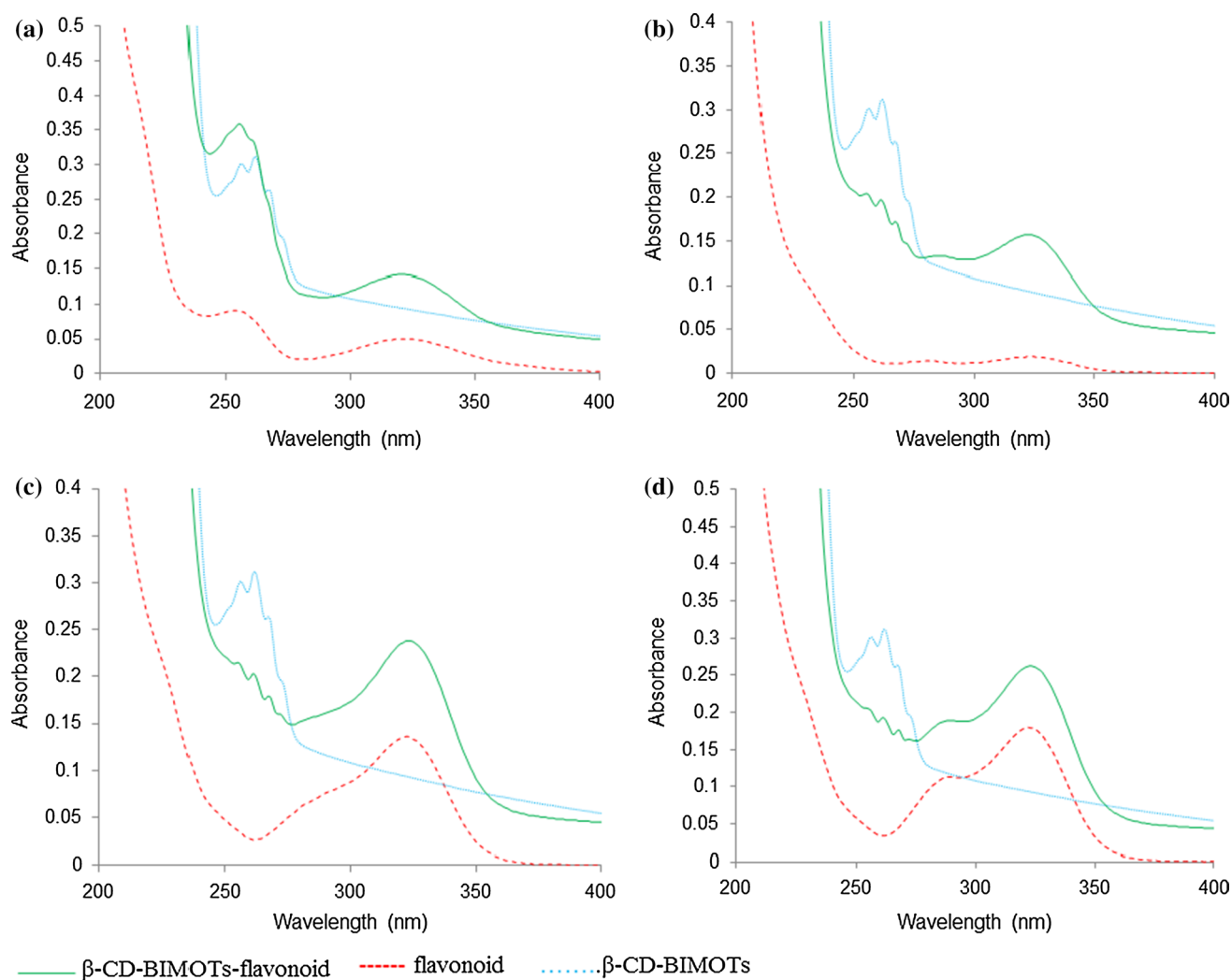


**Fig. 7** Absorption spectra of **a**  $\beta$ -CD-BIMOTs-flavanone, **b**  $\beta$ -CD-BIMOTs-hesperetin, **c**  $\beta$ -CD-BIMOTs-naringenin, **d**  $\beta$ -CD-BIMOTs-eriodictyol with [ $\beta$ -CD-BIMOTs]: 0.032 mM [Flavonoids]: 0.01 mM;  $T = 25^\circ\text{C}$

**Table 3**  $K$  values for  $\beta$ -CD-BIMOTs-flavonoids

Flavonoids	$K$
Flavanone	722
Hesperetin	572
Naringenin	1077
Eriodictyol	6032

shown in Electronic Supplementary Material Fig. S5 using Eq. (5). In Table 3, the  $K$  values obtained are in the following order:  $\beta$ -CD-BIMOTs-hesperetin <  $\beta$ -CD-BIMOTs-flavanone <  $\beta$ -CD-BIMOTs-naringenin <  $\beta$ -CD-BIMOTs-eriodictyol. This deduced that the strength of interaction is correlated with the substituted OH group at flavonoids. Previous study reported that hydrogen bond is the strongest non-covalent interactions with 8.4–41.8 kJ/mol stabilization energy

[32]. Naringenin and eriodictyol that possess 3–4 OH substituents experienced highest  $K$  value due to the stronger hydrogen bond formation. Indeed, these results clarified that naringenin and eriodictyol interacted at the external torus of  $\beta$ -CD-BIMOT. Meanwhile, the small  $K$  values for flavanone and hesperetin proven that the inclusion complex was formed due to hydrophobic interaction thus exhibit the enantioseparation.

## Conclusions

In this work,  $\beta$ -CD-BIMOTs-CSP was successfully synthesized and compared with native  $\beta$ -CD-CSP for enantioseparation of flavonoids. The  $\beta$ -CD-BIMOTs-CSP is performed better than  $\beta$ -CD-CSP due to the combination of multi interactions which is contributed by IL and  $\beta$ -CD. Flavanone and hesperetin obtained good enantioresolution

in reverse phase mode. Meanwhile, the enantiomers of naringenin and eriodictyol are prefer to resolve in polar organic mode due to the high number of OH moiety substitution. From  $^1\text{H}$  NMR and NOESY determination, flavanone and hesperetin are proven to form inclusion complexes with  $\beta$ -CD-BIMOTs. Naringenin and eriodictyol experienced non inclusion but formed hydrogen bonding at exterior torus of  $\beta$ -CD-BIMOTs.

**Acknowledgments** Authors would like to seize this opportunity to express their gratitude to the University Malaya for the IPPP Grant (PG027/2013A) and UMRG Grant (RP006A–13SUS, RP020A–16SUS and RP011B–14SUS). The authors also acknowledge Ministry of Higher Education (MOHE) for providing fellowship to one of the authors-cum-researchers, Ms. NurulYani Rahim.

#### Compliance with Ethical Standards

**Conflict of Interest** All authors declare that they have no conflict of interest.

**Ethical Approval** This article does not contain any studies with human participants or animals performed by any of the authors.

#### References

- Di Carlo G, Mascolo N, Izzo A, Papasso F (1999) Flavonoids: old and new aspects of a class of natural therapeutic drugs. *Life Sci* 65:337–353
- El-Mahdy MA, Zhu Q, Wang QE, Wani G, Patnaik S, Zhao Q, Arafa E, Barakat B, Mir S, Wani AA (2008) Naringenin protects HaCaT human keratinocytes against UVB-induced apoptosis and enhances the removal of cyclobutane pyrimidine dimers from the genome. *J Photochem Photobiol* 84:307–316
- Pietta P (1998) In: Rice-Evans CA, Packer L (eds) *Flavonoids in health and disease*. Marcel Dekker Inc., New York
- Cao G, Sofic E, Prior RL (1997) Antioxidant and pro-oxidant behavior of flavonoids: structure-activity relationships. *Free Radic Biol Med* 22:749–760
- Lees P, Taylor PM, Landoni FM, Arifah AK, Waters C (2003) Ketoprofen in the cat: pharmacodynamics and chiral pharmacokinetics. *Vet J* 1:21–35
- Wolf C (2008) *Dynamic stereochemistry of chiral compounds: principles and applications*. Royal Society of Chemistry, UK
- Schurig V (2002) Chiral separations using gas chromatography. *Trends Anal Chem* 21:647–661
- Juvancz Z, Szejtli J (2002) The role of cyclodextrins in chiral selective chromatography. *Trends Anal Chem* 21:379–388
- Scriba GK, Altria K (2009) Using cyclodextrins to achieve chiral and non-chiral separations in capillary electrophoresis. *LC GC Eur* 22:420
- Stalcup AM, Chang SC, Armstrong DW, Pitha J (1990) (S)-2-hydroxypropyl- $\beta$ -cyclodextrin, a new chiral stationary phase for reversed-phase liquid chromatography. *J Chromatogr A* 513:181–194
- Wang Y, Young DJ, Tan TTY, Ng SC (2010) “Click” immobilized perphenylcarbamated and permethylated cyclodextrin stationary phases for chiral high-performance liquid chromatography application. *J Chromatogr A* 1217:5103–5108
- Li X, Zhou Z (2014) Enantioseparation performance of novel benzimido- $\beta$ -cyclodextrins derivatized by ionic liquids as chiral stationary phases. *Anal Chim Acta* 819:122–129
- Li X, Zhou Z, Zhou W, Dai L, Li Z (2011) Preparation of a novel cyclodextrin derivative of benzimido- $\beta$ -cyclodextrin and its enantioseparation performance in HPLC. *Analyst* 136:5017–5024
- Wasserscheid P, Keim W (2000) Ionic liquids-new “solutions” for transition metal catalysis. *Angew Chem* 39:3772–3789
- Pandey S (2006) Analytical applications of room-temperature ionic liquids: a review of recent efforts. *Anal Chim Acta* 556:38–45
- Canongia Lopes JN, Pádua AA (2006) Nanostructural organization in ionic liquids. *J Phys Chem B* 110:3330–3335
- Anderson JL, Armstrong DW (2003) High-stability ionic liquids. A new class of stationary phases for gas chromatography. *Anal Chem* 75:4851–4858
- Rahim NY, Tay KS, Mohamad S (2016)  $\beta$ -Cyclodextrin functionalized ionic liquid as chiral stationary phase of high performance liquid chromatography for enantioseparation of  $\beta$ -blockers. *J Incl Phenom Macrocycl Chem* 85:303–315
- Raoov M, Mohamad S, Abas MR (2013) Removal of 2, 4-dichlorophenol using cyclodextrin-ionic liquid polymer as a macroporous material: characterization, adsorption isotherm, kinetic study, thermodynamics. *J Hazard Mater* 263:501–516
- Yatabe J, Kageyama T (1994) Preparation of hydrophobic silica with isocyanate. *J Ceram Soc Jpn* 102:595–598
- Manske RHF (1965) *The alkaloids: chemistry and physiology*, vol 5. Academic Press Inc, New York
- Cwiertnia B, Hladon T, Stobiecki M (1999) Stability of diclofenac sodium in the inclusion complex with  $\beta$ -cyclodextrin in the solid state. *J Pharm Pharmacol* 51:1213–1218
- Zhang W, Lee HR (2010) Grafting of polyethylene glycols onto nanometer silica surface by 1,4-phenylene diisocyanate. *Surf Interface Anal* 42:1495–1498
- Ng SC, Ong TT, Fu P, Ching CB (2002) Enantiomer separation of flavour and fragrance compounds by liquid chromatography using novel urea-covalent bonded methylated  $\beta$ -cyclodextrins on silica. *J Chromatogr A* 968:31–40
- Lin C, Liu W, Fan J, Wang Y, Zheng S, Lin R, Zhang W (2013) Synthesis of a novel cyclodextrin-derived chiral stationary phase with multiple urea linkages and enantioseparation toward chiral osmabenzene complex. *J Chromatogr A* 1283:68–74
- Hunter CA, Lawson KR, Perkins J, Urch CJ (2001) Aromatic interactions. *J Chem Soc Perkin Trans* 2(5):651–669
- Kafková B, Bosáková Z, Tesařová E, Coufal P (2005) Chiral separation of beta-adrenergic antagonists, profen non-steroidal anti-inflammatory drugs and chlorophenoxypropionic acid herbicides using teicoplanin as the chiral selector in capillary liquid chromatography. *J Chromatogr A* 1088:82–93
- Chang SC, Reid GL, Chen S, Chang CD, Armstrong DW (1993) Evaluation of a new polar-organic high-performance liquid chromatographic mobile phase for cyclodextrin-bonded chiral stationary phases. *TrAC Trends Anal Chem* 12:144–153
- Van Dijk C, Driessen AJ, Recourt K (2000) The uncoupling efficiency and affinity of flavonoids for vesicles. *Biochem Pharm* 60:1593–1600
- Ventura CA, Giannone I, Musumeci T, Pignatello R, Ragni L, Landolfi C, Milanese C, Paolino D, Puglisi G (2006) Physicochemical characterization of disoxaril-dimethyl- $\beta$ -cyclodextrin inclusion complex and in vitro permeation studies. *Eur J Med Chem* 41:233–240
- Hu Y, Wang X, Pan H, Ding L (2012) Interaction mode between methylene blue-Sm(III) complex and herring sperm DNA. *Bull Chem Soc Ethiop* 3:395–405
- Frieden E (1975) Non-covalent interactions: key to biological flexibility and specificity. *J Chem Educ* 12:754–761

# Chromatographic and spectroscopic studies on $\beta$ -cyclodextrin functionalized ionic liquid as chiral stationary phase: Enantioseparation of NSAIDs

Adsorption Science & Technology  
0(0) 1–19

© The Author(s) 2016

DOI: 10.1177/0263617416686798

journals.sagepub.com/home/adt

**Nurul Yani Rahim and Kheng Soo Tay**

Department of Chemistry, Faculty of Science, University of Malaya, Malaysia

**Sharifah Mohamad**

Department of Chemistry, Faculty of Science, University of Malaya, Malaysia

University of Malaya Centre for Ionic Liquids (UMCiL), University of Malaya, Malaysia

## Abstract

Recently, we reported a new chiral stationary phase prepared using  $\beta$ -cyclodextrin functionalized with aromatic ionic liquid which is aimed to enhance the performance of enantioseparation of flavonoids and  $\beta$ -blockers. In this paper, the characteristics and performance of previously prepared chiral stationary phase denoted as  $\beta$ -CD-BIMOTs were compared with the newly synthesized chiral stationary phase denoted as  $\beta$ -CD-DIMOTs.  $\beta$ -CD-DIMOTs were prepared by functionalization of  $\beta$ -cyclodextrin with aliphatic ionic liquid. The obtained  $\beta$ -CD-BIMOTs and  $\beta$ -CD-DIMOTs stationary phases were compared with native  $\beta$ -CD stationary phase for the enantioseparation of non-steroidal anti-inflammatory drugs (NSAIDs) (ibuprofen, indoprofen, ketoprofen and fenoprofen). The  $\beta$ -CD-BIMOTs stationary phase showed greater chiral resolution capabilities rather than  $\beta$ -CD-DIMOTs and native  $\beta$ -CD stationary phases. Further, in order to understand the interaction of enantioseparation, the inclusion complex formation between NSAIDs and  $\beta$ -CD-BIMOTs was studied using  $^1\text{H}$  NMR, NOESY and UV/Vis. The enantioseparated NSAIDs were found to form multiple interactions with  $\beta$ -CD-BIMOTs-CSP.

## Keywords

 $\beta$ -cyclodextrin, NSAIDs, ionic liquid, enantioseparation, inclusion complex

---

### Corresponding author:

Sharifah Mohamad, Department of Chemistry, Faculty of Science, University of Malaya, Malaysia.

Email: sharifahm@um.edu.my

Creative Commons CC-BY: This article is distributed under the terms of the Creative Commons Attribution 3.0 License (<http://www.creativecommons.org/licenses/by/3.0/>) which permits any use,reproduction and distribution of the work without further permission provided the original work is attributed as specified on the SAGE and Open Access pages (<https://us.sagepub.com/en-us/nam/open-access-at-sage>).

## Introduction

Non-steroidal anti-inflammatory drugs (NSAIDs) are drugs that have been used to provide analgesic, antipyretic and anti-inflammatory effects (Ye et al., 2010). Profen (2-arylpropionic acids) is an important group of NSAIDs, characterized by a chiral carbon atom next to the carboxylic acid group (Ye et al., 2010). This chiral structure of NSAIDs exhibits optical activity and causes the different biological properties of enantiomers (Ye et al., 2010). For example, for ibuprofen, the pharmacological activity resides in the *S*-enantiomer only (Núñez-Agüero et al., 2006). Consequently, the enantioseparation of NSAIDs is an important concern for pharmaceutical use.

High-performance liquid chromatography (HPLC) has been proven to be one of the most widespread techniques for the enantiomeric separation and analysis (Muderawan et al., 2006; Zhang et al., 2008). In this study, the enantioseparation of selected NSAIDs was performed using HPLC with  $\beta$ -cyclodextrin ( $\beta$ -CD)-based chiral stationary phase (CSP).  $\beta$ -CD is a doughnut-shaped cyclic oligosaccharides containing seven  $\alpha$ -(1,4)-glycosidic linkages.  $\beta$ -CD has been used extensively as CSPs in HPLC because of its ability to recognize enantiomeric molecules through the formation of inclusion complexes (Xiao et al., 2012; Zhong et al., 2006) and its  $C_7$  symmetry axis. Fourteen hydroxyl groups located at the mouth of the cavity provide a number of potential interactions with enantiomers during the enantioseparation. Until 1990, most of the enantioseparation studies focused on the preparation of native  $\beta$ -CD-based CSPs modified by different linkage groups (Zhou et al., 2010). However, the application of native  $\beta$ -CD-CSPs was not always satisfactory (Zhou et al., 2010). Therefore, recently, researches have been focused on the preparation of modified  $\beta$ -CD to be used as CSPs (Xiao et al., 2012).

The addition of different substituent groups onto the rim of  $\beta$ -CD provides multiple interactions such as  $\pi$ - $\pi$ , dipole-dipole interaction, electrostatic interaction, and hydrogen bonding which contributes significantly to effective enantioseparation. Ionic Liquids (ILs) are examples of new substituent groups that are been used to modify  $\beta$ -CD (Li and Zhou, 2014; Li et al., 2011). ILs is composed of organic cation and inorganic or organic anion (Wasserscheid and Keim, 2000). It is widely used in environmentally benign chemical processing and analysis (Pandey, 2006). ILs molecules consist of high charge region and low charge region (Canongia Lopes and Pádua, 2006) which contributes to enantioseparation through electrostatic and dispersive interaction (Anderson and Armstrong, 2003).

In our previous work, we introduced the preparation, characterization and chromatographic performance of  $\beta$ -CD-BIMOTs-CSP (Figure 1) (Rahim et al., 2016a, 2016b). It was observed that compared with native  $\beta$ -CD-CSP,  $\beta$ -CD-BIMOTs-CSP possessed excellent chiral recognition abilities towards the selected  $\beta$ -blockers and flavonoids. Herein, we demonstrate another  $\beta$ -CD functionalized IL denoted as  $\beta$ -CD-DIMOTs-CSP (Figure 1) to investigate the effect of the alkyl chain of imidazolium cation of IL on enantioseparation abilities. The characterization of  $\beta$ -CD-BIMOTs-CSP and  $\beta$ -CD-DIMOTs-CSP was compared with native  $\beta$ -CD-CSP using FTIR and thermal analysis. Additionally, the chromatographic performance of  $\beta$ -CD-BIMOTs-CSP,  $\beta$ -CD-DIMOTs-CSP and native  $\beta$ -CD-CSP was compared for the enantioseparation of NSAIDs (Figure 2). To the best of our knowledge, most studies on the interactions of enantioseparation using  $\beta$ -CD functionalized IL-based CSP are often elaborated through computational study (Li and Zhou, 2014; Li et al., 2011). However, none of those studies provided data via experimental data. As a solution to this problem, this article evaluates the inclusion

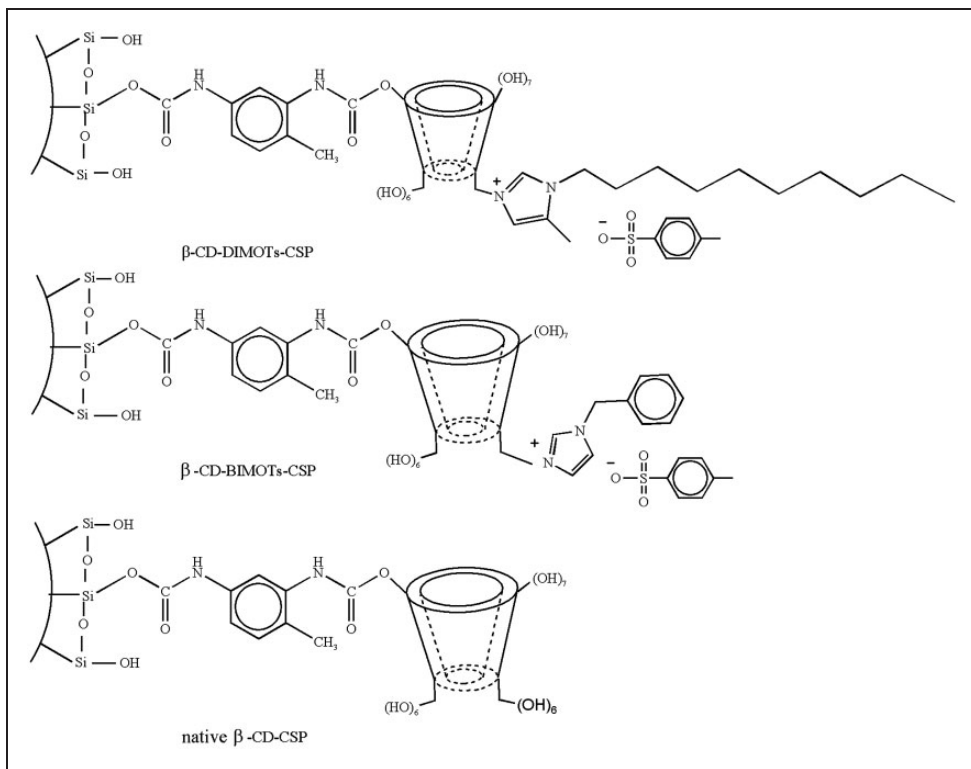


**Figure 1.** The structure of  $\beta$ -CD-DIMOTs-CSP,  $\beta$ -CD-BIMOTs-CSP and native  $\beta$ -CD-CSP.

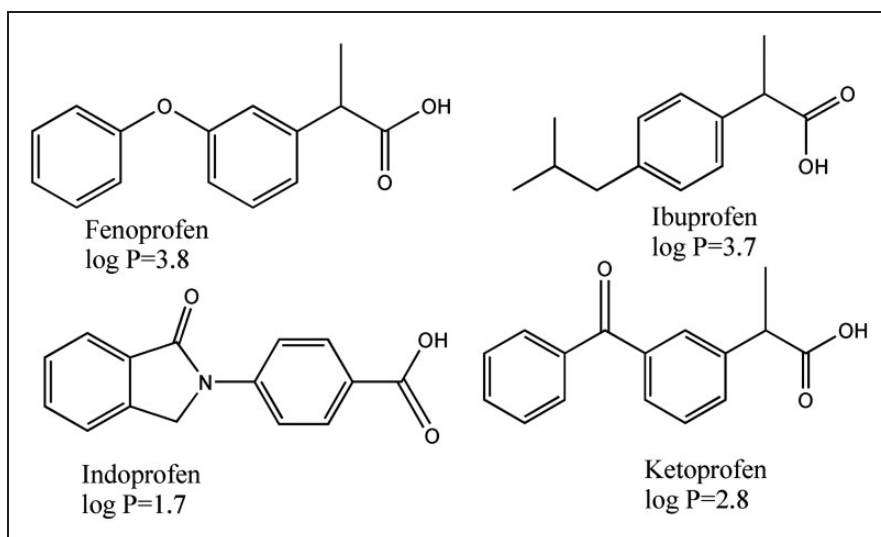


**Figure 2.** The structure of selected NSAIDs.



complex formation between NSAIDs and  $\beta$ -CD functionalized IL CSP in enantioseparation using spectroscopic techniques ( $^1\text{H}$  NMR, NOESY and UV/Vis).

## Experimental

### Materials

$\beta$ -CD was purchased from Acros (Belgium) (99%). 1-benzylimidazole (1-BzlIm), 1-decyl-2-methylimidazole ( $\text{C}_{10}\text{MIm}$ ), 2,4-toluene diisocyanate (TDI) and NSAIDs were purchased from Aldrich (USA). Solvent used for HPLC and synthesis are LC and anhydrous grade solvents, respectively, purchased from Merck (Germany). Kromasil spherical silica gel with a mean pore size 100 Å and particle size of 5  $\mu\text{m}$  was purchased from Merck (Germany). The stainless steel HPLC empty columns (250 mm  $\times$  4.6 mm) were purchased from Grace (USA).

### Instruments

FT-IR spectra were performed on a Perkin–Elmer RX1 FT-IR (Perkin Elmer, Waltham, MA, USA) using KBr pellets. Thermogravimetric (TGA) analyses curves were examined using a TA Instrument Q500 (Perkin Elmer, Waltham, MA, USA). An elemental analysis of the sample was determined with a Leco Truspec CHN Analyzer (Saint Joseph, MI).  $^1\text{H}$  NMR,  $^{13}\text{C}$  NMR and NOESY spectra were recorded using an Avance spectrometer at 600 MHz (Bruker, Fällanden, Switzerland). Absorption spectra measurements were carried out with a Shimadzu UV 1800 (Shimadzu, Japan) spectrophotometer in the range of 190 to 800 nm. The employed HPLC system comprised an LC-20AT pump, an SPD-M20 detector, an SIL-20AHT auto sampler, a CTO-20AC column oven and CBM-20A communication bus module (Shimadzu, Japan).

### Synthesis of CSPs

The  $\beta$ -CD-BIMOTs-CSP was synthesized according to the procedure reported previously (Rahim et al., 2016a, 2016b). Meanwhile, the preparation of  $\beta$ -CD-DIMOTs-CSP involved the following four steps. (i) preparation of *p*-toluene sulfonic anhydride ( $\text{Ts}_2\text{O}$ ), (ii) preparation of 6-O-Monotosyl-6-deoxy- $\beta$ -CD ( $\beta$ -CDOTs), (iii) synthesis of Mono-6-deoxy-6-(3-decyl-2-methylimidazolium tosylate)- $\beta$ -CD ( $\beta$ -CD-DIMOTs) and (iv) immobilization of  $\beta$ -CD-DIMOTs onto modified silica. The synthesis pathway of  $\beta$ -CD-DIMOTs-CSP is illustrated in Figure 3.

$\text{Ts}_2\text{O}$  was prepared according to our previous publications (Rahim et al., 2016a, 2016b), primarily by dissolving *p*-toluene sulfonyl chloride (2.00 g, 10.4 mmol) in dichloromethane (DCM) (12.5 mL). Then, *p*-toluene sulfonic acid (0.52 g, 2.63 mmol) was added gradually with vigorous stirring under nitrogen atmosphere. The resulting mixture was stirred overnight at room temperature. The mixture was then filtered to remove the unreacted *p*-toluene sulfonic acid. Hexane (50 ml) was added to the filtrate and a precipitate was obtained after drying overnight under reduced pressure.  $\beta$ -CDOTs was also prepared according to our previously reported method (Rahim et al., 2016a, 2016b).  $\text{C}_{10}\text{MIm}$  (10 mol equivalent) was then added dropwise to a stirred solution of dry  $\beta$ -CDOTs (1.00 g, 0.78 mmol) in anhydrous DMF (40 ml) to prepare  $\beta$ -CD-DIMOTs. Stirring was continued at 90°C under nitrogen atmosphere for a further 48 h. After cooling to room temperature, acetone was added to precipitate the product. Thereafter, the mixture was



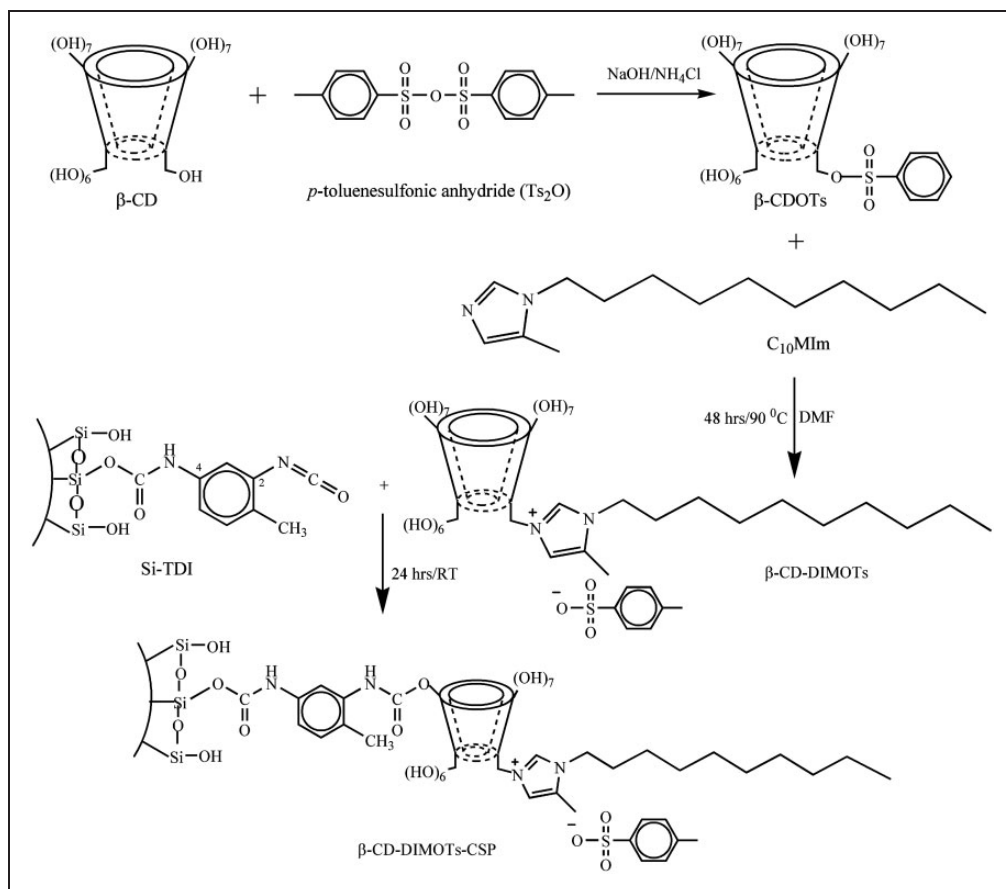


**Figure 3.** Synthesis pathway of  $\beta$ -CD-DIMOTs-CSP.

then stirred for 30 min and the product was filtered and washed with excess amount of acetone. A white yellow precipitate was obtained as the final product. The structure of  $\beta$ -CD-DIMOTs is shown in Figure 4.

The immobilization of  $\beta$ -CD-DIMOTs onto silica was first prepared by modifying silica gel as reported by Yatabe and Kageyama (1994). The silica gel was reacted with 2, 4-toluene diisocyanate (TDI) in dry hexane for 4 h at room temperature to obtain Si-TDI. Upon completion of the reaction, the product was filtered, rinsed thoroughly by hexane and dried under reduced pressure. The immobilization of  $\beta$ -CD-DIMOTs onto Si-TDI was then carried out by stirring Si-TDI (5 g) in anhydrous hexane (200 ml) under nitrogen atmosphere. After 30 min, a solution of  $\beta$ -CD-DIMOTs (1.8 g) in anhydrous hexane was added. Stirring was continued for 24 h. The synthesized solid was filtered and washed with toluene, acetone and distilled water to obtain a purified product. The product was characterized using elemental analysis, FT-IR and TGA. The aforementioned procedure was also applied to immobilize the native  $\beta$ -CD onto the Si-TDI.

FT-IR/KBr,  $\text{cm}^{-1}$ : 3297 (OH), 2922 (C-H), 1652 (C=C), 1152 (C-N).

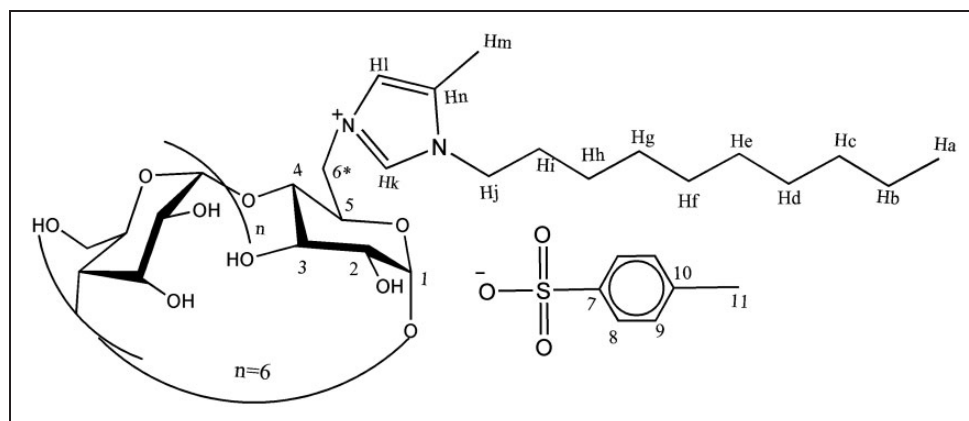


**Figure 4.** The structure of  $\beta$ -CD-DIMOTs.

$^1\text{H}$  NMR, DMSO- $d_6$ : Hl (7.68, s), Hk (7.61, s), Hb-Hj (1.23-1.28, t), Ha (0.85, t), H8 (7.46, d), H9 (7.11, d), OH-2-OH-3 (5.64–5.79, m), H1 (4.83, s), OH-6 (4.44–4.54, m), H6\* (3.91), H3, H5, H6 (3.54–3.63), H2–H4 (3.20–3.34, m), H11 (2.28, s).

$^{13}\text{C}$  NMR, DMSO- $d_6$ : Ca (16.13), Cb (19.79), Cc (28.62), Cd (22.48), Cg (22.48), Ch (21.38), Ci (22.48), Cj (31.37), Ck (126.42), Cl (128.75), Cm (14.40), Cn (129.84), C9 (128.17), C8 (126.06), C1 (102.38), C4 (81.95), C2 (73.49), C3 (72.43), C5 (70.74), C6 (60.36), C6\* (45.66).

CHNS (%): C (40.45), H (6.35), N (1.71), S (1.61).

### Column packing approach

The CSPs (2.5 g) were suspended in approximately 15 ml HPLC-grade hexane and poured into a stainless steel column (250 mm  $\times$  4.6 mm). Thereafter, the CSPs were packed under 35 MPa with hexane for about 24 h.

### HPLC analysis instrumentation and conditions

The newly packed column was flushed with 100% hexane at a flow rate of 0.2 ml/min for 24 h. The flow rate was increased to 0.5 ml/min to obtain a stable baseline. The NSAIDs were prepared at a concentration of 500 mg/l in MeOH. The injection volume was 20  $\mu\text{l}$ . The flow rate was fixed at 0.5 ml/min. The reversed separation mode of mobile phase consisted of ACN/water and MeOH/water, whereas, polar organic consisted of various volume fraction mixture of ACN and MeOH.

### Calculations of chromatographic data

The retention factor ( $k'$ ), selectivity factor ( $\alpha$ ) and resolution factor ( $R_s$ ) were calculated using the following equations

$$k' = \frac{(t_R - t_0)}{t_0} \quad (1)$$

$$\alpha = \frac{k'_2}{k'_1} = \frac{(t_{R2} - t_0)}{(t_{R1} - t_0)} \quad (2)$$

$$R_s = \frac{2 \times (t_{R2} - t_{R1})}{(W_1 - W_2)} \quad (3)$$

The dead time ( $t_0$ ) is the time for the mobile phase to pass through the column. The retention time ( $t_R$ ) is the retention time corresponding to each isomer in the chromatographic separation.  $t_{R2}$  and  $t_{R1}$  represent the retention times of the second and first isomers, respectively, and  $W_1$  and  $W_2$  are the corresponding base peak widths.

### *Preparation of $\beta$ -CD-BIMOTs/NSAIDs complexes*

The complex of  $\beta$ -CD-BIMOTs with NSAIDs was prepared using the conventional kneading method (Cwiertnia et al., 1999; Daruházi et al., 2008).  $\beta$ -CD-BIMOTs and NSAIDs (with the ratio of 1:1) were triturated with mortar and pestle in small amount of ethanol to form homogenous paste. The slurry was kneaded for 30 min and dried to a constant mass. The final product was characterized using  $^1\text{H}$  NMR and NOESY. The prepared samples were dissolved in DMSO- $d_6$ . A 700  $\mu\text{l}$  of the resulting solution was introduced into standard 5 mm NMR tubes, and the spectra of  $^1\text{H}$  NMR and NOESY were recorded at 27°C. For NOESY experiments, the spectra were recorded with a mixing time of 700 ms with 256 increments and 40 scans.

### *Determination of the absorption spectra of $\beta$ -CD-BIMOTs/NSAIDs complexes*

A 2.0 mL of 0.01 mM NSAIDs aliquot and 3.2 ml of 0.0032 M  $\beta$ -CD-BIMOTs solution was transferred accurately into a 10.0 ml standard volumetric flask and diluted to the mark with ultra-pure water. The absorption spectra of  $\beta$ -CD-BIMOTs/NSAIDs complexes were recorded against a blank reagent which was prepared with the same reagent concentration but without the addition of NSAIDs. In addition, absorption spectra of NSAIDs and  $\beta$ -CD-BIMOTs were also recorded. All the absorbance was measured at 200–800 nm separately against blank reagent.

## **Result and discussion**

### *FTIR characterization*

The spectra of  $\beta$ -CD,  $\beta$ -CD-BIMOTs and  $\beta$ -CD-DIMOTs are shown in Figure 5. The broad O-H stretching band around 3200–3300  $\text{cm}^{-1}$  for  $\beta$ -CD,  $\beta$ -CD-BIMOTs and  $\beta$ -CD-DIMOTs is corresponded to the OH group in the  $\beta$ -CD molecules. The intense band at 1657  $\text{cm}^{-1}$  in IR spectra of  $\beta$ -CD-BIMOTs was attributed to C=C of the aromatic ring of 1-BzlIm moieties (Figure 5(b)). The weak bands known as overtones at 1665–2000  $\text{cm}^{-1}$  were also attributed to the aromatic ring (Socrates, 2004) of 1-BzlIm moieties. The C-H band occurred at  $\sim$ 2900  $\text{cm}^{-1}$  of  $\beta$ -CD-BIMOTs and  $\beta$ -CD-DIMOTs spectra (Figure 5(b) and (c)) were found to be more intense than that of  $\beta$ -CD (Figure 5(a)). These results indicate that  $\beta$ -CD was successfully functionalized with 1-BzlIm and  $\text{C}_{10}\text{MIm}$ .

The spectra of Si-TDI, native  $\beta$ -CD-CSP,  $\beta$ -CD-BIMOTs-CSP and  $\beta$ -CD-DIMOTs-CSP are shown in Figure 6. Spectra of Si-TDI (a) show the presence of the isocyanate

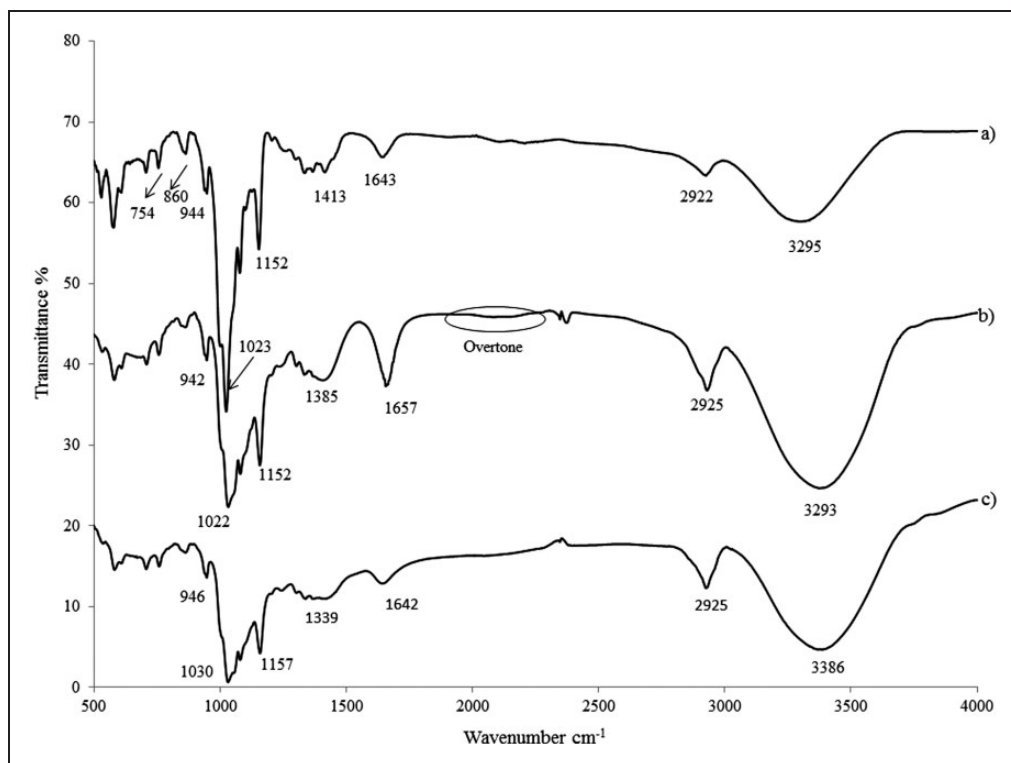


**Figure 5.** FT-IR spectra of (a)  $\beta$ -CD (b)  $\beta$ -CD-BIMOTs (c)  $\beta$ -CD-DIMOTs.

(O=C=N-) group at  $2280\text{ cm}^{-1}$ . The para position isocyanate group is expected to react with OH groups on the surface of silica to form Si-TDI (Arnold, 1957; Rahim et al., 2016a, 2016b). The remaining isocyanate group at ortho-position would react with secondary OH group of  $\beta$ -CD or  $\beta$ -CD functionalized IL. Therefore, the isocyanate peak disappeared after immobilization of native  $\beta$ -CD,  $\beta$ -CD-BIMOTs and  $\beta$ -CD-DIMOTs onto Si-TDI (Figure 6(b) and (d)).

### Thermal analysis

TGA analyses were performed on the Si-TDI, native  $\beta$ -CD-CSP,  $\beta$ -CD-BIMOTs-CSP and  $\beta$ -CD-DIMOTs-CSP in the temperature range of 50 to  $900^\circ\text{C}$ . Based on the thermogram shown in Figure 7, there was an initial loss of weight at temperature below  $100^\circ\text{C}$  for all samples. This was attributed to the removal of physically adsorbed water and/or remaining solvent residues. Physically adsorbed water was further removed completely by heating to around  $200^\circ\text{C}$ . TDI attached to the silica surface decomposed in the region between 125 and  $250^\circ\text{C}$  (Guo et al., 2005). In addition, Si-TDI showed a small but noticeable weight loss in the region  $250\text{--}600^\circ\text{C}$ , caused by the dehydration of the silica surface (Poole et al., 2003). The thermogram of  $\beta$ -CD-BIMOTs-CSP and  $\beta$ -CD-DIMOTs-CSP showed two very distinct weight losses. The weight loss occurred at the range of  $210\text{--}357^\circ\text{C}$  can be attributed to the decomposition of organic moieties at the surface. The weight loss takes place at  $400\text{--}600^\circ\text{C}$

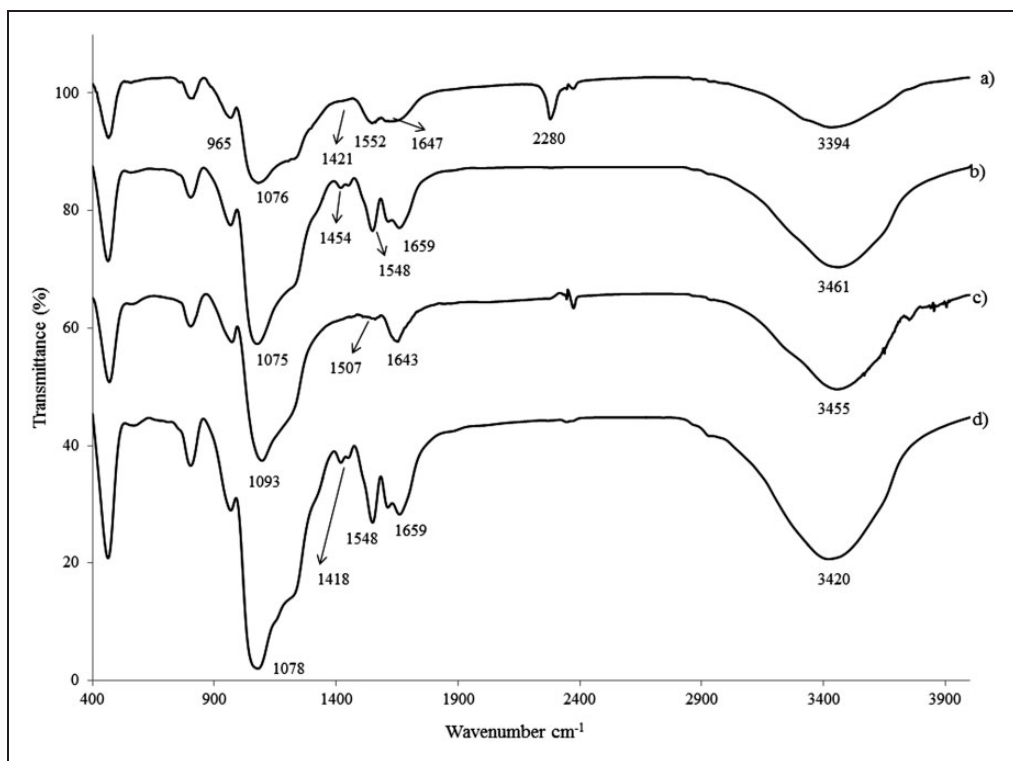


**Figure 6.** FT-IR spectra of (a) Si-TDI (b) native  $\beta$ -CD-CSP (c)  $\beta$ -CD-BIMOTs-CSP (d)  $\beta$ -CD-DIMOTs-CSP.

might be due to the decomposition of the residual methoxy groups on silica (Antochshuk and Jaroniec, 2000). The incessant decrease in weight of native  $\beta$ -CD-CSP,  $\beta$ -CD-BIMOTs-CSP and  $\beta$ -CD-DIMOTs-CSP between 600 and 900°C can be assigned to the decomposition of the  $\beta$ -CD. Overall, the thermogram of  $\beta$ -CD-BIMOTs-CSP showed more pronounced weight loss than  $\beta$ -CD-DIMOTs-CSP at all isothermal temperatures. This is because the long alkyl chain of  $\beta$ -CD-DIMOTs-CSP prevents it from becoming volatile at high temperatures (Lu et al., 2002).

### Elemental analysis

The elemental composition of  $\beta$ -CD-DIMOTs-CSP was C: 15.56%, H: 2.33%, N: 4.72%, S: 1.42%. The degree of surface coverage for  $\beta$ -CD-DIMOTs-CSP was calculated from the following equation (Hongdeng et al., 2014)

$$\beta - \text{CD} - \text{DIMOTs} - \text{CSP} (\mu\text{mol m}^{-2}) = \frac{\%N}{42 \times (1 - \%C - \%H - \%N) \times S} \quad (4)$$

where %C, %H, and %N represent the percentages of carbon, hydrogen, and nitrogen, respectively. S is the specific surface area of the silica support (400 m<sup>2</sup> g<sup>-1</sup>). From the

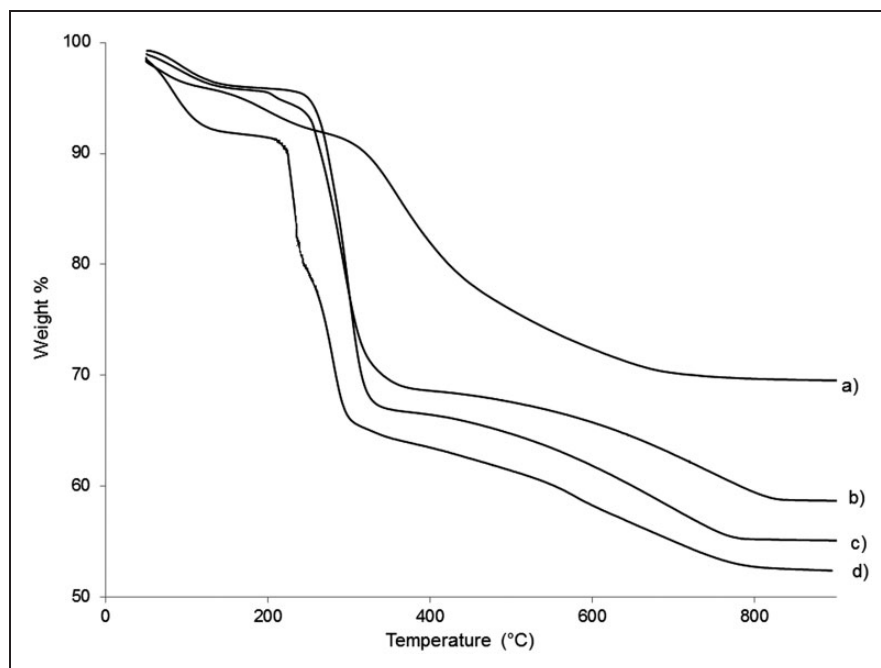


**Figure 7.** Thermogram of (a) Si-TDI (b) native  $\beta$ -CD-CSP (c)  $\beta$ -CD-BIMOTs-CSP (d)  $\beta$ -CD-DIMOTs-CSP.

elemental analysis,  $\beta$ -CD-DIMOTs attached to the silica surface was quantified as  $3.63 \mu\text{mol m}^{-2}$ .

### Screening performance of $\beta$ -CD functionalized ILs

The effect of different groups attached to imidazolium cation (present in  $\beta$ -CD functionalized IL) on the separation of chiral compounds was studied. The performance of  $\beta$ -CD-BIMOTs-CSP and  $\beta$ -CD-DIMOTs-CSP was compared with native  $\beta$ -CD-based CSP for the enantioseparation of NSAIDs. The chromatogram in Figure 8(a) showed that ibuprofen achieved baseline separation while the other NSAIDs (Figure 8(b) and (c)) were poorly enantioseparated using  $\beta$ -CD-BIMOTs-CSP. It is obvious that  $\beta$ -CD-BIMOTs-CSP showed better chromatographic performance as compared to that of  $\beta$ -CD-DIMOTs-CSP and native  $\beta$ -CD based CSP. These results suggest that  $\beta$ -CD-BIMOTs-CSP might provide additional interaction with NSAIDs thus enhanced the enantioseparation. The planar aromatic of 1-BzIm attached to  $\beta$ -CD-BIMOTs-CSP is approached by planar analytes in preference, forming  $\pi$ - $\pi$  interaction (Wang et al., 2012) that contributed to better enantioseparation. The long alkyl chain of  $\beta$ -CD-DIMOTs-CSP is able to cover the partial cavity of  $\beta$ -CD (Meier-Augenstein et al., 1992) resulting in decreased its chiral selectivity. Thus, the optimization of mobile phase for the enantioseparation of NSAIDs was further investigated using  $\beta$ -CD-BIMOTs-CSP. Additionally, the interactions of the enantioseparation on  $\beta$ -CD-BIMOTs-CSP were evaluated.

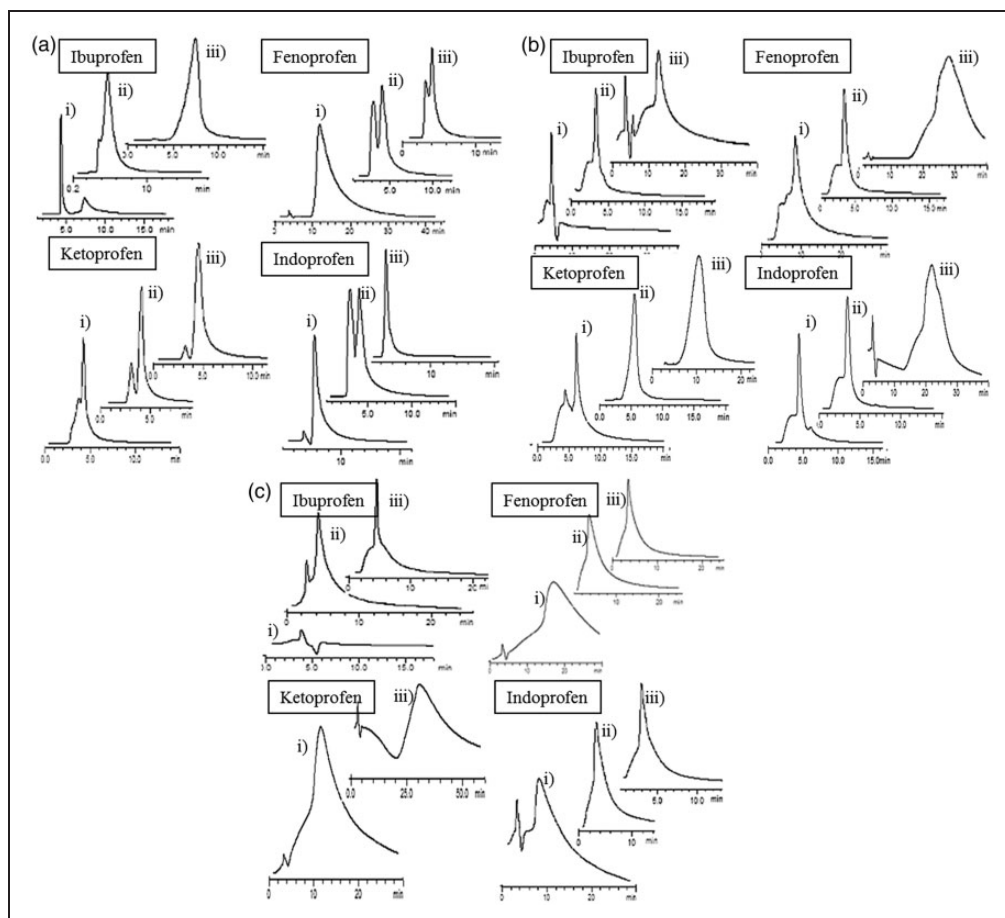


**Figure 8.** The [AQ4]chromatograms for the enantioseparation of selected NSAIDs on (a)  $\beta$ -CD-BIMOTs-CSP (b)  $\beta$ -CD-DIMOTs-CSP (c) native  $\beta$ -CD-CSP condition: (i) 90/10 ACN/water (ii) 50/50 ACN/water and (iii) 30/70 ACN/water.

### Chromatographic data and evaluation on the interactions of enantioseparation on $\beta$ -CD-BIMOTs-CSP

With respect to the chemical structures of NSAIDs shown in Figure 2, we studied the influences of organic solvent composition on enantioseparation of NSAIDs using two different separation modes; reverse phase and polar organic. The effects of various organic solvent compositions (mobile phase) on  $k'$ ,  $\alpha$  and  $R_s$  in the reversed and polar organic separation modes are shown in Table 1. It is apparent that the enantioseparation of NSAIDs achieved better resolution using reversed separation mode than when polar organic mode was used. Furthermore, in the reversed separation mode, high  $R_s$  values of NSAIDs were obtained using different compositions of ACN organic solvent. The high



**Table 1.** Chiral separation data for the NSAIDs on  $\beta$ -CD-BIMOTs CSP.

NSAIDs	Conditions	$k_1'$	$k_2'$	$\alpha$	$R_s$
Ibuprofen	ACN/water-90/10	0.29	1.17	4.04	2.51
	ACN/water-50/50	0.43	0.43	1.00	0
	ACN/water-30/70	1.23	1.23	1.00	0
	MeOH/water-90/10	0.16	0.16	1.00	0
	MeOH/water-50/50	0.77	0.77	1.00	0
	ACN/MeOH-30/70	0.12	0.12	1.00	0
	ACN/MeOH-50/50	0.18	0.18	1.00	0
Indoprofen	ACN/water-90/10	3.35	3.35	1.00	0
	ACN/water-50/50	0.15	0.51	3.39	1.09
	ACN/water-30/70	0.16	0.48	3.02	0.68
	MeOH/water-90/10	0.26	0.26	1.00	0
	MeOH/water-50/50	3.23	3.23	1.00	0
	ACN/MeOH-30/70	0.63	0.63	1.00	0
	ACN/MeOH-50/50	0.79	0.79	1.00	0
Ketoprofen	ACN/MeOH-10/90	2.33	2.33	1.00	0
	ACN/water-90/10	0.76	1.01	1.33	0.43
	ACN/water-50/50	0.46	0.94	2.06	0.72
	ACN/water-30/70	0.52	1.14	2.20	0.88
	MeOH/water-90/10	2.54	2.54	1.00	0
	MeOH/water-50/50	5.12	5.12	1.00	0
	ACN/MeOH-50/50	1.21	1.21	1.00	0
Fenoprofen	ACN/MeOH-10/90	4.93	4.93	1.00	0
	ACN/water-90/10	1.04	1.04	1.00	0
	ACN/water-50/50	0.07	0.07	1.00	0
	ACN/water-30/70	0.11	0.50	4.55	0.54
	MeOH/water-90/10	0.06	0.06	1.00	0
	MeOH/water-50/50	1.05	1.05	1.00	0
	ACN/MeOH-30/70	0.13	0.13	1.00	0
	ACN/MeOH-50/50	0.25	0.25	1.00	0
	ACN/MeOH-10/90	0.52	0.52	1.00	0

values of  $k_1'$  and  $k_2'$  obtained with highest and lowest composition of ACN (90% and 30%) used, revealed that the retention behavior of NSAIDs is mixed aqueous-normal separation mode (Guo et al., 2009). In this separation mode, the retention mechanism was based on the distribution of the analytes between ACN-rich mobile phase and water-enriched layer on stationary phase (Buszewski and Noga, 2012). Apart from composition of organic solvent, the effect of mobile phase pH on the enantioseparation of NSAIDs was also investigated. TEAA buffer was used to control the mobile phase pH. Buffer can influence the degree of ionization of analytes and result in different retention behavior. Referring to the chromatograms shown in Figure 9, there was no  $R_s$  value for NSAIDs at pH 4 and 9. The TEAA buffer is believed to have masked the enantioselective retention sites on the CSP surface and decreased the resolution (Mosiashvili et al., 2013).

As can be seen from Table 1, ibuprofen was completely resolved with  $R_s$  value of 2.51, meanwhile, indoprofen showed partial separation with  $R_s$  value of 1.09. Ketoprofen and fenoprofen were also partially enantioseparated and fenoprofen attained the lowest  $R_s$  value



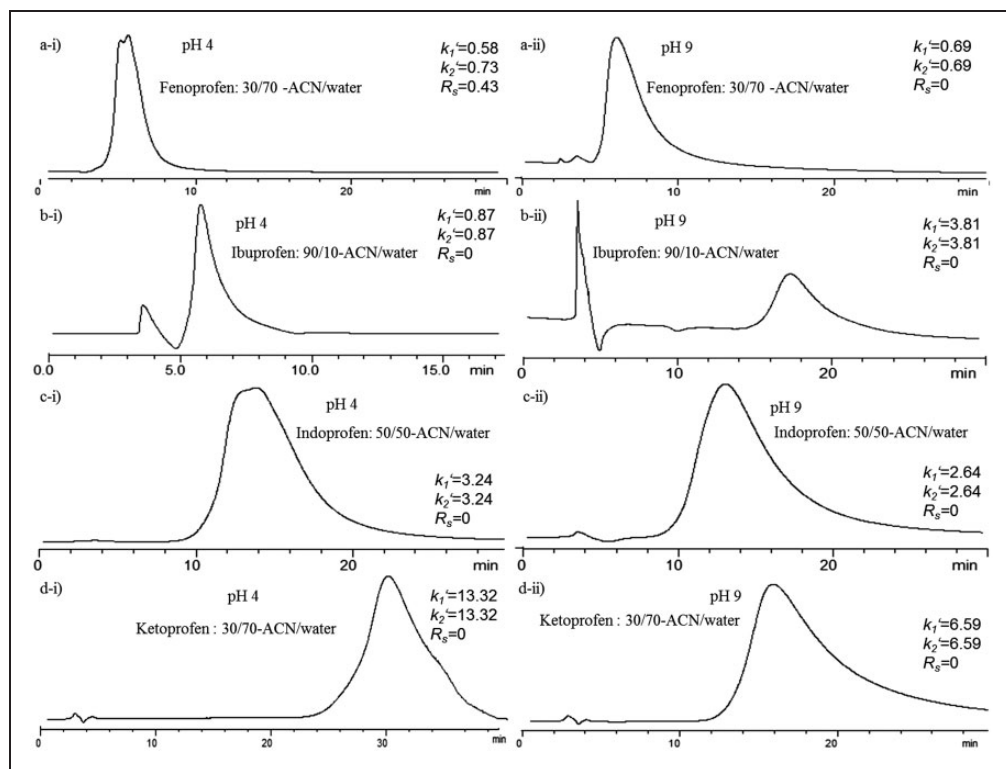


**Figure 9.** The chromatograms of fenoprofen, ibuprofen, indoprofen and ketoprofen responding to different pH of mobile phase.

(0.54). The relatively low  $R_s$  values of ketoprofen and fenoprofen were because of the substituent in the *meta* position that made their orientation in an unfavorable way to fit into the  $\beta$ -CD-BIMOTs cavity (Fanali and Aturki, 1995). The higher  $R_s$  values of ibuprofen and indoprofen are probably due to the *para* position of the substituent (containing the chiral center) on the aromatic ring (Fanali and Aturki, 1995). This is in good agreement with previous studies which also proved that *para*-substituted aromatic rings can fit properly into the CD cavity forming inclusion complex, but the extent of the penetration mode is dependent on the polarity and feature structure of analytes (Fanali and Aturki, 1995; Núñez-Agüero et al., 2006). It can be concluded that the less polar ibuprofen achieved better enantioseparation than polar indoprofen (Velkov et al., 2007).

Even though the polarity of fenoprofen and ibuprofen are close to each other ( $\log P_{\text{fenoprofen}} = 3.8$ ,  $\log P_{\text{ibuprofen}} = 3.7$ ) (Velkov et al., 2007), ibuprofen achieved higher  $R_s$  value when high organic solvent content (90% ACN) was used. This is because ibuprofen can be fitted into  $\beta$ -CD-BIMOTs cavity, whereas fenoprofen with two aromatic rings was less favorable to be fitted into  $\beta$ -CD-BIMOTs cavity due to steric hindrance effect. According to previous simulation study (Núñez-Agüero et al., 2006), there was also moderate and weak hydrogen bonding between the carboxyl group of ibuprofen and hydroxyl groups of  $\beta$ -CD during the complexation. Ketoprofen which is composed of a similar structure (two aromatic rings) as fenoprofen, achieved better enantioseparation

**Table 2.** Chemical shifts corresponding to  $\beta$ -CD-BIMOTs in the presence of NSAID.

$\beta$ -CD-BIMOTs	$\beta$ -CD-BIMOTs/ ibuprofen		$\beta$ -CD-BIMOTs/ indoprofen		$\beta$ -CD-BIMOTs/ ketoprofen		$\beta$ -CD-BIMOTs/ fenoprofen		
	$\delta$	$\Delta\delta$	$\delta$	$\Delta\delta$	$\Delta$	$\Delta\delta$	$\delta$	$\Delta\delta$	
H1	4.8405	4.8369	-0.0036	4.8316	-0.0089	4.8337	-0.0068	4.8280	-0.0125
H2	3.3312	3.3200	-0.0112	3.3474	0.0162	3.3015	-0.0297	3.3118	-0.0194
H3	3.6394	3.6387	-0.0007	3.6323	-0.0071	3.6284	-0.011	3.6326	-0.0068
H4	3.3716	3.4056	<b>0.0340</b>	3.4292	<b>0.0576</b>	3.3985	0.0269	3.4132	<b>0.0416</b>
H5	3.5777	3.5597	<b>-0.018</b>	3.5536	<b>-0.0241</b>	3.5458	<b>-0.0319</b>	3.5530	<b>-0.0247</b>
H6	3.9225	3.9091	-0.0134	3.9045	-0.018	3.9048	-0.0177	3.8803	-0.0422
H8	7.4215	7.4422	0.0207	7.4318	0.0103	7.4182	-0.0033	7.4209	-0.0006
H9	7.1112	7.1189	-0.0077	7.1268	0.0156	7.1196	-0.0084	Overlap	-
H11	2.0847	-	-	-	-	-	-	-	-
Ha	7.4314	7.4877	<b>0.0563</b>	7.4835	<b>0.0521</b>	7.4737	<b>0.0423</b>	7.4834	<b>0.052</b>
Hb	7.7957	7.8149	0.0192	Overlap	-	-	-	7.7896	-0.0061
Hc	7.7542	7.7516	-0.0026	Overlap	-	-	-	7.7410	-0.0132
Hd	-	-	-	-	-	-	-	-	-
He	7.9563	7.9921	<b>0.0358</b>	-	-	7.9378	-0.0185	7.9399	-0.0164
Hf	9.2394	9.3362	<b>0.0968</b>	9.3202	<b>0.0808</b>	9.2240	-0.0154	9.3217	<b>0.0823</b>
Hg	5.4371	5.4514	0.0143	5.4146	-0.0225	5.4036	-0.0335	5.4459	-0.0088

Note: Values in bold refer to the highest induced shift of that particular proton.

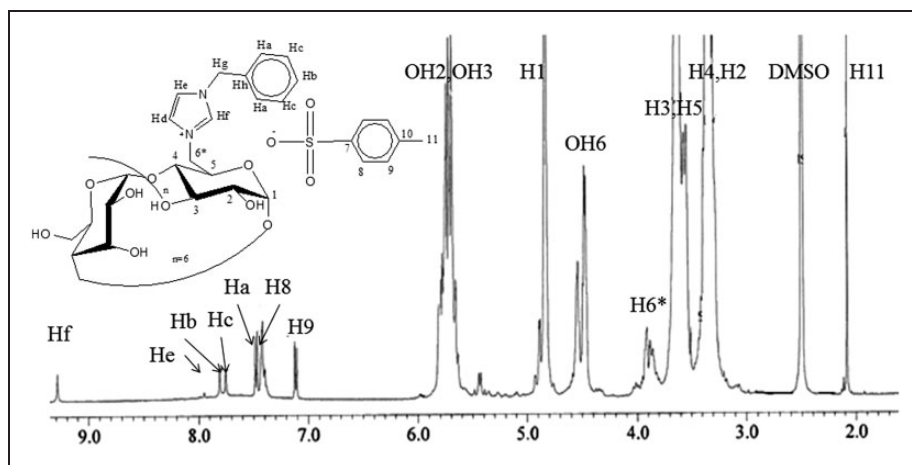
than fenoprofen. This is due to the presence of carbonyl group in ketoprofen which enhanced the formation of hydrogen bonding with  $\beta$ -CD-BIMOTs rather than ether linkage in fenoprofen (Lommerse et al., 1997). Therefore, it can be said that, apart from the inclusion complex formation, hydrogen bonding also played an important role in enhancing the enantioseparation of NSAIDs.

In order to verify the interactions of enantioseparation,  $^1\text{H}$  NMR and NOESY of  $\beta$ -CD-BIMOTs/NSAIDs complexes were studied. The values of chemical shifts ( $\delta$ ) obtained from  $^1\text{H}$  NMR for different protons in  $\beta$ -CD-BIMOTs, NSAIDs and  $\beta$ -CD-BIMOTs/NSAIDs complexes are listed in Tables 2 and 3. The deduced structures of the  $\beta$ -CD-BIMOTs and  $\beta$ -CD-BIMOTs/NSAIDs complexes are shown in Figures 10 and 11, respectively. Normally, the inclusion of non-polar region of an analyte into the hydrophobic cavity would affect the inner protons of the glucose units of  $\beta$ -CD, namely, H3 and H5 (Zhang et al., 1990). However, in the presence of ibuprofen, indoprofen, ketoprofen and fenoprofen, there were appreciable shift at H4 and H5 protons of  $\beta$ -CD-BIMOTs (Table 2) due to the formation of hydrogen bonding and inclusion complex, respectively. In addition, significant change in values of chemical shifts ( $\delta$ ) of Hc' proton of ibuprofen (Table 3) was also observed. This result indicates that isobutyl moiety of ibuprofen was included into the cavity of  $\beta$ -CD-BIMOTs. However, the cross peak between proton of isobutyl ibuprofen with H5 proton of  $\beta$ -CD is absent in the NOESY spectra of  $\beta$ -CD-BIMOTs/ibuprofen (see in Figure S1(a) in supporting information). Perhaps, the great difference between isobutyl size and the internal  $\beta$ -CD diameter, ( $\approx 4.3$  and  $7.8 \text{ \AA}$ , respectively) causes such weak interaction (Núñez-Agüero et al., 2006). Furthermore, cross-peaks between Hf', Hg' and Hj' protons of ibuprofen with H5 proton of  $\beta$ -CD-BIMOTs confirm the penetration of aromatic moiety into the  $\beta$ -CD-BIMOTs cavity.

**Table 3.** Induced shifts corresponding to NSAID in the presence of  $\beta$ -CD-BIMOTs.

	$\beta$ -CD-BIMOTs/ Ibuprofen $\Delta \delta$	$\beta$ -CD-BIMOTs/ Indoprofen $\Delta \delta$	$\beta$ -CD-BIMOTs/ Ketoprofen $\Delta \delta$	$\beta$ -CD-BIMOTs/ Fenoprofen $\Delta \delta$
Ha'	-0.0022	-0.0044	<b>-0.0183</b>	0.0132
Hb'	-0.0041	-0.0022	-0.0048	0.0133
Hc'	<b>0.0072</b>	-0.0044	-0.0083	0.0132
Hd'	-0.0030	<b>-0.0141</b>	-0.0070	<b>0.0677</b>
He'	-0.0033	-0.0051	<b>-0.0119</b>	<b>0.0677</b>
Hf'	-0.0023	-0.0081	-0.0083	0.0237
Hg'	-0.0011	-0.0081	-0.0052	0.0238
Hh'	-0.0020	-0.0086	-0.0046	0.0373
Hi'	-	-0.0086	-0.0042	0.0099
Hj'	-0.0029	-	<b>0.0155</b>	-
Hk'	-	-0.0235	-0.0098	0.0258

Note: Values in bold refer to the highest induced shift of that particular proton.

**Figure 10.** The deduced structure of  $\beta$ -CD-BIMOTs.

Appreciable shifts were also observed for the aromatic proton of indoprofen (Hd', Hh', Hi'), ketoprofen (Ha', He') and fenoprofen (Hd', He') (Table 2), which proves the formation of inclusion complexes. This result was further convinced with the NOESY spectra of  $\beta$ -CD-BIMOTs/indoprofen,  $\beta$ -CD-BIMOTs/ketoprofen and  $\beta$ -CD-BIMOTs/fenoprofen (Figure S1 (b) and (d)), where cross-peaks between Hh', Hi' (proton indoprofen), He' (proton ketoprofen) and Ha', Hc', Hi' (proton fenoprofen) with H5 proton of  $\beta$ -CD-BIMOTs were observed.

Additionally, the UV/Vis absorption spectra of  $\beta$ -CD-BIMOTs/NSAIDs complexes were further investigated to acquire more information on the interactions between NSAIDs and  $\beta$ -CD-BIMOTs. The plots of UV/Vis absorption for  $\beta$ -CD-BIMOTs, NSAIDs and

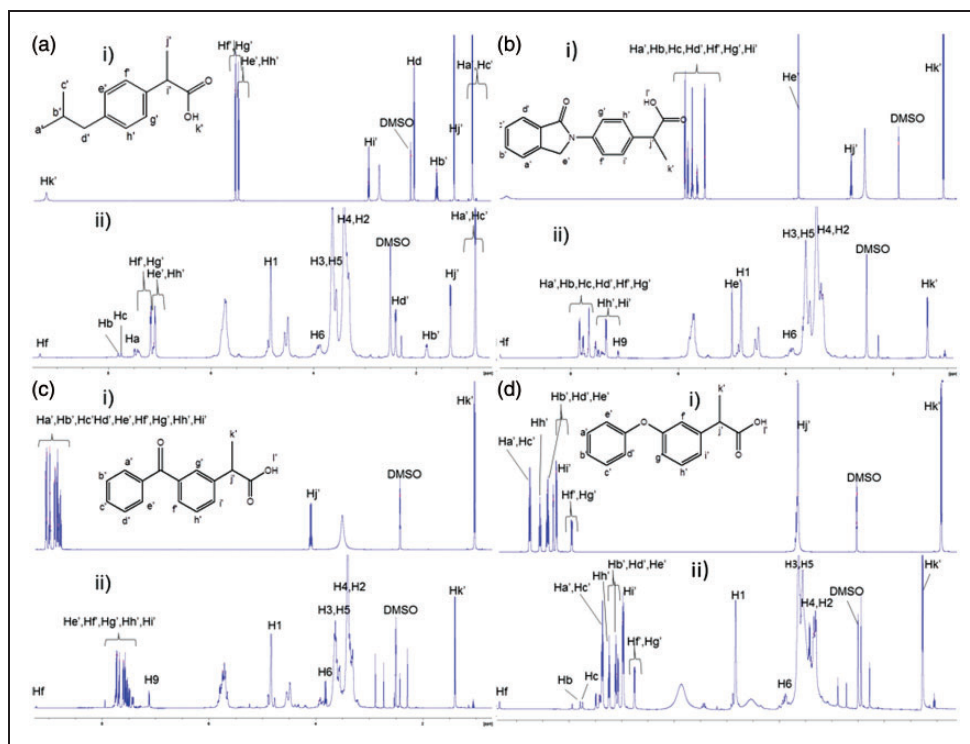


**Figure 11.** The deduced structure of NSAID/ $\beta$ -CD-BIMOTs complexes: (a) (i) ibuprofen (ii)  $\beta$ -CD-BIMOTs/ibuprofen, (b) (i) indoprofen (ii)  $\beta$ -CD-BIMOTs/indoprofen (c) (i) ketoprofen (ii)  $\beta$ -CD-BIMOTs/ketoprofen, (d) (i) fenoprofen (ii)  $\beta$ -CD-BIMOTs/fenoprofen.

$\beta$ -CD-BIMOTs/NSAIDs complexes are presented in Figure 12. The results obtained revealed that  $\beta$ -CD-BIMOTs had  $\lambda_{\max}$  in the range of 230–260 nm. The  $\lambda_{\max}$  of  $\beta$ -CD-BIMOTs/ibuprofen,  $\beta$ -CD-BIMOTs/indoprofen and  $\beta$ -CD-BIMOTs/fenoprofen complexes appeared at 262, 256 and 256 nm, respectively, referring to  $\beta$ -CD-BIMOTs. The absorbance of  $\beta$ -CD-BIMOTs/ibuprofen,  $\beta$ -CD-BIMOTs/indoprofen and  $\beta$ -CD-BIMOTs/fenoprofen underwent the hyperchromic effect (increase in absorbance), while the absorbance of  $\beta$ -CD-BIMOTs/ketoprofen experienced the hypochromic effect (decrease in absorbance). Both the hyperchromic and hypochromic effects observed were due to the  $\pi$ - $\pi^*$  transition of dipole moments of the aromatic ring. The transition dipole moment of this chromophore interacts with the induced dipoles of the neighboring chromophores, depending on their relative orientation. If the dipoles are along the same axis and one behind the other, then the intensity of the absorption band will increase and hyperchromic effect is observed. Conversely, if the dipoles are parallel and adjacent, a decrease in intensity of the absorption band occurs, and hypochromic effect is observed (Peral and Gallego, 2000). The hypochromic effect on  $\beta$ -CD-BIMOTs/ketoprofen can also be attributed to the limitation for  $\pi$ - $\pi^*$  transition because of hydrogen bonding (Peral and Gallego, 2000) at carbonyl group between aromatic rings of ketoprofen. The variations that occurred in the UV/Vis spectra were a consequence of complexation of NSAIDs with  $\beta$ -CD-BIMOTs accompanied by  $\pi$ - $\pi$  interaction and hydrogen bonding. These results clearly

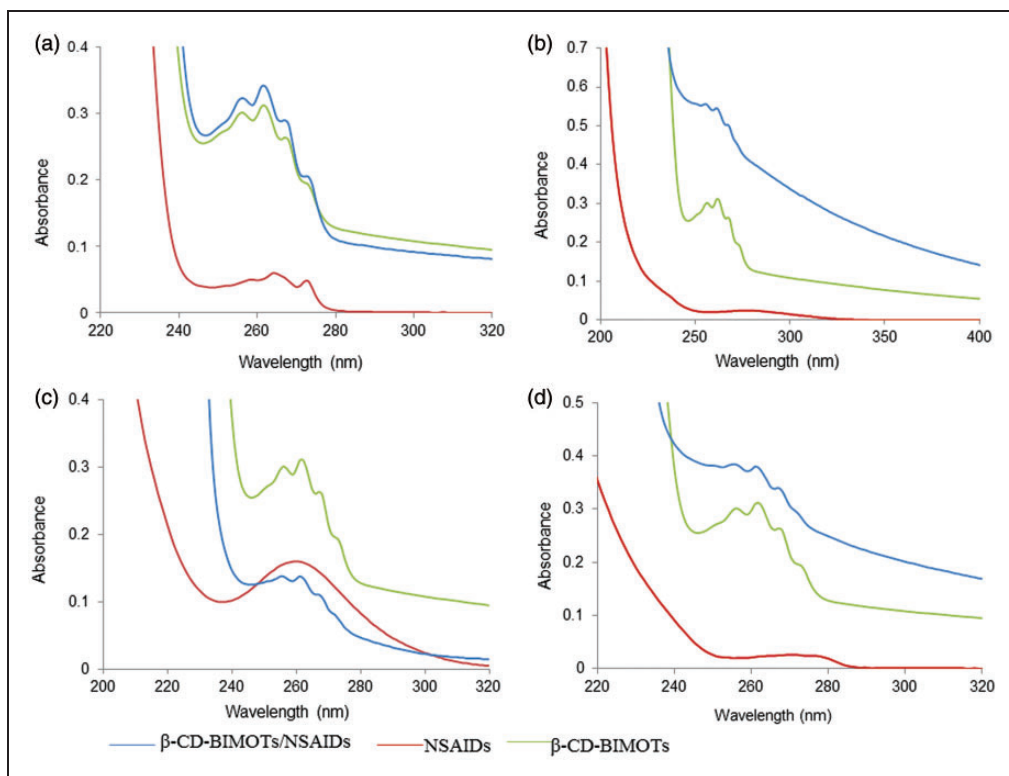


**Figure 12.** Absorption spectra of (a)  $\beta$ -CD-BIMOTs/ibuprofen, (b)  $\beta$ -CD-BIMOTs/indoprofen, (c)  $\beta$ -CD-BIMOTs/ketoprofen and (d)  $\beta$ -CD-BIMOTs/fenoprofen with ( $\beta$ -CD-BIMOTs): 0.032 mM (NSAIDs): 0.01 mM; T = 25°C.

prove the ability of IL to form  $\pi$ - $\pi$  interaction in addition to the existing superposition of inclusion complex and hydrogen bond for the enantioseparation of NSAIDs.

## Conclusions

In this study,  $\beta$ -CD-BIMOTs-CSP and  $\beta$ -CD-DIMOTs-CSP were successfully synthesized and compared for enantioseparation of NSAIDs. The  $\beta$ -CD-BIMOTs-CSP performed better than  $\beta$ -CD-DIMOTs-CSP and  $\beta$ -CD-CSP due to the additional  $\pi$ - $\pi$  interaction which was possible with  $\beta$ -CD-BIMOTs-CSP. Furthermore, a better enantioseparation of ibuprofen, fenoprofen, indoprofen and ketoprofen using  $\beta$ -CD-BIMOTs-CSP were observed due to the superposition of hydrogen bonding, hydrophobic and also  $\pi$ - $\pi$  interactions. From  $^1\text{H}$  NMR, NOESY and UV/Vis studies, NSAIDs were proven to form inclusion complexes with  $\beta$ -CD-BIMOTs-CSP.

## Acknowledgments

The authors acknowledge Ministry of Higher Education (MOHE) for providing fellowship to one of the authors-cum-researchers, Ms. NurulYani Rahim.

## Declaration of conflicting interests

The author(s) declared no potential conflicts of interest with respect to the research, authorship, and/or publication of this article.

## Funding

The author(s) disclosed receipt of the following financial support for the research, authorship, and/or publication of this article: The authors would like to seize this opportunity to express their gratitude to the University Malaya for the IPPP grant PG027/2013A and UMRG grant (RP006A-13SUS and RP011B-14SUS).

## Supplementary Material

Supplementary material for this paper can be found at <http://journals.sagepub.com/doi/suppl/10.1177/0263617416686798>.

## References

- Anderson JL and Armstrong DW (2003) *Anal. Chem* 75: 4851 [AQ1].
- Antochshuk V and Jaroniec M (2000) *Chem. Mater* 12: 2496.
- Arnold R, Nelson J and Verbanc (1957) *J. Chem. Rev* 57: 47.
- Buszewski B and Noga S (2012) *Anal. Bioanal. Chem* 402: 231.
- Canongia Lopes JN and Pádua AA (2006) *J. Phy. Chem. B* 110: 3330.
- Cwiertnia B, Hladon T and Stobiecki M (1999) *J. Pharm. Pharmacol* 51: 1213.
- Daruházi ÁE, Szente L, Balogh B, et al. (2008) *J. Pharm. Biomed. Anal* 48: 636.
- Fanali S and Aturki Z (1995) *J. Chromatogr. A* 694: 297.
- Guo Z, Jin Y, Liang T, et al. (2009) *J. Chromatogr. A* 1216: 257.
- Guo ZX, Liu WF, Li Y, et al. (2005) *J. Macromol. Sci. A* 42: 221.
- Hongdeng Q, Mingliang Z, Jia C, et al. (2014) *Anal. Methods* 6: 469.
- Li X and Zhou Z (2014) *Anal. Chim. Acta* 819: 122.
- Li X, Zhou Z, Zhou W, et al. (2011) *Analyst* 136: 5017.
- Lommerse JP, Price SL and Taylor R (1997) *J. Comput Chem* 18: 757.
- Lu X, Ng HY, Xu J, et al. (2002) *Synthetic Metals* 128: 167.
- Meier-Augenstein W, Burger BV, Spies HS, et al. (1992) *Z. Naturforsch. B Chem. Sci* 47: 877.
- Mosiashvili L, Chankvetadze L, Farkas T, et al. (2013) *J. Chromatogr. A* 1317: 167.
- Muderawan IW, Ong TT and Ng SC (2006) *J. Sep. Sci* 29: 1849.
- Núñez-Agüero CJ, Escobar-Llanos CM, Díaz D, et al. (2006) *Tetrahedron* 62: 4162.
- Pandey S (2006) *Anal. Chim. Acta* 556: 38.
- Peral F and Gallego E (2000) *Spectrochim. Acta Mol. Biomol. Spectrosc* 56: 2149.
- Poole CF (2003) *The Essence of Chromatography*. Elsevier.
- Rahim NY, Tay KS and Mohamad S (2016a) *J. Incl. Phenom. Macrocycl. Chem* 85: 303.
- Rahim NY, Tay KS and Mohamad S (2016b) *Chromatographia* 1.
- Socrates G (2004) *Infrared and Raman characteristic group frequencies: tables and charts*. [AQ2] John Wiley & Sons.
- Velkov T, Horne J, Laguerre A, et al. (2007) *J. Chem. Biol* 14: 453.
- Wang RQ, Ong TT, Tang W, et al. (2012) *Anal. Chim. Acta* 718: 121.
- Wasserscheid P and Keim W (2000) *Angew. Chemie. Int. Ed* 39: 3772.
- Xiao Y, Ng SC, Tan TT Y, et al. (2012) *J. Chromatogr. A* 1269: 52.
- Yatabe J and Kageyama T (1994) *J. Ceram. Soc. Jap* 102: 595.
- Ye J, Yu W, Chen G, et al. (2010) *Biomed. Chromatogr* 24: 799.

- Zhang ZB, Zhang WG, Luo WJ, et al. (2008) *J. Chromatogr. A* 1213: 162.
- Zhang DD, Zhao PY, Huang NJ, et al. (1990) In: *The 5th International symposium on cyclodextrins*. [AQ3]: Editions de Santé, p. 146.
- Zhong Q, He L, Beesley TE, et al. (2006) *Chromatographia* 64: 147.
- Zhou ZM, Li X, Chen XP, et al. (2010) *Talanta* 82: 775.